LIST OF DOCUMENTS:

1. PROGRAM ANNOUNCEMENT, CALLS FOR PROPOSALS, AND PROGRAM RULES ARE ALL CONTAINED IN RESEARCH ANNOUNCEMENT RA 94-30 WHICH WAS PUBLISHED IN THE COMMERCE BUSINESS DAILY (CBD) (3 PAGES)

2. AGREEMENT MDA972-95-3-0008, DEVELOPMENT OF HIGH BANDGAP III-V MATERIAL AND OPTICAL DEVICES WITH ATTACHMENTS 1 THROUGH 5 AND AMENDMENTS 0001, 0002 AND MODIFICATION A0001. (44 PAGES)

3. PROPOSAL BY BLUE BAND CONSORTIUM, BLUE LIGHT AND UV EMITTERS – THE BAY AREA NITRIDE DEVELOPMENT CONSORTIUM, DEVELOPMENT OF HIGH BANDGAP III-V MATERIALS AND OPTICAL DEVICES. (50 PAGES)

4. REPORTS:
MILESTONES 1 AND 2. MILESTONE 6 PARTIALLY COMPLETED (5 PAGES)
MILESTONES 3 THROUGH 6 QUARTER 1 REPORT (29 PAGES)
MILESTONES 7 THROUGH 11 REPORT FOR MONTH 6 (37 PAGES)
MILESTONES 12 THROUGH 16 REPORT FOR MONTH 9 (18 PAGES)
MILESTONES 17 THROUGH 21 REPORT FOR MONTH 12 (11 PAGES)
MILESTONES 22 THROUGH 26 REPORT FOR MONTH 15 (16 PAGES)
MILESTONES 38 THROUGH 43 REPORT FOR MONTH 24 (16 PAGES)
FINAL REPORT AUGUST 1997 JUNE 1995-AUGUST 1997 (19 PAGES)
(TOTAL PAGES FOR REPORTS 151)

NOTE: NO REPORTS WERE LOCATED FOR MILESTONES 27 THROUGH 37.

TOTAL NUMBER OF PAGES: 248

1. PROGRAM ANNOUNCEMENT, CALLS FOR PROPOSALS, AND PROGRAM RULES ARE ALL CONTAINED IN RESEARCH ANNOUNCEMENT RA 94-30 WHICH WAS PUBLISHED IN THE COMMERCE BUSINESS DAILY (CBD) (3 PAGES)

CBD, Thurs, Apr 14

Transmission via CBD Express V. 5.1/S
Defense Advanced Research Projects Agency

1. P!!
2. 0412!!
3. 94!!
4. 97AE!!
5. 22203-1714!!
6. A!!
7. Advanced Research Projects Agency (ARPA), Contracts Management Office (CMO), 3701 North Fairfax Drive, Arlington, VA 22203-1714!!
8. A -- ADVANCED MATERIALS PARTNERSHIPS!!
9. RA94-30!!
10. 072594!!
11. Dr. Ben A. Wilcox, Tech POC, ARPA/DSO, FAX: (703)696-2201.!!
12. N/A!!
13. N/A!!
14. N/A!!
15. N/A!!
16. N/A!!
17. The manufacturing of advanced materials and subsequent components and devices is a crucial enabling factor for developing virtually all military systems. Research results are often transitioned into commercial applications. Advanced materials manufacturing technologies are prominent in many recently released reports, including the report of the National Critical Technologies Panel, The Defense Critical Technologies Plan, The Commerce Department Emerging Technologies Report, and the Aerospace Industries Association. The Defense Sciences Office of the Advanced Research Projects Agency (ARPA/DSO) plans to initiate at least five advanced materials manufacturing "partnerships" with the private sector, institutions of higher education and state and local governments. See 10 U.S.C.2358 and 2371. Approximately thirty million dollars ($30 million) of FY94 funds are available for this activity. Research areas of interest include: (a) affordable polymer matrix composite structures, (b) large area, wide band-gap III-V bulk and epitaxial materials for heterostructures useful in optoelectronics, (c) magnetic materials and devices exhibiting giant magnetoresistance, and (d) metallic alloys, ceramics and their composites and components produced by innovative forming processes. The partnerships are intended to demonstrate management mechanisms and concepts which will facilitate the widespread development and application of affordable advanced materials, components, devices and the manufacturing processes used to produce them. Projects which are aimed at increasing the performance and reducing the cost of materials are of interest, but the primary focus is reducing the cost of components and devices manufactured from advanced materials. These partnerships are also aimed at demonstrating the effectiveness of collaboration between U.S. industry, U.S. universities and colleges, state and local governments and federal laboratories. For the establishment of these partnerships, ARPA is seeking innovative and creative technical approaches and management ideas and concepts which involve the active participation of large and small U.S. industrial firms, U.S. academic institutions of higher education, federal laboratories, and state and local governments. It is anticipated that, in most situations, a U.S. industrial firm will serve as the lead organization. All efforts must be cost shared. Federal government funding will not exceed 50 percent of the total

required resources except as noted below for small business participants. Non-federal contributions can include the fair market value for the program utilization of equipment, services, materials, technology transfer activities, and other assets. However, cash contributions are preferred. A small business participant in an Advanced Materials Partnership may count as non-federal cost share any funds received under a Small Business Innovation Research (SBIR) or Small Business Technology Transfer (STTR) contract, whether awarded by ARPA or any other agency. In order to qualify, a funded SBIR or STTR effort must be clearly identified in the proposal as integral to the proposal effort or is clearly related to the work being performed under the ARPA agreement and capable of being integrated into that effort. For successful proposals, funds which are expended after the proposal due date may be counted as cost sharing even before the commencement of work under the partnership agreement. Funds expended prior to the proposal due date will not be considered as a direct cost share. However, where expended SBIR/STTR funds have resulted in a product which will defray the cost of a project, that product may be counted as "in-kind" cost share. A merit-based process will be used to select partnerships to participate in this program. Evaluation criteria, listed in order of decreasing value, to be used in that process include: (1) technical excellence and innovativeness of proposed ideas and approach, and the impact on cost-effective manufacturing of materials, components, and devices, (2) extent to which the program advances and enhances the national security interests of the United States, and the potential effectiveness of the partnership to further develop widespread application (dual-use) of the products to be developed (pervasive impact), (3)commitment of the partnership to productize the results of the proposed effort, (4)qualifications of the personnel proposed to participate and adequacy of facilities, and (5)financial commitments of the eligible institutions to the proposed partnership. It is anticipated that projects of up to two years in duration will be supported. Longer term options may be proposed. Goals of the partnership must include demonstration of a component or device of military interest. A substantial effort of each partnership will be devoted to modeling and simulation of materials manufacturing. Each effort should emphasize "intelligent manufacturing" of materials concepts and include a cost model and business plan for productization. Partnerships having the management and technical capabilities, facilities and experience necessary to conduct this program are invited to submit brief preproposals to describe their technical approach, management concepts, participants, relevant experience and estimates of the overall cost and timing of the project. This procedure is intended to minimize unnecessary effort in proposal preparation and review. Preproposals should not exceed 20 pages of text plus a one page work breakdown structure for the program and a proposed task schedule chart. Ten single sided hard copies, each 8.5 by 11 inches, should be submitted. They should have 1.25-inch maximum margins, and a font size not smaller than 12 pitch. Within approximately seven (7) business days of receipt, ARPA will acknowledge receipt of the submission and assign a control number that should be used in all further correspondence regarding the preproposal. ARPA intends to respond to preproposals within 30 days of receipt with a recommendation of whether or not to submit a full proposal. Regardless of the recommendation, the decision to propose is the responsibility of the proposer. All submitted proposals will be fully reviewed regardless of the disposition of the preproposal. All those who submit full proposals are required to supply eight copies

of the proposal. A p osals must be in the ollo ing "page" format: double-spaced, not greater than 8.5 by 11 inches, typed single-side with 1.25 inch minimum margins, with a font size not smaller than 12 pitch. Volume 1 of submitted proposals shall include an Abstract, Executive Summary, Technical Approach, Program Plan, Statement of Work, Milestone Chart, Facilities and Equipment Description, Relevant Prior Work, Management Plan, Cost Model, Business Plan for Productization, and Resumes of Key Individuals. The page count of Volume 1 should be limited to a maximum of 50 pages, which includes all figures, tables, and charts. Volume 2 of submitted proposals shall contain a complete cost breakdown. Details of any cost sharing to be undertaken by the offerer should be included in the proposal. The merit of submitted proposals will be evaluated in relation to the proposed cost and availability of funds. The Government plans to make award decisions within 30 days after receipt of full proposals. It is anticipated that in most cases the award instrument will be an ARPA "agreement" (10 U.S.C. 2358/2371) rather than a procurement contract or grant. These "agreements" will be eligible for Independent Research and Development (IR&D) cost sharing. All proprietary material submitted should be clearly marked as such and will be held in strict confidence. All preproposals and proposals must reference ARPA RA #94-30. No additional information is available nor will a formal RFP or other solicitation regarding this announcement be issued. Requests for same will be disregarded. The Government reserves the right to select for award all, some, or none of the proposals received in response to this announcement and to negotiate for less than the entire effort proposed. All responsible sources capable of satisfying the Government's needs may submit proposals which will be evaluated as received. ARPA expects the response to this announcement to be large. Therefore, telephone inquiries are strongly discouraged. All questions regarding this RA must be submitted in writing or via FAX: (703)696-2201)to the technical contact indicated. Bidders should submit preproposals to: Advanced Research Projects Agency, Defense Sciences Office, REF: RA #94-30 ATTN: Dr. Ben A. Wilcox, 3701 North Fairfax Drive, Arlington, VA 22203-1714. All preproposals are due no later than 4 pm EST, 16 May 1994. Full proposals are due no later than 4 pm EST, 25 July 1994.

*****

2. AGREEMENT MDA972-95-3-0008, DEVELOPMENT OF HIGH BANDGAP III-V MATERIAL AND OPTICAL DEVICES WITH ATTACHMENTS 1 THROUGH 5 AND AMENDMENTS 0001, 0002 AND MODIFICATION A0001. (44 PAGES)

MODIFICATION A0001 TO THE TECHNOLOGY DEVELOPMENT AGREEMENT

BETWEEN

BLUE LIGHT AND UV EMITTERS – THE BAY AREA NITRIDE DEVELOPMENT (BLUE BAND) CONSORTIUM
c/o SDL, INC.
80 ROSE ORCHARD WAY
SAN JOSE, CA 95134-1365

AND

THE DEFENSE ADVANCED RESEARCH PROJECTS AGENCY
3701 NORTH FAIRFAX DRIVE
ARLINGTON, VA 22203-1714
(POC: J. CARTER, DCMC SAN DIEGO, (619) 495-7462)

CONCERNING

DEVELOPMENT OF HIGH BANDGAP III-V MATERIALS AND OPTICAL DEVICES

Agreement No:	MDA972-95-3-0008
Modification No:	**A0001**
Authority:	10 U.S.C. § 2371
Effective Date:	Date of Grants Officer Signature

1. This modification hereby:
   A. Extends the Term of this Agreement from 24 to 27 months.
   B. Revises the Schedule of Payments and Payable Milestones to extend the ninth payable milestone period by three months.

2. Paragraph A of Article II, TERM, is hereby deleted from this Agreement and replaced with the following paragraph:

ARTICLE II: TERM

A. The Term of this Agreement

The Program commences upon the date of the last signature hereon and continues for twenty-seven (27) months. If all funds are expended prior to the 27-month duration, the Parties have no obligation to continue performance and may elect to cease development at that point. Provisions of this Agreement, which, by their express terms or by necessary implication ,apply for periods of time other than specified herein, shall be given effect, notwithstanding this Article.

3. Attachment 3, Schedule of Payments and Payable Milestones, is revised to delete Month 24 and insert Month 27 as the required delivery date for the ninth payable milestone period.

4. The total Agreement amount remains unchanged. All provisions, terms, and conditions set forth in this Agreement are applicable and in full force and effect except as specified otherwise herein.

FOR THE BLUE BAND CONSORTIUM
SDL, INC.

John P. Melton 5/23/97
(Date)
John P. Melton
Vice President, Business Operations

FOR THE UNITED STATES OF AMERICA
DCMC SAN DIEGO, San Diego, CA

5/23/97
Joan R. Carter (Date)
Administrative Grants Officer
Agreements Administrator

AMENDMENT 0002 TO THE TECHNOLOGY DEVELOPMENT AGREEMENT

Between

BLUE LIGHT AND UV EMITTERS - THE BAY AREA NITRIDE DEVELOPMENT (BLUE BAND) CONSORTIUM

And

THE DEFENSE ADVANCED RESEARCH PROJECTS AGENCY
3701 North Fairfax Drive
Arlington, VA 22203-1714

CONCERNING

DEVELOPMENT OF HIGH BANDGAP III-V MATERIALS AND OPTICAL DEVICES

Agreement No.: MDA972-95-3-0008
Amendment No.: 0002
ARPA Order No.: N/A

Total Amount of the Agreement:	$	8,364,000
Total Estimated Government Funding of the Agreement:	$	4,136,000
Total Estimated Consortium Cost Share:	$	4,228,000
Funds Obligated by this Action:	$	0
Total Government Funds Obligated:	$	4,136,000

Authority: 10 U.S.C. § 2371

This modification is for administrative purposes only. The Agreement administration is hereby revised to incorporate and add to Article IV and Attachment 5 the following Agreement Administration Office and the Agreements Administrator:

DCMC San Diego
DCMDW/GSTB(Ms. J. Carter)
7675 Dagget Street, Suite 200
San Diego, CA 92111-2241

Phone: (619)495-7462
FAX: (619) 495-7626
DSC 972
Email:jcarter@sndao.dcmdw.dla.mil

Ms. Jean R. Carter is hereby delegated the responsibility to represent the Government as an Agreements Administrator for the following Articles:

ARTICLE	TITLE
ARTICLE II	Term
ARTICLE III	Management of the Project
ARTICLE IV	Agreement Administration
ARTICLE V	Obligation and Payment
ARTICLE VI	Disputes
ARTICLE VII	Patent Rights
ARTICLE VIII	Data Rights

Others areas delegated to Ms. Jean R. Carter are as follows:

(a) Milestone payment approvals
(b) Tracking of total expenditures under the Agreement
(c) Processing of reports
(d) Participate in program reviews and/or other equivalent meetings
(e) Monitor cost share
(f) Property administration
(g) Attachments 2 through 4

Copies of business related documents referenced in the aforementioned are to be sent to Ms. Jean R. Carter.

The total Agreement amount remains unchanged. All provisions, terms, and conditions set forth in this Agreement are applicable and in full force and effect except as specified otherwise herein.

FOR THE UNITED STATES OF AMERICA
THE DEFENSE ADVANCED RESEARCH PROJECTS AGENCY

BY: GRANT MAYBERRY — NOV 12 1996 (Date)
Agreements Officer
Contracts Management Office

AGREEMENT

BETWEEN

BLUELIGHT AND UV EMITTERS - THE BAY AREA NITRIDE DEVELOPMENT (BLUE BAND) CONSORTIUM
c/o SDL, INC.
80 ROSE ORCHARD WAY
SAN JOSE, CA 95134-1356

AND

ADVANCED RESEARCH PROJECTS AGENCY
3701 NORTH FAIRFAX DRIVE
ARLINGTON, VA 22203-1714

CONCERNING

DEVELOPMENT OF HIGH BANDGAP III-V MATERIALS AND OPTICAL DEVICES

Agreement No.: MDA972-95-3-0008
Modification No.: 0001
ARPA Order No.: N/A
Effective Date: October 25, 1995
Authority: 10 U.S.C. § 2371

This Agreement is administratively modified to change the Agreements Administrator as follows:

1. In Article IV, AGREEMENT ADMINISTRATION, the ARPA Agreements Administrator is revised from:

<u>ARPA:</u> Elaine Ely - Agreements Administrator
ARPA / CMO (703) 696-2411

to:

<u>ARPA:</u> Grant E. Mayberry - Agreements Administrator
ARPA / CMO (703) 696-2438

2. In Attachment 5, List of Government and Consortium Representatives, revise the second listed government representative from:

<u>Elaine Ely, Agreement Administrator</u>
ARPA / CMO
3701 N. Fairfax Drive
Arlington, VA 22203-1714
phone: (703) 696-2411
FAX: (703) 696-2208
Email: eely@arpa.mil

to:

Grant E. Mayberry, Agreement Administrator
ARPA / CMO
3701 N. Fairfax Drive
Arlington, VA 22203-1714
phone: (703) 696-2438
FAX: (703) 696-2208
Email: gmayberry@arpa.mil

All provisions, terms, and conditions set forth in this Agreement are applicable and in full force and effect except as specified otherwise herein.

FOR THE UNITED STATES OF AMERICA
THE ADVANCED RESEARCH PROJECTS AGENCY

By:
SCOTT R. ULREY
Agreements Administrator
Contracts Management Office

10/25/95
(Date)

ORIGINAL

AGREEMENT

BETWEEN

BLUE LIGHT AND UV EMITTERS - THE BAY AREA NITRIDE DEVELOPMENT (BLUE BAND) CONSORTIUM

AND

THE ADVANCED RESEARCH PROJECTS AGENCY
3701 NORTH FAIRFAX DRIVE
ARLINGTON, VA 22203-1714

CONCERNING

DEVELOPMENT OF HIGH BANDGAP III-V MATERIALS AND OPTICAL DEVICES

Agreement No.: MDA972-95-3-0008
ARPA Order No.: C197
Total Amount of the Agreement: $ 8,364,000
Total Estimated Government Funding of the Agreement: $4,136,000
Funds Obligated: $ 4,136,000
Authority: 10 U.S.C. 2371
Line of Appropriation: AA 9740400 1320 C197 P4V10 2525 DPAC 4 5018 503733 $4,136,000.00

This Agreement is entered into between the United States of America, hereinafter called the Government, represented by The Advanced Research Projects Agency (ARPA), and the Blue Band Consortium (CONSORTIUM) pursuant to and under U.S. Federal law.

FOR THE BLUE BAND CONSORTIUM

John P. Melton 4/28/95
(Signature) (Date)
SDL, INC.

John P. Melton
~~Vice President, Business Operat~~ions
(Typed Name and Title)

FOR THE UNITED STATES OF AMERICA
ADVANCED RESEARCH PROJECTS AGENCY

[signature]
RON H. REGISTER
DEPUTY DIRECTOR FOR MANAGEMENT

5/26/95
EFFECTIVE DATE

TABLE OF CONTENTS

ARTICLES		PAGE
ARTICLE I	Scope of the Agreement	03
ARTICLE II	Term	05
ARTICLE III	Management of the Project	06
ARTICLE IV	Agreement Administration	08
ARTICLE V	Obligation and Payment	09
ARTICLE VI	Disputes	10
ARTICLE VII	Patent Rights	11
ARTICLE VIII	Data Rights	15
ARTICLE IX	Foreign Access to Technology	16
ARTICLE X	Officials Not to Benefit	17
ARTICLE XI	Civil Rights Act	17
ARTICLE XII	Order of Precedence	18
ARTICLE XIII	Execution	18

ATTACHMENTS

ATTACHMENT 1	Blue Band Consortium Statement of Work
ATTACHMENT 2	Report Requirements
ATTACHMENT 3	Schedule of Payments and Payable Milestones
ATTACHMENT 4	Funding Profile
ATTACHMENT 5	List of Government and Consortium Representatives

ARTICLE I: SCOPE OF THE AGREEMENT

A. Background and Vision Statement

Industry leaders and universities have formed a fully vertically integrated Consortium to collaboratively develop advanced technology leading to the demonstration and volume manufacturing of laser diodes and light emitting diodes (LED) operating in the blue and green regions of the spectrum. The visible emitter technology will enable a broad range of military applications including high-density optical storage systems, lightweight countermeasures, cockpit displays, solar-blind communication, submarine communication and combat protection systems. Commercial applications include high density optical data storage systems, full color displays, and high resolution printers. In addition, the material developments of the ARPA program will lead to substantial advances in high-power and high-temperature electronic components.

The Blue Band Consortium was formed in conjunction with ARPA to create a forum that would not otherwise exist to address the technological issues of blue/green emitters in a two year program that will result in dramatic acceleration of the time to market for both components and systems. The key to any program intended to leverage both military and commercial markets is the development of technology in organizations that have demonstrated sustained manufacturing capabilities. The strategy in the formation of the Blue Band Consortium is to draw from industry leaders in both technology and manufacturing, maintain a common technology focus while having vertically integrated team members covering issues from substrate growth through high volume components manufacturing and system integration. This Consortium represents a unique coupling of the technical and market leaders in visible emitter technology, thus insuring a successful demonstration and commercialization of visible semiconductor devices.

The core members of the Consortium consist of Hewlett Packard (HP), the world's largest manufacturer of high brightness visible LEDs; SDL - the largest U.S. manufacturer of commercial and consumer laser diodes; and Xerox, the leading manufacturer of document equipment in the United States. HP and SDL will be responsible for the epitaxial growth of the Gallium Nitride (GaN) and related films, while Xerox will utilize its expertise in materials characterization to assist Hewlett Packard and SDL in the characterization of epitaxial grown crystals. In addition to the core members, the Consortium consists of two substrate manufacturers, American Crystal Technologies and ATMI, both of whom have demonstrated high quality substrate growth. The two participating universities, The University of Texas and Boston University, have demonstrated some of the highest quality GaN films fabricated to date. The four associate members will concentrate on the development of advanced substrate and epitaxial growth technologies, in particular the university efforts are to concentrate on high risk, long range technology. Device fabrication will be performed at HP and SDL where LEDs and laser diodes will be fabricated, respectively.

The technical approach is focused on materials growth techniques, substrate technologies, materials characterization, device fabrication and prototype demonstration. The final demonstration of the Consortium will be manufacturable LEDs and laser diodes (LDs) operating in the blue and green regions of the spectrum. Consortium members are highly committed to the commercialization of the technology and will perform the device development within their existing manufacturing facilities for ease of transfer to already existing high volume production lines. It is the intent of the Consortium, within two years following the completion of this Agreement, to produce high-volume components to satisfy existing and emerging military and commercial applications and to integrate these enabling components into consumer products produced both by members of the Blue Band Consortium and other manufacturing firms.

B. Definitions

1. "Consortium" is a group of independent entities, specified in Article IV herein, which have chosen to be bound together under a set of Articles of Collaboration for the purpose of performing the tasks set forth herein.

2. "Articles of Collaboration" (hereinafter "Articles") are the agreed upon rules and procedures which

govern the activities and relationships of the Consortium and the Consortium Members.

3. "Consortium Executive Committee" (hereinafter "CEC") is the technical and financial management body of the Consortium, as defined in the Articles.

4. "Consortium Member" - Each of the participating entities, once having executed the Articles, is a member of the Consortium and therefore a participant to this Agreement.

5. "Party" - For purposes of this Agreement, there are only two Parties: ARPA (The Government) and the Consortium (comprised of all Consortium Members).

6. "Technical Program Manager" (hereinafter "Program Manager") is the Government's technical representative from ARPA charged with overall responsibility for review and verification of completion of Payable Milestones and the Statement of Work, including amendments or modification thereto, as set forth herein.

7. "Consortium Technical Coordinator" (hereinafter "Technical Coordinator"] is the authorized technical agent of the Consortium charged with maintaining a technical / administration point-of-contact function with responsibilities including receipt and distribution of all communications between ARPA and the Consortium, monitoring of technical program progress toward payable milestones, and facilitation of overall program technical and reporting requirements on behalf of the Consortium. acting as the principal technical point of contact.

8. "Consortium Administrator" is the authorized agent of the Consortium charged with maintaining the program financial management function including receipt and distribution of program funds, monitoring of financial program progress toward payable milestones, and facilitating overall program financial and reporting requirements on behalf of the Consortium.

9. "Agreement Administrator" is the Government's principal point of contact for all administrative, financial or other non-technical issues arising under the Agreement.

10. "Intellectual Property" means any inventions, creations, improvements, technical data, mask works, works of authorship or other developments, including software, and improvements thereto, whether patentable, copyrightable or not, conceived and developed during the term of this Agreement with joint (i.e., Consortium and Federal) funding. "Intellectual Property Rights" means any Rights in Intellectual Property including patents, copyrights, technical data, mask works, trade secrets and confidential information.

C. Scope

1. The Consortium shall perform a coordinated research and development program (Program) designed to develop High-Bandgap III-V Materials and Optical Devices. The research shall be carried out in accordance with the Statement of Work incorporated in this Agreement as Attachment 1. The Consortium shall submit or otherwise provide all documentation required by Attachment 2, Report Requirements.

2. The Consortium shall be paid for each Payable Milestone accomplished in accordance with the Schedule of Payments and Payable Milestones set forth in Attachment 3 and the procedures of Article V. Both the Schedule of Payments and the Funding Schedule set forth in Attachments 3 and 4 respectively may be revised or updated in accordance with Article III.

3. The Government and the Consortium (Parties) estimate that the Statement of Work of this Agreement can only be accomplished with the Consortium aggregate resource contribution as set forth in Attachments 3 and 4 of this Agreement to be provided from the effective date of this Agreement through twenty-four (24) months thereafter, including, if applicable, any ARPA approved pre-Agreement costs. The Consortium intends and, by entering into this Agreement, undertakes to cause to be provided these funds. As a condition of this Agreement, it is herein understood and agreed that Federal funds and funds identified as Consortium contributions are

to be used only for costs that: (i) a reasonable and prudent person would incur in carrying out the advanced research project herein; and (ii) are consistent with the purposes stated in the governing Congressional authorizations and appropriations. Consortium contributions will be provided as detailed in the Funding Schedule set forth in Attachment 4. If either ARPA or the Consortium is unable to provide its respective total contribution, the other party may reduce its project funding by a proportional amount.

D. Goals/Objectives

1. The overall goal of this Consortium is the rapid development and demonstration of optoelectronic components operating in the green, blue and ultraviolet portion of the optical spectrum. To realize this goal, the technical objectives will focus on three major efforts:

- a highly integrated development of core materials growth technologies;
- identification and development of key substrate technologies;
- prototype demonstration of the integrated growth and materials characterization efforts in Light Emitting Diodes and Laser Diodes.

2. The Government will have continuous involvement with the Consortium. The Government will also obtain access to research results and certain rights in data and patents pursuant to Articles VII and VIII. ARPA and the Consortium are bound to each other by a duty of good faith and reasonable research effort in achieving the goals of the Consortium. This Agreement reflects the collaborative document identified as "Articles of Collaboration for Blue Band," which document binds Consortium participants.

3. This Agreement is an "other transaction" pursuant to 10 U.S.C. 2371. The Parties agree that the principal purpose of this Agreement is for the Government to support and stimulate the Consortium to provide its reasonable efforts in advanced research and technology development and not for the acquisition of property or services for the direct benefit or use of the Government. The Federal Acquisition Regulation (FAR) and Department of Defense FAR Supplement (DFARS) apply only as specifically referenced herein. This Agreement is not a procurement contract or grant agreement for purposes of FAR Subpart 31.205-18. This Agreement is not intended to be, nor shall it be construed as, by implication or otherwise, a partnership, a corporation, or other business organization.

ARTICLE II: TERM

A. The Term of this Agreement

The Program commences upon the date of the last signature hereon and continues for twenty-four (24) months. If all funds are expended prior to the 24-month duration, the Parties have no obligation to continue performance and may elect to cease development at that point. Provisions of this Agreement, which, by their express terms or by necessary implication, apply for periods of time other than specified herein, shall be given effect, notwithstanding this Article.

B. Termination Provisions

Subject to a reasonable determination that the project will not produce beneficial results commensurate with the expenditure of resources, or as a result of recognition that technical objectives and market conditions cannot be realized, either Party may terminate this Agreement by written notice to the other Party, provided that such written notice is preceded by consultation between the Parties. In the event of a termination of the Agreement, it is agreed that disposition of Data developed under this Agreement, shall be in accordance with the provisions set forth in Article VIII, Section B. The Government, acting through the Agreement Administrator, and the Consortium, acting through its Consortium Administrator, will negotiate in good faith a reasonable and timely adjustment of all

outstanding issues between the Parties at the time of termination. Failure of the Parties to agree to a reasonable adjustment will be resolved pursuant to Article VI. The Government has no obligation to reimburse the Consortium beyond the last completed and paid milestone if the Consortium, acting through its Consortium Executive Committee, decides to terminate.

C. Extending the Term

The Parties may extend by mutual written agreement the term of this Agreement if funding availability and research opportunities reasonably warrant. Any extension shall be formalized through modification of the Agreement by the Agreements Administrator and the Consortium Administrator.

ARTICLE III: MANAGEMENT OF THE PROJECT

A. Consortium Members

The Members of the Consortium shall be those identified in the Articles of Collaboration. Changes to the membership of the Consortium require the approval of ARPA as described below. Consortium Members, as set forth in the Articles of Collaboration of the Consortium, are either Principal or Associate Members, as follows:

Principal Members:	HEWLETT-PACKARD	San Jose, CA
	SDL	San Jose, CA
	XEROX	Palo Alto, CA
Associate Members:	AXT	Dublin, CA
	ATMI	Danbury, CT
	The University of Texas at Austin	Austin, TX
	Boston University	Boston, MA

B. Consortium Executive Committee (CEC)

1. There shall be a Consortium Executive Committee ("CEC") comprised of representatives of the Principal Members, constituted in accordance with the Articles of Collaboration. The CEC shall have the authority to bind the Consortium Members by the mechanisms set forth in the Articles of Collaboration.

The following CEC decisions are subject to ARPA approval (which shall not be unreasonably withheld):

(a) Changes to the Articles of Collaboration if such changes substantially alter the relationship between the Parties as originally agreed upon when the Agreement was executed;

(b) Changes to the Articles of Collaboration if such changes substantially alter the relationship among the Consortium Members in effect when the Agreement was executed;

(c) Changes to, or elimination of, any ARPA funding allocation to any Consortium Member for technical or financial reasons;

(d) Revisions to the Statement of Work or the Funding Schedule of this Agreement; and

(e) Admission, removal or replacement of Consortium Members, excluding the down-select process identified in the Statement of Work.

2. The CEC shall establish a schedule of quarterly technical meetings. The CEC shall notify all Consortium Members and the ARPA Program Manager of the established meeting schedule and, in the event of changes to this schedule, shall notify all Consortium Members and the ARPA Program Manager thirty (30) calendar days prior to the next scheduled meeting. Meetings of the CEC, other than quarterly technical meetings, may be called at any time upon at least fifteen (15) calendar days' notice by the written request of any Consortium Member representative on the CEC to the CEC chair.

3. Subject to procedural requirements as set forth in the Articles, decisions of the CEC shall be reached by consensus or mutual agreement.

C. Management and Program Structure

1. Technical and program management of the coordinated research program established under this Agreement shall be accomplished through the management structures and processes described in this Article and the Articles of Collaboration.

(a) Subject to the terms and conditions of this Agreement and of the Articles of Collaboration of the Consoritum, the CEC shall be responsible for the overall management of the Consortium including technical, programmatic, reporting, financial and administrative matters.

(b) The ARPA Program Manager shall be a non-voting member of the CEC, but shall otherwise fully participate in regular technical meetings of the CEC. Other Government personnel as deemed appropriate by the ARPA Program Manager may also participate in the technical portion of these meetings.

(c) A Program Board, consisting of one senior level management person appointed by each Principal Member and one person appointed by ARPA will be established to oversee the research program. The Program Board function and membership shall be as set forth in the Articles of Collaboration.

2. The ARPA Program Manager shall be responsible for the review and verification of the completion of each Payable Milestone, and shall have continuous interaction to cause effective collaboration between ARPA and the Consortium.

D. Program Management Planning Process

The program management and planning process shall be subject to quarterly and annual reviews with inputs and review from the CEC and the ARPA Program Manager.

1. Initial Program Plan: The Consortium will follow the initial program plan that is contained in the Statement of Work (Attachment 1), and the Schedule of Payments and Payable Milestones (Attachment 3).

2. Overall Program Plan Annual Review

(a) The CEC, with ARPA Program Manager participation and review, will prepare an overall Annual Program Plan in the first quarter of each Agreement year. (For this purpose, each consecutive twelve (12) month period from (and including) the month of execution of this Agreement during which this Agreement shall remain in effect shall be considered an "Agreement Year.") The Annual Program Plan will be presented and reviewed at an annual site review concurrent with the appropriate quarterly meeting of the CEC which will be attended by the Consortium Members, the ARPA Program Manager, Senior ARPA management or other ARPA program managers and personnel as appropriate. The CEC, with ARPA participation and review, will prepare a final Annual Program Plan.

(b) The Annual Program Plan provides a detailed schedule of research activities, commits the Consortium to use reasonable research efforts to meet specific performance objectives, includes forecasted

expenditure and describes the Payable Milestones. The Annual Program Plan will consolidate all prior adjustments in the research schedule, including revisions/modifications to payable milestones. Recommendations for changes, revisions or modifications to the Agreement which result from the Annual Review shall be made in accordance with the provisions of Article III, Section E.

E. Amendments / Modifications

1. As a result of quarterly meetings, annual reviews, or at any time during the term of the Agreement, research progress or results may indicate that a change in the Statement of Work or Schedule of Payments and Payable Milestones (Attachment 3) would be beneficial to program objectives. Recommendations for modifications, including justifications to support the recommended changes to the Statement of Work or Schedule of Payments and Payable Milestones, will be documented and submitted in writing by the CEC to the ARPA Program Manager for review and approval, with a copy to the ARPA Agreements Administrator. This submission will detail the technical, schedule, and financial impacts of each proposed modification. The Government is not obligated to pay for additional or revised Payable Milestones until the CEC-recommended changes are approved by the ARPA Program Manager and the Schedule of Payments and Payable Milestones is formally revised by the ARPA Agreements Administrator and made part of this Agreement.

2. The ARPA Program Manager shall be responsible for the review and approval of any CEC recommendations to revise or otherwise modify this Agreement's Statement of Work or Schedule of Payments and Payable Milestones or other proposed changes to the terms and conditions of this Agreement.

3. For minor or administrative Agreement modifications such as changes in the paying office or appropriation data, or changes to Government personnel identified in this Agreement, no signature is required by the Consortium. For administrative changes initiated by the CEC, such as changes in Consortium personnel identified in this Agreement and address or phone number changes, the CEC may authorize the Consortium Administrator to act as agent in signing such minor Administrative amendments or modifications.

ARTICLE IV. AGREEMENT ADMINISTRATION

Unless otherwise provided in this Agreement, approvals permitted or required to be made by ARPA may be made only by the ARPA Agreements Administrator. Administrative and contractual matters under this Agreement shall be referred to the following representatives of the parties:

<u>ARPA</u>: Elaine Ely - Agreements Administrator
ARPA / CMO (703) 696-2411

<u>CONSORTIUM</u>: Janelle Johnson - Consortium Administrator
SDL (408) 943-9411, ext. 232

Technical matters under this Agreement shall be referred to the following representatives:

<u>ARPA</u>: Anis Husain - Program Manager
ARPA / MTO (703) 696-2236

<u>CONSORTIUM</u>: David Welch - Technical Coordinator
SDL (408) 943-9411

Jo Major - Principal Investigator
SDL (408) 943-9411

Each party may change its representatives named in this Article by written notification to the other party.

ARTICLE V: OBLIGATION AND PAYMENT

A. Obligation

1. The Government's liability to make payments to the Consortium is limited to only those funds obligated under this Agreement or by amendment to the Agreement. ARPA may incrementally fund this Agreement.

2. If modification becomes necessary in performance of this Agreement, pursuant to Article III, paragraph E, the ARPA Agreements Administrator and Consortium Administrator shall negotiate and execute a revised Schedule of Payable Milestones consistent with the then current Program Plan.

3. Obligation levels are subject to change only by written amendment or modification to the Agreement in accordance with Article III.E.

B. Payments

1. In addition to any other financial reports provided or required, the CEC shall notify the ARPA Agreements Administrator immediately if any contribution from a Consortium Member is not made as required.

2. Prior to the submission of invoices to ARPA by the Consortium Administrator, the Consortium shall have and maintain an established accounting system which complies with Generally Accepted Accounting Principles, and with the requirements of this Agreement, and shall ensure that appropriate arrangements have been made for receiving, distributing and accounting for Federal funds. The Parties recognize that as a conduit, the Consortium does not incur nor does it allocate any indirect costs of its own to the Consortium Member cost directly incurred pursuant to this Agreement. Consistent with this, an acceptable accounting system will be one in which all cash receipts, disbursements, and engineering hours are controlled and documented properly in accordance with each Consortium Members' normal business practice.

3. The CEC shall document the accomplishments of each Payable Milestone by submitting or otherwise providing the Payable Milestones Report required by Attachment 2, Part D. The Consortium shall submit an original and five (5) copies of all invoices to the Agreements Administrator for payment approval. After written verification of the accomplishment of the Payable Milestone by the ARPA Program Manager, and approval by the Agreements Administrator, the invoices will be forwarded to the payment office within thirty (10) calendar days of receipt of the invoices at ARPA. Payments will be made by AFDW/FW, Attn: Commercial Services, 170 Luke Avenue, Suite 280, Bolling Air Force Base, Washington, DC 20332-5113 within twenty (20) calendar days of ARPA's transmittal. Subject to change only through written Agreement modification, payment shall be made to the address of the Consortium Administrator set forth below.

4. Address of Payee:

BLUE BAND CONSORTIUM
Attn: Janelle Johnson, Consortium Administrator
SDL, Inc.
80 Rose Orchard Way
San Jose, CA 95134-1356

Payment shall be made by domestic electronic wire transfer**

To:	**SIL VLY BK SJ**
Route & Transit:	**121140399**
For Credit of:	**SDL, Inc.**
Credit Account:	**03516628-70**
By Order of:	**(name of sender)**

**** Each Payment Must Be Marked With Invoice Number**

5. Payments shall be made no more frequently than quarterly in the amounts set forth in the Attachment No. 3 (B) "Detailed Schedule of Payable Milestones," provided the ARPA Program Manager has verified the accomplishment of the Payable Milestones. It is recognized that the quarterly accounting of current expenditures reported in the "Quarterly Business Status Report" submitted in accordance with Attachment No. 2 is not necessarily intended or required to match the Payable Milestones until submission of the Final Report; however, payable milestones shall be revised during the course of the program to reflect current and revised projected expenditures.

6. Limitation of Funds: In no case shall the Government's financial liability exceed the amount obligated under this Agreement.

7. Financial Records and Reports: The Consortium and Consortium Members shall maintain adequate records to account for Federal funds received under this Agreement and shall maintain adequate records to account for Consortium Participant funding provided under this Agreement. Upon completion or termination of this Agreement, whichever occurs earlier, the Consortium Administrator shall furnish to the Agreements Administrator a copy of the final report required by Attachment 2, Part E. The Consortium's and Consortium Members' relevant financial records are subject to examination or audit on behalf of ARPA by the Government for a period not to exceed three (3) years after expiration of the term of this Agreement. Such audits or examination may be conducted by independent certified public accounting or auditing firms designated by the Consortium Members with complete reports made available to the Government upon request. The cost of any independent audit shall be paid by the Consortium Member. The Agreements Administrator or designee shall have direct access for a period of three (3) years after completion of this Agreement to sufficient records and information of the Consortium and Consortium Members, to ensure full accountability for all funding under this Agreement. Such Government audit, examination, or access shall be performed during business hours on business days upon prior written notice to the Consortium Member and shall be subject to the security requirements of the audited party. This Agreement shall not be construed as requiring the Consortium Members to establish systems extending beyond their current systems to account for costs in accordance with generally accepted accounting principles.

ARTICLE VI: DISPUTES

A. General

Parties shall communicate with one another in good faith and in a timely and cooperative manner when raising issues under this Article.

B. Dispute Resolution Procedures

1. Any disagreement, claim or dispute between ARPA and the Consortium concerning questions of fact or law arising from or in connection with this Agreement, and, whether or not involving an alleged breach of this Agreement, may be raised only under this Article.

2. Whenever disputes, disagreements, or misunderstandings arise, the Parties shall attempt to resolve the issue(s) involved by discussion and mutual agreement as soon as practicable. In no event shall a dispute, disagreement or misunderstanding which arose more than three (3) months prior to the notification made under subparagraph B.3 of this article constitute the basis for relief under this article unless the Director of ARPA in the interests of justice waives this requirement.

3. Failing resolution by mutual agreement, the aggrieved Party shall document the dispute, disagreement, or misunderstanding by notifying the other Party (through the ARPA Agreements Administrator or Consortium Administrator, as the case may be) in writing of the relevant facts, identify unresolved issues, and specify the clarification or remedy sought. Within five (5) working days after providing notice to the other Party, the aggrieved Party may, in writing, request a joint decision by the ARPA Deputy Director for Management and Representative of the CEC of the Consortium ("Consortium Representative"). The other Party shall submit a written position on the matter(s) in dispute within thirty (30) calendar days after being notified that a decision has

been requested. The Deputy Director for Management and the Consortium Representative shall conduct a review of the matter(s) in dispute and render a decision in writing within thirty (30) calendar days of receipt of such written position. Any such joint decision is final and binding unless a Party shall within thirty (30) calendar days request further review as provided in this Article.

4. Upon written request to the Director of ARPA, made within thirty (30) calendar days of a joint decision, or upon unavailability of a joint decision under subparagraph B.3 above, the dispute shall be further reviewed. The Director of ARPA may elect to conduct this review personally or through a designee or jointly with a representative of the other Party who is a senior official of the Party. Following the review, the Director of ARPA or designee will resolve the issue(s) and notify the Parties in writing. Such resolution is not subject to further administrative review and, to the extent permitted by law, shall be final and binding.

5. Subject only to this article and 41 U.S.C. 321-322, if not satisfied with the results of completing the above process, either Party may within thirty (30) calendar days of receipt of the joint decision notice in subparagraph B.3 above pursue any right and remedy in a court of competent jurisdiction.

C. Limitation of Damages

Claims for damages of any nature whatsoever pursued under this Agreement shall be limited to direct damages only up to the aggregate amount of ARPA funding disbursed as of the time the dispute arises. In no event shall ARPA be liable for claims for consequential, punitive, special and incidental damages, claims for lost profits, or other indirect damages. ARPA agrees that there is no joint and several liability within the Consortium. The Consortium disclaims any liability for consequential, indirect, or special damages, except when such damages are caused by willful misconduct of the Consortium Managerial personnel. In no event shall the liability of a Consortium Member or any other entity performing research activities under this Agreement exceed the funding it has received up to the time of incurring such liability.

ARTICLE VII: PATENT RIGHTS

A. Definitions

1. "Invention" means any invention or discovery which is or may be patentable or otherwise protectable under Title 35 of the United States Code.

2. "Made" when used in relation to any invention means the conception or first actual reduction to practice of such invention.

3. "Practical application" means to manufacture, in the case of a composition of product; to practice, in the case of a process or method, or to operate, in the case of a machine or system; and, in each case, under such conditions as to establish that the invention is capable of being utilized and that its benefits are, to the extent permitted by law or Government regulations, available to the public on reasonable terms.

4. "Subject invention" means any invention of a Consortium Member conceived or first actually reduced to practice in the performance of work under this Agreement.

5. "Consortium" as used in this Article means individual Consortium Member.

B. Allocation of Principal Rights

Unless the Consortium shall have notified ARPA (in accordance with subparagraph C.2 below) that the Consortium does not intend to retain title, the Consortium shall retain the entire right, title, and interest throughout the world to each subject invention consistent with the provisions of the Articles of Collaboration, this Article, and 35 U.S.C. 202. With respect to any subject invention in which the Consortium retains title, ARPA shall have a non-exclusive, nontransferable, irrevocable, paid-up license to practice or have practiced on behalf of the United States the

subject invention throughout the world for Government military and research purposes only. Notwithstanding the above, the Consortium may elect as defined in its Articles of Collaboration to provide full or partial rights that it has retained to Consortium Participants or other parties.

C. Invention Disclosure, Election of Title, and Filing of Patent Application

1. The Consortium shall disclose each subject invention to ARPA within four (4) months after the inventor discloses it in writing to his company or university personnel responsible for patent matters. The disclosure to ARPA shall be in the form of a written report and shall identify the Agreement under which the invention was made and the identity of the inventor(s). It shall be sufficiently complete in technical detail to convey a clear understanding to the extent known at the time of the disclosure, of the nature, purpose, operation, and the physical, chemical, biological, or electrical characteristics of the invention. The disclosure shall also identify any publication, sale, or public use of the invention and whether a manuscript describing the invention has been submitted for publication and, if so, whether it has been accepted for publication at the time of disclosure.

2. If the Consortium determines that it does not intend to retain title to any such invention, the Consortium shall notify ARPA, in writing, within twenty-four (24) months of disclosure to ARPA. However, in any case where publication, sale, or public use has initiated the one (1)-year statutory period wherein valid patent protection can still be obtained in the United States, the period for such notice may be shortened by ARPA through written notice to the CEC to a date that is no more than sixty (60) calendar days prior to the end of the statutory period.

3. The Consortium shall file its initial patent application on a subject invention to which it elects to retain title within one (1) year after election of title or, if earlier, prior to the end of the statutory period wherein valid patent protection can be obtained in the United States after a publication, or sale, or public use. The Consortium may elect to file patent applications in additional countries (including the European Patent Office and the Patent Cooperation Treaty) within either ten (10) months of the corresponding initial patent application or six (6) months from the date permission is granted by the Commissioner of Patents and Trademarks to file foreign patent applications, where such filing has been prohibited by a Secrecy Order.

4. Requests for extension of time for disclosure election, and filing under Article VII subparagraph C, may be granted by the Government. Requests for extension are to be forwarded to the ARPA Agreement Administrator. If the request for extension is consistent with the intent of the Agreement and based on a sound business rationale, the approval of the Government for a reasonable time extension shall not be withheld.

D. Conditions When the Government May Obtain Title

Upon ARPA's written request, the Consortium shall convey title to any subject invention to ARPA under any of the following conditions:

1. If the Consortium fails to disclose or elects not to retain title to the subject invention within the times specified in paragraph C of this Article; provided, that ARPA may only request title within sixty (60) calendar days after learning of the failure of the Consortium to disclose or elect within the specified times.

2. In those countries in which the Consortium fails to file patent applications within the times specified in paragraph C of this Article; provided, that if the Consortium has filed a patent application in a country after the times specified in paragraph C of this Article, but prior to its receipt of the written request by ARPA, the Consortium shall continue to retain title in that country; or

3. In any country in which the Consortium decides not to continue the prosecution of any application for, to pay the maintenance fees on, or defend in reexamination or opposition proceedings on, a patent on a subject invention.

E. Minimum Rights to the Consortium and Protection of the Consortium's Right to File

1. The Consortium shall retain a non-exclusive, royalty-free license throughout the world in each subject invention to which the Government obtains title, except if the Consortium fails to disclose the invention within the times specified in paragraph C of this Article. The Consortium license extends to the domestic (including Canada) subsidiaries and affiliates, if any, of the Consortium Participants within the corporate structure of which the Consortium Participant is a party and includes the right to grant licenses of the same or lessor scope to the extent that the Consortium was legally obligated to do so at the time the Agreement was awarded. The license is transferable only within the approval of ARPA, except when transferred to the successor of that part of the business to which the invention pertains. ARPA approval for license transfer shall not be unreasonably withheld.

2. The Consortium domestic license may be revoked or modified by ARPA to the extent necessary to achieve expeditious practical application of subject invention pursuant to an application for an exclusive license submitted consistent with appropriate provisions at 37 CFR Part 404, provided that such revocation or modification shall not take place less than (5) years after the end of the term of the Agreement. This license shall not be revoked in that field of use or the geographical areas in which the Consortium has achieved practical application and continues to make the benefits of the invention reasonably accessible to the public. The license in any foreign country may be revoked or modified at the discretion of ARPA to the extent the Consortium, its licensees, or the subsidiaries or affiliates have failed to achieve practical application in that foreign country.

3. Before revocation or modification of the license, ARPA shall furnish the Consortium a written notice of its intention to revoke or modify the license, and the Consortium shall be allowed thirty (30) calendar days (or such other time as may be authorized for good cause shown) after the notice to show cause why the license should not be revoked or modified.

F. Action to Protect the Government's Interest

1. The Consortium agrees to execute or to have executed and promptly deliver to ARPA all instruments necessary to (i) establish or confirm the rights the Government has throughout the world in those subject inventions to which the Consortium elects to retain title, and (ii) convey title to ARPA when requested under paragraph D of this Article and to enable the Government to obtain patent protection throughout the world in that subject invention.

2. The Consortium agrees to require that employees of the Participants of the Consortium working on the Consortium, other than clerical and nontechnical employees, agree to disclose promptly in writing, to personnel identified as responsible for the administration of patent matters and in a format acceptable to the Consortium, each subject invention made under this Agreement in order that the Consortium can comply with the disclosure provisions of paragraph C of this Article. The Consortium may follow standard company or university policies with respect to employee disclosure of Subject Inventions.

3. The Consortium shall notify ARPA of any decisions not to continue the prosecution of a patent application, pay maintenance fees, or defend in a reexamination or opposition proceedings on a patent, in any country, not less than thirty (30) calendar days before the expiration of the response period required by the relevant patent office.

4. The Consortium shall include, within the specification of any United States patent application and any patent issuing thereon covering a subject invention, the following statement: "This invention was made with Government support under Agreement No. MDA972-95-3-0008 awarded by ARPA. The Government has certain rights in the invention."

G. Lower Tier Agreements

1. The Consortium shall include this Article, suitably modified, to identify the Parties, in all

subcontracts or lower tier agreements, regardless of tier, for experimental, developmental, or research work.

2. In the case of a lower tier agreement with a vendor, at any tier, ARPA, the vendor, and the Consortium agree that the mutual obligations of the parties created by this Article flow down to the vendor and constitute an agreement between the vendor and ARPA with respect to the matters covered by this Article.

H. Reporting on Utilization of Subject Inventions

The Consortium agrees to submit, during the term of the Agreement, periodic reports no more frequently than annually on the utilization of a subject invention or on efforts at obtaining such utilization of a subject invention or on efforts at obtaining such utilization that are being made by the Consortium or licensees or assignees of the inventor. Such reports shall include information regarding the status of development, date of first commercial sale or use, gross royalties received by the Consortium subcontractor(s), and such other data and information as the agency may reasonably specify. The Consortium also agrees to provide additional reports as may be requested by ARPA in connection with any march-in proceedings undertaken by ARPA in accordance with paragraph J of this Article. Consistent with 35 U.S.C. 202(c)(5), ARPA agrees it shall not disclose such information to persons outside the Government without permission of the Consortium.

I. Preference for American Industry

Notwithstanding any other provision of this clause, the Consortium agrees that it shall not grant to any person the exclusive right to use or sell any subject invention in the United States or Canada unless such person agrees that any product embodying the subject invention or produced through the use of the subject invention shall be manufactured substantially in the United States or Canada. However, in individual cases, the requirements for such an agreement may be waived by ARPA upon a showing by the Consortium that reasonable but unsuccessful efforts have been made to grant licenses on similar terms to potential licensees that would be likely to manufacture substantially in the United States or that, under the circumstances, domestic manufacture is not commercially feasible.

J. March-in Rights

The Consortium agrees that, with respect to any Subject Invention in which it has retained title, ARPA has the right to require the Consortium, an assignee, or exclusive licensee of a subject invention to grant a non-exclusive license to a responsible applicant or applicants, upon terms that are reasonable under the circumstances, and if the Consortium, assignee, or exclusive licensee refuses to comply with such a requirement, ARPA has the right to grant such a license itself if ARPA determines that:

1. Such action is necessary because the Consortium or assignee has not taken within a reasonable time, or is not expected to take within a reasonable time, effective steps consistent with the intent of this Agreement, to achieve practical application of the Subject Invention;

2. Such action is necessary to alleviate health or safety needs which are not reasonably satisfied by the Consortium, assignee, or their licensees;

3. Such action is necessary to meet requirements for public use and such requirements are not reasonably satisfied by the Consortium, assignee, or their licensees; or

4. Such action is necessary because the agreement required by paragraph (I) of this Article has not been obtained or waived or because a licensee of the exclusive right to use or sell any Subject Invention in the United States is in breach of such Agreement.

ARTICLE VIII: DATA RIGHTS

A. Definitions

1. "Government Purpose Rights", as used in this article, means rights to use, duplicate, or disclose Data, in whole or in part and in any manner, for Government purposes only. Government purposes include military and research purposes, and use by Government research laboratories. Government purposes do not include the right to have or permit others to use, modify, reproduce, release, or disclose Data for commercial purposes, unless the Data has been delivered to the Government in accordance with the March-In process specified in subparagraph B.2 of this Article.

2. "Data", as used in this article, means recorded information, regardless of form or method of recording, which includes but is not limited to, technical data, software, trade secrets, and mask works, developed in performance of this Agreement. The term does not include financial, administrative, cost, pricing or management information and does not include subject inventions included under Article VIII.

B. Allocation of Principal Rights

1. This Agreement shall be performed with mixed Government and Consortium funding. The Parties agree that in consideration for Government funding, the Consortium intends to reduce to practical application items, components and processes developed under this Agreement.

2. The Consortium agrees to retain and maintain all Data in good condition until five (5) years after completion or termination of this Agreement. In the event of exercise of the Government's March-in Rights as set forth under Article VII, or subparagraph B.3 of this Article, the Consortium, acting through its Consortium Executive Committee, agrees, upon written request from the Government, to deliver, within sixty (60) days from the date of the written request, at no additional cost to the Government, all Data necessary to achieve practical application, consistent with the intent of this Agreement, of either a Subject Invention or a particular technology developed under this Agreement.

3. The Consortium agrees that, with respect to Data necessary to achieve practical application, consistent with the intent of this Agreement, of either a Subject Invention or a particular technology developed under this Agreement, ARPA has the right to require the Consortium Member(s) to grant a non-exclusive license to a responsible applicant or appliants, upon terms that are reasonable under the circumstances, and if the Consortium Member(s), assignee, or exclusive licensee refuses to comply with such a requirement, ARPA has the right to grant a non-exclusive, royalty-free, license itself if ARPA determines that:

(a) Such action is necessary because the Consortium Member(s), assignee, or licensee has not taken within a reasonable time, or is not expected to take within a reasonable time, effective steps consistent with the intent of this Agreement, to achieve practical application of a particular technology developed under this Agreement, or

(b) Such action is necessary to alleviate health or safety needs which are not reasonably satisfied by the Consortium Member(s), assignees, or licensees; or

(c) Such action is necessary to meet requirements for public use and such requirements are not reasonably satisified by the Consortium Member(s), assignees, or licensees.

4. With respect to Data delivered pursuant to Attachment 2, the Government shall have Government Purpose Rights, as defined in paragraph A above. With respect to data which has been developed solely with private funds, either prior to or outside the scope of this mixed-funding Agreement, the Government has no right, title or interest therein.

5. In the event this Agreement is terminated under the conditions set forth in Article II.B, the Consortium agrees to deliver all outstanding Data pursuant to Attachment 2, documenting all major developments and progress under the Agreement up to the time of termination. The Government shall have Government Purpose Rights to such Data, as defined in paragraph A above.

C. Marking of Data

Pursuant to paragraph B above, any Data delivered under this Agreement shall be marked with the following legend:

Use, duplication, or disclosure is subject to the restrictions as stated in Agreement MDA972-95-3-0008 between the Government and the Consortium.

D. Lower Tier Agreements

The Consortium shall include this Article, suitably modified to identify the Parties, in all subcontracts or lower tier agreements, regardless of tier, for experimental, developmental, or research work.

ARTICLE IX: FOREIGN ACCESS TO TECHNOLOGY

This Article shall remain in effect during the term of the Agreement and for three (3) years thereafter.

A. Definition

"Foreign Firm or Institution" means a firm or institution organized or existing under the laws of a country other than the United States, its territories, or possessions. The term includes, for purposes of this Agreement, any agency or instrumentality of a foreign government; and firms, institutions or business organizations which are owned or substantially controlled by foreign governments, firms, institutions, or individuals.

"Know-How" means all information including, but not limited to discoveries, formulas, materials, inventions, processess, ideas, approaches, concepts, techniques, methods, software, programs, documentation, procedures, firmware, hardware, technical data, specifications, devices, apparatus and machines.

"Technology" means discoveries, innovations, Know-How and inventions, whether patentable or not, including computer software, recognized under U.S. law as intellectual creations to which rights of ownership accrue, including, but not limited to, patents, trade secrets, maskworks, and copyrights developed under this Agreement.

B. General

The Parties agree that research findings and technology developments arising under this Agreement may constitute a significant enhancement to the national defense, and to the economic vitality of the United States. Accordingly, access to important technology developments under this Agreement by Foreign Firms or Institutions must be carefully controlled. The controls contemplated in this Article are in addition to, and are not intended to change or supersede, the provisions of the International Traffic in Arms Regulation (22 CFR pt. 121 et seq.), the DoD Industrial Security Regulation (DoD 5220.22-R) and the Department of Commerce Export Regulation (15 CFR pt. 770 et seq.)

C. Restrictions on Sale or Transfer of Technology to Foreign Firms or Institutions

1. In order to promote the national security interests of the United States and to effectuate the policies that underlie the regulations cited above, the procedures stated in subparagraphs C.2, C.3, and C.4 below shall apply to any transfer of Technology. For purposes of this paragraph, a transfer includes a sale of the company, and sales or licensing of Technology. Transfers do not include:

(a) sales of products or components, or
(b) licenses of software or documentation related to sales of products or components, or
(c) transfer to foreign subsidiaries of the Consortium participants for purposes related to this Agreement, or
(d) transfer which provides access to Technology to a Foreign Firm or Institution which is an approved source of supply or source for the conduct of research under this Agreement provided that such transfer shall be limited to that necessary to allow the firm or institution to perform its approved role under this Agreement.

2. The Consortium shall provide timely notice to ARPA of any proposed transfers from the Consortium of Technology developed under this Agreement to Foreign Firms or Institutions. If ARPA determines that the transfer may have adverse consequences to the national security interests of the United States, the Consortium, its vendors, and ARPA shall jointly endeavor to find alternatives to the proposed transfer which obviate or mitigate potential adverse consequences of the transfer but which provide substantially equivalent benefits to the Consortium.

3. In any event, the Consortium shall provide written notice to the ARPA Program Manager and Agreements Administrator of any proposed transfer to a foreign firm or institution at least sixty (60) calendar days prior to the proposed date of transfer. Such notice shall cite this Article and shall state specifically what is to be transferred and the general terms of the transfer. Within thirty (30) calendar days of receipt of the Consortium's written notification, the ARPA Agreements Administrator shall advise the Consortium whether it consents to the proposed transfer. In cases where ARPA does not concur or sixty (60) calendar days after receipt and ARPA provides no decision, the Consortium may utilize the procedures under Article VI, Disputes. No transfer shall take place until a decision is rendered.

4. Except as provided in subparagraph C.1 above and in the event the transfer of Technology to Foreign Firms or Institutions is approved by ARPA, the Consortium shall, prior to any transfer of Technology, negotiate a license with the Government to the Technology being transferred under terms that are reasonable under the circumstances.

D. Lower Tier Agreements

The Consortium shall include this Article, suitably modified, to identify the Parties, in all subcontracts or lower tier agreements, regardless of tier, for experimental, developmental, or research work.

ARTICLE X: OFFICIALS NOT TO BENEFIT

No member of Congress shall be admitted to any share or part of any contract or agreement made, entered into, or accepted by or on behalf of the United States, or to any benefit to arise thereupon.

ARTICLE XI: CIVIL RIGHTS ACT

This Agreement is subject to the compliance requirements of Title VI of the Civil Rights Act of 1964 as amended (42 U.S.C. 2000-d) relating to nondiscrimination in Federally assisted programs. Each Consortium participant entity has signed an Assurance of Compliance with the nondiscriminatory provisions of the Act. The Parties recognize that since the Consortium has no employees, that compliance is the responsibility of each participant.

ARTICLE XII: ORDER OF PRECEDENCE

In the event of any inconsistency between the terms of this Agreement and language set forth in the Consortium's Articles of Collaboration, the inconsistency shall be resolved by giving precedence in the following order: (1) The Agreement, (2) Attachments to the Agreement, (3) Consortium Articles of Collaboration.

ARTICLE XIII: EXECUTION

This Agreement constitutes the entire agreement of the Parties and supersedes all prior and contemporaneous agreements, understandings, negotiations and discussions among the Parties, whether oral or written, with respect to the subject matter hereof. This Agreement may be revised only by written consent of the CEC and ARPA Agreements Administrator. This Agreement, or modifications thereto, may be executed in counterparts each of which shall be deemed as original, but all of which taken together shall constitute one and the same instrument.

BLUE BAND CONSORTIUM STATEMENT OF WORK

INTRODUCTION

The BLUE BAND Consortium is composed of two industrial optoelectronic component manufacturers, Hewlett Packard and SDL, Inc., a major optoelectronic systems manufacturer, Xerox, two manufacturers of semiconductor substrates, AXT and Advanced Technology Materials, Inc., and two universities, The University of Texas at Austin and Boston University.

The goal of the BLUE BAND Consortium is the rapid commercialization of optoelectronic components operating in the green, blue, and ultraviolet portion of the optical spectrum. To realize this goal, the Consortium is divided into three efforts: (1) a highly integrated development of core growth technologies; (2) identification and development of key substrate technologies; and (3) cutting-edge materials growth research performed at university facilities.

The integrated growth and characterization effort is the centerpiece of the Consortium. Within the growth effort, the three optoelectronic houses freely share all MOCVD (Metal-organic Chemical Vapor Deposition) information. In regular technical meetings, the critical MOCVD growth problems will be discussed and multiple technical approaches will be identified. These potential solutions will then be divided and assigned to individual institutions, thus permitting the parallel examination of multiple pathways without duplication of effort. With this approach, the central problems of nitride materials growth will be rapidly solved.

Substrate issues will be addressed primarily by the substrate vendors and the universities. The clear advantage provided by the consortium is the ability of the Consortium to (1) aid in the characterization of the various substrates, and (2) to provide the substrate vendors with a critical link with MOCVD growth technology. The Consortium therefore provides the substrate vendors with substantial information concerning the performance of their substrates in actual growth situations.

Industrial institutions generally cannot address very high risk technologies. Therefore, this Consortium includes university efforts addressing molecular beam epitaxy (MBE) and MOCVD growth technologies. Although the universities are less closely linked to the main MOCVD effort, this independence is considered a valuable asset in that it substantially broadens the Consortium effort.

Contained within this document are the overall Statement of Work for the entire Consortium, including the downselect process for substrate manufacturers prior to the second year effort, and individual statements of work from each Member.

BLUE BAND CONSORTIUM SOW / TASKS

The BLUE BAND Consortium will develop key technologies for the commercialization of GaN and related materials. The development of these core technologies will be used to launch an aggressive LED (Light Emitting Diode) commercialization program and a demonstration program for the first blue semiconductor laser based upon the III-V nitrides. At the conclusion of the program, demonstrations of commercially viable LEDs and prototype laser diodes will be achieved. The goal specifications for the LED demonstrations are >4% external quantum efficiency with an emitted power >4 mW for devices emitting in the wavelength range of 480 to 570 nm. The goal specifications for the laser diode demonstrations are continuous wave operation of a p/n laser diode emitting at a wavelength shorter than 500 nm.

Tasks

1. The development of high-quality, low-defect density GaN and related alloys.

   - Optimization of MOCVD parameters to achieve high-quality buffer layers.
   - Optimization of MOCVD parameters for high-quality epitaxial GaN layers.
   - Characterization of nitride films: characterization techniques include TEM, AFM, X-ray diffraction, SEM, optical transmission, photoluminescence and photopumping.

2. The development of low-defect density heterojunctions.

   - Optimization of MOCVD parameters for ternary AlGaN alloys.
   - Optimization of MOCVD parameters for ternary InGaN alloys.
   - Optimization of MOCVD parameters for quaternary AlGaInN alloys.
   - Characterization of nitride heterojunctions. Analysis will include electronic measurements, TEM, and X-ray diffraction.
   - Modelling of nitride heterojunctions. The theoretical effort will address topics such as band-edge offsets and strain-related effects.

3. The development of n- and p-type GaN and related alloys. The development of low-resistance contact technologies for these alloys.

   - Modeling of atomic and electronic structure, formation energies for native defects, doping and compensation.
   - Calculation of formation energy, solubility, and doping efficiency of p-type dopants (Mg, C, and Zn) in GaN.
   - Controllable n-type doping.
   - Controllable p-type doping.
   - Ohmic contacts to n-type GaN
   - Ohmic contacts to p-type GaN
   - Electronic characterization of doped GaN and related alloys. Techniques include

variable-temperature Hall measurements, variable-temperature DLTS, optical DLTS, SIMS, C-V and I-V measurements.
- Demonstrations of p/n homojunctions and heterojunctions.

4. Advanced substrate identification and development

- Hybrid GaN substrate development.
- Bulk GaN substrate development.
- Evaluation of existing commercially available substrates.

5. Fabrication technology development.

- Wet etching techniques.
- Dry etching techniques.

6. LED fabrication and characterization.

- Optimization of LED epitaxial design.
- Wafer dicing development.
- Die attach, die bonding and encapsulation technique development.
- Characterization of LED technology including LED I-V and LOP behavior, radiation patterns, and reliability.

7. Laser diode fabrication and characterization.

- Development of facet formation techniques.
- Optimize epitaxial layers for laser diode operation.
- Laser die attach and die bonding technique development.
- Characterization of the optical properties of the AlGaInN material system.
- Characterization of AlGaInN laser diode structures under optical and electrical excitation.
- Fabrication of the laser program demonstrations.

8. Preparation of the Final Report.

DOWN-SELECT PROCESS / PROCEDURE FOR SUBSTRATE VENDORS

The BLUE BAND program is structured such that at the end of the first program year, the Consortium will decide to fund either AXT or ATMI through the second program year. If both vendors show promising results, reasonable efforts will be given by the Consortium Members to find additional resources to permit both substrate vendors to proceed through the second year. In any event, ARPA is not obligated to provide additional funds.

PROCESS:

1. The three primary members of the consortium, HP, XEROX, and SDL, will decide to fund either AXT or ATMI for the second year of the Blue Band Agreement. The decision will be reached by consensus.

2. The substrate vendors will present to the consortium the results of the first year research at the end of the first year. Within 10 working days of the meeting, the Consortium will inform ARPA, AXT and ATMI of the funding decision reached by the Primary Consortium Members.

3. The ARPA program manager shall be present throughout the subtrate selection process.

4. The Blue Band Consortium will deliver a written report describing the decision to ARPA.

5. Neither the Consortium nor ARPA will be financially liable beyond the first year funding to the vendor not selected for participation through the second year.

PROCEDURE:

1. AXT and ATMI will provide to the BLUE BAND Consortium examples of substrate technical progress at the end of the third quarter of the program. The samples should have surfaces suitable for MOCVD growth.

   1a. The Consortium will characterize the sample substrates provided by AXT and ATMI.

   1b. The Consortium will grow epitaxial layers of GaN on the sample substrates and characterize the epitaxial layers.

2. During the meeting at the end of year one, AXT and ATMI will present data addressing these points:

   2a. The current technical progress in the program.
   2b. An estimate of the substrate quality achievable under continued funding.
   2c. The path to the realization of commercially available substrates, including
      - information on size, both current and anticipated,
      - estimates of substrate pricing, and
      - substrate delivery estimates.

3. Following the presentations of AXT and ATMI, the results of the Consortium analysis of the AXT and ATMI substrates, and GaN epi growth upon these substrates will be presented. The Consortium will also present technical and commercial information of devices produced using current substrate technologies to determine the commercial

impact, through improving or enabling device performance, of the substrate technologies under development at AXT and ATMI.

4. The successful substrate technology will be selected on the basis of the Consortium determination, taking all foregoing analyses into account, as to which substrate technology will best enable or improve the performance of devices constructed on currently available substrates.

INDIVIDUAL CONSORTIUM MEMBERS' SOW / TASKS

HEWLETT-PACKARD

HP will work with team members and develop nitride MOCVD growth technology employing and EMCORE, vertical flow, high volume production reactors. Using the films grown by the team members, HP will develop wafer fabrication, die fabrication, and packaging technologies for LEDs. The LEDs will be characterized for (i) light output and emission wavelength spectra as a function of forward current, (ii) forward and reverse voltage behavior, and (iii) long-term reliability under a variety of stress conditions. Low-cost production techniques will be investigated to establish manufacturability, and high-volume manufacturing will be initiated. Prototype lamps will be supplied both to ARPA and potential users for commercial evaluation.

HP TASKS

HP.1 In collaboration with team members, develop nitride MOCVD growth technology using an EMCORE, vertical flow, high volume production reactor.

- Install and accept the reactor for nitride MOCVD growth.
- Perform parametric studies of the growth process and establish relations between growth parameters and materials properties.
- Develop buffer layer growth processes for both sapphire and SiC substrates.
- Develop n- and p-doped, single layer, binary composition growth processes.
- Develop processes for growth of p/n homojunctions in binary composition layers.
- Develop processes for growth of multilayers of n- and p-doped heterostructures.
- Develop processes for growth of p/n junction, double-heterostructure devices
- Provide epitaxial layers to Xerox PARC on an ongoing basis to provide for material characterization studies.

HP.2 In collaboration with team members, develop routine characterization techniques for rapid feedback of information critical to the epi growth team.

- Establish PL characterization capability for both single point and wafer scanning.
- Establish C-V and Hall effect measurement capability.
- Optimize X-ray rocking curve measurement capability.
- Develop a rapid turn-around LED device process for epi evaluation.

HP.3 Examine various device designs aimed at giving the desired emitted light wavelength and maximize the light output. Develop wafer and die fabrication processes suitable for the processing of nitride epi wafers into LEDs. Device goals are >4% external quantum efficiency with an emitted power >4 mW for a device emitting in the wavelength range of 480 nm to 570 nm.

- Investigate various epitaxial layer designs (number of layers, compositions, thicknesses and doping levels) which provide carrier confinement, minimize current crowding, and optimize light emission efficiency at specific wavelengths.
- Develop metal contacting schemes to provide ohmic contacts to both n- and p-type nitride-based materials.
- Develop dry and/or wet etching processes for defining contact areas and/or chip shaping.
- Develop wafer dicing processes to give damage-free, regular shaped chips.
- Develop suitable die attach, die bonding and encapsulation processes for producing packaged nitride LEDs.

HP.4 Fully characterize packaged LED lamps with respect to their electrical and optical properties, and determine their long-term reliability.

- Determine LED I-V and LOP (light output) behavior under a variety of temperature and drive conditions.
- Determine operating lifetimes under a variety of stress conditions including high temperature (55°C), high humidity (85%)/high temperature (55°C), and low temperature (-30°C).
- Determine the radiation patterns for standard lamp packed devices.

HP.5 Initiate high volume manufacturing and investigate low-cost production technology.

- Examine multiwafer epi growth of double-heterostructure devices.
- Investigate run-to-run and wafer-to-wafer layer uniformity -- thickness, composition, doping -- and device performance uniformity -- V_f (forward voltage), and LOP, and l_d (dominant wavelength).

HP.6 In collaboration with team members, prepare Final Report for submission to ARPA.

SDL, INC.

SDL will work with other team members to develop semiconductor laser diodes operating in the blue and ultraviolet portions of the optical spectrum. SDL will contribute growth technology, developed using custom low-pressure MOCVD reactors, to aid in the rapid development of GaN and related materials. Using the epitaxial layers developed by SDL and other team members, SDL will develop processing techniques applicable to semiconductor injection lasers, including

contact technology, facet formation techniques, and chip-shaping techniques. The prototype laser diodes will be delivered to ARPA. At the conclusion of the agreement, it is the goal of SDL to be in a position to begin to examine issues of commercialization, including output power capablity, spectral characteristics, modulation characteristics, and reliability.

SDL TASKS

SDL.1 In collaboration with team members, develop nitride MOCVD growth technology using custom SDL reactors.

- To facilitate material studies and characterization efforts, SDL will provide MOCVD nitride material to Xerox as an ongoing task.
- Perform parametric studies of the growth process and establish relations between growth parameters and materials properties.
- Develop buffer layer growth processes for both sapphire and SiC substrates.
- Develop n- and p-doped, single layer, binary composition growth processes for both sapphire and SiC substrates.
- Develop processes for growth of p/n heterojunctions

SDL.2 In collaboration with team members, develop routine characterization techniques for rapid feedback of information critical to the epi growth team.

- Establish PL and photopumping capability.
- Establish C-V and Hall effect measurement capability.
- Establish high-resolution X-ray rocking curve measurement capability

SDL.3 Examine processing techniques unique to laser diode fabrication.

- Develop facet fabrication techniques, either cleavage, etching, or polishing.
- Develop metal contacting schemes to provide Ohmic contacts to both n- and p-type nitride-based materials.
- Develop dry and/or wet etching processes for defining contact areas and/or chip shaping.
- Develop die separation techniques.
- Develop die match and wire bonding techniques.

SDL.4 Fabricate and characterize short-wavelength laser diodes.

- Fabricate and characterize LEDs as a material diagnostic.
- Fabricate and characterize single-mode ridge-waveguides to determine the optical properties of the AlGaInN material system.
- Photopump AlGaInN heterostructures.
- Fabricate and test AlGaInN heterostructure laser diodes under pulsed excitation.
- Fabricate and test AlGaInN heterostructure laser diodes under CW excitation.

SDL.5 In collaboration with team members, prepare Final Report for submission to ARPA.

XEROX PARC (Palo Alto Research Center)

Xerox PARC, in collaboration with the team members, will work towards the realization of optoelectronic devices based upon the III-V nitrides. The three general objectives of the work to be performed at Xerox PARC in support of the BLUE BAND effort are: (1) to provide timely feedback information on the properties of III-V nitride layers to assist other team members in optimizing growth conditions, (2) to contribute to the determination of key materials parameters and processing strategies for fabricating optoelectronic devices, and (3) to contribute to the fundamental understanding of these materials. These objectives will be pursued in close coordination with the other team members.

Within each quarter, Xerox will pursue studies to aid the experimental growth effort. The mechanism designed to aid this interaction is a steady flow of materials, from all other members of the team, to Xerox, with information flowing back to the Consortium concerning the properties of these samples. In each quarter, materials characterization will be provided on a minimum of four specimens of GaN or related materials. For each specimen, results will be provided from a minimum of one of the following experimental techniques: TEM, SIMS, X-ray diffraction, PL, Hall effect, CV, IV, or DLTS.

XEROX TASKS

XE.1 Characterization of the electronic and optical properties of GaN and related alloys.

- The development of Ohmic contacts and Schottky barrier contacts to GaN and related materials.
- C-V and I-V measurements.
- Coordinated electrical (C-V, I-V, DLTS) and optical measurements (PL) to identify defect structure in n-type and p-type GaN.
- Perform experiments to determine the acceptor doping efficiency in doped p-type GaN.
- Perform variable-temperature Hall measurements on speciments of GaN to obtain electron transport parameters (e.g., Hall mobility and electron concentration versus temperature).
- Perform SIMS analysis on GaN and related materials for identification of impurities and determination of doping efficiencies.

XE.2 Characterization of the structural properties of GaN and related alloys. Included in this task are TEM, SEM, AFM and X-ray diffraction studies.

- Study the GaN/Al_2O_3 interface using TEM.
- Study the GaN/SiC interface using TEM.
- Study the AlGaN and InGaN heterostructure system with TEM.
- Study the effect of high n-type and p-type doping on the crystal structure of GaN.

- Study the interaction of dislocations and impurities.

XE.3 Modelling of the physical properties of GaN and related alloys.

- Investigate atomic and electronic structure, and formation energies for native defects and describe the role of point defects in doping and compensation.
- Calculate the formation energy, solubility, and doping efficiency of p-type dopants.
- Calculate the formation energy, solubility, and doping efficiency of n-type dopants.
- Enumerate key parameters for the operation and performance of optoelectronic devices.
- Calculate bandoffsets in the AlGaInN materials system.
- Calculate energetics of hydrogen and hydrogen diffusion in GaN.

XE.4 In collaboration with team members, prepare Final Report for submission to ARPA.

AXT

AXT believes that the most reliable route to a long-lived, commercially viable semiconductor laser based on GaN and related materials is through homoepitaxy on low defect density substrates. AXT will team with the Polish Academy of Sciences High Pressure Research Center (Unipress) to develop the high pressure solution growth GaN single-crystal technology which has been reported by Unipress. Substrate growth will be conducted at Unipress and preparation of substrates for epitaxy will be conducted at AXT. The Unipress technology is similar to vertical gradient freeze (VGF) growth of GaAs in its approach. AXT's extensive experience in VGF indicates that, using a scaled Unipress technology, GaN substrates which are commercially cost effective for optoelectronic applications can be developed. The goal of AXT is the development of high quality GaN substrates on the scale of 2.5 cm suitable for epitaxial growth of high-quality optoelectronic devices.

AXT TASKS

AXT.1 In collaboration with UNIPRESS, AXT will develop growth reactors capable of synthesizing 2.5 cm scale GaN substrates suitable for epitaxial growth.

- Complete a transfer of growth information from UNIPRESS.
- Develop growth criteria to enable substrate production of commercially viable size.
- Design and construct a growth reactor capable of producing 2.5 cm GaN substrates.

AXT.2 In collaboration with the team members, AXT will develop high crystallinity GaN substrates suitable for the production of high-performance optoelectronic devices.

- As an ongoing substate evaluation, AXT will deliver to the Consortium GaN substrates of varying size for evaluation and epitaxial growth.
- Develop manufacturing processes to produce epi-ready substrates; surface

preparation, cleaning, orientation are included in this task.

AXT.3 AXT will present a presentation summarizing first year research and the second year program to the CEC and ARPA at the end of year one.

AXT.4 In collaboration with team members, prepare Final Report for submission to ARPA.

ADVANCED TECHNOLOGY MATERIALS, INC. (ATMI)

ATMI, in partnership with other team members, will develop GaN substrate materials using a "hybrid" growth technique. The substrates developed using this method will be of large size, have good crystallinity and will be fully compatible with the MOCVD approaches of the larger Consortium. In addition, the surface finish and other preparation techniques of these large area substrates will be studied. ATMI will deliver sample substrates to ARPA and the other team members as described in the detailed milestone

ATMI TASKS

ATMI.1 Reactor design, fabrication and characterization

- Design reactors for both Year 1 and Year 2
- Construction of the improved reactor of Year 2
- Characterization of the GaN growth reactor, including gas flow, thermal gradients, etc.

ATMI.2 GaN substrate growth and characterization

- Characterization of growth rate and morphology
- Characterization of general crystallinity using X-ray diffraction
- Surface preparation techniques.

ATMI.3 In collaboration with team members, prepare Final Report for submission to ARPA.

BOSTON UNIVERSITY

Boston University will use the unique capabilities of Molecular Beam Epitaxy (MBE) to evaluate materials growth issues. The particular focus will be the study of the effect of substrate type and quality upon the growth of AlGaInN. Substrates to be evaluated include:
6H-SiC, ZnO, M-plane sapphire and GaN grown by the Vapor Phase Epitaxy (VPE) method. All of these substrates are closely lattice-matched to the AlGaInN system. The first three substrates will be obtained from commercial vendors while the GaN substrates are being currently developed at Boston University. Substrate preparation and surface cleaning procedures will be developed. Characterization of the materials will be carried out in collaboration with the Xerox group.

Boston University TASKS

BU.1 Boston University will grow VPE GaN on selected substrates

- Design and construct a hydride VPE reactor.
- Grow VPE GaN.
- Deliver samples of the VPE GaN to the consortium, particularly Xerox PARC, for evaluation.

BU.2 Boston University will use MBE growth techniques to evaluate several possible substrates for AlGaInN materials growth.

- Grow and characterize GaN and AlGaInN on 6H-SiC.
- Grow and characterize GaN and AlGaInN on VPE-grown GaN.
- Grow and characterize GaN and AlGaInN on ZnO.
- Grow and characterize GaN and AlGaInN on M-plane sapphire.

BU.3 Boston University will provide samples of the materials grown in BU.2 to the consortium, particularly Xerox PARC, for materials characterization.

BU.4 Boston University will fabricate optoelectronic devices, including LEDs and laser diodes, as a materials characterization tool for the optical and electrical properties of materials grown in Task BU.2.

BU.5 In collaboration with team members, prepare Final Report for submission to ARPA.

UNIVERSITY OF TEXAS AT AUSTIN

The proposed program will develop practical materials and device technologies for the fabrication of high-performance injection electroluminescent devices that will provide high-energy visible light emission in the blue spectral region as well as emission in the near ultraviolet. These injection-laser and light-emitting-diode (LED) devices will be fabricated from wide-bandgap III-V compound semiconductor epitaxial heterostructures in the InAlGaN system grown by low-pressure metalorganic chemical vapor deposition (LP-MOCVD). Characterization of the physical properties of materials produced at UT will be performed in collaboration with Xerox PARC, via coordinated delivery of epitaxial materials to Xerox.

University of Texas at Austin TASKS

UT.1 In collaboration with team members, UT-Austin will develop LP-MOCVD growth technology for wide-bandgap III-V nitrides.

- Initiate growth studies in the existing Emcore UTM reactor system (B reactor).

- Study the relationship between growth parameters and the resulting structural, optical, electrical, and optoelectronic properties of the epitaxial films.
- Study novel precursors suitable as MOCVD nitrogen sources.
- Study the effect of the introduction of molecular nitrogen into the MOCVD gas phase.
- Establish growth parameters for the initiation of nitride film growth on Al_2O_3 and SiC substrates.
- Install and characterize a new Emcore HT MOCVD growth system designed specifically for high-temperature growth (C reactor).
- Develop an understanding of p- and n-type doping in GaN and related alloys.
- Establish conditions of the growth of p-n junction devices.
- Develop processes for the growth of heterostructures, quantum wells, and superlatices.

UT.2 In collaboration with team members, UT-Austin will develop characterization techniques for the wide-bandgap III-V nitrides.

- Perform studies of the fundamental optical properties of nitride materials.
- Study the structural properties and defects of the epitaxial films.
- Establish capability for the study of the photoluminescence characteristics of these materials.
- Establish the capability to measure the electrical characterization of thin films.

UT.3 In collaboration with other team members, UT-Austin will design, fabricate, and test light-emitting devices, including coherent and incoherent light sources.

- Evaluate various device designs to provide optical and electrical characteristics required for high-performance light-emitting devices.
- Study the formation of Ohmic contacts to p- and n-type nitride materials.
- Develop etching techniques for the controlled formation of device structures in these materials.

UT.4 In collaboration with team members, prepare Final Report for submission to ARPA.

REPORT REQUIREMENTS

A. QUARTERLY REPORT

On or before ninety (90) calendar days after the effective date of the Agreement and quarterly thereafter throughout the term of the Agreement, the Consortium shall submit or otherwise provide a quarterly report. Two (2) copies shall be submitted or otherwise provided to the ARPA Program Manager, and one (1) copy shall be submitted or otherwise provided to the ARPA Agreement Administrator. The report will have two (2) major sections.

1. Technical Status Report. The technical status report will detail technical progress to date and report on all problems, technical issues or major developments during the reporting period. The technical status report will include a report on the status of consortium collaborative activities during the reporting period.

2. Business Status Report. The business status report shall provide summarized details of the resource status of this Agreement, including the status of the contributions by the Consortium participants. This report will include a quarterly accounting of current expenditures as outlined in the Annual Program Plan. Any major deviations shall be explained along with discussions of the adjustment actions proposed.

B. ANNUAL PROGRAM PLAN DOCUMENT

The Consortium Executive Committee (CEC) shall submit or otherwise provide to the ARPA Program Manager one (1) copy of a report which describes the Annual Program Plan as described in Article IV. This document shall be submitted not later than thirty (30) calendar days following the Annual Site Review as described in Article IV.

C. SPECIAL TECHNICAL REPORTS

As agreed to by the Consortium and the ARPA Program Manager, the CEC shall submit or otherwise provide to the ARPA Program Manager one (1) copy of special reports on significant events such as significant target accomplishments by Consortium Members, significant tests, experiments, or symposia.

D. PAYABLE MILESTONES REPORTS

The CEC shall submit or otherwise provide to the ARPA Program Manager, documentation describing the extent of accomplishment of Payable Milestones. This information shall be as required by Article IV, and shall be sufficient for the ARPA Program Manager to reasonably verify the accomplishment of the milestone of the event in accordance with the Statement of Work.

E. FINAL REPORT

(a) The Consortium Executive Committee (CEC) shall submit or otherwise provide a Final Report making full disclosure of all major developments by the Consortium within sixty (60) calendar days of completion or termination of this Agreement. With the approval of the ARPA Program Manager, reprints of published articles may be attached to the Final Report. Two (2) copies shall be submitted or otherwise provided to the ARPA Program Manager, one (1) copy shall be submitted to the ARPA Agreement Administrator, and one (1) copy shall be submitted or otherwise provided to ARPA/ MTO (Attn: Assistant Director for Program Management. One (1) copy shall be submitted to the Defense Technical Information Center (DTIC) addressed to Bldg. 5 / Cameron Station, Alexandria, VA 22314.

(b) The Final Report shall be marked with a distribution statement to denote the extent of its availability for distribution, release, and disclosure without additional approvals or authorizations. The Final Report shall be marked on the front page in a conspicuous place with the following marking:

> "DISTRIBUTION STATEMENT B. Distribution authorized to U.S. Government agencies only to protect information not owned by the U.S. Government and protected by a contractor's "limited rights" statement, or received with the understanding that it not be routinely transmitted outside the U.S. Government. Other requests for this document shall be referred to ARPA Security and Intelligence Office."

BLUE BAND CONSORTIUM
SCHEDULE OF PAYMENTS & PAYABLE MILESTONES

SOW	#	Month	PAYABLE MILESTONES	ARPA PAYMENT	Consortium PAYMENT
BB.1	1	1	Complete plans & piping for install. of Emcore HT "D" reactor system. AlGaN films grown on $A1_2O_3$ substrates in existing Emcore UTM "B" system. Deliver samples to Xerox. Install Si doping source on "B" reactor and begin n- and p-doping studies of GaN.	$173,000	$173,000
BB.4	2	1	Establish detailed program plan & schedule w/ UNIPRESS (AXT) Complete plans & facilities for reactor for GaN growth (ATM)	$40,000	$40,000
			END OF FIRST PAYABLE MILESTONE PERIOD		
BB.1	3	3	Emcore reactor installed & operational. Studies of superlattice buffer layers initiated. Prepare GaN/Al_2O_3 and GaN/SiC layers & deliver samples to Xerox. Structural Characterization of GaN-Al_2O_3 interface.	$188,000	$128,000
BB.2	4	3	Initiate studies of InGaN growth in "B" reactor	$10,000	$10,000
BB.3	5	3	Metal contacts for n-type GaN films. Deliver GaN w/ n-type impurities to Xerox for materials characterization. Initiate electrical characterization of GaN. Investigate native defects in GaN.	$227,000	$162,000
BB.4	6	3	Develop undoped GaN films on 6H-SiC substrates & introduce n- and p-type dopants. Deliver samples to Xerox. Characterization of reactor for GaN growth. Deliver 2mm scale GaN single crystal substrates to the consortium for study.	$110,000	$110,000
			END OF SECOND PAYABLE MILESTONE PERIOD		
BB.1	7	6	Complete installation of new Emcore HT "D" reactor. Demonstrate GaN and AlGaN growth in D reactor. Deliver samples to Xerox. Scanning PL operational. Whole wafer scans of member's GaN available. Structural characterization of the GaN/SiC interface.	$99,000	$84,000
BB.2	8	6	AlGaN/GaN heterostructures demonstrated. Deliver samples to Xerox.	$90,000	$70,000
BB.3	9	6	Controllable n-type doping in GaN demonstrated, with doping levels between $2x10^{17}$ and 5×10^{18} cm^{-3}. Electrical characterization of donor-doped n-type GaN. Calculate properties of p-type dopants (Mg & Zn) in GaN. Deliver GaN with p-type impurities to Xerox for materials characterization.	$182,000	$192,000

SOW	#	Month	PAYABLE MILESTONES	ARPA PAYMENT	Consortium PAYMENT
BB.4	10	6	Deliver 5mm scale GaN single crystal substrates to Consortium for epitaxian growth. Develop GaN substrates by the VPE method. Such substrates will be grown on Zn0 coated sapphire substrates. Characterization of GaN on growth template.	$110,000	$110,000
BB.5	11	6	RIE etching of GaN films demonstrated.	$40,000	$35,000
			END OF THIRD PAYABLE MILESTONE PERIOD		
BB.1	12	9	Photopumping set-up completed; PL studies initiated.	$10,000	$10,000
BB.2	13	9	Structural characterization of AlGaN layers.	$40,000	$40,000
BB.3	14	9	Controllable p-type doping in GaN demonstrated between 10^{17} and 10^{18} cm^{-3}. Demonstration of p/n homojunction, w/ goal specs. of turn-on voltage less than 4.5 V and reverse breakdown voltage greater than 10 V. Deliver sample to Xerox. Metal contacts for p-type GaN films. Deliver heavily n-doped and p-doped samples to Xerox for material study. Electrical characterization of acceptor-doped GaN. Calculate properties of n-type dopants (Si, O, C) in GaN. Studies of passivation in nitride films initiated. Doping demonstrated for p- and n-type GaN in D system.	$320,000	$330,000
BB.4	15	9	Development of GaN films on single crystalline Zn0 substrates. Deliver GaN samples for Consortium growth & characterization. Deliver 1cm scale GaN single crystal substrates to Cons. for eval.	$105,000	$105,000
BB.6	16	9	First LED chip configuration & processing designed. n- and p-type GaN film etching.	$50,000	$55,000
			END OF FOURTH PAYABLE MILESTONE PERIOD		
BB.1	17	12	Structural characterization of heavily n-doped & p-doped GaN.	$30,000	$30,000
BB.2	18	12	Heterojunction growth for fundamental band offset studies.	$15,000	$15,000
BB.3	19	12	p/n AlGaN/GaN heterojunction demonstrated. Performance parameters to be characterized include I-V, optical power measurements, and spectral measurements. Turn-on voltage goal specification is less than 4.4 V. Deliver samples, including a single heterojunction to Xerox.	$138,000	$330,000
BB.4	20	12	Complete evaluation of SiC vs. Al203. Develop AXT program plan for Phase II. Develop ATMI program plan for second year. Development of GaN films on the M-plane of saphhire.	$81,000	$81,000
BB.6	21	12	GaN LED demonstration. Enumerate materials/modeling parameters that critically influence LED operation.	$30,000	$30,000
			END OF FIFTH PAYABLE MILESTONE PERIOD		
			YEAR ONE TOTALS	$2,088,000	$2,140,000

SOW	#	Month	PAYABLE MILESTONES	ARPA PAYMENT	Consortium PAYMENT
BB.2	22	15	Structural characteristics of AlGaN/GaN heterojunctions. InGaN film growth demonstrated. InGaN/GaN structures delivered to Xerox for study. Theoretical investigation of band offsets of the AlGaInN material system.	$225,000	$185,000
BB.3	23	15	Electronic characterization and PL study of defects in n-type GaN.	$40,000	$40,000
BB.4	24	15	IF AXT: Design new reactor ; or IF ATMI: Scale-up of GaN growth system. Comparison of GaN devices on sapphire and SiC substrates. Develop n-type and p-type AlGaInN on 6H-SiC substrates.	$200,000	$200,000
BB.6	25	15	Bonding to smple devices demonstrated.	$70,000	$60,000
BB.7	26	15	Development of facet formation technologies, including polishing, END OF SIXTH PAYABLE MILESTONE PERIOD	$80,000	$80,000
BB.1	27	18	Photopumping set-up complete.	$20,000	$20,000
BB.2	28	18	Structural characterization of InGaN/GaN heterojunctions. Undoped and doped InGaN/GaN double heterostructure films demonstrated.	$130,000	$95,000
BB.3	29	18	Electrical characterization and PL of defects in p-doped GaN and calculation of energetics of hydrogen in GaN.	$75,000	$75,000
BB.4	30	18	IF AXT: Deliver 1 cm scale GaN single crystal substrate(s) to other Cons. Members. Fabricate new reactor. Development of GaN films on the VPE-grown GaN substrates. IF ATMI: Develop GaN films on VPE-grown GaN substrates. Characterization of n-type GaN grown at ATMI.	$125,000	$125,000
BB.6	31	18	p/n InGaN/GaN heterojunction LED demonstrated. Demonstrate, via measurements of the optical emission spectra, goal in corporation levels in excess of 4% (In0.04Ga0.96N) within the InGaN active region. Deliver to Xerox a homogeneous alloy representative of an LED active region for analysis. AlGaN/InGaN heterostructures and LEDS demonstrated.	$140,000	$125,000
BB.7	32	18	Fabricate single mode ridgewaveguide with facets and characterize END OF SEVENTH PAYABLE MILESTONE PERIOD	$100,000	$100,000
BB.2	33	21	Structural characterization of a homogeneous alloy representative of a light emitting active region.	$40,000	$40,000
BB.3	34	21	Electrical characterization of a homogeneous alloy representative of a light emitting active region and theoretical investigation of hydrogen/impurity interaction.	$75,000	$75,000
BB.4	35	21	IF AXT: Establish growth conditions for new reactor. IF ATMI: Characterization of 2" GaN substrate. Development of AlGaInN films on VPE-grown GaN substrates.	$75,000	$75,000

SOW	#	Month	PAYABLE MILESTONES	ARPA PAYMENT	Consortium PAYMENT
BB.6	36	21	Double heterostructure, packaged LED devices demonstrated and characterized. Goal performance spec. is an emitted power >4 mW. mW. Goal efficiency specification is >4% external quantum efficiency.	$160,000	$120,000
BB.7	37	21	Demonstrate AlGaInN ridgewaveguide heterostructure under photo-pumped excitation. Goal performance spec. is the demonstration of stimulated emission. Demonstrate AlGaInN ridgewaveguide p/n junction under pulsed electrical excitation. Goal spec. is the demonstration of pulsed laser operation. Optically pump AlGaN/InGaN QW laser structures. Optically pump AlGaN/GaN DH laser structure.	$180,000	$180,000
			END OF EIGHTH PAYABLE MILESTONE PERIOD		
BB.1	38	24	Structural characterization of dislocations after simulated diode operation.	$30,000	$30,000
BB.2	39	24	Calculate formation energies of selected native defects & dopant impurities in AlN and InN. Electrical characterization of a doped AlGaN/GaN single heterojunction.	$44,000	$44,000
BB.4	40	24	Development of AlGaInN alloys on single crystalline ZnO substrates IF AXT: Deliver substrates grown in new reactor to Cons. Members. IF ATMI: Further substrate development	$50,000	$50,000
BB.6	41	24	Characterization of best current LED technology.	$0	$180,000
BB.6	42	24	Demonstration of AlGaInN ridgewaveguide p/n junction under CW electrical excitation. Goal spec. is CW laser action with an emission wavelength in the blue portion of the electromagnetic spectrum. Characterization of AlGaN/InGaN QW diode laser structures.	$133,000	$133,000
BB.7	43	24	Completion of Final Report.	$56,000	$56,000
			END OF NINTH PAYABLE MILESTONE PERIOD		
			YEAR TWO TOTALS	$2,048,000	$2,088,000
			PAYMENT TOTALS FOR THE AGREEMENT	$4,136,000	$4,228,000

FUNDING PROFILE

A. CONSORTIUM MEMBER CONTRIBUTIONS

Member	Contribution
Hewlett-Packard	$1,117,000
SDL	$ 979,000
Xerox PARC	$ 846,000
University of Texas at Austin	$ 446,000
Boston University	$ 280,000
AXT (year one)	$ 140,000
ATMI (year one)	$ 140,000
AXT or ATMI (year two)	$ 280,000
TOTAL	**$4,228,000**

B. PROJECTED PROGRAM FUNDING COMMITMENTS*

	ARPA Payments	Consortium Contribution
FY95	$1,269,000	$1,114,000
FY96	$2,024,000	$2,131,000
FY97	$ 843,000	$ 983,000
TOTAL	**$4,136,000**	**$4,228,000**

* The ARPA "Payments" and Consortium "Contributions" listed here coincide with the projected schedule for actually accomplishing the Payable Milestones. In terms of Fiscal Year Appropriated Funds, the Government's cost-share is from FY94 Appropriated Funds.

LIST OF GOVERNMENT AND CONSORTIUM REPRESENTATIVES

GOVERNMENT:

Anis Husain, Program Manager
ARPA/ MTO
3701 N. Fairfax Drive
Arlington, VA 22203-1714
phone: (703) 696-2236
FAX: (703) 696-2201
Email: ahusain@arpa.mil

Elaine Ely, Agreement Administrator
ARPA / CMO
3701 N. Fairfax Drive
Arlington, VA 22203-1714
phone: (703) 696-2411
FAX: (703) 696-2208
Email: eely@arpa.mil

CONSORTIUM:

Dave Welch, Technical Coordinator
SDL
80 Rose Orchard Way
San Jose, CA 95134-1365
phone: (408) 943-9411
FAX: (408) 943-1070
Email: 73173.3155@compuserve.com

Jo Major, Principal Investigator
SDL
80 Rose Orchard Way
San Jose, CA 95134-1365
phone: (408) 943-9411
FAX: (408) 943-1070
Email: 74151.753@compuserve.com

Janelle Johnson, Consortium Administrator
SDL
80 rose Orchard Way
San Jose, CA 95134-1365
phone: (408) 943-1070
FAX: (408) 943-1070

CONSORTIUM MEMBER REPRESENTATIVES

George Craford
Hewlett-Packard Company
370 West Trimble Road
San Jose, CA 95131
phone: (408) 435-6561
fax: (408) 435-6335
Email: none

Bill Imler
Hewlett-Packard Company
370 West Trimble Road
San Jose, CA 95131
phone: (408) 435-4900
fax: (408) 435-6335
Email: Bill_Imler@SJ.HP.com

Noble Johnson
Xerox Corporation, PARC
3333 Coyote Hill Road
Palo Alto, CA 94304
phone: (415) 812-4161
fax: (4315) 812-4105
Email: Connell.parc@xerox.com

Neville Connell
Xerox Corporation, PARC
3333 Coyotte Hill Road
Palo Alto, CA 94304
phone: (415) 812-4132
fax: (415) 812-4105
Email: n_johnson@parc.xerox.com

Russ Dupuis
The University of Texas at Austin
MER 1.606D1R990
Austin, TX 78712-1100
phone: (512) 471-0537
fax: (512) 471-8575
Email: dupuis@ece.Utexas.edu

Ted Moustakas
Boston University
44 Cummington Drive
Boston, MA 02215
phone: (617) 353-5431
fax: (617) 353-6440
Email: tdm@buenga@bu.edu

Heikki Helava
American Crystal Technoilogy (AXT)
6780 Sierra Court, Suite 1
Dublin, CA 94568
phone: (510) 833-0553
fax: (510) 833-2667
Email: HHelava@holonet. net

Mike Tischler
Advanced Technology Materials, Inc.
7 Commerce Drive
Danbury, CT 06810
phone: (203) 794-1100
fax: (203) 830-4116
Email: tisch@atmi.com

3. PROPOSAL BY BLUE BAND CONSORTIUM, BLUE LIGHT AND UV EMITTERS – THE BAY AREA NITRIDE DEVELOPMENT CONSORTIUM, DEVELOPMENT OF HIGH BANDGAP III-V MATERIALS AND OPTICAL DEVICES. (50 PAGES)

A proposal in response to **ARPA SOL RA94-30**

by the *BLUE BAND* Consortium
Blue Light and UV Emitters - the Bay Area Nitride Development Consortium

Development of High-Bandgap III-V Materials and Optical Devices

SDL
San Jose, CA

Hewlett-Packard
San Jose, CA

Xerox PARC
Palo Alto, CA

Prof. Russell D. Dupuis
University of Texas at Austin

Prof. Ted Moustakas
Boston University

AXT
Dublin CA

ATMI
Danbury CT

Abstract 2
I. Executive Summary 2
II. Technical Approach 4
III. Program Plan 25
IV. Statement of Work 27
V. Milestone Chart 27
VI. Facilities and Equipment Description 28
VII. Relevant Prior Work 29
VIII. Business Plan for Productization 45
IX. Key Personnel 48
X. References 49

This document contains **PROPRIETARY INFORMATION** that shall not be duplicated, used or disclosed in whole or in part, for any purpose other than to evaluate this proposal. If, however, a contract is awarded to any member of the consortium as a result of, or in connection with the submission of this data, the parties shall have the right to duplicate, use or disclose the data to the extent provided in the resulting contract. This restriction does not limit the parties' right to use the information contained in this proposal if it is obtained from another source without restriction. Proprietary information is contained within all pages of this proposal.

Abstract

SDL, HP, Xerox, the University of Texas at Austin, Boston University, American Xtal Technology and Advanced Technology Materials, Inc., have formed a strategic consortium to develop and commercialize optoelectronics based upon the nitride alloys. This proposal describes the prior art achieved within the consortium and outlines a research and development program to achieve high performance nitride-based LEDs and laser diodes operating in the visible and ultra-violet portions of the electromagnetic spectrum.

I. Executive Summary

SDL, Hewlett Packard (HP), Xerox, the University of Texas at Austin (UT), Boston University, Advanced Technology Materials, Inc. (ATMI), and American Xtal Technology (AXT) have teamed together to develop nitride materials for the demonstration of visible LEDs and laser diodes from the near ultra-violet (UV) to the yellow regions of the spectra. This proposal is in response to ARPA solicitation 94-30, addressing the development of large area, wide-bandgap bulk and epitaxial materials for heterostructures useful in optoelectronics. The proposed program is unique in that: i) the partners have demonstrated the highest quality GaN material made to date, ii) the partners represent the largest commercial manufacturers of optoelectronics in the United States, iii) the partners have successfully fabricated LED's in GaN materials, iv) the program is the only combination of all technologies required to produce and commercialize LEDs and laser diodes, and v) the consortium has unique systems expertise to allow the immediate integration of the devices into commercial systems. The attributes of the team are discussed below.

The consortium has demonstrated the highest crystalline quality GaN materials. GaN material quality is best measured via X-ray full width at half maximum (FWHM). SDL has grown GaN with a FWHM of 27 seconds. UT has demonstrated GaN films grown on sapphire with FWHM of 38 seconds. The demonstration of 27 seconds FWHM is the narrowest reported X-ray and represents the world's highest quality GaN. The materials grown by the UT and SDL are the only demonstration of fully planar growth and single crystal growth of GaN films. The background carrier concentration of GaN grown at SDL is $2x10^{15}/cm^3$, the lowest demonstrated by MOCVD. Both p- and n-type conductivity has been observed in SDL and BU material.

The consortium members represent world leaders in the field of crystal growth, materials characterization and device fabrication. All five team members have demonstrated their expertise in developing the highest quality materials in their respective areas; HP in the fabrication of high brightness LED materials, SDL in the development of high power laser diode materials, UT in the development of advanced materials, Xerox in the development of characterization and processing of semiconductor materials and ATMI and AXT in the fabrication of high quality substrate materials. BU is an expert in MBE growth and processing of GaN and has achieved a deep-blue GaN injection LED.

HP and SDL represent the largest commercial optoelectronics manufacturers in the United States. The key to any program intended to leverage both military and commercial markets is the development of technology in organizations that have demonstrated sustained manufacturing capabilities. In the area of optoelectronics there are no companies, even in Japan, that surpass the commercial impact of either HP or SDL in their respective market areas. HP is the world's largest dollar volume manufacturer of visible LEDs and is the single largest optoelectronics manufacturer in the U.S. SDL is the world's largest dollar volume commercial manufacturer of laser diodes and is the largest volume commercial manufacturer of laser diodes in the U.S.. SDL has been chosen as the company

Use or disclosure of the information contained on this sheet is subject to the restrictions on the title page of this proposal. This information is proprietary to the consortium.

with the greatest impact on the optoelectronics market over the past five years by Laser Focus World. The incorporation of these two program members into the consortium insure the rapid introduction of components into both military and commercial systems. In addition, HP and Xerox are two of the largest manufacturers of optoelectronic systems. The systems businesses of Xerox and HP will provide strong internal markets for this technology.

Corporate Commitment: HP is committed to the proposed program as a result of strategic alliances with other members. Their corporate commitment to GaN materials development exceeds $10M over the next several years. SDL, in anticipation of the success of the program has begun negotiations with leaders in the data storage to manufacture and supply high volume laser diode products. Both SDL and HP are firmly committed to the rapid introduction of high-bandgap optoelectronics.

The program is designed to address the crystal growth of GaN and related films by MOCVD, the studies of growth on and fabrication of appropriate substrate materials, the processes required for high quality buffer layers, and materials characterization to understand the crystallographic, electronic and optical properties of GaN alloys. Efficient LED demonstration will be made within the first year with the subsequent demonstration of laser diodes occurring towards the end of the second year. Although devices are the program goal, the technical emphasis will be the development of high quality GaN-based materials. The program will address the following issues in the development of GaN-based visible emitters.

Single crystal growth of GaN. The consortium will leverage the existing expertise of UT and SDL in the growth of high quality films to demonstrate single crystal low dislocation density GaN materials. Emphasis will be placed on the development of low dislocation epitaxy. The growth will be investigated in MOCVD reactors at SDL, HP and UT with characterization performed at Xerox.

Substrate fabrication and definition. Critical to the successful growth of GaN films is the fabrication of appropriate substrates. GaN LEDs are currently grown on sapphire substrates. For higher performance devices, the program will develop advanced substrates. AXT will develop bulk GaN growth and ATMI will develop GaN substrates grown by vapor phase epitaxy (VPE) on sacrificial substrates. Boston University will evaluate the growth of GaN films on existing and developmental substrate materials including sapphire, ZnO, SiC, and hybrid substrates (i.e. VPE grown GaN substrates), and bulk GaN.

Advanced materials development. The demonstration of visible emitters in the blue-green portions of the spectrum from band-to-band transitions requires the fabrication of low stress, low bandgap films. Due to critical thickness issues in the growth of InGaN materials the band-to-band recombination may be limited to high energy emission. As part of this program the consortium will develop both GaAsN and InGaN materials as the active regions of blue/green emitters. SDL has pioneered the development of GaAsN materials.

Device development. The program goals are to demonstrate both LEDs and laser diodes in the visible spectrum. The development of LED technology will occur first due to the high quality of existing GaN films grown by the consortium members. The final goal of the program is to demonstrate a laser diode operating at room temperature.

Modeling and calculations of electronic properties. Xerox will develop theoretical bandstructure models to study the material characteristics including band alignment, doping properties, transition strengths and gain.

Business plan. The industrial members have strong motivation to rapidly commercialize the advances of the program. The consortium is active in pursuing

Use or disclosure of the information contained on this sheet is subject to the restrictions on the title page of this proposal. This information is proprietary to the consortium.

the market introduction of advanced laser diodes, LEDs, opto-electronic systems, and advanced substrate materials.

The program is proposed as the core research effort to be partially funded by ARPA. The corporate members are committed to developing viable GaN-based emitting devices and view the consortium as providing the critical mass necessary for success. Without ARPA funding , materials and device development will be considerably slower, a narrower range of parameter space will be investigated and there will be substantial duplication of effort and unneeded expenditures of funds. In conclusion, this proposal represents a teaming of the industry leaders in optoelectronic devices for the development of GaN-based materials. In addition the corporate members are heavily investing in this technology and view this consortium as a mechanism to insure rapid technology development for commercial introduction. The team members have demonstrated the greatest impact on the US based optoelectronic markets, the highest quality GaN films grown and the development of high quality substrate materials. This consortium represents a unique coupling of the technical and market leaders in visible emitter technology, thus insuring a successful demonstration and commercialization of visible semiconductor devices.

II. Technical Approach

Due to the high bond strength, large bandgap energies and present quality of materials, nitride alloys have been chosen as the preferred materials for visible optoelectronic devices. The majority of commercially based optoelectronic companies have concentrated their efforts on the development of GaN films for both LEDs and laser diodes. Recent demonstrations by Nichia Chemical of GaN based LEDs has spawned a number of concentrated research efforts in this area including efforts at SDL, HP, Xerox, and the University of Texas at Austin. Although the current LED demonstrations have been encouraging, the reliability of such devices are insufficient for most commercial applications. As a result the consortium members have begun significant efforts in the areas of GaN based visible optoelectronics. In particular HP has initiated an internally funded program at greater than $10M over the next several years for the development of GaN based LEDs. SDL has initiated negotiations with data storage corporations for the strategic development of blue laser sources. Although the development of the GaN is being actively pursued by the consortium members with internal funding the proposed program is highly strategic joining the individual expertise in a strategic direction that would not otherwise exist. Not only are the team members committed to GaN materials, they are the industry leaders and are the best avenue for successful commercialization of nitride technologies.

To achieve the goals of the program the program is designed to address the technical issues including the development of efficient active regions that utilize direct band-to-band emission, the development of dislocation-free quaternary AlGaInN materials, the development of appropriate substrate technologies, and device process technology development.

The technical approach to these issues is divided into four areas:

- **MOCVD growth techniques.**
- **Substrate technologies.**
- **Materials characterization.**
- **Device fabrication and development.**

The goal at the end of the program is to demonstrate both high brightness LEDs and CW room temperature laser diodes.

II.1 Materials Growth

The MOCVD epitaxial growth process as pioneered by Dupuis and co-workers has been applied to a wide variety of important III-V, II-VI, IV-VI and II-IV-V compound semiconductors. MOCVD is in world-wide use for the commercial production of compound semiconductor optoelectronic and electronic devices. Because of the commercial

Use or disclosure of the information contained on this sheet is subject to the restrictions on the title page of this proposal. This information is proprietary to the consortium.

suitability of MOCVD crystal growth to large area production, the primary emphasis of the program will be the investigation of MOCVD based GaN materials.

Currently, the highest quality nitride materials are grown at SDL, Inc. and the University of Texas at Austin. The material crystallinity of these materials, as measured by surface morphology, high-resolution transmission electron microscopy, high-resolution reciprocal-space x-ray diffraction mapping, and background carrier concentration, is substantially superior to any other material yet discussed in the literature or through the nitride bulletin board. The current state-of-the-art in GaN growth, at either SDL or UT , produces material with the following characteristics:

•X-ray rocking curve full-width at half-maximum (FWHM) of 27 seconds, external to the consortium, the best value is 85 seconds.

•Smooth epitaxial films, with full planarity achieved immediately.

•Low dislocation materials, with dislocation densities 1000 times lower than GaN grown by Nichia.

•Extremely low, n~2 x 10^{15} cm^{-3}, background carrier concentrations in undoped GaN materials.

These material advances lie along a critical path to the fabrication of reliable semiconductor devices, and will significantly improve the device performance as demonstrated by the Nichia Chemical Co. As will be discussed in detail within this proposal, the LED lamp of Nichia, although exciting, has several difficulties. A primary difficulty is a relatively short lifetime, with degradation observable almost immediately. The second difficulty with the current LED is that the optical recombination mechanism is based upon donor-acceptor recombination. For both LED operation with good color saturation and for any laser diode, a spectrally narrow recombination mechanism is required, i.e., an active region typified by direct band-to-band recombination. Finally, the compositions used in the Nichia diode span a limited range of the AlGaInN alloy composition range.

The role of dislocations in optical recombination processes in the nitride alloys is an ongoing research topic within the consortium. It is obvious that dislocations are less harmful to the operation of nitride devices than in comparable arsenide or phosphide devices, however, it is believed that dislocations still impair device performance. Dislocations may impair operation in the following ways: i) non-radiative recombination at or near dislocations, ii) gettering of impurities during the actual growth process, iii) impeding carrier motion.

Dislocation-free materials will be developed by pursuing growth strategies where (1) buffer layers and other epitaxially strategies produce a starting nitride layer free of dislocations and (2) all of the subsequent epitaxial layers are grown with a single lattice constant that matches the "seed" nitride layer. This epitaxial growth strategy uses quaternary layer structures to achieve this lattice matching. Thus, quaternary layer development is included within this proposal.

The achievement of dislocation-free structures will also be aided by the development of alternate substrate which more closely match the lattice spacing and thermal coefficients of expansion of the nitride alloys. These substrates include ZnO, 6-H SiC, bulk GaN, and hybrid substrates fabricated by vapor phase epitaxy.

To achieve a spectrally narrow output for the LED lamp and to achieve the optical gain required for the semiconductor laser, an active region that is typified by efficient band-to-band optical recombination must be developed. Furthermore, particularly for the LED, the

Use or disclosure of the information contained on this sheet is subject to the restrictions on the title page of this proposal. This information is proprietary to the consortium.

active regions developed must be capable of operation throughout the green and blue portions of the electromagnetic spectrum.

II.1.1 MOCVD Growth Development

The recent breakthroughs of the groups at SDL and UT are critical in setting the framework for the MOCVD development of this program. There are several critical MOCVD technologies to be developed within this program including i) the elimination of threading dislocations, ii) the development of lattice-matched quaternary AlGaInN materials, and iii) the development of efficient active regions typified by band-to-band recombination.

The epitaxial films for the UT-Austin portion of this program in a new state-of-the-art commercial Emcore Model GS3200 LP-MOCVD reactor system. This MOCVD growth system will be dedicated entirely to the growth of III-V nitrides and will be available for the growth of LED and laser device structures in this program. The Emcore reactor has a capacity for simultaneously growing highly uniform epitaxial films on up to three 2.0 in. dia. wafers. A diagram of this system is shown in Fig. 2.1.

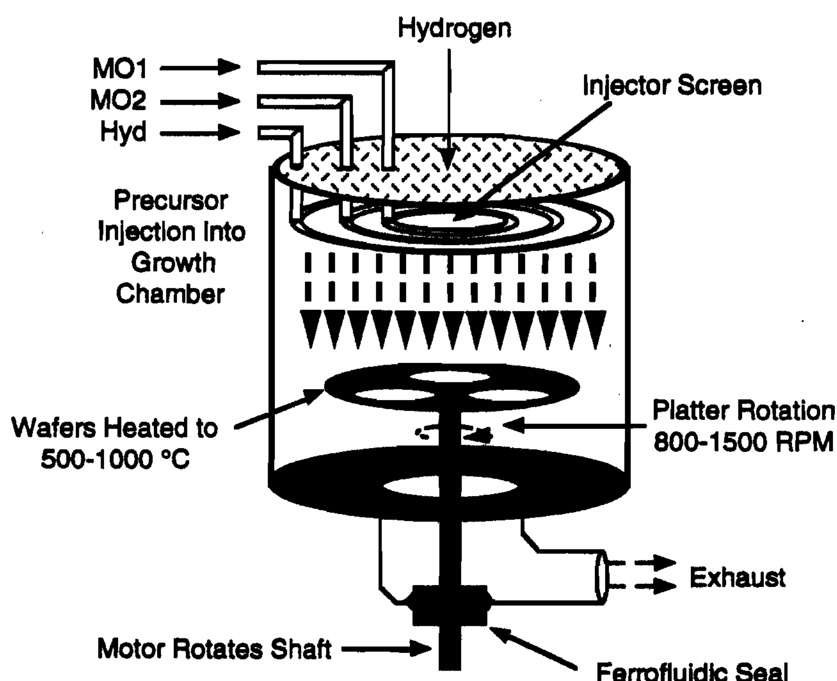

Fig. 2.1 Schematic diagram of the Emcore GS3200 LP-MOCVD reactor to be used for the low-temperature growth of InAlGaN epitaxial films.

Reactors of this type are widely used throughout the world for the production of AlGaAs-GaAs and InGaAsP-InP low-threshold injection lasers and high-efficiency AlInGaP-InGaP LED's, including at various US and Japanese companies, in particular, at HP Optoelectronics. The UT-Austin Emcore GS3200 system is similar to the design of the larger production-scale Emcore GS3300 system that Hewlett-Packard Optoelectronics Division presently has in operation for the growth of III-V heterostructure materials. These larger growth systems employ a 7 in. diameter wafer carrier that can accommodate up to seven 2.0 in. diameter wafers. The reactor in use at SDL is a vertical low-pressure reactor designed for the commercial laser diode fabrication. The differing reactor designs will be compared throughout the program to ascertain the dependence of nitride film quality upon specific reactor geometry. In addition, aspects of growth technology unique to the Nichia design, such as N_2 carrier gas flow, will be examined for efficacy in the program.

Use or disclosure of the information contained on this sheet is subject to the restrictions on the title page of this proposal. This information is proprietary to the consortium.

II.1.2 Visible Active Region Development

The bandgap of the binary GaN is 3.4 eV, thus, band-to-band recombination from GaN is not visible but in the ultra-violet portion of the electromagnetic spectrum. The achievement of an UV laser diode is desirable for many applications, however, active regions emitting in the blue and green portions of the visible spectrum are absolutely critical for visual applications. The emission of GaN may be extended into the visible by: (1) doping of the active region with acceptors and donors (Nichia), and (2) the use of an alloy active region, i.e., the addition of indium as a substitute for gallium or the addition of arsenic or phosphorous as a substitute for nitrogen. The latter approach leads to the formation of active regions under biaxial compressive strain.

The use of donor-acceptor (D-A) recombination to achieve optical emission is less efficient than direct band-to-band recombination. Furthermore, the emission exhibits a strong saturation effect. In current GaN based LEDs, the D-A recombination saturates at a current density of ~250 A/cm^2, as shown in the Section VII. Above this current level the emission shifts to a band-to-band transition which radiates in the near UV. Consequently, for the LED, the light output power saturates at relatively low drive current, thus limiting the output power achievable from the LED. In the laser diode, the D-A transition saturation prevents any possibility of stimulated emission. Therefore, for higher output power in an LED or for the high optical gain required for a semiconductor laser diode, efficient direct band-to-band recombination becomes a necessity.

Strained-layer alloy active regions are in wide use within commercial optoelectronic devices, however, the use of strained-layer technology in the fabrication of nitride materials is very immature. The active region of the current LED technology employs an InGaN active region, grown upon a GaN substrate, however, the indium content of the active region is limited to ~6%. Incorporation of higher levels of indium will be a focus of the research program. <u>In addition, a novel active region is suggested: a GaAsN strained-layer quantum well.</u>

The literature describes band-bowing effects in the ternary GaNP.[1,2] Extensions of this work have led to the prediction of large band-bowing parameters in the ternary GaAsN. In addition, TEM studies at Xerox of the GaAsN films grown at SDL have shown the incorporation of ~10% As in the GaN hexagonal matrix. This is sufficient to reduce the bandgap of GaN throughout the blue, green, yellow, and amber portions of the visible spectrum. The bandgap of GaAsN versus As content is shown in Fig. 2.2 .

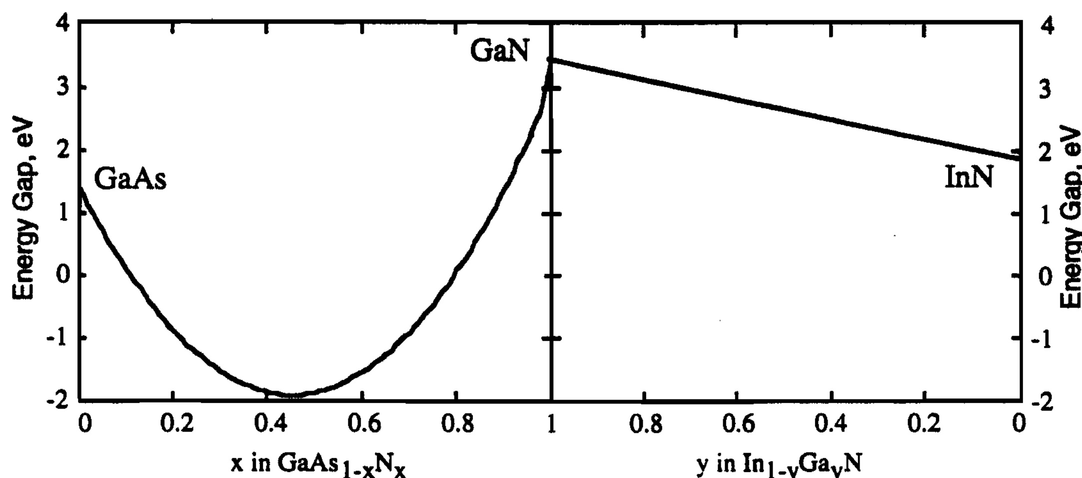

Fig. 2.2 The bandgap of GaAsN and InGaN.

The principal issues in designing the active region of either LEDs or laser diodes are (1) minimizing the bandgap of the active region and (2) maintaining the crystallinity of the

Use or disclosure of the information contained on this sheet is subject to the restrictions on the title page of this proposal. This information is proprietary to the consortium.

active region, i.e., not exceeding the active layer critical thickness. Thus, the bandgap as a function of strain is a figure of merit for any active layer alloy. For all values of strain, GaAsN has a substantially lower bandgap than InGaN. At a strain of 3%, where the critical thickness is ~100Å, the bandgap of GaAsN is ~ 2 eV (~600 nm, amber) while the bandgap of InGaN is still ~3 eV (~410 nm, a barely visible blue). The GaAsN active region is capable of extending nitride-based LEDs and laser diodes throughout the visible spectrum.

II.1.3 Substrate Development

In all epitaxial growth techniques, the quality of the epitaxial layers is closely tied to the crystallinity and thermal matching of the substrate. The ideal substrate for the growth of GaN is bulk GaN. However, at this point bulk GaN technology is incapable of offering substrates larger than ~2 mm in diameter. Furthermore, the issues associated with the development of bulk GaN substrates are extremely difficult. Due to the high risk/high payoff of the bulk GaN substrate issue, two substrate vendors have been selected to attack GaN substrate issue. During the first year, proof-of-concept and scalability will be demonstrated. In year two, a single substrate vendor is selected, with an accelerated funding rate.

In addition to the long-term investigation, this program addresses the short-term substrate needs of the consortium, i.e., for any given application, what substrate is best suited for the fabrication of high-quality epitaxial structures. Molecular beam epitaxy (MBE), with its attendant real-time in-situ growth monitoring, is ideal for evaluating the quality of the initial growth stages of nitride alloys on various substrates. Therefore, Boston University will evaluate the existing substrate technologies, i.e. sapphire, including m-plane, SiC (4-H and 6-H), ZnO, for which the consortium has identified a supplier, and "hybrid substrates" to be fabricated both at ATMI and Boston University.

It is useful to discuss these currently available options. Sapphire substrates may be considered a commodity item. SiC substrates, while readily available are priced 40X that for sapphire, thus hindering research efforts. Further, the quality of the SiC surface preparation, as examined by high-resolution TEM performed at Xerox PARC, is inferior to that of sapphire.

Another potentially suitable substrate is the aforementioned ZnO, where the lattice mismatch for GaN growth is 1.88%. The problems with ZnO as a substrate are that (i) there is a high equilibrium vapor pressure of Zn over ZnO at moderate temperatures, i.e., ZnO decomposes readily, starting at about 400 C, and (ii) ZnO is readily reduced upon exposure to hydrogen and/or ammonia at moderate temperatures. Surface passivation techniques were used in order for the ZnO to serve as a substrate. ZnO substrates currently are not available commercially. Good quality material has been grown in the past using hydrothermal growth techniques, but the processes were mothballed when it could not compete economically competing materials for acoustic wave applications. The consortium has access to these ZnO substrates and will evaluate their potential utility as a substrate material. Given positive research results within this program, ZnO could again become commercially available.

II.1.3.1 GaN Substrate Development

A recognized solution to the problems inherent in GaN heteroepitaxy is the development of a high-quality GaN substrate. The refractory properties of GaN which make it attractive for high-bandgap device applications also make it difficult to synthesize in large, single-crystal form. Additionally, GaN is impervious to hot acids and impervious to most hot bases. This makes any conventional surface preparation of GaN substrates for epitaxial growth extremely difficult.

II.1.3.1.1 American Xtal Technology

Recently, the High Pressure Research Center (HPRC) of the Polish Academy of Sciences, Warsaw, Poland has demonstrated the growth of high quality GaN single crystals by a gas pressure cell technique[3]. Although the originally-reported crystals were also only a few mm

Use or disclosure of the information contained on this sheet is subject to the restrictions on the title page of this proposal. This information is proprietary to the consortium.

in size, the group first reported and showed (at the Electronic Semiconductor Materials Symposium, San Jose, March 1994) platelet GaN single crystals with 1 cm dimensions. Although the surface morphology of the platelets was poor, X-ray Bragg diffraction studies at the Cu Kα-line demonstrated that the crystallographic structure of the platelets was reasonable good (FWHM 25-30 arcsec).

The platelet substrates which have been grown by the HPRC are degenerate n-type. For laser applications, it would be useful to have p-type semiconducting substrates also. For electronic applications, semi-insulating substrates offer significant advantages. The properties of GaN substrates and epitaxial materials were discussed in detail at the 8th International Conference of Semi-insulating III-V Materials in Warsaw, Poland (6-10 June 1994). No fundamental limitation to achieving semi-insulating, n-type or p-type single-crystal GaN substrates were identified, although the native defect properties of GaN are not thoroughly understood yet.

Under the present proposal, AXT proposes to the development of high quality substrates and the surface preparation techniques required for homoepitaxy. AXT will supply GaN substrates to the consortium for homoepitaxial growth of III-nitride compounds. The size and quality of substrates to be supplied will depend on the status of the development program with epi-ready substrates available late in the second year of the program.

Since conventional techniques of substrate preparation are not applicable to GaN, AXT proposes to explore unconventional methods of surface preparation. AXT will explore diamond turning and excimer laser processing. Diamond turning can be used for the initial polish of the surface with excimer laser ablation used for the final surface polish. AXT proposes to explore include cutting and dicing. Due to the high strength of the material, controlled cleaving of GaN substrates of any substantial thickness is expected to be difficult. Although we have experience of cutting ceramic AlN, which is more refractory and harder than GaN, with a diamond-coated wire saw, other techniques such as abrasive blasting or excimer laser scribing may provide a higher quality final surface for improved voltage hold-off and/or optical facets.

II.1.3.1.2 Advanced Technology Materials, Inc.

In this program, ATMI will examine a novel technique to produce low defect density GaN substrates. The key feature is the use of a sacrificial substrate which is removed from the deposited GaN layer at the growth temperature. This will eliminate the formation of defects wafer warpage or cracking resulting from differences in thermal coefficients of expansion. The dislocation density will be reduced by growing thick GaN layers (25-1000μm).

In addition to reducing the defect density, this sacrificial technique has several significant advantages. First, large diameter substrates can be produced, limited only by the size of available sacrificial substrates. For a silicon sacrificial substrate, this technique can produce GaN substrates greater than 10" in diameter. Second, the substrates are essentially epi-ready; no substrate fabrication, i.e. sawing and polishing, is required. Third, substrates of varying compositions and doping density can be easily produced because these parameters are controlled by the gas phase deposition process. The doping can easily be varied throughout the thickness of the substrate, for example to produce a heavily doped layer at the back for low resistance ohmic contacts. The dopant may be introduced either from the gas phase or by diffusion from the sacrificial substrate. And finally, many substrates can be produced simultaneously.

Efficient growth of GaN and removal of the sacrificial substrate requires a specially designed reactor. This reactor must be able to deposit GaN only on the front of the sacrificial substrate and not on the back. It must then be able to expose the back of the sacrificial substrate to a gas stream containing an etchant for the sacrificial substrate. If the etchant is selective, that is it will etch the sacrificial substrate but not the GaN, then both sides of the wafer may be exposed to the gas stream. If the etch is not selective, the reactor

Use or disclosure of the information contained on this sheet is subject to the restrictions on the title page of this proposal. This information is proprietary to the consortium.

may have to be designed to expose only the back to the etchant. Removal of the sacrificial substrate can be greatly eased by using a thinned substrate.

Figure 2.3 shows a schematic of a two chamber system that we will utilize for this growth technique. The two chambers are separated by a carrier that has holes in it the same size as the sacrificial substrate, as seen in Fig. 2.3a. Small tabs on the bottom of the carrier hold the substrate in place. GaN growth occurs in the top chamber. Growth proceeds both perpendicular to as well as parallel to the substrate surface. After several hundred microns of growth, the GaN will extend over the edge of the sacrificial substrate. This overhang helps provide a seal between the two chambers. Sealing is further enhanced during the growth step by keeping the pressures in the two chambers equal to minimize diffusion.

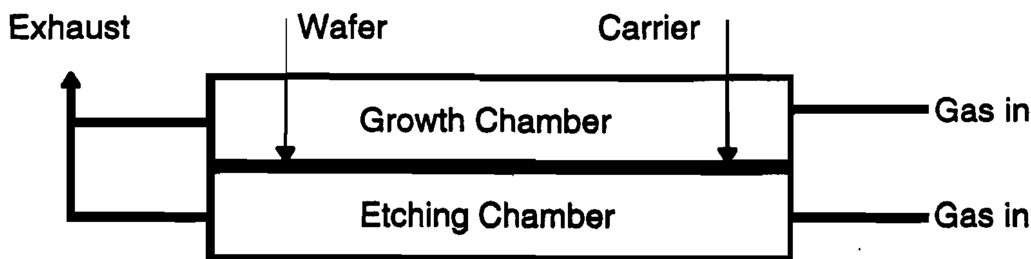

Fig. 2.3 Schematic of two-chamber growth system.

When the GaN growth is completed, the system is represented by Fig. 2.4. Without reducing the temperature, the etchant species is introduced into the lower chamber. The sacrificial substrate is etched away, leaving the GaN substrate sitting in the recess of the carrier as shown in Fig. 2.4c. During the etching sequence, cross-diffusion is minimized by keeping the pressure in the upper chamber slightly higher than in the lower chamber. The carrier can then be withdrawn to unload the system. It is clear that this or a similar system can be scaled up to grow on many substrates simultaneously.

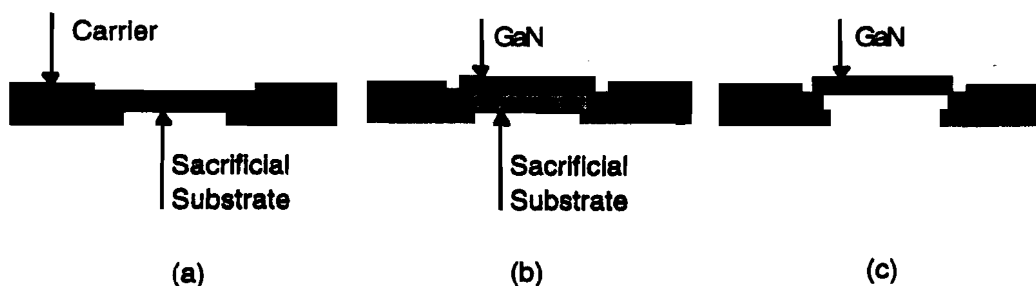

Fig. 2.4 Schematic of wafer carrier showing (a) sacrificial substrate at start of growth, (b) GaN grown on sacrificial substrate and (c) GaN substrate after removal of sacrificial substrate.

Growth of GaN

The GaN will be grown using vapor phase epitaxy (VPE) in which HCl is reacted with Ga and NH_3 in a hot wall system. VPE is chosen over metal-organic vapor phase epitaxy (MOVPE) because of the lower cost of the precursors and the ability to scale to larger systems.

Silicon Etching

Gas phase silicon etching is a well established procedure in the fabrication of silicon microcircuits. It is commonly performed using gases such as HCl or SF_6 in H_2 at elevated temperatures. Silicon can be etched using HCl over a wide range of temperatures, 700-

Use or disclosure of the information contained on this sheet is subject to the restrictions on the title page of this proposal. This information is proprietary to the consortium.

1200°C. Since typical GaN growth temperatures are around 1000-1100°C, it is clear that we will be able to etch the silicon at the same temperature used for GaN deposition.

II.1.3.2 Alternate Substrate Development

A parallel effort at Boston University will prepare and evaluate alternate substrate preparation and subsequent growth technology. The growth system of Boston University, a molecular beam epitaxy machine with an electron cyclotron resonance nitrogen source (ECR-MBE) is used to study the nucleation and growth kinetics on the alternate substrates. ECR-MBE is ideal for this task due to the extensive in-situ monitoring capabilities contained on the machine, allowing real-time evaluation of film growth.

•Hybrid GaN substrates: These substrates will be grown at Boston University using the hydride VPE method. In this method, the GaN is formed by the reaction of GaCl with NH3 and has been reported to have high growth rates (> 100 mm/hr.). The films will be grown on sapphire substrates, coated first by the method of sputtering with (0001) oriented films of ZnO. The sapphire substrates will be separated and reused by dissolving the ZnO with NaOH. The produced GaN wafers (1-2 inches in diameter and 0.5-1.0 mm thick) will be used in the epitaxial growth of III-V nitride thin films and junctions by the MBE and MOCVD method.

•Bulk ZnO substrates: ZnO has a wurtzite structure, like that of III-V nitrides, and a lattice constant of 3.25 Å. Thus this substrate can be used to fabricate lattice matched heterostructures out of the In-Ga-Al-N family, with energy gaps varying from 2.7 to 4.5eV. As previously mentioned, a source for such substrates has been identified.

•M-plane (1100) sapphire substrates: This substrate has the smaller lattice mismatch (about 2.6%) compared to the C-plane and R-plane sapphire. There is one report in the literature which shows that without either a GaN or AlN buffer, GaN films grown on this substrate have the best surface morphology and photoluminescence, and good electrical properties.[5]

II.2 Analysis of Critical Materials Issues

Xerox PARC proposes to conduct basic materials studies on III-V nitrides and their alloys in support of the development of these materials for optoelectronic applications. There are three general objectives of these studies: (1) to provide timely feedback information on the properties of these materials to assist other members of the Consortium in optimizing growth and processing for high-performance devices, (2) to contribute to the determination of key materials parameters and the identification of key processing strategies for fabricating these devices, and (3) to make major contributions to the fundamental understanding of these materials in order to establish the scientific underpinnings for emerging high-bandgap optoelectronic technologies. These objectives will be pursued in close coordination with the other members of the Consortium.

II.2.1 Crystallinity and Device Performance

In all III-V materials, a close link between dislocation density and optoelectronic device performance has been observed. Fig. 2.5 shows the optical recombination efficiency versus dislocation densities for a number of III-V binary and ternary compounds. The observed trend is that a reduction of dislocation density in III-V semiconductors raises the optical recombination efficiency. Second, the figure shows that dislocations are worse in some compounds than in others.

Because of the good performance of the Nichia LED, a device with a high dislocation density, some members of the nitride community believe that dislocations, and poor crystal quality, have no deleterious role in nitride device physics. However, specific effects of dislocations are unknown, i.e., the performance of dislocation-free nitrides has never been measured. From Fig. 2.4 and extensive experience at HP and SDL with optical recombination processes, it is anticipated that low-dislocation nitride materials will have dramatically improved optical and electrical performance.

Use or disclosure of the information contained on this sheet is subject to the restrictions on the title page of this proposal. This information is proprietary to the consortium.

In all other III-V alloys, dislocations impact device performance in other areas including:

•Carrier mobility degradation,

•Dopant gettering at dislocations, reducing dopant activation,

•Degradation of planar growth, and

•Reliability degradation.

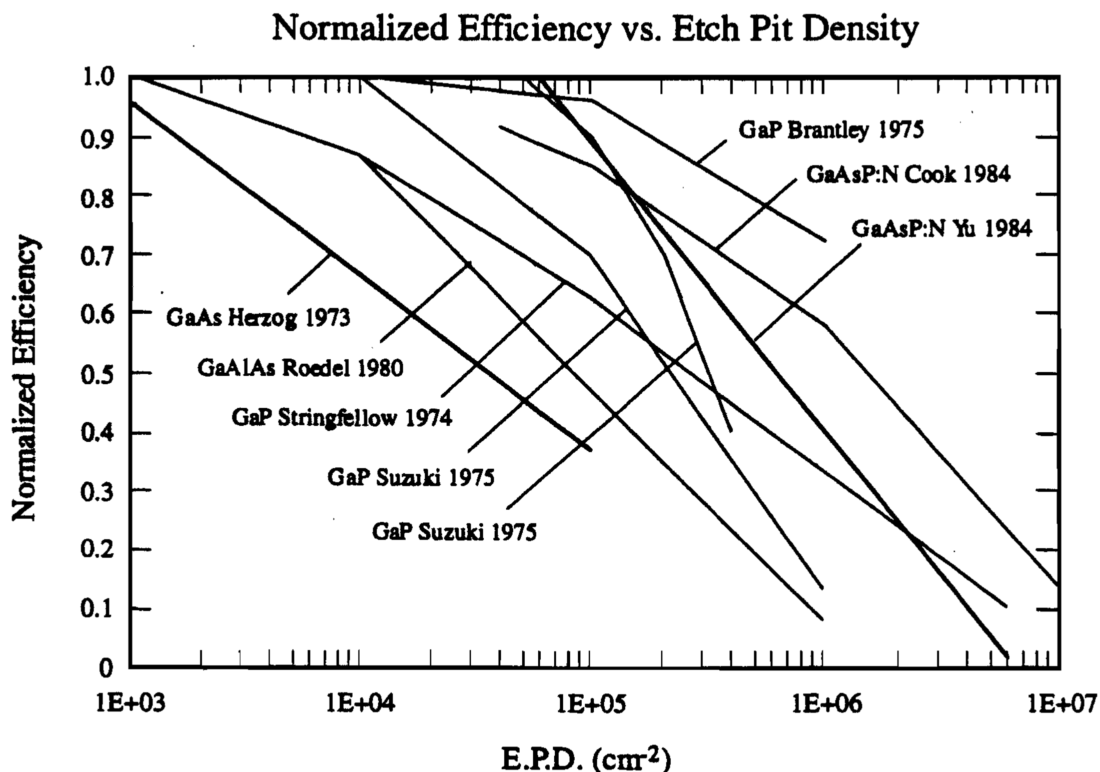

Fig. 2.5 Efficiency versus dislocation density in III-V semiconductors.

Dislocation elimination and understanding the impact of dislocations upon nitride performance are central to this proposal and will lead to the demonstration of significant device performance improvements.

II.2.1.1 High Resolution X-Ray Diffractometry

To achieve rapid advances in materials growth, convenient characterization techniques must be employed. X-ray diffractometry is commonly used to assess the crystallinity of films. For the films commonly grown in the nitride community, i.e., with X-ray FWHM of hundreds of seconds, relatively unsophisticated X-ray techniques may be employed. For films of higher crystallinity, sophisticated X-ray techniques can provide substantial information concerning variations in lattice spacing within the epitaxial layer and also measure the mosaicity of the sample. Simply stated, mosaicity is a measure of the amount of tilt in local areas of the crystalline structure. A high degree of mosaicity indicates poor nucleation leading to 3-dimensional growth, thus high resolution X-ray studies will be used to further optimize buffer layer nucleation and crystallization.

Use or disclosure of the information contained on this sheet is subject to the restrictions on the title page of this proposal. This information is proprietary to the consortium.

A schematic of the high resolution X-ray system is shown in Fig. 2.6. The X-ray source is collimated with a four germanium crystal monochromator having beam dispersion of 2-3 arc second. The sample serves as the fifth crystal. The beam exiting the sample is passed through a triple axis optic with a double bounce germanium crystal and collected with a standard X-ray detector. As shown is the prior work section, this enables reciprocal space mapping of the diffracted spot, allowing a separation of lattice parameter variation from mosaicity effects. This provides a key analytic tool required for characterization of the very high quality films grown within the consortium.

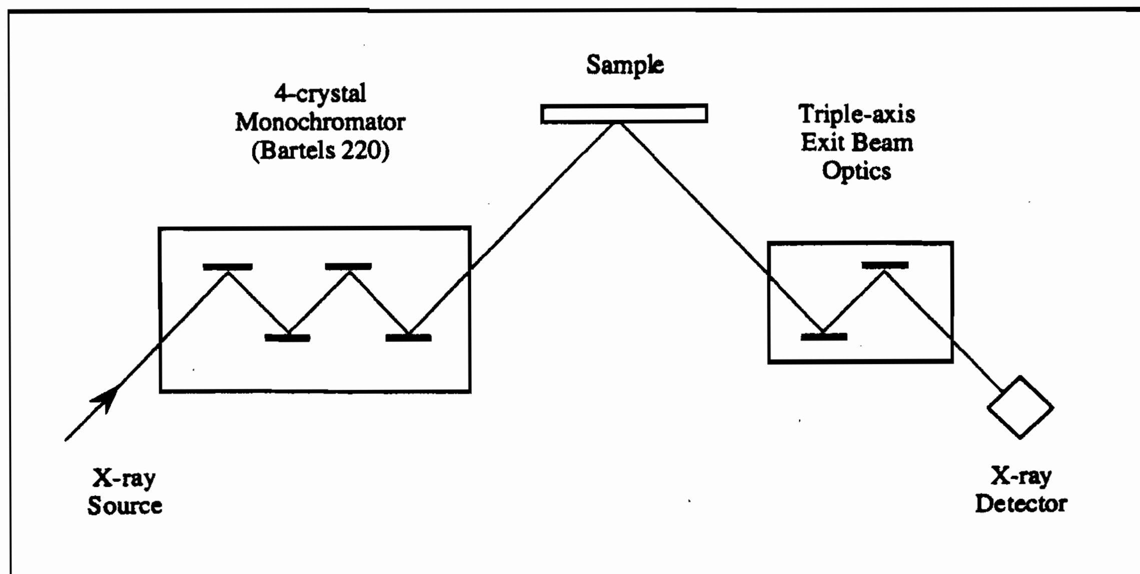

Fig. 2.6 A schematic of the X-ray reciprocal-space mapping system.

II.2.1.2 Transmission Electron Microscopy

The fundamental quality of the epitaxial film is dictated within the first few monolayers of growth. Therefore, understanding the initial substrate/film interface is important. The initial stages of growth are regulated by the quality of the thin buffer layers used as nucleation layers in GaN growth. Prior to the SDL/Xerox/UT collaborative effort the development of buffer layer technology was based on trial-and-error methods. Because of this approach, the crystallinity of most nitride films has been relatively constant, at 100-400 arc seconds, for a number of years. The on-going MOCVD/TEM consortium collaboration has resulted in rapid improvements in the general crystallinity of nitride films, ultimately yielding films with low dislocation densities and narrow X-ray rocking curves, FWHM 27 seconds, which are superior to any other epitaxial nitride film; indeed the consortium epitaxial nitride films now approach the crystallinity of the bulk nitride films grown at the HPRC in Poland.

Within the program, the detailed study of the interface structure of GaN thin films grown on various substrates such as sapphire, SiC and ZnO will be expanded. These studies involve high-resolution cross-section transmission electron microscopy (TEM) and modeling of the atomic bonding at the interface.

As the program advances to the construction of heterostructures, the understanding of the mechanisms of strain relaxation due to lattice mismatch will become essential for the design of heterojunctions in the AlGaInN system. Of particular interest are misfit dislocations on the basal plane, their separation into partials with stacking faults, and in the relationship with threading dislocations.

Dislocation densities may be a limiting factor in the production of high quality materials for laser applications. The consortium is currently monitoring threading dislocation densities

Use or disclosure of the information contained on this sheet is subject to the restrictions on the title page of this proposal. This information is proprietary to the consortium.

via cross-sectional TEM characterization, however, this technique is rapidly becoming of limited utility as the dislocation density of high-quality nitride films drops below the detection limit of cross-sectional TEM characterization. Therefore, plan-view TEM, etching and X-ray topography are now being integrated into the characterization of more modern nitride films.

II.2.2 Electrical and Optical Properties

II.2.2.1 Optical Deep Level Transient Spectroscopy

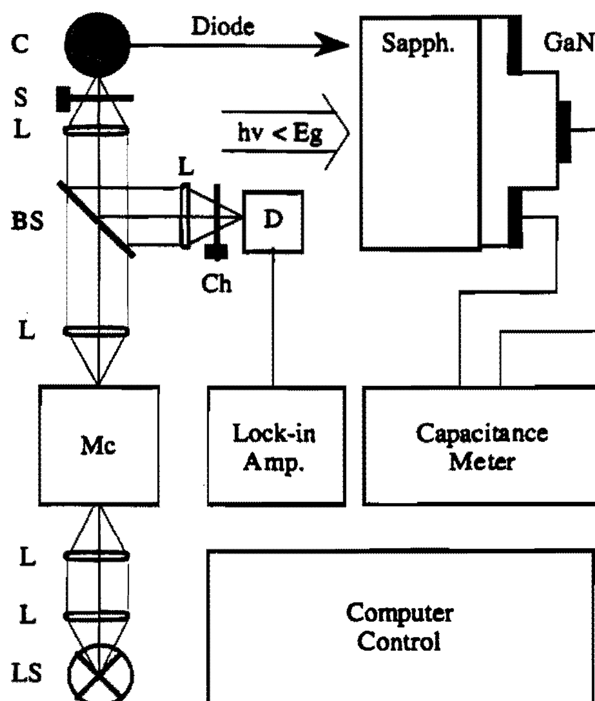

Fig. 2.7. **Apparatus for photoemission DLTS on III-V nitrides. Subbandgap photons are used to emit charge from deep levels in the depletion layer of a Schottky diode at low temperature, with the transitions detected by a time-varying capacitance. The components are labeled as follows: light source LS, lens L, monochromator Mc, beam splitter BS, shutter S, cryostat C, chopper Ch, and detector D.**

Deep levels can degrade device performance by introducing competing recombination channels for injected free carriers. Characterization and identification of deep level defects will be performed with two forms of deep level transient spectroscopy (DLTS). Conventional DLTS, which utilizes thermal energy for charge emission, will be used to characterize deep levels, but is limited to within approximately 0.8 eV of the band edges,. To overcome this limitation, we have developed an apparatus for photoemission DLTS on wide bandgap semiconductors (Fig. 2.7). In combination with other techniques, such as PL, we expect to achieve a detailed understanding of the nature and kinetics of deep-level luminescence centers in the III-V nitrides and their alloys. The DLTS techniques will also be applied, in combination with TEM, to determine whether dislocations introduce deep levels in these materials.

Use or disclosure of the information contained on this sheet is subject to the restrictions on the title page of this proposal. This information is proprietary to the consortium.

II.2.2.2 Photoluminescence and Photopumping

The routine study of the photoluminescence (PL) and optical characteristics of the epitaxial layers in this program will be made at HP, SDL Inc, Xerox, and also at UT and BU. It is essential that each of the organizations with growth responsibilities have a rapid-turn-around PL materials evaluation capability so that results can be used in the optimization of growth conditions on a timely basis. In addition, detailed optical studies will be carried out at specific laboratories in the consortium that have specific specialized capabilities.

Photoluminescence (PL) techniques will be used to characterize the radiative recombination. Both low-temperature and time-resolved measurements will be performed. As a routine characterization technique, the PL intensity of selected emission bands provides a quick and convenient relative measure of material quality. As a research instrument, PL will be used to distinguish among the several channels of recombination, i.e., band-to-band transitions, bound exciton transitions, donor-acceptor pair transitions, and transitions to deep states, to determine phonon coupling , and to determine transition lifetimes. Given the range of PL emission bands that have been previously reported for heteroepitaxial GaN (i.e., band-edge, near band-edge, and deep-level transitions), it is anticipated that a comprehensive PL study will yield invaluable information for improving material quality and eliminating parasitic radiative.

Time-resolved PL studies, photoluminescence-excitation (PLE) measurements, and optical pumping studies of epitaxial films and laser structures will be performed with the system shown schematically in Fig. 2.8. This high-performance laser system permits PLE and PL measurements in bulk, DH, and quantum-well samples in the AlGaInN system. The system will be used to photopump single layers and heterostructures at temperatures ranging from 4.2 K to 300 K to evaluate the crystal quality of materials through the study of the fundamental optical transition energies in these materials due to both intrinsic and extrinsic processes.

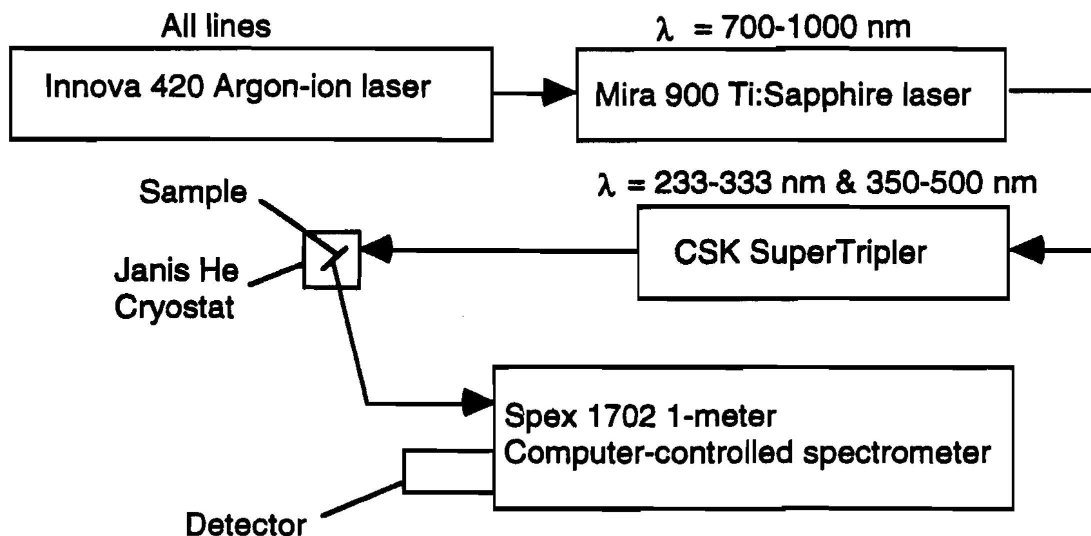

Fig. 2.8 Schematic diagram of tripled femtosecond Ti:Sapphire UV laser system

In addition to the characterization of "bulk" optical properties of these materials, detailed information can be obtained about bound exciton states, carrier lifetimes, heterostructure interface recombination velocities, and impurity bands. Selected samples will be optically characterized via variable-temperature photopumping to access the characteristics of stimulated emission in the nitride alloys. Samples will be characterized by pumping at 77K

Use or disclosure of the information contained on this sheet is subject to the restrictions on the title page of this proposal. This information is proprietary to the consortium.

and 300K to evaluate the heterostructure quality. The information gained will be a guide for the design of injection lasers.

the band offsets in these wide-bandgap materials. While theoretical and experimental data for the bandgaps of these binary and ternary materials is available, not much (if anything) is currently experimentally known about the band alignments in heterostructures in the InAlGaN system. We propose to make detailed studies of the PL of low-temperature QW heterostructures in this system and internal photoemission measurements to determine the conduction band and valence band offsets. These measurements will be correlated with theoretical calculations and photoemission data. These results will be important for the design and realization of low-threshold lasers and high-efficiency LEDs.

II.2.3 Electrical Conductivity in Nitride Alloys

A hurdle to the realization of high-performance optoelectronic devices will be the ability to controllably achieve high p-type doping. In Mg-doped GaN grown by MOCVD, activation of acceptor dopants (e.g., Mg and Zn) requires either low-energy electron beam irradiation (LEEBI) or thermal annealing, or a combination of the two. The formation of acceptor-H complexes under the presence of hydrogen during the MOCVD growth is likely responsible for the need for a post-growth activation. The understanding *and control* of the compensation of p-doped GaN is a significant part of the program.

High dislocation densities may impact impurity incorporation, distribution, and activation. The very high quality of the nitride films, as measured by dislocation densities and x-ray rocking curve FWHMs, grown within the consortium will allow the separation of properties *intrinsic to the nitride alloys* from the consequences of poor crystallinity.

II.2.3.1 P-type Nitride Alloys

Workers in Japan have published data describing the successful MOCVD growth of p-type GaN using Mg doping.[6] In the first report of p-type GaN:Mg on a AlN buffer layer, Amano et al, used Mg-doping in MOCVD-grown GaN films to dope the films with acceptors. After growth, the GaN layers were annealed using low-energy (5 keV) electron beam irradiation (LEEBI). After irradiation, the layers showed p-type behavior with a resistivity of 0.2 Ω-cm.[6] In other work, Nakamura, et al, grew p-type GaN:Mg films on GaN buffer layers made conductive with post-growth thermal annealing at ~700°C for 20 min. These results show promise for the achievement of low-resistivity p-type AlInGaN alloy films grown by MOCVD. Other workers have speculated that the process of annealing (either by thermal treatment alone or in conjunction with LEEBI) can reduce the H-ion content of films, which contributes to the reduction of the compensation in p-type wide-bandgap semiconductors.[7] Note that LEEBI produced only a thin layer of "p-type" material ~500 nm thick, while thermal annealing produced p-type conduction throughout the Mg-doped GaN epitaxial layer.

Our initial approach will be to study the thermal and electron-beam induced dissociation kinetics for activation of acceptor impurities. An effective experimental technique to obtain phenomenological parameters for such dissociation processes involves the use of capacitance-voltage measurements to monitor in situ the recovery of dopants in the depletion layer of a diode as the dopant-impurity complexes are thermally dissociated; the technique will be extended to examine electron irradiation. Such studies will identify (1) the microscopic mechanism responsible for low p-type doping efficiencies in MOCVD-grown GaN, (2) the mechanism utilized in the LEEBI technique, and (3) processing strategies that will maximize p-type doping efficiency. Electron and hole concentrations and their mobilities will be characterized by variable-temperature Hall effect measurements, which also provide information on charge scattering processes and dopant activation energies. These measurements will be supplemented with capacitance-voltage measurements (variable temperature and ac frequency) on current rectifying devices. SIMS studies will be used to determine the actual concentrations of dopant atoms incorporated under different growth conditions.

Use or disclosure of the information contained on this sheet is subject to the restrictions on the title page of this proposal. This information is proprietary to the consortium.

The thermal annealing facilities required for the dopant activation experiments are in place at all facilities. During this program, p-type dopants and growth/post-growth procedures for AlInGaN alloys will be established to produce low-resistivity p-type materials. In Year II these results will be furthered and utilized for the construction of improved injection electroluminescent devices. Again, it is critically important to the growth of dislocation-free materials for these measurements to be meaningful.

In most MOCVD nitride systems, the background doping level of GaN is heavily n-type. The high background level interferes with p-type doping and is not desired. In GaN grown within the consortium, the background dopant level is $\sim 2 \times 10^{15}$ cm^{-3}. This level is a significant indication of the MOCVD capability of the consortium, since the control of the background doping level is tied to precise control of the III-V ratio in the gas phase, the growth temperature and the cleanliness of the MOCVD reactor. Although a complete discussion of the defects/contaminants in MOCVD GaN is beyond the scope of this text, a brief discussion of the current scientific difficulties with this issue is warranted.

It has been proposed that the dominant n-type behavior of the III-V nitrides is primarily due to native defects, namely, N vacancies.[8] This analysis has been called into question since Khan, et al.[9] An alternative explanation for these effects could be due to background C and O incorporation into the films grown at different temperatures. As was pointed out by Jenkins and Dow in 1989, the effects of defects and contaminants can be critically important in the realization of low-resistivity p-type AlInGaN films.[10] Dupuis has also seen defect-related doping effects in the growth of AlGaAs-GaAs injection lasers on Si substrates.[11] The LP-MOCVD systems to be used in this program have been specially constructed to eliminate O contamination with high-purity proprietary sources used to reduce unintended dopant incorporation.

II.2.3.3 Ionic Bonding in Nitride Alloys

Compared to conventional III-V arsenides and phosphides, the character of atomic bonding in the nitrides is highly ionic. The importance of this was first pointed out by Kurtin, McGill, and Mead in 1969.[12] Based on a wide variety of empirical evidence they described a fundamental transition in the electronic nature of solids. It was shown that valence band excitations (holes) are expected to be much more localized in III-V nitrides than they are in more covalent semiconductors. This localization affects the electronic and optical properties of the materials.

Specifically, ionic semiconductors such as GaN are expected to show limited Fermi level pinning at their free surfaces. That is, any states associated with the surface are either few in number or energetically located outside the energy gap of the material. As a consequence, ohmic contacts to n-type materials should be relatively simple to make using low work function metals such as In, Al, or Ti. Indeed, we have already fabricated non-alloyed ohmic contacts to n-type GaN using a TiAl composite contact. Ohmic contacts to p-type GaN are expected to be more difficult, though ohmic AuNi contacts have been demonstrated by Nichia Chemical.

Another implication is that hole mobilities may be low in GaN. In fact, with the exception of one literature report, which has been widely disputed in the nitride community, hole mobilities have been reported to be less than 10 cm^2/V-sec. This is clearly important in the design of LED or laser structures, dictating that the current path through the p-type layers must be kept very short.

Finally, it is recognized that dislocations and other extended defects can sometimes behave like internal surfaces within semiconductors. If surface states are less important in ionic materials it follows that dislocations and other defects may be more benign than they are in covalent materials such as GaAs or InP. This is certainly born out by the fact that the LEDs produced by Nichia Chemical have dislocation densities in excess of 10^{10} cm^{-2}. However, even if dislocations are more benign in the nitrides, they impose an upper limit on the efficiency of visible LEDs made from every other material system. Their role in limiting the

Use or disclosure of the information contained on this sheet is subject to the restrictions on the title page of this proposal. This information is proprietary to the consortium.

efficiency and lifetime of laser diodes is also well documented. Therefore, we believe that substantial improvements in epitaxial material growth will be needed before GaN devices can be fully exploited on a commercial basis.

II.2.4 Heterojunction Development

All commercial laser diodes and high-efficiency LEDs are formed of layered structures that are optimized to produce high quality materials of varying refractive index and bandgap *while maintaining a common epitaxial lattice constant.* By maintaining an invariant lattice constant throughout the crystal, a dislocation-free crystal may be grown. The only exception to this rule is the usage of strained-layer quantum well active regions, however, strained-layer active regions are grown with thicknesses less than the so-called critical thickness and therefore introduce no new dislocations. As described throughout this text, dislocations and defects in III-V materials can interfere with conduction processes, dopant activation and optical recombination and significantly degrade the reliability of an optoelectronic component.

The ternary materials AlGaAs and AlGaP, where Al and Ga are nearly the same size in the crystal lattice, are nearly lattice-matched across their entire compositional range. However, AlGaN is not an inherently lattice-matched system with ~3% mis-match from AlN to GaN. Therefore, to grow nitride alloy heterostructures, as needed for high-performance optoelectronics, requires by definition quaternary alloy development. In this section of the proposal, an overview of the heterostructure systems available in the AlGaInN system is presented.

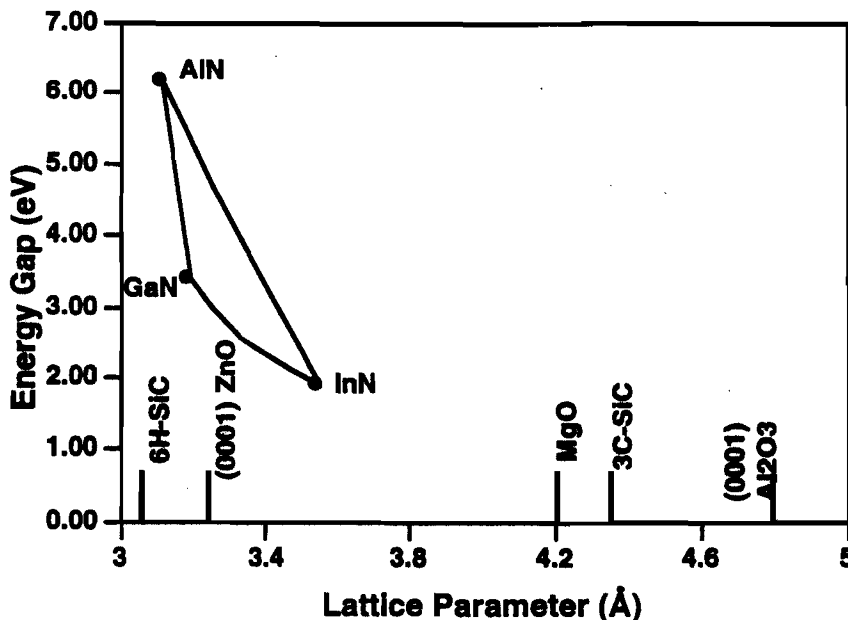

Fig. 2.9 **Dependence of the energy gap, E_g, upon lattice parameter, a_o, for materials in the Al-In-Ga-N system; also indicated are the lattice constants for some commonly used substrates.**

The dependence of the energy gap upon the lattice parameter of materials in the Al-In-Ga-N system are shown in Figure 2.9, along with the lattice parameters of several possible single-crystal substrates, e.g., α(6H)-SiC and (0001) Al_2O_3. Important physical properties of the III-V nitrides are listed in Table 2.1. Note that AlInGaN films grown on α(6H)-SiC substrates will be under tension and that a range of compositions can be grown lattice-matched to (0001) ZnO. Several approaches to reducing the dislocation density and strain in the epitaxially grown films will be evaluated, as discussed below. One possibility is the use of low-temperature GaN buffer layers. As discussed more fully below, the groups at

Use or disclosure of the information contained on this sheet is subject to the restrictions on the title page of this proposal. This information is proprietary to the consortium.

SDL and UT-Austin have recently produced the highest quality heteroepitaxial films of GaN using (0001) Al_2O_3 using at low-temperature GaN buffer layer.

Dupuis has done extensive research in the heteroepitaxial growth of GaAs on (100) Si substrates where the lattice mismatch is approximately +4%.[13-15] Many of the considerations that apply to the growth of GaAs/Si are also relevant for the growth of Al-Ga-In-N semiconductors on lattice-mismatched substrates such as those listed in Table 2.2. For the case of lattice-mismatched heteroepitaxy, it is advantageous to be able to grow films at lower temperatures since the strain in an epitaxial layer at room temperature can be directly related to the lattice mismatch at the growth temperature and the differential coefficient of linear thermal expansion, $\Delta\alpha_T$, between the substrate and the film. It is desirable to use a film/substrate combination for which the layers are not only lattice-matched but which also have similar coefficients of thermal expansion. A comparison of the α_T data of Tables 2.1 and 2.2 shows that both α-SiC and α-ZnO have thermal expansion coefficients that are much closer to the experimentally determined values for AlN and GaN than does sapphire. It is expected that InN will have a similar value for α_T. As a result, epitaxial films in the AlInGaN system grown on SiC or ZnO substrates will have less residual strain due to differential thermal expansion than for $AlGaInN/Al_2O_3$ films.

Table 2.1 Properties of Wurtzite Binary Compounds in the Al-Ga-In-N System‡

Material	Eg (eV; nm)	a (Å)	c (Å)	n†	αT (106 K^{-1})*
AlN	6.2; 200	3.104	4.978	2.20[a]/1.95[R19]	5.6[c]
GaN	3.5; 354	3.180	5.178	2.29[a]/2.5[b]	5.6[R11]
InN	2.2; 563	3.533	5.705	2.24[a]	not known

‡ Data from Ref. R10 except as indicated.
† Measured near the band edge.

* Measured for "a-axis" in the temperature range 300 - 1273 K.

[a] Calculated values from W. A. Harrison, *Electronic Structure and the Properties of Solids,* (W. H. Freeman & Co., San Francisco, CA, 1980.), p. 114, 115.

[b] D. D. Manchon, A. S. Barker, P. J. Dean, and R. B. Zetterstrom, Solid State. Commun. 8, 1227 (1970).

[c] M. Neuberger, *Handbook of Electronic Materials, Vol. 2, III-V Semiconducting Compounds,* IFI/Plenum, New York, 1971), p. 18.

Table 2.2 Properties of Possible Substrates for Epitaxy in the Al-Ga-In-N System‡

Material	Orientation	Structure	E_g (eV)	a (Å)	c (Å)	α_T ($10^6 K^{-1}$)*
α-Al_2O_3	(0001)	rhombohedral	> 6	4.76	12.99	8.8[a]
α(6H)-SiC	(0001)	wurtzite	2.86	3.0865†	15.11†	4.7[a]
α-ZnO	(0001)	wurtzite	3.2	3.250	5.207	4.3

‡ Data from *CRC Handbook of Chemistry and Physics,* R. C. Weast, ed. (CRC Press, Boca Raton, Fl, 1983) except as indicated.

* Measured for "a" axis over the range 300-1273K.

† C. M Wolfe, N. Holonyak, Jr., and G. E. Stillman, *Physical Properties of Semiconductors,* (Prentice Hall, Englewood Cliffs, NJ, 1989), p. 340.

[a] W. D. Kingery, H. K. Brown, D. R. Uhlmann, *Introduction to Ceramics, Second Edition* (John Wiley & Sons, New York, 1976), p. 594.

Probably the most important single recent contribution to the improved growth of AlGaN has been the use of low-temperature buffer layers for heteroepitaxial growth of GaN and AlGaN alloys on sapphire and other substrates.[16] The first reports of the improvement of GaN/Al_2O_3 films using low-temperature buffer layers was made by Amano, et al, in 1986.

Use or disclosure of the information contained on this sheet is subject to the restrictions on the title page of this proposal. This information is proprietary to the consortium.

In retrospect, this work should be "obvious" to anyone familiar with the area of GaAs on Si because this same approach was used in the first demonstration of improved heteroepitaxial growth of GaAs on (100) Si substrates. It is not surprising that many of the same "tricks" can be used for both types of heteroepitaxial growth for, in many respects, the major problems, i.e., lattice and expansion coefficient mismatch, are the same. In the proposed program, work on various schemes for the growth of dislocation-free, lattice-matched heterostructures will be undertaken.

As mentioned above, the use of alternate "nearly lattice-matched" substrates will be studied extensively. For example, as indicated in Table 2.2 and shown in Fig. 2.3, α(6H)-SiC has a wurtzite lattice structure with a (0001) growth plane that has an "a" lattice parameter of 3.087 Å corresponding to a lattice mismatch of $\Delta a/a_0 \sim -3\%$ relative to GaN and ~ -2% for AlN. This is to be compared with a measured lattice mismatch for GaN on α-Al_2O_3 (which is rhombohedral) of $\Delta a/a_0 > \sim 18\%$. This is a significant improvement of over an order magnitude of reduction in the mismatch. Furthermore, it is important to note that the films will be under compression instead of tension. This could significantly alter the dislocation density and defect structure of GaN/SiC films relative to GaN/Al_2O_3 films.[17] We will explore these effects and compare the results with GaN/ZnO films (which will be under tension) where the mismatch is ~+2%. It is also interesting to note that $Ga_{0.8}In_{0.2}N$ alloys can be grown which are lattice-matched (at 300K) to ZnO. This alloy has a calculated energy gap of $E_g \sim 3.1$ eV (~400 nm) and would be a possible candidate for the active region of a UV semiconductor laser. In addition, calculations of the electronic structure and donor and acceptor energy levels of the AlGaInN alloys show that both p- and n-type doping should be possible in these ternary systems, suggesting that low resistivity layers required for efficient injection luminescence should be achievable.[10]

It should be noted that our experience with the growth of InGaAs and InGaAsP lattice-matched to InP has shown that somewhat better epitaxial layers can be obtained by growing films lattice-matched to the substrate *at the growth temperature* instead of at room temperature. Because of the differential coefficient of linear expansion between the film and the substrate, cooling from the growth temperature to 300K can contribute to some additional strain in the epitaxial layer. It is also relevant to consider the improved performance of strained-quantum-well lasers in the AlGaAs-InGaAs-GaAs system. These results suggest that some strain in the laser active region may be desirable. We will study these effects in the nearly-lattice-matched film/substrate systems and determine the optimum alloy compositions which can be grown.

Another significant feature of the proposed research program is the growth and characterization of AlInGaN quaternary epitaxial layers. It is well known that the growth of lattice-matched quaternaries of InGaAsP (for long wavelength infrared as well as visible red lasers) and AlGaInP (for short-wavelength red and yellow lasers) has resulted in the demonstration of high-performance lasers in wavelength ranges for which there is no corresponding lattice-matched ternary composition in these systems.[18] In fact, most of the current technological and commercial developments in the area of semiconductor injection lasers today are focused on the growth of quaternary laser active regions in these systems. While only recently has a limited report of the growth of AlInGaN quaternary alloys been made[19], the ternaries AlGaN[20] and GaInN[21] have been grown throughout the entire composition range and it is known that there are no fundamental reasons why well-behaved quaternary alloys should not exist. In fact, as shown above in Figure 2.9, the bandstructure calculations for the GaInN and AlInN ternaries show well-behaved conduction bands as a function of alloy composition.[10] Combining the available experimental and theoretical data for the three ternaries, AlGaN, GaInN, and AlInN, we expect that the entire parameter space of composition vs. lattice constant for the AlInGaN quaternary can be calculated with good accuracy. Using these calculations, lattice-matched quaternaries with different compositions and energy gaps can be grown.

Use or disclosure of the information contained on this sheet is subject to the restrictions on the title page of this proposal. This information is proprietary to the consortium.

In summary, the ternary and quaternary alloys of GaN will be developed throughout this research program, leading to the fabrication of dislocation-free nitride alloys, the foundation of high-performance optoelectronics.

II.3 Device Development

The program consists of two efforts: the LED effort of HP with the goal of rapid introduction of blue LEDs, and the laser diode effort with the goal of demonstrating CW operation of an injection laser diode by the conclusion of the program. In this section of the proposal, basic device considerations are outlined.

II.3.1 Laser Design and Processing

II.3.1.1 Optical and Electronic Confinement

The design of optimized low-threshold heterojunction semiconductor lasers and high-efficiency LED's will be guided by the already established principles for high-performance III-V heterostructure lasers. The key features of the required device structure are the confinement of the optical field to the waveguide layer(s) in the direction normal to the junction plane and the confinement of injected carriers to the active region. The confinement of carriers and the optical field can be readily accomplished in the InAlGaN system through the use of the lattice-matched ternary and quaternary alloys. Using the experimentally determined values of the index difference, Δn, and the energy gap difference, ΔE_g, between the "cladding layers" and the "active region" required for low-threshold AlGaAs-GaAs injection lasers, we can get some feeling for how feasible UV lasers in the InAlGaN system will be. As an example, consider the case of a conventional $Al_{0.4}Ga_{0.6}As$-GaAs DH laser structure, which is a standard low-threshold laser structure in the AlGaAs system. In this case, the index difference, Δn, between the $Al_{0.4}Ga_{0.6}As$ cladding layers and the GaAs active region is $\Delta n \sim 0.28$ at the GaAs laser energy of $E_{laser} = 1.38$ eV and $\Delta E_g \sim 0.476$eV. These values will be used as a benchmark to develop a "first guess" laser structure in the InAlGaN system.

As a specific case, let us consider the possibility of using alloys lattice-matched to (0001) ZnO substrates. These have an energy gap, E_g and an index of refraction, $n(E_g)$, at the corresponding bandgap energy that is intermediate between the values of the binaries of which they are composed. If we take the values of n given in Table 1 and use a linear function for the dependence of n(E', x) upon x in the $Ga_{1-x}In_xN$ system, we find that at the bandgap energy of $Ga_{0.8}In_{0.2}N$ ($E_g = 3.1$ eV), the estimated value for the index of refraction of $Ga_{0.8}In_{0.2}N$ is $n(E_g = 3.1 \text{ eV}) = 2.44$.

If we take the simple approach that we require a cladding layer for this $Ga_{0.8}In_{0.2}N$ "active region" that has an energy gap ~0.48 eV higher, (as determined above for the $Al_{0.4}Ga_{0.6}As$-GaAs laser above) we conclude that we need an alloy with a bandgap energy ~3.58 eV. Using the equation for $E_g(x)$ calculated in Ref. 10 for the $Al_{1-x}In_xN$ system, we calculate that this energy gap corresponds to an alloy of composition $Al_{0.49}In_{0.51}N$. This alloy has an estimated value of $n(E_g = 3.58 \text{ eV}) = 2.08$. We conclude that a DH structure consisting of cladding layers of $Al_{0.49}In_{0.51}N$ and an active region of $Ga_{0.8}In_{0.2}N$ emitting light at $E_g = 3.1$ eV ($\lambda = 400$ nm, in the UV) will have values of $\Delta n \sim 0.36$ and a $\Delta E_g \sim 0.5$ eV and will thus satisfy both the requirements of $\Delta n \sim 0.28$ and $\Delta E_g \sim 0.476$ eV. Thus, we expect that such a DH structure is capable of confining electrons to the active region of the laser structure. The estimated lattice mismatch between the active region and the cladding layers in this DH structure will be $\Delta a/a_0 \sim 1.7\%$ which is small enough to be acceptable. Note that, as discussed above, the lattice mismatch can be entirely eliminated by employing quaternary AlGaInN cladding layers.

The DH laser structure is shown schematically below in Fig. 2.10a. The active region of this laser could also be designed to include a MQW structure with $Ga_{0.8}In_{0.2}N$ QW's and barriers of $Al_{0.42}In_{0.58}N$ ($E_g = 3.3$ eV) which have a lattice mismatch of ~ 0.8% relative to the active region. Based upon the experience with other III-V quantum-well injection lasers, this would probably result in the lasing at slightly higher energy, a lower threshold

Use or disclosure of the information contained on this sheet is subject to the restrictions on the title page of this proposal. This information is proprietary to the consortium.

current, and higher differential quantum efficiency. This QW device structure is shown schematically in Fig. 2.10b.

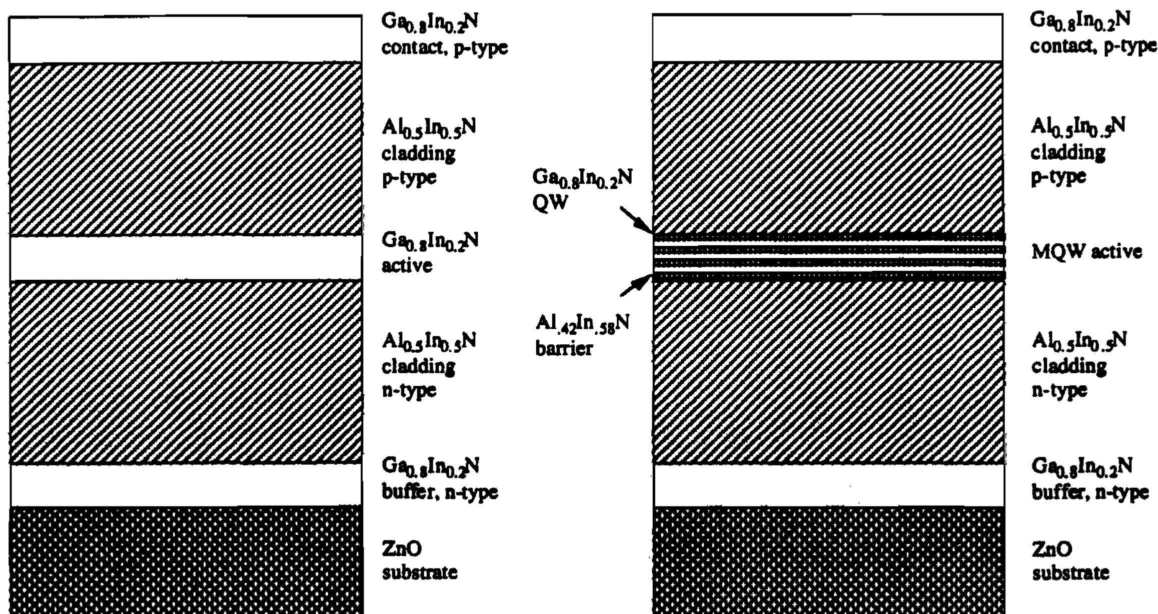

Fig. 2.10 Preliminary heterostructure laser designs. (a) is a double-heterostructure while (b) is a strained-layer multi-quantum well design.

II.3.1.2 Facet Formation

A fundamental consideration in the fabrication of conventional injection lasers is the formation of cleaved facets for the Fabry-Perot mirrors to provide feedback for the optical field. The consortium has extensive experience in the fabrication of Fabry-Perot (FP) geometry injection lasers. Cleaving the (0001)-oriented InAlGaN films on (0001) Al_2O_3 substrates is expected to be more difficult than cleaving (100) GaAs substrates. However, cleavage appropriate for FP laser diodes has been demonstrated at SDL. If cleaving proves unsatisfactory, specialists at SDL will use reactive ion etching (RIE) for the formation of stripe-geometry device structures. SDL has an on-going technology development program in the etching of FP mirrors for high-power AlGaAs-GaAs lasers and has demonstrated highly reliable high-power AlGaAs and AlGaInAs laser diodes using etched mirrors.

II.3.2 LED Processing

The bright blue LED announced by Nichia Chemical Co., Japan, in November 1993 was a singular achievement, placing the wide bandgap nitride technology in the forefront for visible emitters. While the potential of the group III nitrides had been recognized for many years, attainment of useful devices had been, until now, elusive. The feasibility for practical, working light emitting devices was proven, and with this achievement the whole spectrum of UV and visible wavelengths became available for exploitation. The Nichia blue and green devices indicate that with this materials system, and suitable improvements in the technology to enhance the light output, a bridge may be made with HP's current AlInGaP LED technology to achieve total visible spectrum coverage. LEDs will then compete directly with fluorescent lamps as light sources.

The luminescence mechanism in the Nichia LEDs, both blue and green, is dominated by D-A pair recombination at low currents. With increasing current the impurity emission becomes saturated and band edge emission becomes dominant. The resulting emission spectrum, is quite broad. This leads to an LED that exhibits poorly saturated color output,

Use or disclosure of the information contained on this sheet is subject to the restrictions on the title page of this proposal. This information is proprietary to the consortium.

and is thus of limited utility for full color displays. This will severely limit the market access of the Nichia lamp.

By moving away from impurity dominated recombination to pure band edge emission one achieves two things: brighter LED devices and color purity. Both enhancements are required to be successful in the market place. To attain this, both purity and crystal quality of the grown layers in the device must be improved. Also, greater indium content in the grown layers must be achieved in order to extend the range of emitted wavelengths into the yellow-green. Direct band-to-band recombination is a key for commercially successful LEDs and is thus a primary effort of the LED program.

The current Nichia LED is a "pseudo-" double heterostructure, having an n-type GaN confining layer on the bottom and a p-type AlGaN confining layer on top of the Zn-Si-doped $In_{.06}Ga_{.94}N$ active layer. While this configuration works, it is not optimized. More closely matched confining layers will be required for a band edge emitting active layer, and lattice matching layers may be necessary to reduce defects. Fully lattice-matched symmetric structures, using quaternary AlGaInN layers, are obviously the preferred approach to the fabrication of highly efficient LED heterostructure and thus form the second effort of the LED program.

The primary degradation mechanism of the Nichia LEDs leading to their short lifetime of ~3500 Hrs, has been identified as failures in their p-contact current blocking layer. This layer, thought to be a Ti_3Ni compound, appears to short out under stress conditions. Thus, the poor reliability observed with these devices does not seem to be associated with the nitride materials system, per se, but with the device design and processing. More suitable current blocking layer schemes and more robust device designs will be selected. Possibly the blocking layer will be eliminated and current spreading window layers used instead. This could improve both the efficiency (light extraction) and high current reliability.

An approach to increase the light extraction from these nitride devices, would be to try window layers of suitable thickness. This has proved very advantageous for the AlInGaP LEDs. As much as 10% more light can be extracted from the chip than without such a layer. However, a primary issue with these nitride based LED devices is the low conductivity of the nitride materials, especially, the p-layer. Assuming a hole mobility of 10 cm^2/V-sec, a hole concentration of 10^{18} cm^{-2}, an electron mobility of 100 cm^2/V-sec and an electron concentration of 10^{18} cm^{-2}, one calculates the slab resistance shown in Figure Fig. 2.11 as a function of slab thickness.

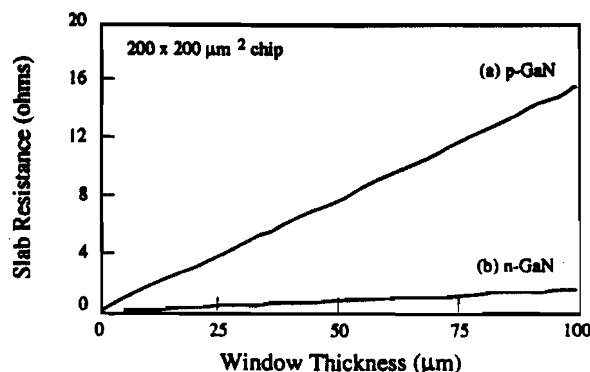

Fig. 2.11 Slab resistance of GaN as a function of slab thickness.

More importantly, one must consider the effect on current spreading. This is shown in Fig. 2.12, which gives the normalized current density at a distance of 100 from the contact edge for various slab thicknesses. A comparison with p-GaP is included which is used as a window layer for light extraction from AlInGaP LED devices. The normalized current density as a function of distance for the contact edge for various slab thicknesses is shown

Use or disclosure of the information contained on this sheet is subject to the restrictions on the title page of this proposal. This information is proprietary to the consortium.

in Figure 2.13. Clearly, both the p-doping mobility and concentration must be increased in order to enhance device performance.

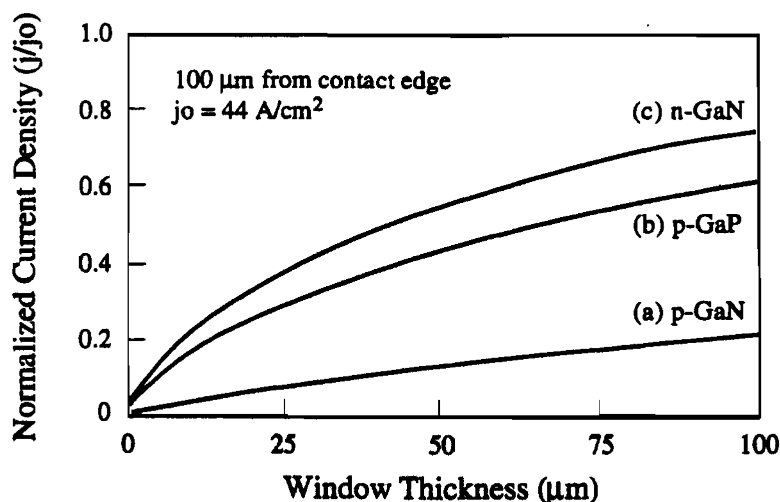

Fig. 2.12 Normalized current density versus window thickness.

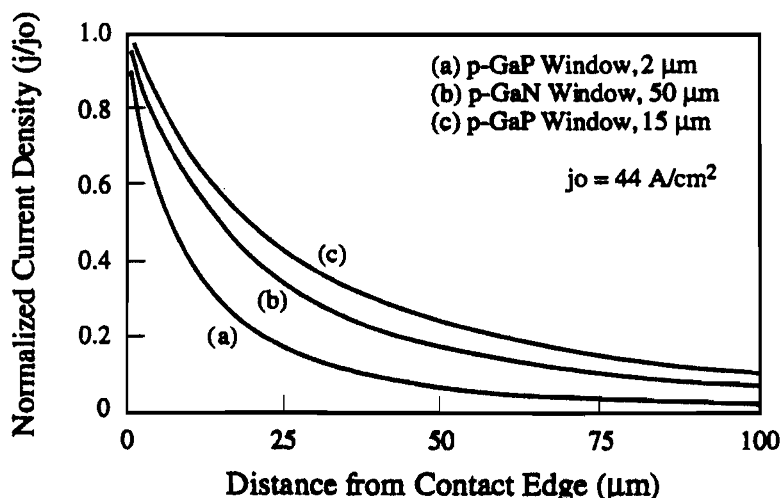

Fig. 2. 13 Normalized current density as a function of distance from contact.

If suitable nitride based window layers can not be grown, it may be possible to wafer bond suitable layers to the device. This technique has been pioneered by HP in their development of transparent substrate AlInGaP LEDs.[23]

To compete in the LED marketplace, high volume manufacturing procedures must be in place with high yielding processes at each step of the way. This requires the use of multi-wafer epi reactors capable of handling 2 inch and/or 3 inch diameter wafers. Maintaining composition uniformity (including dopant incorporation) and layer thickness uniformity, both across the wafers and from wafer to wafer is required. Extensive optimization of growth conditions will be required to achieve this. Obtaining growth uniformity will be facilitated by in situ monitoring, robust device design, and robust processes. It is paramount to understand the sources of variability in the process and the interplay between reactor hardware and process variables. Failure Mode Effects and Criticality Analysis[24] will be used as well as HP's extensive experience in the high volume production of AlInGaP to produce the efficient and uniform materials required for high volume LED production.

Use or disclosure of the information contained on this sheet is subject to the restrictions on the title page of this proposal. This information is proprietary to the consortium.

III. Program Plan

III.1 Management Plan

The consortium consists of SDL, HP, Xerox, University of Texas at Austin (UT), Boston University, AXT, and ATMI. The program manager will be Dr. David F. Welch, Vice President of R+D at SDL. The core industrial partners to the program are SDL, HP and Xerox. These team members will collaborate fully and openly on the MOCVD crystal growth of nitrides. Inputs into this industrial team will come from the other consortium members. UT and BU will transfer growth and processing technology to the industrial core members. AXT and ATMI will develop GaN substrate growth technologies and deliver evaluation substrates to the growth members. The program managers and principal investigators by organization are listed below.

Institution	Program Managers	Principal Investigators
SDL	Dr. David F. Welch	Dr. Jo Major
HP	Dr. George Craford	Dr. Grant Elliot
Xerox	Dr. Neville Connell	Dr. Noble Johnson
UT	Prof. Russell Dupuis	Prof. Russell Dupuis
Boston University	Prof. Ted Moustakas	Prof. Ted Moustakas
AXT	Dr. Heikki Helava	Dr. Heikki Helava
ATMI	Dr. Duncan Brown	Dr. Michael Tischler

III.2 Task Division

To achieve the goals, the program is divided into several tasks to be performed at each organization. The MOCVD crystal growth will be performed at HP, SDL and UT. The material characterization will be performed at Xerox. The theoretical and empirical analysis of the physical properties of the nitride alloys will be achieved at Xerox. This effort will supply the needed fundamental knowledge base to aid in the fabrication of high-performance LEDs and laser diodes. In the second year of program funding, Xerox will begin investigation of processing techniques unique to the construction of the nitride injection laser diode while HP and SDL will pursue device structures necessary to demonstrate the LED and laser diodes. An industrial task breakdown is shown is Table 3.1

Table 3.1 The task breakdown of the industrial partners.

HP-OED	Xerox-PARC	SDL
Growth	**Structure**	**Growth**
•Horizontal	•Dislocations	•Vertical Quartz
•Buffer Layer	•Heterojunctions	•Buffer Layer
•Substrates	**Electronic**	•GaAsN
•InGaN	•Transport	•Substrates
Processing	•Defects, modeling	**Processing**
•LED specific	**Processing**	•laser diode specific
•Contacts	•Dopant Activation	•WG Fabrication
	•Etching, Diffusion	•laser diode Facets

The university efforts are focused at the development and characterization of alternate substrate technology, at Boston University, and the development of MOCVD growth technologies at UT .

Use or disclosure of the information contained on this sheet is subject to the restrictions on the title page of this proposal. This information is proprietary to the consortium.

The device effort of the program is divided into two tracks: the LED manufacturing effort led by HP and the laser diode effort led by SDL and Xerox. The LED effort is a rapid track to prototype LED fabrication. The laser diode effort will focus upon continued material improvements, ultimately leading to the consortium demonstrating the first CW laser diode based upon nitride alloys.

Table 3.2 The task breakdown of the academic partners.

Boston	UT
ECR-MBE	Growth
Hybrid GaN	Emcore MOCVD
ZnO	Quaternary Development
M-Plane Sapphire	Source Issues
Doping, Contacts	

The substrate development effort will be handled in parallel by AXT and ATMI during the first program year. This approach is chosen because of the high risk of GaN substrate development. The emphasis will be on a thorough proof-of-concept with particular emphasis on developing methods compatible with the demonstration of technologies compatible with industrial and technological needs. In year 2, the consortium will select the substrate vendor with the most technically sound approach to substrate development and fund this company at an accelerated rate. The bulk substrates will be made available to the consortium. BU will pursue evaluation of commercially available substrates and evaluate the substrate technologies developed within the program. BU will use MBE growth as a tool to ascertain the quality of the substrates used throughout the program.

The work of ATMI. will be supported by a subcontract from ATMI to Professor Thomas Kuech at the University of Wisconsin.

III.3 Cost Model

The cost of the program as broken down by year and company is shown in Table 3.3. Within the table, the price is represented as ARPA funds/Matched funds. All values are in thousands of dollars.

Table 3.3 The cost breakdown of the proposed program.

Company/Year	1	2	Total
HP	550/550	550/550	1100/1100
SDL	500/500	550/550	1050/1050
Xerox	447/458	460/474	907/932
UT-Austin	293/358	186/200	479/558
BU	150/172	150/128	300/300
AXT	150/150	*	150/150
ATMI	150/150	*	150/150
AXT/ATMI		300/300	300/300
Total	**2240/2338**	**1896/1902**	**4136/4240**

Although not formally committed as matching funding, HP is estimating internal nitride funding to exceed $10 million over the next several years due to the high commercial importance of nitride development.

Use or disclosure of the information contained on this sheet is subject to the restrictions on the title page of this proposal. This information is proprietary to the consortium.

IV. Statement of Work

The consortium proposes to develop GaN and related alloys for the purpose of demonstrating advanced optoelectronic devices. The goal at the end of the base two year program is to demonstrate CW LEDs and laser diodes. The goal specifications of the LED are optical power exceeding 4 mW, operating wavelength between 480 nm and 570 nm and an external efficiency exceeding 4%. The goal specifications of the laser diode are continuous wave operation between 360 nm and 540 nm at room temperature.

- LED: > 4% , p > 4 mW, 480 nm < λ < 570 nm
- Laser Diode: CW, 360 < λ < 540 nm

To achieve these goals the consortium will separate the tasks of epitaxial growth, substrate fabrication, materials characterization, and device fabrication as discussed in the task description above. In addition to the technical tasks the consortium will support quarterly review reports and an annual meeting, and a program final report. At the conclusion of the program the consortium will supply ARPA with working devices, LEDs (10) and laser diodes (5), that best represent the above stated goal specifications.

The consortium will provide ARPA with samples of the substrates that are produced during the program that best meet the technical and manufacturing needs of the consortium.

V. Milestone Chart

The milestones of the program are designed to ensure efficient collaboration and to rapidly develop materials and device technology leading to the final demonstration of LEDs and laser diodes based on nitride materials.

Milestones for Materials and Device Development Program

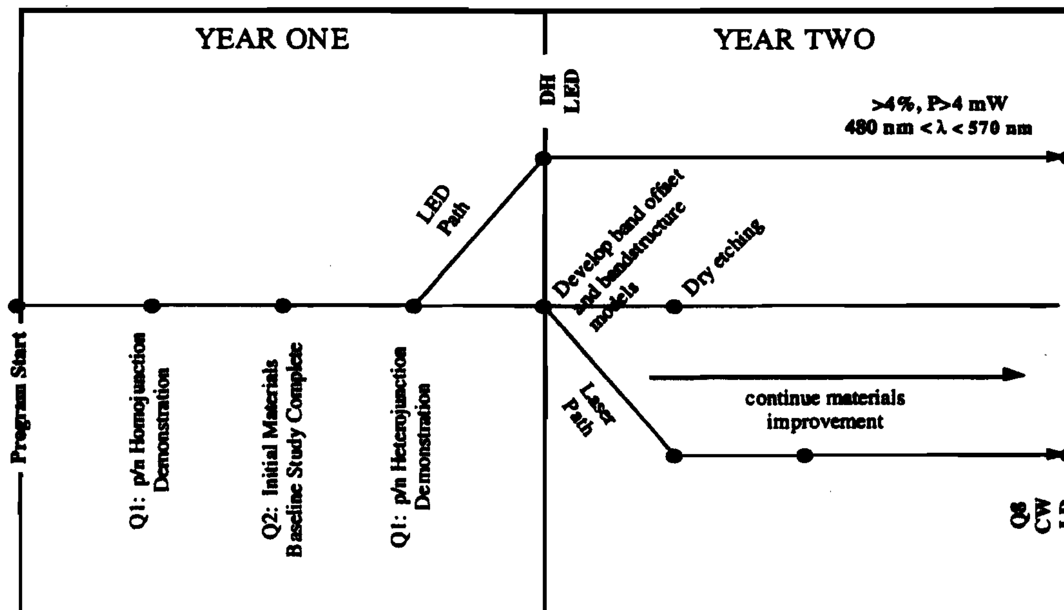

Fig. 5.1(a) The milestones of the Materials and Device Development Program.

The milestones of the proposal as outlined in Fig. 5.1(a) and 5.1(b) are divided into four categories, basic materials research and processing techniques, LED performance , laser diode performance, and substrate milestones.

Use or disclosure of the information contained on this sheet is subject to the restrictions on the title page of this proposal. This information is proprietary to the consortium.

Milestones for Substrate Development Program

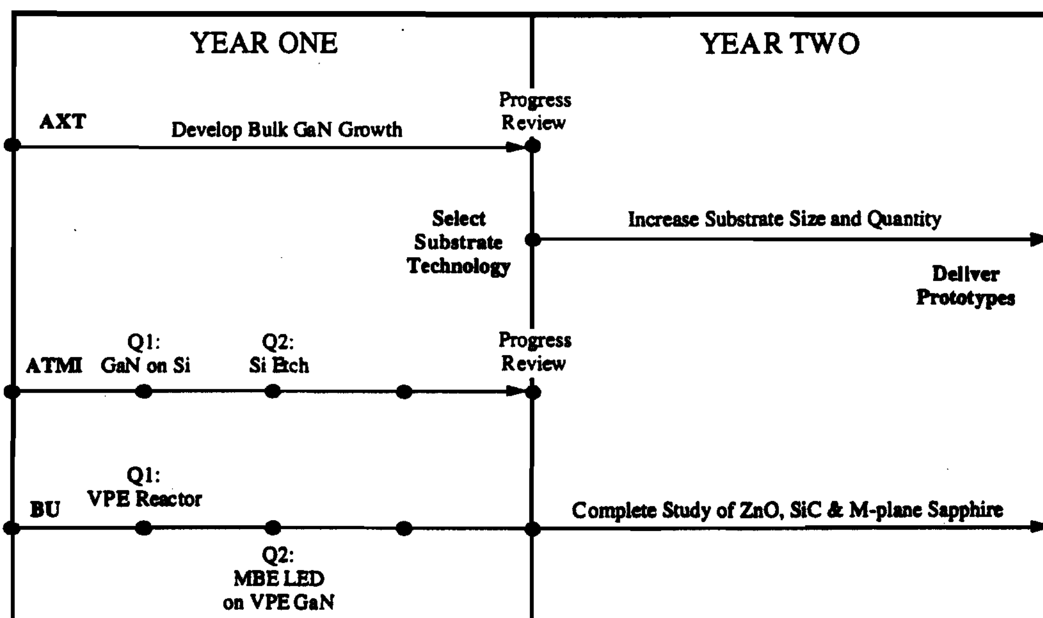

Figure V.1 The Technical Milestones of the Substrate Development Program.

VI. Facilities and Equipment Description

Materials Growth:

HP: LEC GaAs and GaP substrate growth, GaAsP hydride VPE, AlGaAs LPE, AlInGaP and AlGaInN MOCVD. The largest substrate capability in the U.S.

SDL: AlGaAs, AlGaInAs, AlGaInP/GaAs, GaInAsP/GaAs, GaInAsP/InP and AlGaInN MOCVD. Three reactors on-line, fourth reactor in pre-construction phase;

ATMI: Full facilities for bulk and epitaxial SiC and III-V materials growth.

AXT: Full bulk growth facilities for GaAs and InP substrate production.

Xerox: Xerox-PARC has full MOCVD capability.

University of Texas at Austin: EMCORE MOCVD reactor, procurement of second reactor for dedication to AlGaInN growth contingent upon funding availability.

Boston University: A Varian GEN II MBE System with a compact ECR microwave plasma source used for the formation of active nitrogen and a complete set of surface analytical equipment (mass spectrometer, RHEED, etc.)

Material Characterization:

Optical: Variable-temperature PL and EL, Time-resolved PL, wafer mapping, IR and microscopic IR, FTIR, Ellipsometry, Cathodoluminescence, optical recombination lifetime measurements, and Raman Spectroscopy.

Structure: X-ray rocking curve and reciprocal space diffraction mapping, Laue X-Ray, High-Resolution TEM with energy dispersive spectroscopy micro-probe, atomic force microscopy, SEM, Alpha-step,

Electrical: Photoexcitation DLTS, Mercury Probe, E.B.I.C., C-V, Polaron, Variable-Temperature Hall Measurement, Sheet Resistance Measurement, DLTS, Raman spectroscopy.

Facilities are readily available in the immediate area for SIMS, Auger, EBIC, EDAX, and a wide variety of other materials characterization techniques.

Processing Equipment:

Use or disclosure of the information contained on this sheet is subject to the restrictions on the title page of this proposal. This information is proprietary to the consortium.

Full equipment is in place for the mass production of both LEDs and laser diodes. This equipment includes: Reactive Ion etching, Diffusion Furnaces, Passivation Deposition (SiN, SiON), Back Lapping, Edge Profilers, Evaporators (Resistance and E-beam), Sputtering Machines, Rapid Thermal Annealing, Photolithography, Etching (Semiconductor and Metal), Plasma Etching, Wafer Sawing, Wafer Scribing, 1 μm projection lithography, an optical coating facility and other processing equipment.

Packaging Equipment:

The packaging facilities for LEDs and laser diodes, at HP-OED and SDL, respectively, are the largest such facilities in the United States and represent a substantial advantage over other potential consortia.

LED and laser diode Test Equipment:

The most complete LED and laser diode evaluation facilities in the United States exist at HP and SDL, respectively. Xerox PARC also has a complete laser diode test facilities.

High-Bandgap Materials Modeling:

IBM RS-6000 scientific work station, Silicon Graphics IRIS graphics work station, custom software for total-energy calculations and materials simulations.

VII. Relevant Prior Work

The members of the consortium represent the cutting edge in optoelectronic device technology. The consortium members have demonstrated the highest quality GaN materials grown to date and have extensive experience in the areas of materials development and characterization, device design and fabrication, substrate fabrication, and commercialization of the technology. Thus, the consortium members uniquely meet the goals of the ARPA program, which is to develop and commercialize advanced optoelectronic materials and devices based on nitride alloys. In this section of the proposal, recent work relating to the development of GaN and related alloys performed by the consortium members is discussed. The work includes systematic transmission electron microscopic (TEM) investigations of buffer layers in GaN growth, characterization of the electrical and optical properties of the nitrides, growth of GaN with unmatched crystallinity, and a thorough analysis of the current Japanese LED effort including degradation effects of the current commercial LED.

VII.1 Structural Properties of Nitride Alloys

During the past year, groups at UT-Austin and SDL, Inc. have begun to study the use of MOCVD to grow heteroepitaxial AlInGaN films. In a very short time, extremely high-quality GaN heteroepitaxial films having world-record X-ray diffraction rocking curve FWHM values have been grown. At UT the epitaxial layers are grown in a specially modified Emcore GS3200 UTM MOCVD system, while at SDL the layers are grown in a vertical low-pressure reactor. Fig. 7.1 shows the optical transmission spectra for three GaN films of varying thickness. The absorption spectra shows band-edge absorption at 3.4 eV with interference fringes reflecting the GaN layer thickness.

Use or disclosure of the information contained on this sheet is subject to the restrictions on the title page of this proposal. This information is proprietary to the consortium.

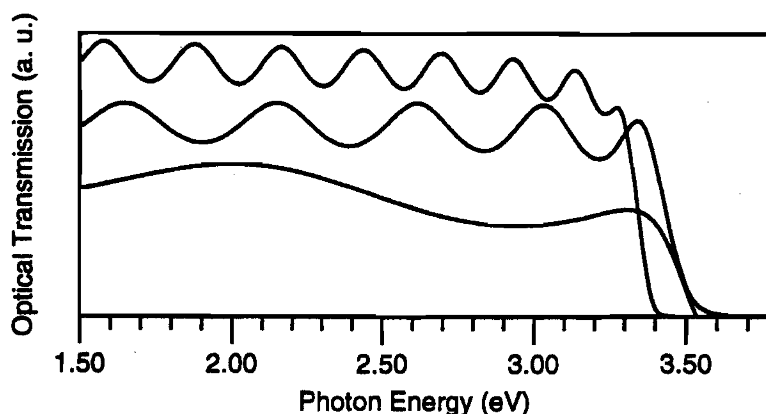

Fig. 7.1: Room-temperature (300K) optical transmission spectra for various GaN heteroepitaxial layers grown on (0001) Al_2O_3.

The structural quality of the GaN epitaxial films is analyzed using a five-crystal diffractometer. Cu K_α radiation is used and rocking curves through the (0002) GaN and Al_2O_3 lattice Bragg peaks are made. The FWHM of the (0002) GaN diffraction peak has been studied as a function of the thickness of the GaN film. The FWHM of the ~0.25 μm-thick films are ~100 arc sec while thicker films, ~0.5 μm, have reproducible FWHM values $\Delta\Theta$~38-40 arc sec. A typical (0002) X-ray rocking curve for a 0.48 μm-thick GaN/Al_2O_3 film is shown in Fig. 7.2. Pendellösung fringes appear on either side of the main GaN peak. These fringes are only observed for thin, very high-quality epilayers. This is the first observation of Pendellösung fringes in any GaN X-ray rocking curve. These fringes offer evidence of high structural quality and allow film thickness to be determined from fringe spacing. The spacing of ~38 arc sec gives a thickness of 0.44 μm, in agreement optical transmission data of Fig. 7.1.

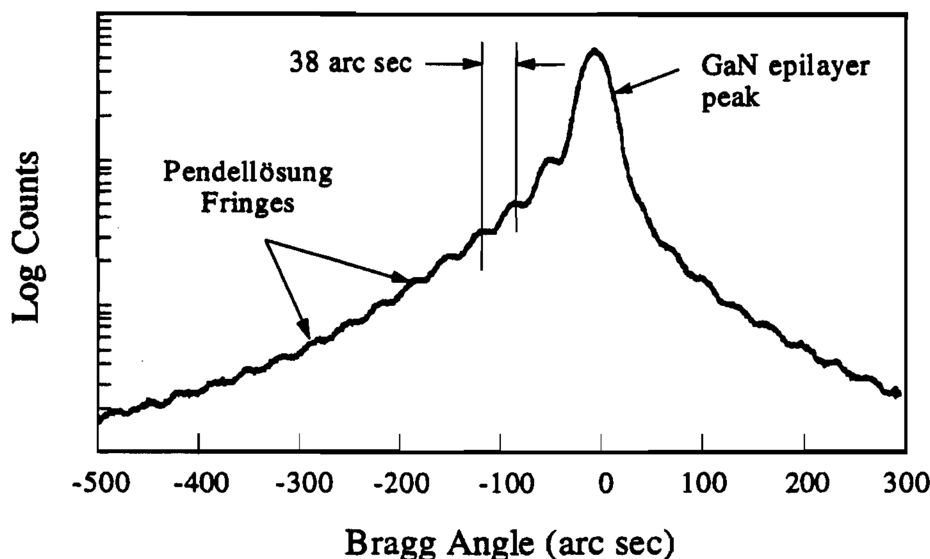

Fig. 7.2: Five-crystal (0002) X-ray rocking curve of a ~0.48 μm-thick GaN epitaxial layer on a (0001) Al_2O_3 substrate. Note that the observation of Pendellösung fringes indicates that the film is of very high quality.

Subsequent to the achievement of the UT group, SDL has produced GaN films with rocking curve FWHM of 27 arc seconds as shown in Fig. 7.3. The rocking curve is nearly symmetric. This profile is actually one of 140 profiles performed during a fifteen hour reciprocal space mapping of the 0002 diffraction peak. The incident optics are a four crystal

Use or disclosure of the information contained on this sheet is subject to the restrictions on the title page of this proposal. This information is proprietary to the consortium.

monochromator; the sample is the fifth crystal, with a triple axis, double crystal collection optic system. The noise in the measurement, when compared to the UT film, is due to limiting the collection time per data point.

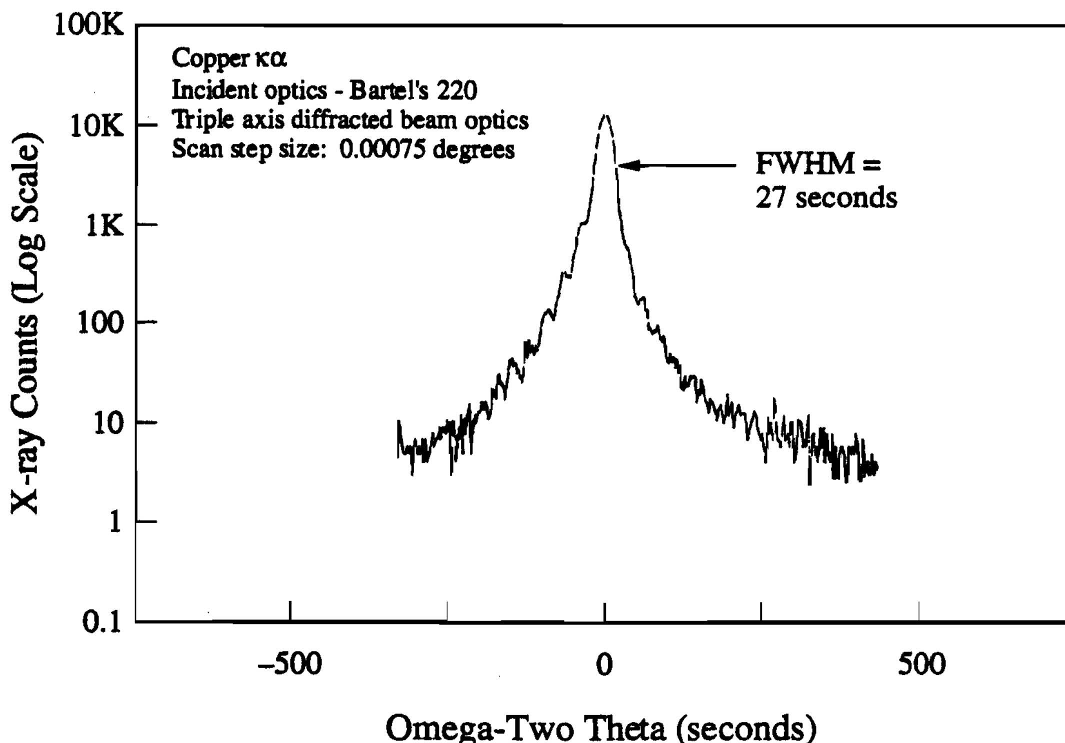

Fig. 7.3 The omega- two theta scan of an SDL GaN film.

The reciprocal space mapping of the 0002 diffraction point is shown in Fig. 7.4. The plot is a contour mapping of the omega versus omega-two theta scan. The vertical distribution is a measure of the mosaicity of the film. The SDL film has a narrow mosaicity distribution with a FWHM in the vertical direction of 35 arc seconds. The horizontal distribution is the standard omega-two theta scan shown in Fig. 7.3, and measures variation in the lattice spacing of the crystal. The diagonal trace is an instrument artifact; the secondary divergence of the X-ray beam.

The dependence of the FWHM of the X-ray rocking curve upon thickness of GaN/Al_2O_3 films as reported by previous workers includes a "best" result of $\Delta\Theta$~96 arc sec for a film having a thickness ~4 µm grown by MOCVD on a GaN buffer layer[25] while a more typical "best" FWHM is $\Delta\Theta$~360 arc sec or more for ~4 µm-thick films.[26-29] Recently, an X-ray rocking curve having a FWHM value of $\Delta\Theta$~98 arc sec was reported for an MOCVD-grown AlN/(0001) Al_2O_3 film but the film thickness was not indicated.[30] The X-ray studies of SDL and UT represent both superior crystallinity and, for the case of reciprocal space mapping, more thorough characterization than has been performed by other researchers.

Use or disclosure of the information contained on this sheet is subject to the restrictions on the title page of this proposal. This information is proprietary to the consortium.

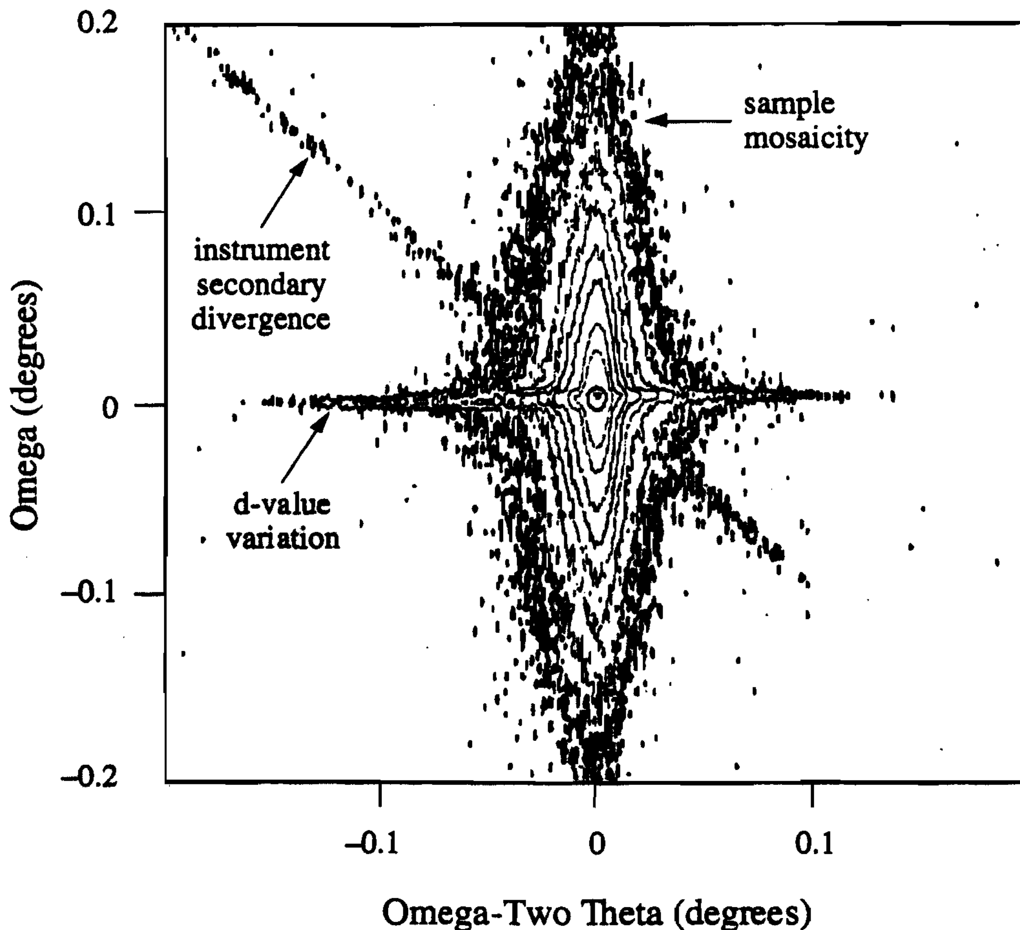

Fig. 7.4 The reciprocal space mapping of the 0002 diffraction point of GaN.

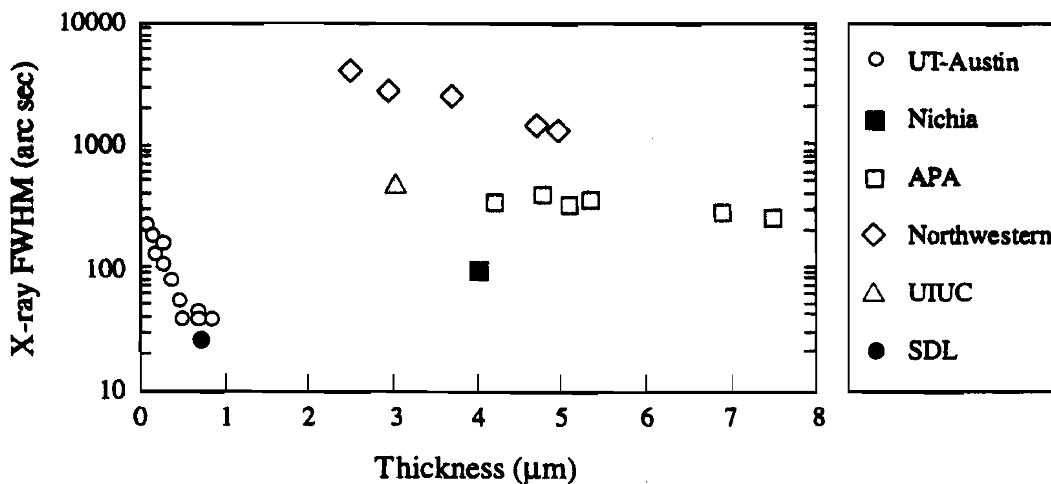

Fig. 7.5 Comparison of reported X-ray FWHM values of GaN/Al_2O_3 heteroepitaxial films vs. layer thickness. Data are from indicated references.

Figure 7.6 shows a room-temperature photoluminescence spectrum of a ~0.5 μm-thick GaN film grown . The narrow linewidth of the band-edge peak at ~367 nm and the high intensity of this peak compared to the deep-level emission at longer wavelengths further

Use or disclosure of the information contained on this sheet is subject to the restrictions on the title page of this proposal. This information is proprietary to the consortium.

indicate the samples to be of good optical quality. Room-temperature cathodoluminescence spectra taken on other samples showed narrow, intense band-edge peaks at ~367 nm.

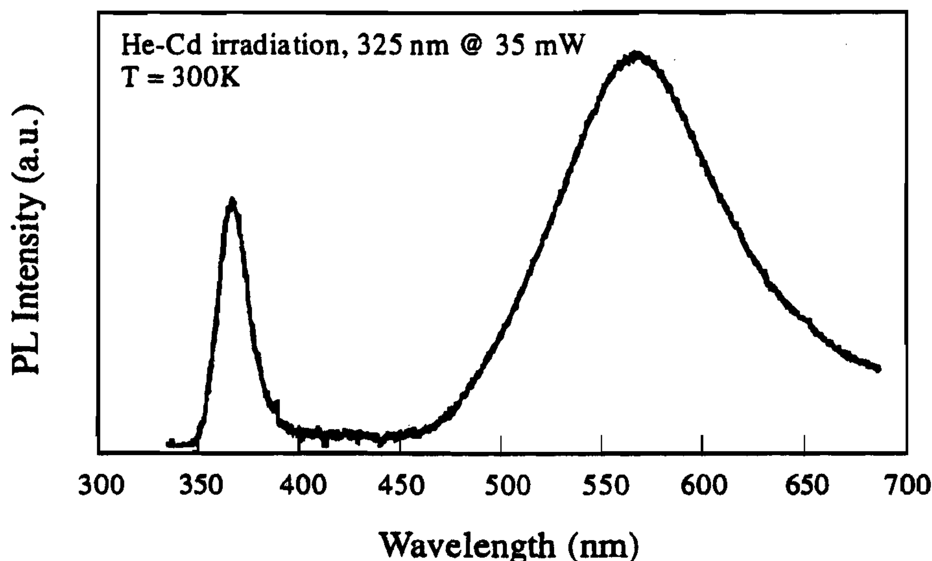

Fig. 7.6 **Room-temperature (300K) photoluminescence spectrum of a relatively thin (~0.5 μm) GaN/sapphire epitaxial film. A He-Cd laser (λ ~325 nm, 35 mW CW input power) was used as an excitation source.**

The results presented here were obtained for relatively thin layers. Kuznia, *et al.* [26] have reported that improved film properties are consistently observed for films employing an AlN buffer layer, an optimal buffer layer thickness, and a total film thickness greater than ~4 μm. Thus, while we have not fully optimized our growth procedure, the structural and electrical properties of our relatively thin GaN heteroepitaxial films represent a significant improvement in the quality of heteroepitaxial III-V nitride films.

Fig. 7.7 **A TEM image of Nichia LED. The dislocation density is ~10^{11} cm^{-2}.**

From a structural standpoint, the material grown within the consortium, at UT and SDL, Inc, is the best available GaN epitaxy. Indeed, the rocking curves generated within the consortium, with a FWHM of 27 arc seconds, are now comparable with the best ***bulk*** substrate GaN material available.[3] The consortium has compared these next-generation nitride films with the existing technology of the Nichia LED. Fig. 7.7 shows the micro-structure of the Nichia lamp with a dislocation density of ~10^{11} cm^{-2}. In addition, many regions of three-dimensional growth are easily observable.

Use or disclosure of the information contained on this sheet is subject to the restrictions on the title page of this proposal. This information is proprietary to the consortium.

Fig. 7.8 shows a TEM cross-section of UT GaN. Our observations show dislocation densities lower than Nichia, by about two orders of magnitude. In addition, the UT GaN has a nearly perfect interface with the sapphire substrate and is planar throughout the entire growth.

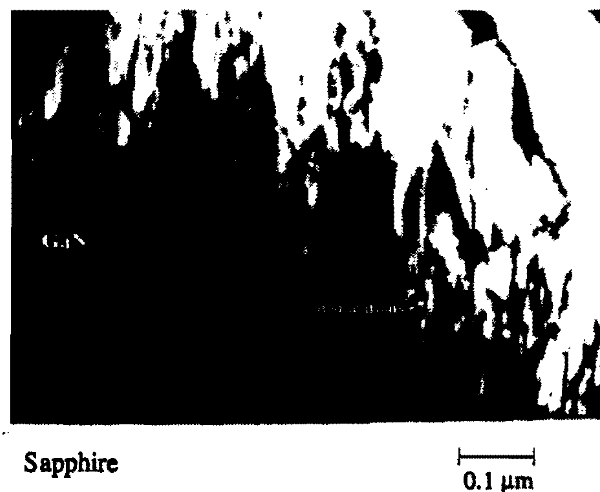

Fig. 7.8 Cross-sectional TEM of GaN film grown at the Univ. of Texas by Russ Dupuis. The dislocation density is ~10^9 cm^{-2}, two orders of magnitude lower than the Nichia material.

TEM work has also explored the characteristics of nitride films grown upon SiC substrates. SiC is an interesting alternative to sapphire as a substrate for epitaxy of AlGaN films. Its main advantages lie on the good lattice match and thermal expansion properties between the nitride alloys and SiC. We have studied the crystalline structure of GaN films grown on SiC by MOCVD, using AlN buffer layers.[31] A TEM image of a GaN film grown on SiC at SDL is shown in Fig. 7.9. The density of dislocations observed is approximately 10^8 dislocations/cm^2, ~1000X lower than the Nichia sample.

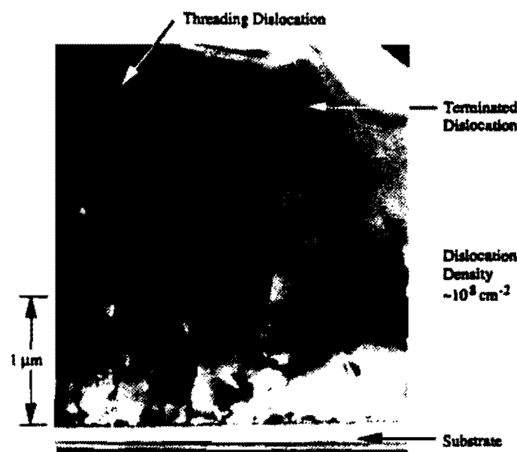

Fig. 7.9 TEM micrograph showing the GaN/AlN/SiC epitaxial structure grown at SDL. The dislocation density is ~10^8 cm-2.

A micrograph of the film is shown in Fig. 7.10. The stacking of the 6-H SiC is visible. The SiC/AlN/GaN interface is seen due to the change in sequence between SiC and GaN. The interface structure is almost entirely coherent, and few misfit dislocations are observed. The surface of the SiC is not perfectly polished with large steps in the SiC surface

Use or disclosure of the information contained on this sheet is subject to the restrictions on the title page of this proposal. This information is proprietary to the consortium.

identifiable. The hardness of SiC makes surface preparation difficult, however, a planar SiC surface would obviously increase the crystallinity of the epitaxy.

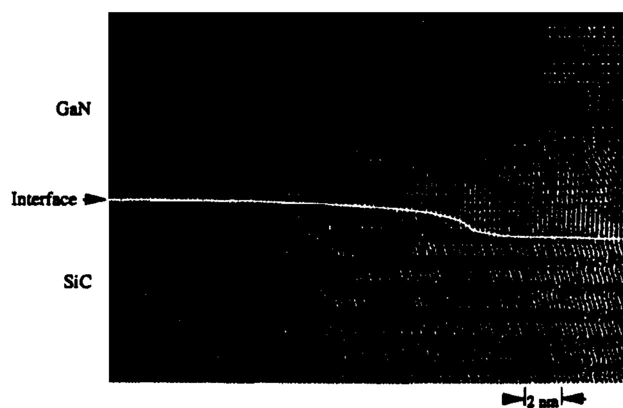

Fig. 7.10 Lattice image of the substrate region of a GaN/AlN/SiC thin film. The AlN/SiC interface is visible by the change in stacking sequence.

The GaN films grown on the SiC substrates also have reasonable X-ray FWHM (Fig. 7.11). The typical rocking curve FWHMs of GaN grown on SiC at SDL vary from 80-120 second, with 95 seconds being a typical value.

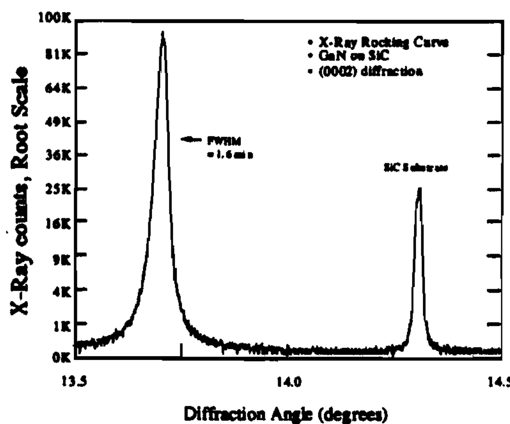

Fig. 7.11 The x-ray rocking curve of a GaN epitaxial layer grown upon an AlN buffer layer on a 6-H SiC wafer.

VII.2 Electrical and Optical Properties of Nitride Alloys

Controlled doping is a critical requirement for the realization of light emitting diodes. In p-type material grown by MOCVD, activation of acceptor dopants (e.g., Mg and Zn) requires either low-energy electron beam irradiation (LEEBI) or thermal annealing, or a combination of these two processes. In contrast, p-type films have been obtained by MBE without the need of such post-growth treatments. The formation of Mg-H complexes during the MOCVD growth is likely. To understand such processes, direct hydrogenation of p-type GaN were studied.[32] Hydrogenation substantially decreases the hole concentration in p-type material but has little effect in n-type material. (Fig. 7.12) Further studies will identify strategies to maximize doping.

Use or disclosure of the information contained on this sheet is subject to the restrictions on the title page of this proposal. This information is proprietary to the consortium.

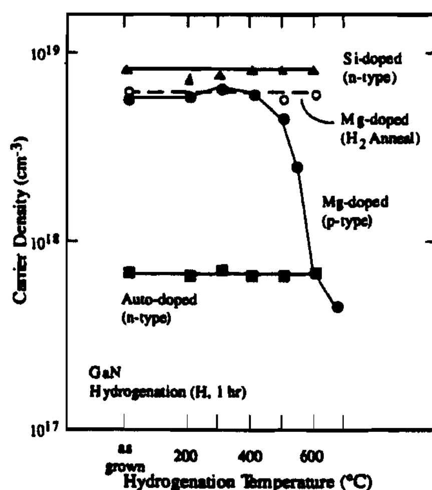

Fig. 7.12 Dependence of the carrier density on hydrogeneation temperature in epitaxial layers of GaN.

We recently discovered new vibrational modes in Mg-doped GaN with incorporated hydrogen.[33] The modes are shown in Fig. 7.13 and form two pairs. Based on selection rules, one pair, room temperature frequencies of 2168 and 2219 cm-1 was assigned to distinct Mg-H complexes. The Mg-H complexes appear to be responsible for low doping efficiencies in as-grown p-type GaN. The origin of the second pair of modes at 2151 and 2185 cm^{-1} is speculatively linked to the presence of diatomic molecules such as N_2.

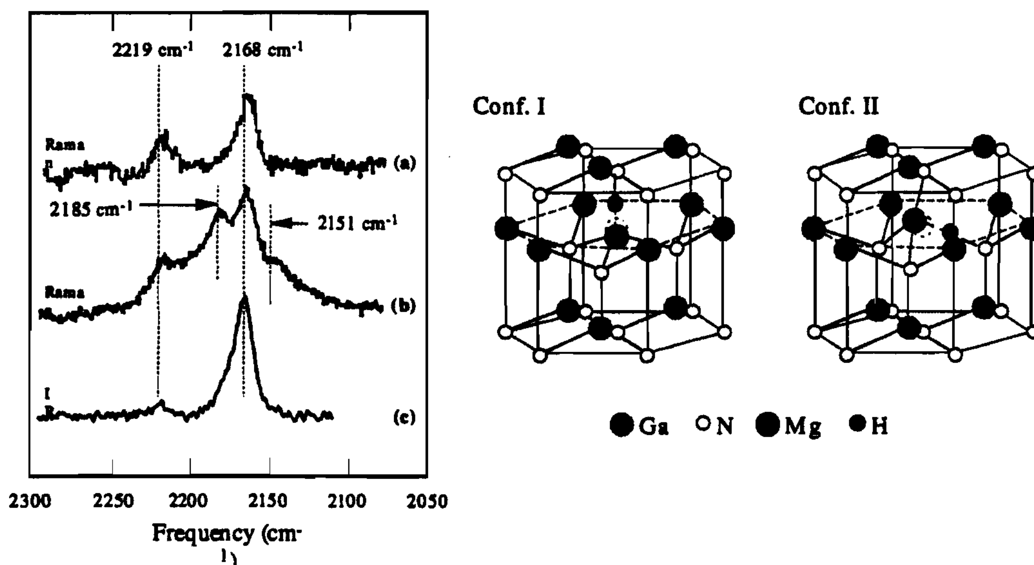

Fig. 7.13 Local vibrational modes in Mg-doped, hydrogenated GaN. Also shown are possible hypothetical structural configurations of two inequivalent sites for the Mg-H complex in GaN.

In the DLTS evaluation of GaN (see Fig. 7.14), two new electronic defects (at 0.49 eV and 0.18 eV) were characterized in near-ideal Schottky diodes fabricated on MOCVD-grown GaN.[34] Important future studies will include the determination of the prevalence of the two newly revealed deep level defects and identification of their chemical nature.

Use or disclosure of the information contained on this sheet is subject to the restrictions on the title page of this proposal. This information is proprietary to the consortium.

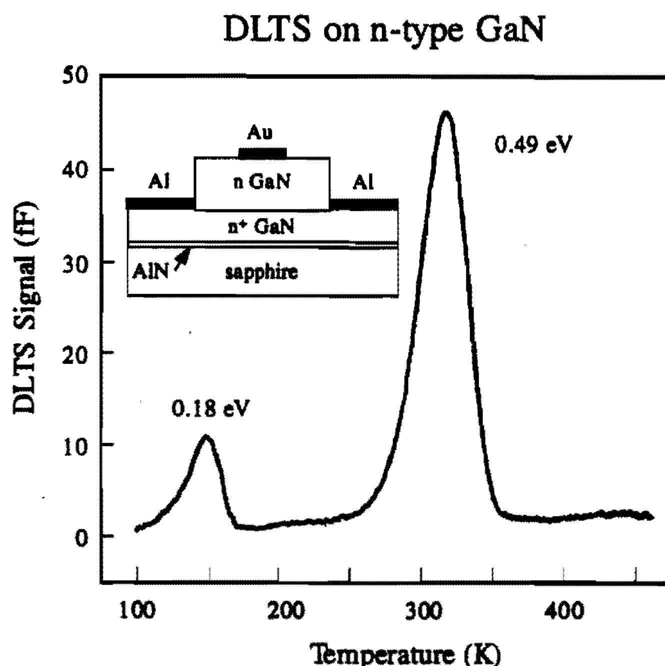

Fig. 7.14. DLTS spectrum for a Schottky diode on n-type GaN. The thermal activation energy for electron emission is listed next to each peak. The diode structure is shown in the inset.

Doping studies of the MOCVD GaN samples of SDL and UT are now beginning. The SDL samples are characterized by very low background doping by optimizing growth temperature, gas chemistry, growth rate and other reactor specifics provides a solid starting point for the attainment of reliable n- and p-type doping. Fig. 7.15 shows the background doping of a GaN sample grown at SDL. P-type conduction following a 700°C anneal step has been observed in GaN:Mg grown at SDL.

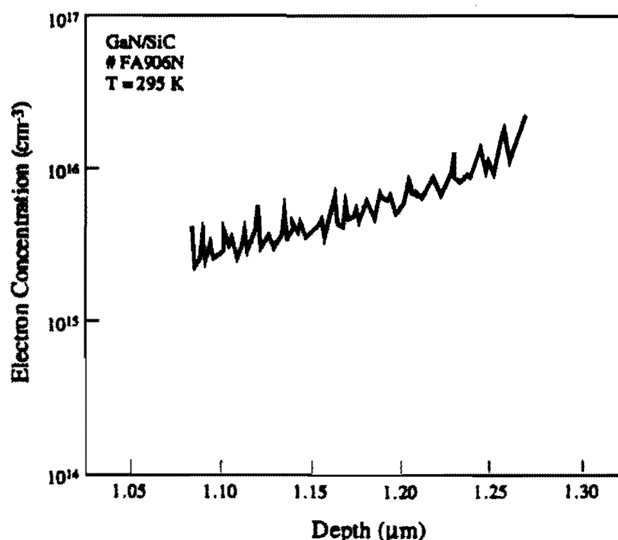

Fig. 7.15 The background carrier concentration of undoped GaN grown at SDL, Inc. Carrier concentration decreases to 2 x 10^{15} cm^{-3} near the sample surface.

The samples grown at UT exhibit n-type doping with a very high conductivity, implying that the carrier mobility may be substantially higher in these higher quality films. A Tencor

Use or disclosure of the information contained on this sheet is subject to the restrictions on the title page of this proposal. This information is proprietary to the consortium.

Sonogauge RT instrument was used to obtain room-temperature resistivity data on several UT samples at HP Labs. These experiments yielded very reproducible resistivity values of ~0.004 Ω-cm for the best samples. The corresponding mobility-carrier concentration product was found to be ~1.5×10^{21} $(V\text{-}s\text{-}cm)^{-1}$. The Tencor instrument routinely produces GaAs resistivity values in excellent agreement with van der Pauw measurements taken on the same GaAs samples. Initial Hall measurements on our GaN layers using the van der Pauw technique were inconclusive, but indicated the films to be heavily *n*-type with net carrier concentrations of $n \sim 8 \times 10^{18}$ cm^{-3}. Coupled with the mobility-carrier concentration product, this would imply a mobility of $\mu_n \sim 190$ $cm^2/V\text{-}s$, which is encouragingly high for this doping level and film thickness. For comparison, Figure 7.16 shows the mobility-carrier concentration product as a function of thickness for our best sample along with previously reported GaN/Al_2O_3 electrical characterization data.

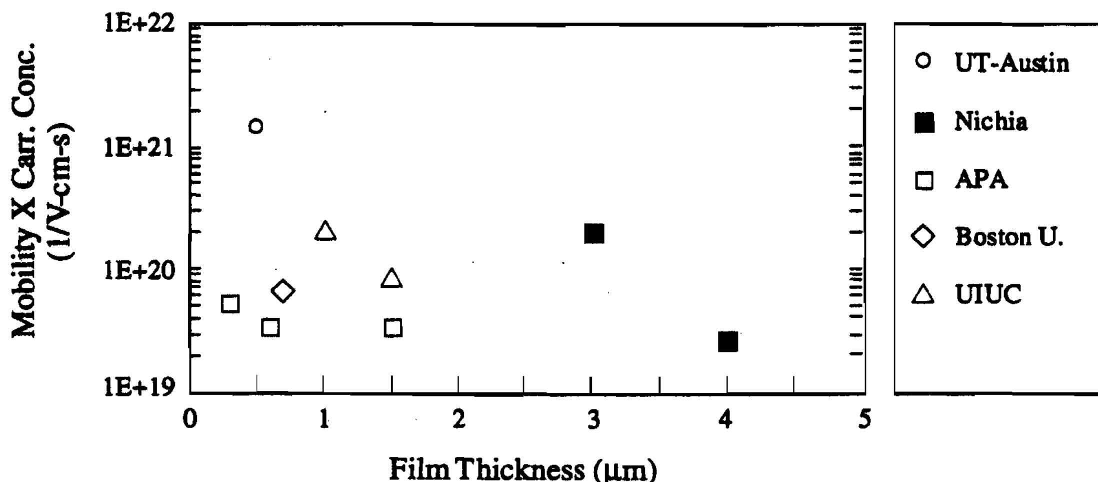

Fig. 7.16 Dependence of the mobility-carrier concentration product (at 300K) upon layer thickness for one of our GaN/sapphire films and recently published data from other groups for thicker GaN/sapphire films.

VII.3 Computational Analysis

Xerox PARC has carried out state-of-the-art first-principles calculations on atomic and electronic structures of compound semiconductors, including properties of binary bulk materials, alloys, defects, and interfaces. Previous work on many aspects of III-V material physics places Xerox PARC in an excellent position to tackle the theoretical understanding of GaN, its alloys, defects, and interfaces. Extensive test calculations brought to light severe deficiencies in the computational approaches used by other groups. In particular, it is important to include both proper treatment of the Ga 3d electrons in the calculations[35] and interactions beyond nearest neighbors. Because of the small lattice constant of GaN, interactions between second-nearest-neighbor Ga atoms can be quite sizable, and affect the electronic properties. The tight-binding approach does not reveal this detail.

While the wurtzite phase is the ground state for GaN, the cubic phase has been found to occur during growth on appropriate substrates. Analysis shows that the atomic structure is extremely similar, and that the differences in formation energies are negligible. The electronic structure exhibits some change, attributable to the lowering of the symmetry when going from zincblende to wurtzite. These effects are illustrated in Fig. 7.17, for the case of vacancies. Overall, the native defects are expected to behave very similarly in the both phases.

The shortcomings of a tight-binding treatment[36] in predicting the properties of the nitrogen vacancy are due to considering only nearest-neighbor interactions. As a result, the splitting of the Ga-dangling-bond-related defect levels is severely underestimated.

Use or disclosure of the information contained on this sheet is subject to the restrictions on the title page of this proposal. This information is proprietary to the consortium.

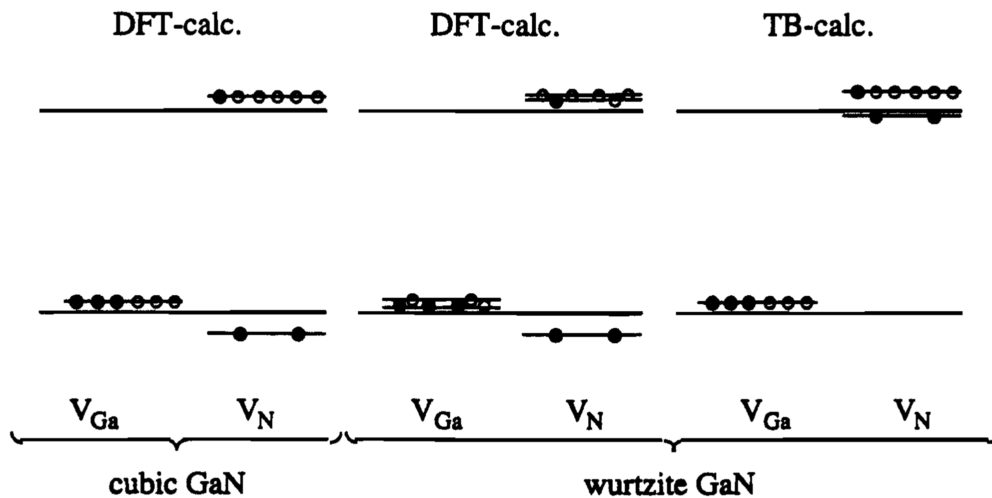

Fig. 7.17 **Schematic illustration of the electronic structure of the gallium and nitrogen vacancies in cubic and wurtzite GaN. For comparison the results of a tight-binding calculation are shown.**

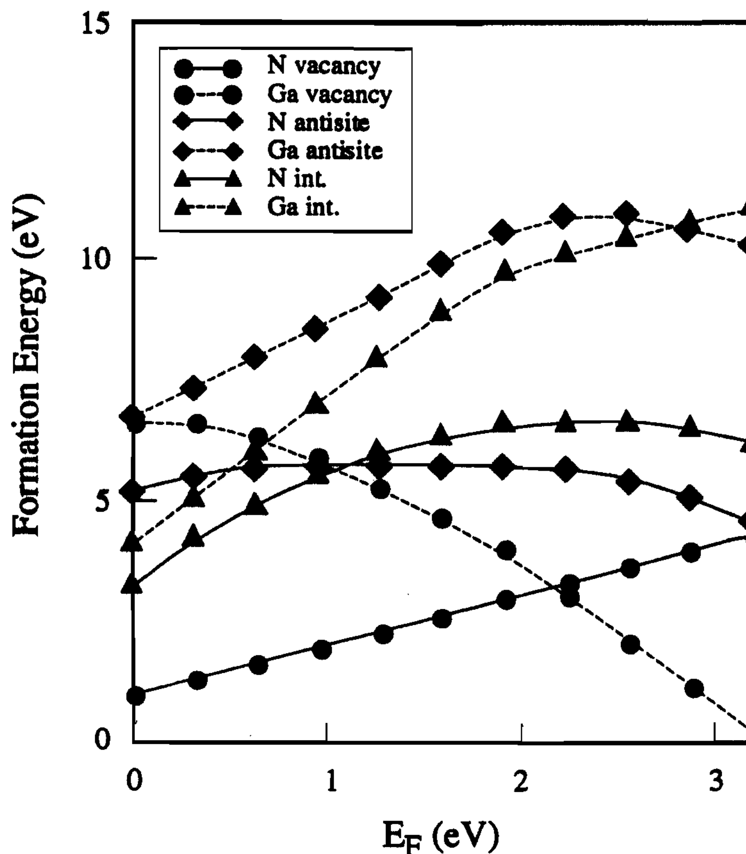

Fig.7.18 **Formation energies of native defects in GaN as a function of the Fermi level, under nitrogen-rich conditions. E_F=0 corresponds to the top of the valence band. Only vacancies have formation energies which are low enough to allow them to occur in appreciable concentrations.**

The results for formation energies of the various native defects are displayed in Fig. 7.18.[37] Under conditions of thermodynamic equilibrium, the formation energy of a defect

Use or disclosure of the information contained on this sheet is subject to the restrictions on the title page of this proposal. This information is proprietary to the consortium.

determines the concentration of the defect. It is seen from Fig. 7.18 that interstitials and antisites have formation energies which are too high to allow these defects to appear in appreciable concentrations. Only vacancies are found to be energetically favorable.

The fact that the formation energy depends on the Fermi level is related to the occurrence of native-defect-induced levels in the band gap. The N vacancy behaves as a donor. However, as can be seen from Fig. 7.18, the formation energy of the isolated nitrogen vacancy in n-type material is quite high, ~4 eV, so that its concentration will be negligible. Thus, *the n-type conductivity of as-grown GaN is not attributed to the nitrogen vacancy.*

VII.4 Device Related Prior Work

Boston University has begun device development including the characterization of p-type films, the development of working contact schemes, the construction of working p-n junctions, LEDS, and preliminary work concerning reactive ion etching (RIE) of nitride alloy thin films.

Recent progress in the etching of nitride alloys is summarized in Fig. 7.19 and Table 7.1. A typical etch rate, for a base pressure of 11 mT and a cathode voltage of 600 V, is a maximum of 200 Å/min, or approximately 1 μm/hour. These rates are sufficiently high for many device fabrication steps, including the fabrication of semiconductor laser diode facets. The etch rate can be raised further by decreasing the base pressure of the system as shown in Fig. 7.19.[38]

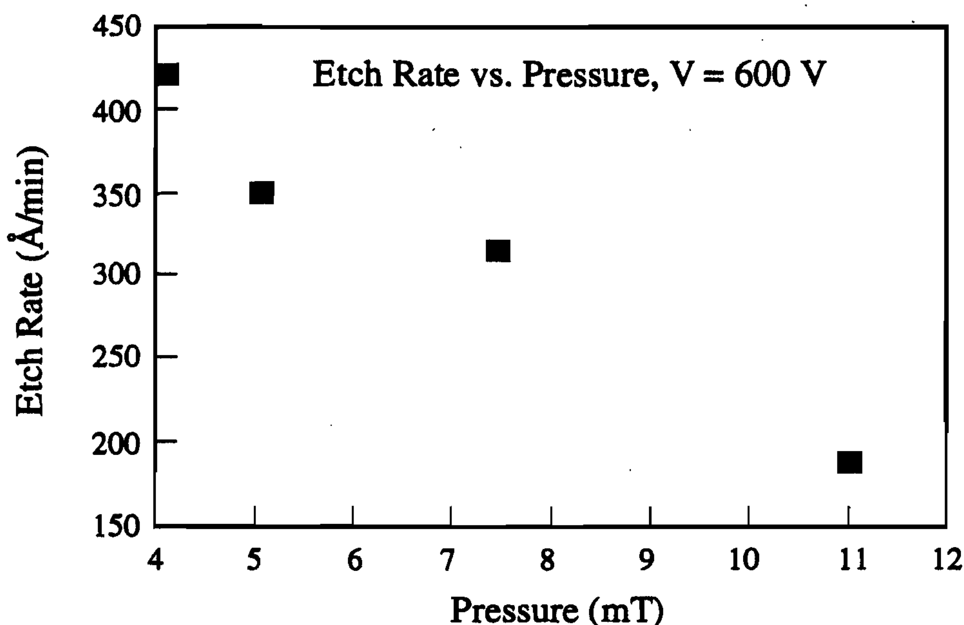

Fig. 7.19 The etch rate of GaN as a function of gas pressure.

Table 7.1 Etching rates of GaN (11mT and V = 600 V)

Gas	Etching Rate (Å/min)
CCl_2F_2	185
CF_3Br	150
CF_3Br/Ar (3:1)	200
CF_4	120
SF_6	100
H_2CH_4 (2:1)	30
Ar	65

Use or disclosure of the information contained on this sheet is subject to the restrictions on the title page of this proposal. This information is proprietary to the consortium.

The achievement of p-type doping is illustrated in Fig. 7.20 which shows (left panel) the mobility of p-type GaN versus reciprocal temperature and (right panel) the hole concentration of Mg-doped GaN from ECR-MBE.

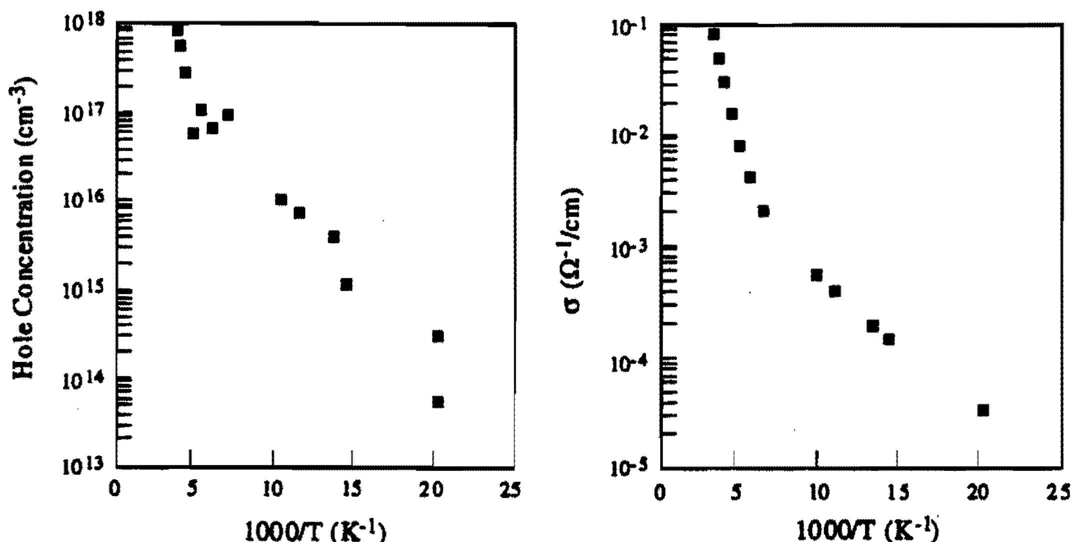

Fig. 7.20 P-type doping in ECR-MBE GaN.

The achievement of p-type doping coupled with the achievement of reliable Ohmic contacts has produced a working p-n junction LED from the Boston group as shown in Fig. 7.21. The LED has a turn-on voltage of approximately 3 V DC and has an emission spectrum centered at ~2.8 eV, a deep blue color.[39,40]

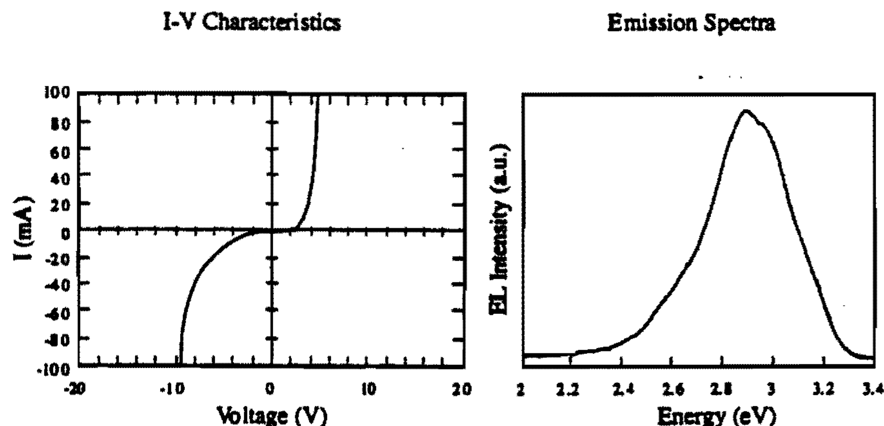

Fig. 7.21 The operation of the p-n junction LED.

VII.4 Current Commercial LED Technology

HP has been collaborating with outside laboratories to evaluate the various blue technologies for the past few years. With the commercial availability now of bright blue and green LEDs from Nichia Chemical Corp., it seems apparent that the GaN system will dominate the wide bandgap LED field. The II-VI devices have severe reliability problems and there is no solution on the horizon. The reliability of the GaN system is expected to be much better. HP has been evaluating LEDs from Nichia Chemical Corp. While the early results have not confirmed their long term reliability, as will be discussed below, the primary degradation exhibited by the Nichia devices is due to device design and processing rather than an inherent problem with the materials system. Extensive longer term reliability

Use or disclosure of the information contained on this sheet is subject to the restrictions on the title page of this proposal. This information is proprietary to the consortium.

studies are not yet complete. A summary of the salient features which have not been published by Nichia or others follows.

Table 7.2 compares the performance of the Nichia blue and green LEDs with existing high brightness LED technologies. The efficiency of the blue GaN device is >40X the efficiency of the existing commercially available SiC blue LEDs.

TABLE 7.2. LED Performance Comparison

Material System(color)	λ (nm)	E.Q.E. (%)	Flux (mlm)	Vf (V)
TS AlGaAs(red)	650	16	320	1.85
TS AlInGaP(amber)	590	11	800	1.95
LPE GaP: N(green)	572	0.4	120	2.2
SiC(blue)	482	0.04	4	3
InGaN(blue)	471	2.5	190	3.8
InGaN(green)	527	2.6	480	3.6

The efficiency and power out versus drive current for the Nichia blue and green LEDs are shown in Figure 7.22(a) and (b) respectively. The LEDs exhibit a well-behaved I-V characteristic with external efficiencies that peak at 3% and 4% for the green and blue emitters, respectively. The saturation of the efficiency is a consequence of utilizing a D-A recombination mechanism for optical recombination.

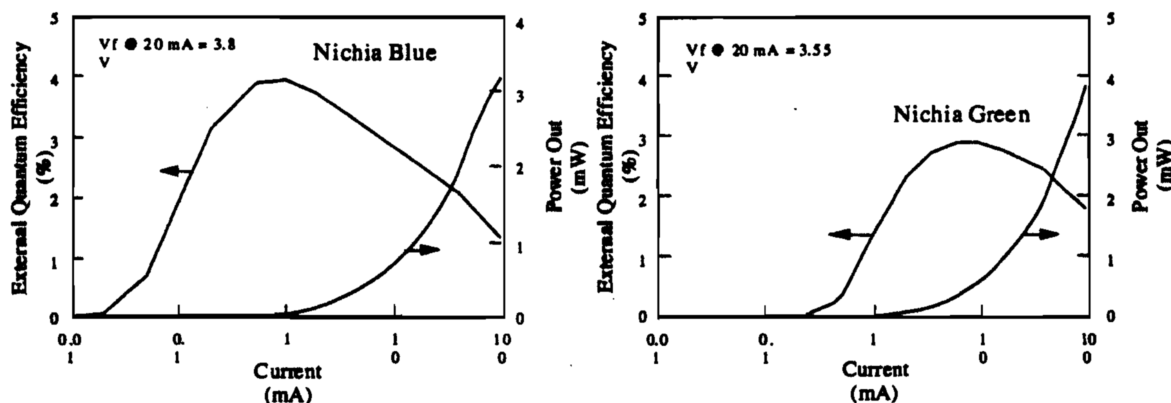

Fig. 7.22 The electro-optical performance of the Nichia LEDs.

Luminescence spectra for both the blue and green emitting devices are shown in Fig. 7.23. The dominant emission mechanism is due to donor-acceptor pair recombination. At high current levels the impurity band saturates and bandedge emission becomes predominant. The LED chips are separated by scribe and break techniques, which appear to result in a low yielding process. Most LED chips are separated by sawing.

Use or disclosure of the information contained on this sheet is subject to the restrictions on the title page of this proposal. This information is proprietary to the consortium.

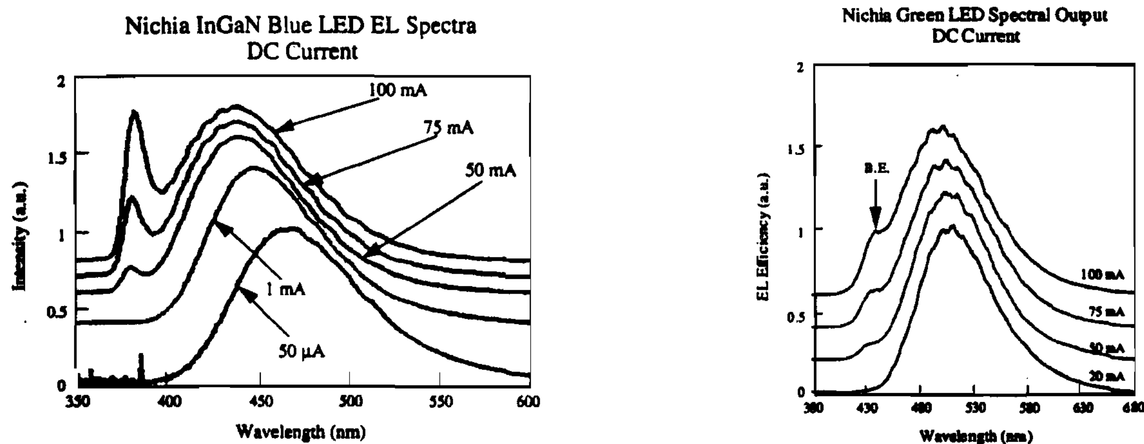

Fig. 7.23 The optical emission spectra for the blue (left) and green (right) LED.

An SEM micrograph showing an overview of the Nichia LED is presented in Fig. 7.23. As noted thereon, a semi-transparent metallic current spreading layer is used to provide uniform emission from the diode, increasing the extraction efficiency. The n- and p-type metallization schemes have been determined as Al/Ti and Au/Ni, respectively. A current-blocking layer is used to prevent light generation below the top (p-type) bonding pad and force the current through the emitting region. This further increases the extraction efficiency of the die.

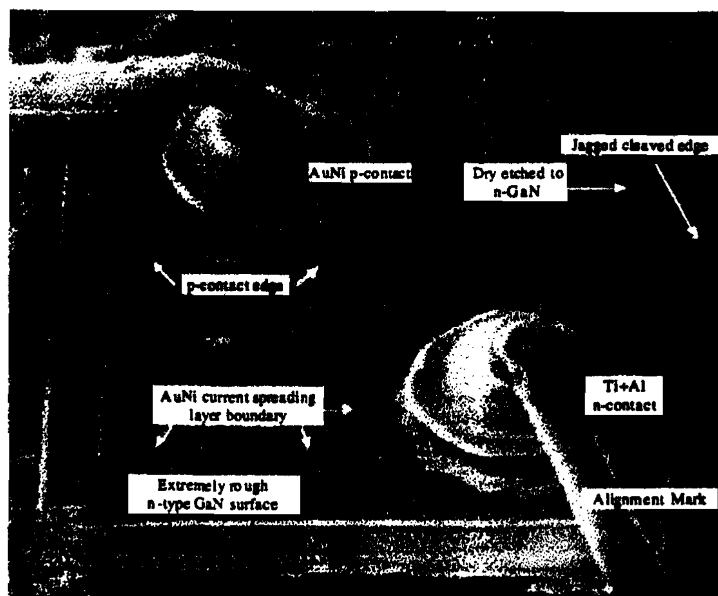

Fig. 7.23 An SEM image of the Nichia LED.

The epitaxial layer structure has been determined by SIMS. The structure differs from what has been published by Nichia in that the lower cladding layer of the double-heterostructure does not contain Al. This data is presented in Fig. 7.24.

Use or disclosure of the information contained on this sheet is subject to the restrictions on the title page of this proposal. This information is proprietary to the consortium.

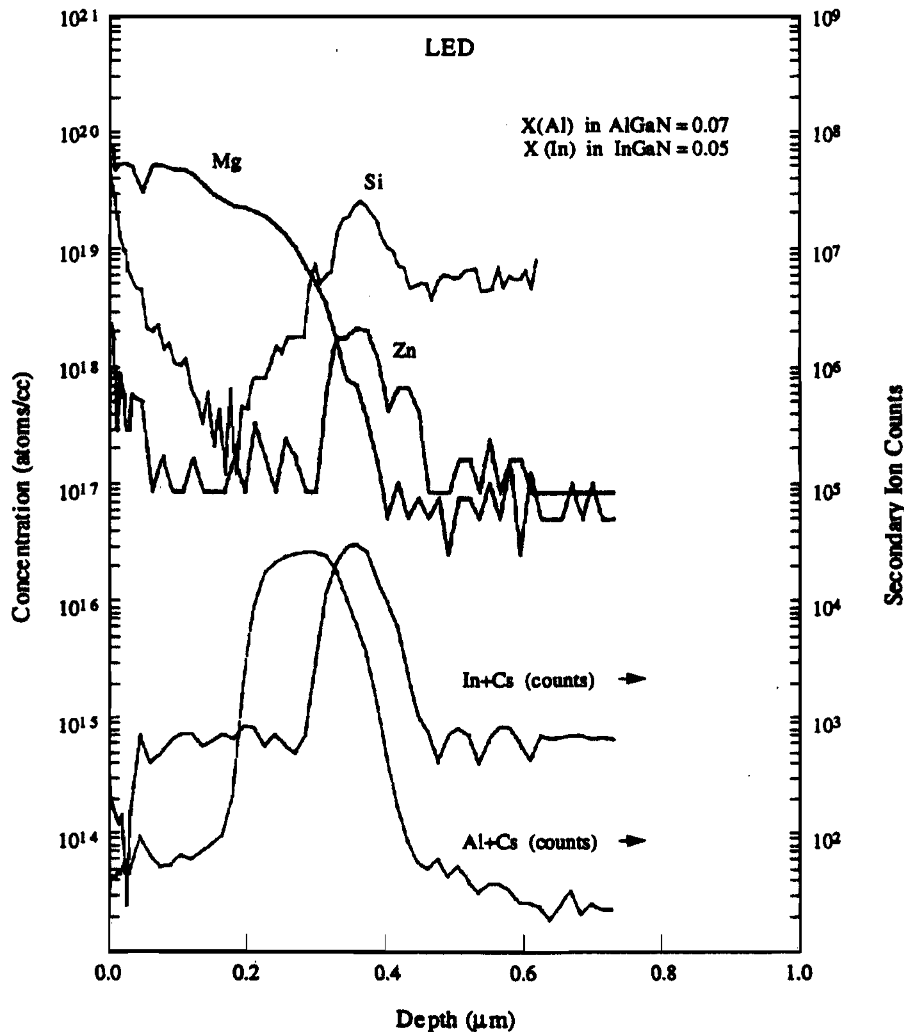

Fig. 7.24 A SIMS analysis of the Nichia LED.

The Nichia LED exhibits considerable degradation, even under normal operation at room temperature as shown in Fig. 7.25. An intensive effort well beyond the limitations of this text, has revealed that the primary failure mechanism is breakdown and leakage through the current-blocking layer underneath the p-type contact. The structural integrity of the nitride materials appears to be unaffected by normal operation of the LED.

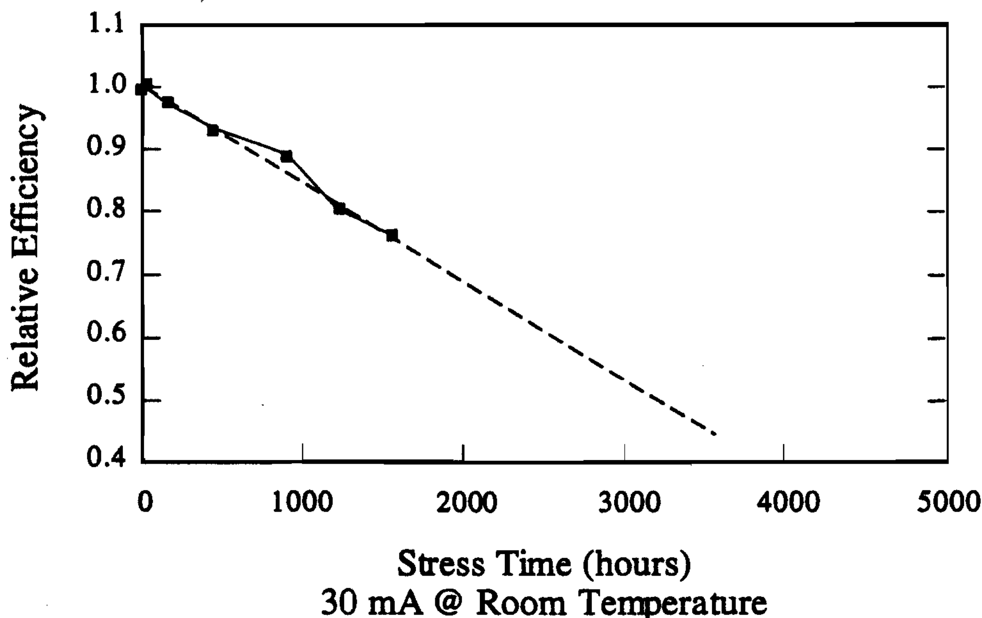

Fig. 7.25 Lifetesting of the Nichia LED.

VIII. Business Plan for Productization

VIII.1 Introduction:

The industrial partners of the consortium are leading manufacturers of optoelectronic components and systems. HP is the largest supplier, in dollar volume, of visible light emitting diodes in the world with strong product lines throughout the red, amber, yellow, and green portions of the visible spectrum. HP is also a systems company involved in sophisticated instrumentation, computers and computer memories, and printing. Xerox is a world leader in high-performance optical systems including copiers, printers, systems reprographics and network systems. SDL is the leading supplier, worldwide, of OEM high-power laser diodes and laser diode optical systems.

The material development program will lead to the demonstration of commercially viable LED technology and prototype LD technology. Blue and green LED commercial introduction, while not a milestone of the program, is certainly the over-riding goal of HP. At the end of the two-year base program, HP will have a solid materials knowledge base with prototype high-performance LEDs, and will begin the development of high-volume manufacturing technologies. At the end of the third year option, HP will be well into the process of commercialization of the technologies developed throughout this program.

The LD technology will be at the prototype demonstration at the end of year two. The third year program is focused on the fabrication of single-mode CW laser diodes with output powers on the order of 10 mW. The single-mode laser diode technology is required to access many of the markets listed below. The development of volume manufacturing technology for the laser diode would begin in year four.

It is the intent of the consortium to produce high-volume components to satisfy existing and emerging applications and to integrate these enabling components into consumer products produced both by members of the consortium and other manufacturing firms.

Use or disclosure of the information contained on this sheet is subject to the restrictions on the title page of this proposal. This information is proprietary to the consortium.

VIII.2 Market Analysis for AlGaInN Materials:

The introduction of blue LEDs and laser diodes addresses existing markets and enables future markets, primarily via cost reduction when compared to existing component technologies. The markets immediately available for the LED consist of automotive applications, traffic management displays, and the commercial signage industry. The availability of cost effective, high performance blue and blue-green LEDs alone would rapidly double the market for LED lamps and displays, which is currently estimated at $1.2B.

HP Optoelectronics Division is the world's leading manufacturer of light emitting diodes in terms of sales dollars, and is among the largest (including Japanese) producers in volume. HP is much larger than any non-Japanese producer. Most recently HP has announced its super bright TS AlInGaP LED which exhibits 80 Cd at 20 mA drive current. These LEDs are manufactured using MOCVD technology. HP is vertically integrated, growing bulk single crystals, growing epi layers via hydride VPE, LPE, and MOCVD, fabricating LED chips and displays and shipping these to customers worldwide. HP has a renowned III-V materials technology R&D effort. This expertise has allowed the development of the worlds brightest LEDs and the transfer to cost effective, large volume manufacturing (many millions of devices per month). HP is accelerating its GaN program over the next several years to bring this blue and blue-green technology to the market place. HP intends to leverage the high volume MOCVD technology utilized for AlInGaP production to develop a AlInGaN devices. In order for blue LEDs to find wide market acceptance, their price must be in the $0.20 ea. range, with an unpackaged chip cost somewhere in the $0.05 ea. range.

Automotive industry designers consider LEDs the technology of choice for back lighting of instrument clusters, convenience switches, LCD displays and climate control panels. Availability of blue LED technology would enable all vehicle lighting to be fulfilled with LEDs. In the traffic management industry, makers of traffic signals have demonstrated substantially reduced electrical power consumption and operating costs through the use of high performance red (stop) and amber (caution) LEDs. Blue-green LED technology (go) will enable an all-LED traffic light. Blue LEDs will enable substantially greater usage of LEDs as full color signs capable of conveying greater information through graphical displays become common.

To project the cost of the finished devices, HP will use cost models developed for the AlInGaP high brightness devices. The overriding cost factor is overhead: occupancy, depreciation, maintenance materials, expensed equipment, indirect labor, and direct labor payroll tax and benefits. Direct costs for materials and labor play a relatively small part. Lamp cost ultimately is driven by (1) process yields (epi, wafer fab, die fab, and assembly), (2) die size (influences the number of die per wafer; important since a wafer is the primary unit processed through the majority of the high costing steps), and (3) volume - the greater the volume the lower the cost since the relatively fixed overhead costs are spread thinner and thinner with increasing volume.

SDL, Inc., is the largest dollar volume manufacturer of semiconductor lasers worldwide. The facilities of SDL are vertically integrated containing a complete semiconductor laser diode fabrication facility, opto-mechanical packaging facility and global marketing. The semiconductor lasers developed within the framework of this proposal will rapidly exploit existing high-end markets, where a high unit cost can be tolerated, followed by penetration into mass consumer marketplaces where the laser unit cost must be on the order of a few dollars for a read blue laser diode and ~$10-100 for a higher-power single-mode read/write laser.

For the semiconductor laser diode, the most immediate market is the replacement of the Ar ion gas laser. The Ar laser is used at the 5-25 mW output power level. The market for these lasers, selling at $3.5K each, is approximately 12,000 units per year giving a total revenue for this market of $42M. The second market is biotechnology, where blue lasers are used

Use or disclosure of the information contained on this sheet is subject to the restrictions on the title page of this proposal. This information is proprietary to the consortium.

for cell sorting and DNA sequencing. This market is price sensitive, however, at the laser unit price of $1K, the biotech market will be expanded by an additional 40,000 units per year. Thus, immediate replacement markets represent yearly revenue of approximately $80M.

In the longer term, three broad markets are available; printing, optical storage, and displays. The projected market for optical printing is shown in Table 1. All dollar figures are for constant 1993 dollars, i.e., zero inflation.

Table 1. The market for optical printing.

Year	1993	1998	2003	2008	2013
Units (Millions of Units)	3.6	7.2	11.6	16.3	20.8
Revenue (Billions of Dollars)	3.3	5.1	8.2	11.5	14.8

Although many companies sell laser printers the vast majority of low-end printers use the Canon engine, with an OEM price of $75. The price of the complete laser printer is likely to decrease slowly from a current average printer price of $920 to an average printer price of $710 in the year 2013. The cost of the laser diode source will at maximum represent 10% of the engine price, thus, the printing market will likely require laser diodes in the price range of $5. Furthermore, blue laser diodes will be a minority of the lasers used for printing; potentially capturing 10% of the market. Based upon unit sales of 3.6 million in 1993 increasing to 20.8 million in 2013, the total potential market for blue laser diodes in printing is currently $1.8M and increases to $10.8M in 2013.

In the high-end printing market, the laser is not such a price-sensitive element. According to detailed market studies of general office usage, the xerographic marks on paper industry in the US had a value of $48B in 1990 and is expected in increase to about $125B in the year 2000. With the advent of high speed xerographic engines an increasing fraction of the much larger print shop market will be captured. The blue diode lasers made available in this program will complement the red and IR lasers already used in laser printing systems. The immediate impact will be to allow the use of more stable photoreceptors for high speed printing.

The optical storage industry represents a much larger market. Data storage, both magnetic and optical, represented a $24B market in 1992. Currently, CD-ROM is the most visible optical storage device. The CD-ROM uses low-power 780 nm laser diodes. Because the packing density of optical storage varies as the reciprocal of the wavelength squared, moving the wavelength to UV wavelengths dramatically increases the capacity of the CD-ROM system.

Table 2. Worldwide Optical Memory Market

Year	1993	1998	2003	2008	2013
CD-ROM					
Units (Million)	2.5	8.0	8.0	3.0	2.0
Revenues ($ Billion)	1.0	2.4	2.0	0.6	0.4
Read/Write					
Units (Million)	0.5	3.5	8.8	16.9	26.8
Revenues ($ Billion)	1.0	3.9	8.7	15.4	24.2

Due to the development of optical data storage systems that feature read/write capabilities, CD-ROM market will peak at approximately $2.4B and subsequently decrease. The market for read/write optical systems is $1.0B and increases to $24.2B in 2013. The pricing of the read/write data storage system is ~$1000 dollars/unit. Of the system total price, ~$100 will be directed to the read/write engine. The blue LD will require an output power of ~10 mW for writing and a power of ~1 mW CW for reading. In volume, the laser price can only represent ~10% of the total cost of the read/write unit, or about $10 dollars/laser diode.

Use or disclosure of the information contained on this sheet is subject to the restrictions on the title page of this proposal. This information is proprietary to the consortium.

Thus, the blue laser diode market is currently $5.1M and will increase rapidly to $0.27B in the year 2013. The comparison of the CD-ROM and read/write market is shown in Table 2. It should be stressed that although most laser printing applications can be envisioned without the fabrication of the blue laser diode, optical storage is absolutely reliant upon the blue or UV laser. The alternatives to the LD include frequency-doubled high-power semiconductor LDs or semiconductor pumped upconversion lasers. The complexity of the frequency-doubled source virtually insures pricing incompatible with consumer markets. Although interesting, the upconversion laser is expensive, extremely fragile, and requires external components for modulation, three attributes that the consumer market will not tolerate. Thus, for consumer-oriented optical memories, the blue LD is an enabling technology. The fabrication of a blue LD will exclude other blue sources from the marketplace in optical storage. The last market that should be considered is simple illumination. The efficiency of red, orange and yellow LED lamps now exceed that of common tungsten lamps. Highly efficient green and blue emitters will make feasible efficient semiconductor light sources.

IX. Key Personnel

DAVID F. WELCH, - Vice-President of Research, SDL, Inc.

Education

B.S. Electrical Engineering, University of Delaware, 1981
Ph.D Electrical Engineering, Cornell, 1985

JO S. MAJOR, JR. - Staff Scientist, SDL, Inc.

Education

B.S. Electrical Engineering, University of Illinois, 1985
M.S. Electrical Engineering, University of Illinois, 1986
Ph.D Electrical Engineering, University of Illinois, 1990

NOBLE J. JOHNSON - Principal Scientist, Xerox Palo Alto Research Center

Education

Ph.D. Princeton University, 1974
M.S.(EE) University of California, Davis, 1970
B.S.(EE) University of California, Davis, 1967

FERNANDO A. PONCE - Member Research Staff, Xerox Palo Alto Research Center

Education

B. S. Physics, U. N. I., Lima, Peru, 1971
M. S. Materials Science and Engineering, Stanford University, 1978
Ph.D. Materials Science and Engineering, Stanford University, 1981

CHRIS G. VAN DE WALLE - Member of Research Staff, Xerox PARC

Education

Engineer, Electrical Engineering, University of Gent, Belgium, 1982
M. S. Electrical Engineering, Stanford University, 1986
Ph.D. Electrical Engineering, Stanford University, 1986

M. GEORGE CRAFORD - R&D Manager, Hewlett-Packard Optoelectronics Division

Education

B.A. Physics, University of Iowa 1961
M.S. Physics, University of Illinois 1963
Ph.D. Physics, University of Illinois 1967

A. GRANT ELLIOT - R&D Project Manager, Hewlett-Packard Optoelectronics

Education:

B.S. Ceramic Engineering, University of California, Berkeley 1962
M.S. Materials Science, San Jose State University 1967

Use or disclosure of the information contained on this sheet is subject to the restrictions on the title page of this proposal. This information is proprietary to the consortium.

Ph.D. Materials Science and Engineering, Stanford University 1973

RUSSEL D. DUPUIS - Professor and Judson S. Swearingen Regents Chair in Engineering, University of Texas at Austin

Education:

Ph.D. Electrical Engineering, University of Illinois, 1973
M.S. Electrical Engineering,.University of Illinois, 1971
B.S. Electrical Engineering, University of Illinois, 1970.with Highest Honors (Bronze Tablet).

THEODORE MOUSTAKAS - Professor, Boston University

Education :

Ph. D. degree in 1974 from Columbia University (IBM Doctoral Fellowship)

HEIKKI I. HELAVA - Program Manager, AXT

Education:

SB Physics MIT 1969
MA Physics Columbia University 1971
MPhil Physics Columbia University 1974
PhD Physics Columbia University 1975

MICHAEL A. TISCHLER - Manager, Wide Bandgap Semiconductors, ATMI

Education:

B.S. Electrical Engineering, The University of Michigan 1978
M.S. Electrical Engineering, The University of Michigan 1980
Ph.D. Electrical Engineering, North Carolina State University 1986

X. References

1. J. N. Baillargeon, K. Y. Cheng, G. E. Hofler, P. J. Pearah, and K. C. Hsieh, Appl. Phys. Lett., **60,** 2540-2542, (1992).
2. S. Miyoshi, H. Yaguchi, K. Onabe, and R. Ito, Appl. Phys. Lett., **63**, 3506-3508. (1993).
3. P. Perlin, I Gorczyca, S. Prorwski and T. Suski, "III-V Semiconducting Nitrides: Physical Properties Under Pressure," Jpn J. Appl. Phys., Vol. 32 Sup. 32-1, pp. 334-339 (1993).
4. T. Detchprohm, H. Amano, K. Hiramatsu and I. Akasaki, J. Cryst. Growth, **128**,384 (1993).
5. T. Matsuoka, T. Sasaki and A. Katsui, OPTOELECTRONICS - Devices and Technologies, **5**, No. 1, 53 (1990).
6. The LEEBI work was reported by H. Amano, M. Kito, K. Hiramatsu, and I Akasaki, Jap. J. Appl. Phys. **28**, L2112 (1989); the thermal annealing results were reported by S. Nakamura, T. Mukai, M. Senoh, and N. Iwasa, Jap. J. Appl. Phys. **31**, L139 (1992).
7. J. A. Van Vechten, J. D. Zook, R. D. Horning, and B. Goldenberg, Jap. J. Appl. Phys. **31**,1258 (1992).
8. H. P. Maruska and J. J. Tietjen, Appl. Phys. Lett. **15**, 327 (1969).
9. M. A. Khan, J. N. Kuznia, J. M. Van Hove, D. T. Olson, S. Krishnankutty, and R. M. Kolbas, Appl. Phys. Lett. **58**, 526 (1991).
10. D. W. Jenkins and J. D. Dow, Phys. Rev. B **39**, 3317 (1989).
11. R. D. Dupuis in *Semiconductor-Based Heterostructures: Interfacial Structure and Stability*, Ed. M. L. Green, et al (The Metallurgical Society, Warrendale PA, 1986) p. 75.
12. Kurtin, McGill, and Mead, Phys Rev. Lett. **22**, 1433 (1969).
13. R. D. Dupuis, J. P. van der Ziel, R. A. Logan, J. M. Brown, and C. J. Pinzone, Appl. Phys. Lett. **50**, 407 (1987).

Use or disclosure of the information contained on this sheet is subject to the restrictions on the title page of this proposal. This information is proprietary to the consortium.

14. R. D. Dupuis in *Semiconductor-Based Heterostructures: Interfacial Structure and Stability*, Ed. M. L. Green, et al (The Metallurgical Society, Warrendale PA, 1986) p. 75.
15. R. D. Dupuis, J. C. Bean, J. M. Brown, A. T. Macrander, R. C. Miller, and L. C. Hopkins, J. Electron. Mat. 16, **69** (1987).
16. H. Amano, N. Sawaki, and I. Akasaki, Appl. Phys. Lett. **48**, 353 (1986).
17. Large-area (1 in. dia.) single-crystal (6H)-SiC substrates are commercially available from Cree Research.
18. R. D. Dupuis, unpublished.
19. T. Matsuoka, N. Yoshimoto, S. Sasaki, A. Katsui, and S. Zembutsu, Paper F6 in *Technical Program of the 33rd Electronic Materials Conf.*, Boulder CO, June 19-21, 1991, p.16.
20. S. Yoshida, S. Misawa, and S. Gonda, J. Appl. Phys. **53**, 6844 (1982).
21. K. Osamura, K. Nakajima, Y. Murakami, P. H. Shingu, and A. Ohtsuki, Solid State Commun. **11**, 617 (1972).
22. H. C. Casey and M. B. Panish, *Heterostructure Lasers, Part A Fundamental Principles* (Academic Press, New York, 1978), p. 45.
23. F.A. Kish, F.M. Steranka, D.C. DeFevere, D.A. Vanderwater, K G. Park, C.P. Kuo, T.D. Osentowski, M.J. Peanasky, J.G. Yu, R.M. Fletcher, D.A. Steigerwald, M.G. Craford, and V.M. Robbins, Appl. Phys. Lett., 64, 2839 (1994).
24. A.G. Elliot, A. Gerami, D.C. Boblet, A.J. McIntyre, SSA Journal, **5**,34 (1991)
25. M. A. Khan, J. N. Kuznia, J. M. Van Hove, D. T. Olson, S. Krishnankutty, and R. M. Kolbas, Appl. Phys. Lett. **58**, 526 (1991).
26. D. K. Gaskill, N. Bottka, and M. C. Lin, Appl. Phys. Lett. **48**, 1449 (1986).
27. M. Mizuta, S. Fujieda, Y. Matusmoto, Jap. J. Appl. Phys. **25**, L945 (1986).
28. S. Zembutsu and T. Sasaki, Appl. Phys. Lett. **48**, 870 (1986).
29. F. Hasegawa, T. Takahashi, K. Kubo, and Y. Nannichi, Jpn. J. Appl. Phys. **26**, 1555 (1987).
30. Y. Someno, M. Sasaki, and T. Hirai, Jpn. J. Appl. Phys. **29**, L358 (1990).
31. F. A. Ponce and J. E. Northrup, "Atomic arrangement at the AlN/Al2O3 interface," Phys. Rev. B, submitted July 1994): F. A. Ponce, J. S. Major, Jr., W. E. Plano and D. F. Welch, "Structure of GaN/AlN/SiC epitaxial films grown by MOCVD," APL., submitted July 1994).
32. M. S. Brandt, N. M. Johnson, R. J. Molnar, R. Singh, and T. D. Moustakas,Appl. Phys. Lett. 64, 2264 (25 April 1994).
33. M. S. Brandt, J. W. Ager III, W. G. GHotz, N. M. Johnson, J. S. Harris, Jr., R. J. Molnar, and T. D. Moustakas, Phys. Rev. B 49, 14768 (15 May 1994)
34. W. Gotz, N. M. Johnson, H. Amano, and I. Akasaki, "Deep Level Defects in n-type GaN," Appl. Phys. Lett., in press (25 July 1994).
35. J. Neugebauer and C. G. Van de Walle, in "Diamond, SiC and Nitride Wide Bandgap Semiconductors", edited by Carter, Gildenblat, Nakamura, and R. J. Nemanich, MRS Proceedings, Vol. 339 (MRS, Pittsburgh, Pennsylvania).
36. D. W. Jenkins and J. D. Dow, Phys. Rev. B 39, 3317 (1989).
37. J. Neugebauer and C. G. Van de Walle, Phys. Rev. B (Rapid Commun.),
38. M. Manfra, S. Berkowitz, R. Molnar, A. Clark, T.D. Moustakas and W. Skocpol, MRS Symp. Proc. (1994).
39. R.J. Molnar. R. Singh and T.D. Moustakas, (in preparation).
40. J. Foresi and T.D. Moustakas, Appl. Phys. Lett., 62, 2859 (1993).

Use or disclosure of the information contained on this sheet is subject to the restrictions on the title page of this proposal. This information is proprietary to the consortium.

4. REPORTS:
MILESTONES 1 AND 2. MILESTONE 6 PARTIALLY COMPLETED (5 PAGES)
MILESTONES 3 THROUGH 6 QUARTER 1 REPORT (29 PAGES)
MILESTONES 7 THROUGH 11 REPORT FOR MONTH 6 (37 PAGES)
MILESTONES 12 THROUGH 16 REPORT FOR MONTH 9 (18 PAGES)
MILESTONES 17 THROUGH 21 REPORT FOR MONTH 12 (11 PAGES)
MILESTONES 22 THROUGH 26 REPORT FOR MONTH 15 (16 PAGES)
MILESTONES 38 THROUGH 43 REPORT FOR MONTH 24 (16 PAGES)
FINAL REPORT AUGUST 1997 JUNE 1995-AUGUST 1997 (19 PAGES)
(TOTAL PAGES FOR REPORTS 151)

BLUE BAND

Blue Light and Ultra-Violet Emitters, the Bay Area Nitride Consortium
Report for Month 1
Contract: MDA972-95-3-0008

DISTRIBUTION: SDL, HP, Xerox, AXT, ATM, Boston University, the University of Texas at Austin, D. Scifres, J. Endriz, R. Craig, J. Johnson, and R&D	**To:** Distribution **From:** Jo S. Major **Date:** 7.12.95

Distribution authorized to U.S. Government agencies only to protect information not owned by the U.S. Government and protected by a contractor's "limited rights" statement, or received with the understanding that it not be routinely transmitted outside the U.S. Government. Other requests for this document shall be referred to ARPA Security and Intelligence Office.

Summary: Milestones 1 and 2 are completed. Milestone 6 is partially completed.

Milestone #1 (UT), Milestone Complete

UT Austin

- **Prepared by:** Russ Dupuis, UT Austin
- **Milestone #1:** Complete plans and piping for installation of Emcore HT "D" reactor system.
- **Summary:**

1. We have completed the installation of the EMCORE D125 Nitride reactor, including connection of the electrical power, cooling water, process gas lines hydrogen line, toxic gas monitors, exhaust, etc.
2. We has sent samples of AlGaN/sapphire to Dr. Fernando Ponce of Xerox PARC for analysis.
3. We have installed a SiH_4 gas line for n-type doping of the EMCORE GS3200 existing reactor.
4. We have initiated further studies of undoped and doped GaN/Sapphire films.

Milestone #2 (ATM, AXT), Milestone Complete.

ATM, Inc.

- **Prepared by:** Mike Tischler, ATM
- **Milestone #2:** Complete plans and facilities for reactor for GaN growth
- **Summary:**

The program to date is ahead of schedule. Our objectives were to complete the plans and facilities for the GaN reactor. The reactor is virtually completely constructed at this point. This includes a vented reactor cabinet, the plumbing for all gases and exhaust, the heating system, quartzware and valve control electronics. Safety features built into the reactor include automatic shutdown upon detection of hydrogen, overpressure of the reactor, loss of carrier gas or loss of compressed air. All facilities including electricity, compressed air, process gases, cabinet and process exhaust have been hooked up. The process exhaust is scrubbed using an ATMI/EcoSys dry scrubber.

Plans for Forthcoming Reporting Period
In the next reporting period we will focus on bringing the reactor on line. This will include leak checking and temperature profiling.

AXT

- **Prepared by:** Heikki Helava, AXT
- **Milestone #2:** Establish detailed program plan and schedule with HPRC/UNIPRESS
- **Summary:**

Gantt Chart included with report; however, it is subject to revision. AXT has initiated the effort for bulk crystal growth which is required under the Blue Band Program. Discussions and negotiations have been carried out with the High Pressure Research Center (HPRC, also called UNIPRESS) to establish the effort required to meet the deliverables objectives of the program. A subcontract has been established with HPRC by AXT and HPRC has delivered a program plan and the first samples of bulk single crystal GaN to AXT.

Milestone #6 (AXT, ATM, BU), Milestone Partially Complete.

AXT

- **Prepared by:** Heikki Helava, AXT
- **Description:** BB.4 #6 Deliver 2 mm scale GaN single crystal substrates to the consortium for study
- **Summary:**

Completed. Sample and micrograph delivered to Noble Johnson at Xerox-PARC 6/12/95.
The 2 mm scale GaN samples which were delivered to AXT cover a range of growth modes of the crystal ranging from rod-like structures to smooth platelets. One platelet (SN 0065, copy of micrograph included with this report), as per AXT's SOW, with a smooth surface was delivered to XEROX-PARC for characterization. According to HPRC's characterization, the smooth face is atomically flat and epi-ready; however, the samples need cleaning and HPRC has not been able to establish entirely satisfactory cleaning procedures. The other face of the sample and both faces of very large crystals grow in 20-40 angstrom steps. In order to utilize these crystals as substrates for epi-growth surface preparation will be necessary.
AXT is exploring the ductile diamond grinding of ultra-hard materials with Horizon Technology Group and NIST. AXT is also examining the laser polishing of GaN surfaces using excimer lasers. We plan to submit one sample to LPL, Inc. or Lambda-Physik to explore the energy requirements for laser processing GaN. Results from these tests will be reported in subsequent periods.

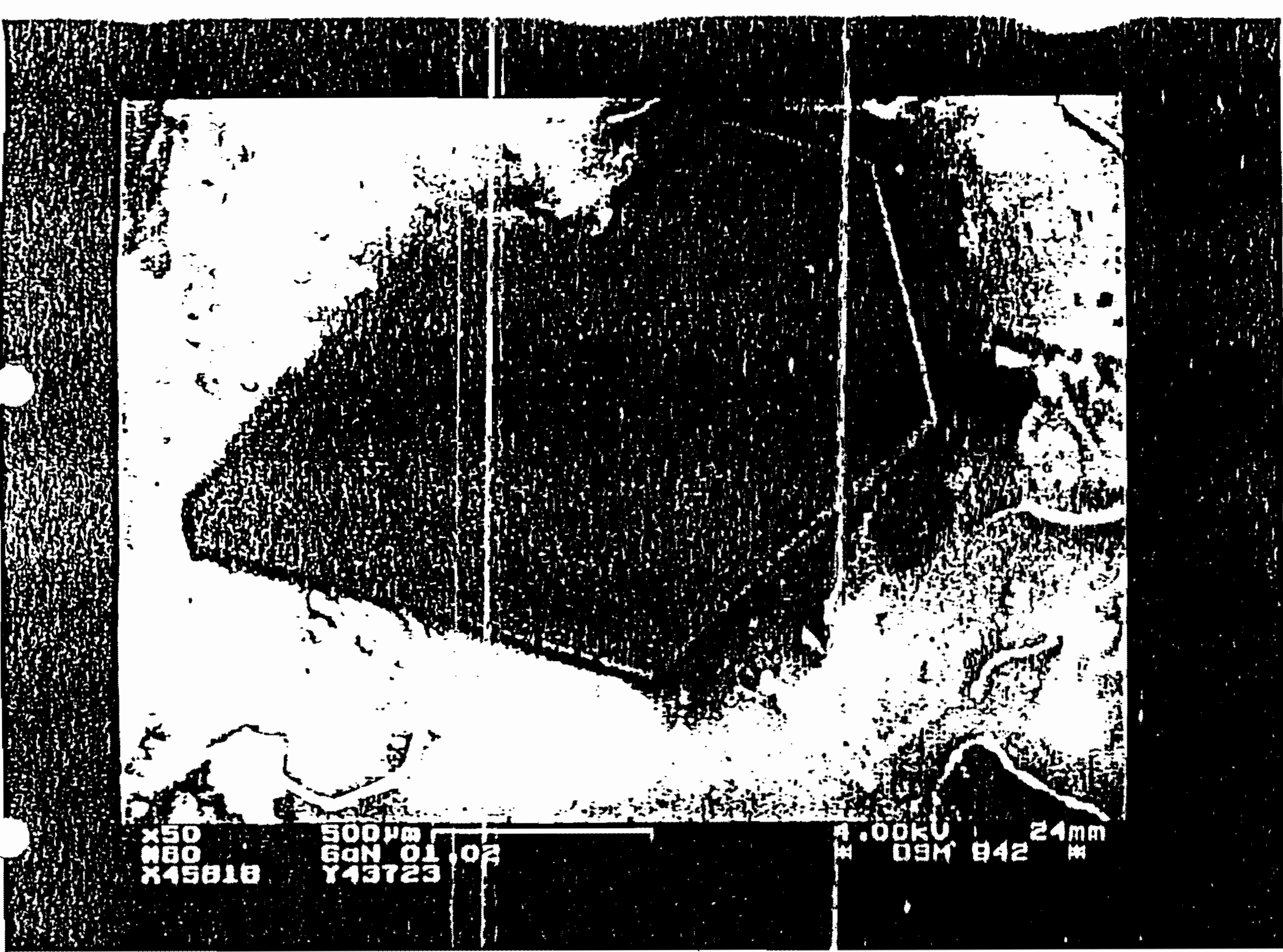

II

Sample delivered
to Xerox Parc
6/12/95
per request of
Noble Johnson

0065

HPRC Subcontract AXT

ID	Task Name
1	Prepare program plan and schedule
2	Program plan completed
3	Calculation & verification 18 mM crucible
4	18 mM crucible unseeded growth
5	18 mM seeded growth
6	Intentional acceptor doping
7	Growth in 18 mM crucible
8	Deliver 3 crystals of 2 mM
9	Deliver 1 crystal of 5 mM
10	Deliver 3 crystals of 5 mM
11	Analyze 25 mM crucible
12	Calculation & verification 25 mM crucibles
13	Fabrication & testing 25 mM crucibles
14	25 mM crucible unseeded growth
15	25 mM crucible seeded growth
16	Deliver 1 GaN crystal of 1 cM
17	Deliver 3 GaN crystals of 1 cM
18	Phase I Downselect Review
19	Deliver 3 GaN crystals of 1 cM
20	Analysis for Phase II
21	Analysis of 35 mM crucible
22	Calculation & verification 35 mM crucible

Project: Blue Band
Date: 95/06/20

Task Progress Milestone Summary

HPRC Subcontract AXT

ID	Task Name
23	Fabricate and test 35 mM crucible
24	35 mM seeded growth
25	Deliver 1 crystal >2 cM
26	Final report

1995: May Jun Jul Aug Sep Oct Nov Dec
1996: Jan Feb Mar Apr May Jun Jul Aug Sep Oct Nov Dec
Jan Feb Mar Apr May

04/

Project: Blue Band
Date: 95/06/20

Task | Progress | Milestone | Summary

BLUE BAND

Blue Light and Ultra-Violet Emitters, the Bay Area Nitride Consortium
ARPA Quarter One Report
Contract: MDA972-95-3-0008

DISTRIBUTION: SDL, HP, Xerox, AXT, ATM,
Boston University, the University of Texas at Austin,
D. Scifres, J. Endriz, R. Craig, J. Johnson, and R&D

To: Distribution
From: Jo S. Major
Date: 10-5-95

Distribution authorized to U.S. Government agencies only to protect information not owned by the U.S. Government and protected by a contractor's "limited rights" statement, or received with the understanding that it not be routinely transmitted outside the U.S. Government. Other requests for this document shall be referred to ARPA Security and Intelligence Office.

Administrative Details

The electronic address of Jo Major is now JoMajor@AOL.com.

Technical Summary

- All milestones of Quarter One have been met.
- The Blue Band gave a kick-off presentation at Big Sky '95, copy of presentation included.

Milestone Report:

Milestone 3.

- **Emcore reactor installed and operational**

  Hewlett-Packard

  The Emcore 3300 GaN MOCVD reactor (S/N 5182) installation was completed 25 January 1995 and the initial acceptance growth runs were begun 6 February 1995. Early hardware problems were corrected, and the reactor acceptance was

completed on 8 March 1995. Over 150 growth runs have been performed in this reactor to date, investigating the effect of process variables such as GaN growth pressure 55-200 Torr), temperature 1020-1055°C), susceptor rotation (500-1000 rpm) and process gas flow rates (TMG, SiH_4 NH_3 and H_2).

Both GaN and AlN buffer layers have been investigated. It was determined that the best electron mobilities in n-type GaN films were achieved for those grown on GaN buffer layers 21 nm thick, with significant reductions in mobility as one moves away from the optimum thickness. The mobility of n-type GaN grown on AlN buffer layers is much less sensitive to buffer layer thickness, but has lower peak mobility than those grown on GaN buffer layers.

- **Studies of SL Buffer Layers**
  University of Texas at Austin
  Studies of SL buffer layers have been initiated. We have been working on superlattices constructed of AlN and GaN thin layers grown on (0001) Al_2O_3 substrates. Our first efforts are still being characterized at this time.

- **Deliver GaN/Al2O3 and GaN/SiC to Xerox SDL, Inc.**
  SDL, Inc. has sent GaN grown on Al_2O_3 and SiC to Xerox for characterization. The sample of GaN/Al_2O_3 will be discussed in detail within this milestone summary. The results of the GaN/SiC characterization will be discussed in Milestone 7 of the next quarterly report.

- **Structural Characterization of GaN/Al_2O_3**
  Xerox
  The role of the substrate interface is critical for heteroepitaxy. The atomic arrangement at the interface between the substrate and the thin film determines the structural characteristics of the epilayer. One of the first activities in our research on III-V nitrides for blue laser diodes has been in the understanding of the crystalline structure in the region next to the substrate. GaN thin films have been studied using cross-section TEM. The films were grown by metal organic chemical vapor deposition on (0001) Al_2O_3 substrates, using the well established approach of growth of buffer layers at low temperatures (520 to 550°C), followed by growth of the GaN epilayer at high temperatures (1020 to 1050°C). The most commonly used buffer layers are AlN and GaN. In this portion of the report we present the results we have obtained about the crystalline structure associated with growth using AlN and GaN buffer layers. No intentional doping was introduced.

A. Epitaxy of GaN using AlN buffer layers

These films were grown at SDL using TMGa, TMAl, and ammonia as sources. The film exhibited good crystalline and electronic properties, with x-ray diffraction rocking curves full width at half-maximum (FWHM) between 4 and 5 arcmin, and room-temperature electron concentrations at about 5×10^{15} cm^{-3}.

A lattice image of the AlN/Al_2O_3 interface is shown in Fig. 1. The sapphire lattice is viewed in the <1-100> projection, with the basal (0006) plane and the (11-20) type planes appearing in horizontal and vertical projections, respectively. The buffer layer and the AlGaN film are observed in their <11-20> projection, where the horizontal corresponds to the basal (0002) planes and the vertical to the {1-100} type planes. A schematic diagram of the AlN/Al_2O_3 is shown in Fig. 2, where proportional projections of the lattices indicate the relative arrangement of the atomic species viewed in Fig. 1. Fig. 3 shows the atomic arrangement of the (0006) and (0002) basal planes of sapphire and AlN, respectively. A configuration satisfying the valence requirements is shown in Fig. 4. This configuration, where an aluminum atom is bonded to three oxygen atoms in the lower atomic layer, and to two nitrogen atoms in the upper layer, would give rise to a coherent, neutral interface. However, AlN grows in the direction of the basal planes, and instead of a two bonds to N in the vertical direction, it either has one or three depending on whether growth is in the polar (000-1) or (0001) directions, corresponding to growth with Al or N on top of the basal plane, respectively. In the following analysis we consider the implications of the two polar orientations, on the observed high resolution images.

Figure 1: Cross section, TEM, lattice image of the substrate region of a GaAlN/AlN/Al_2O_3 thin film showing the atomic arrangement at the respective interfaces.

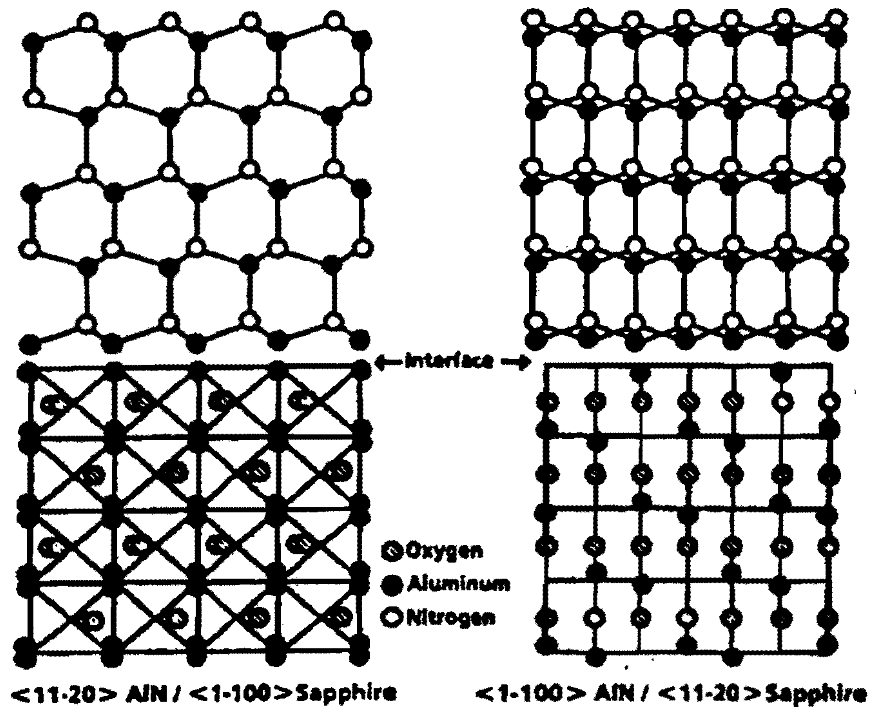

Figure 2. The atomic arrangement of the (a) Al_2O_3 and (c) AlN lattice structures projected onto the basal plane. The bonding configuration between aluminum and the adjacent neighbors is viewed in direction normal to basal plane in (b) Al_2O_3 and (d) AlN.

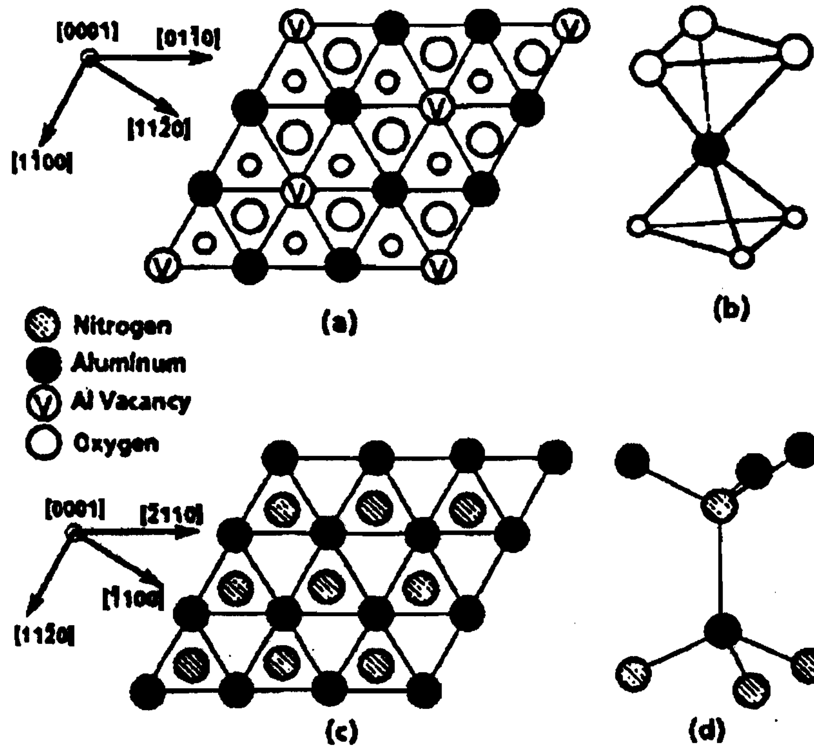

Figure 3 the atomic arrangement of the (a) Al_2O_3 and (C) AIN lattice structures projected onto the basal plane. The bonding configuration between aluminum and the adjacent neighbors is viewed in direction normal to basal plane in (b) Al_2O_3 and (d) AIN.

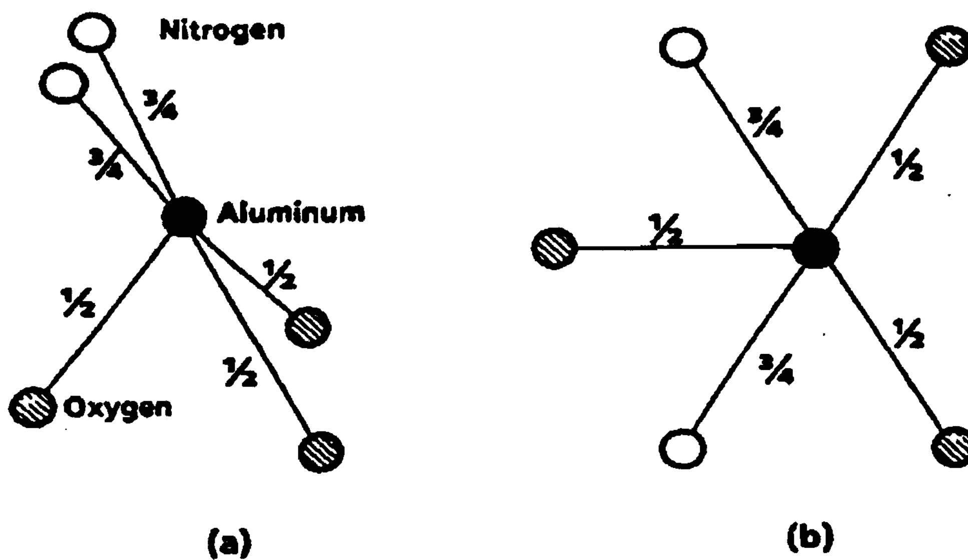

Figure 4. Atomic bonding configuration of Aluminum between its oxide and its nitride, satisfying the covalent bonding requirements.

Figure 5 shows two different projections of the same region of the AlN/Al_2O_3 interface. These are the same projections depicted in Fig. 2, and are obtained by rotating the specimen 30 degrees about the c-axis. The symmetry of the spots observed in these two projections indicates that the atomic sites are represented by bright regions of the image. For AlN, each bright spot corresponds to an Al-N pair in the [01-10] projection, and a bright line (spots are not always resolved) in the 11-20 projection.

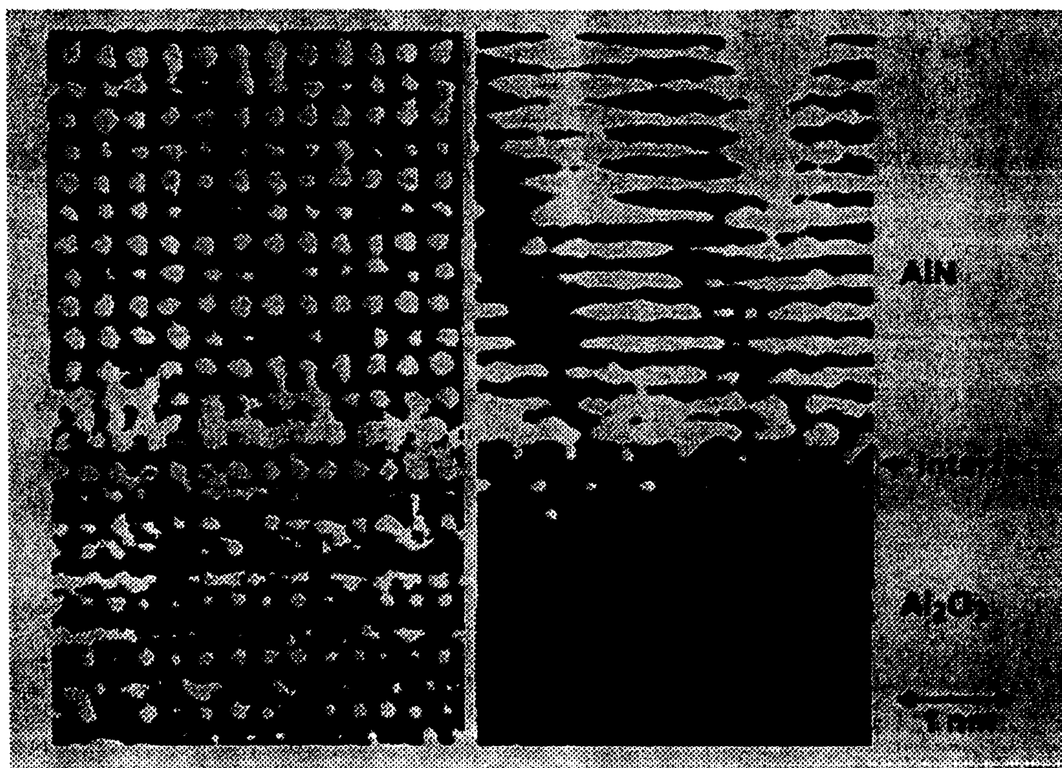

Figure 5. Lattice images of the AlN/ Al_2O_3 interface taken in the (a) [01-10] and (b) [11-20] projections of the same interface region.

Figure 6 shows the atomic arrangement expected for the two possible polarities discussed above. In model A, Al occupies the top position in the AlN lattice. Interatomic separations of the Al-N and the Al-O bonds are used in these diagrams. The interplanar separations in the c-axis direction is plotted in Figure 6. A comparison of the two models and the experimental values, as shown in Figure 7, indicates that Model B is most likely associated with our

observations. This means that the AlN film has grown with N at the top position of the basal plane. It must be noted that the polarity of growth is determined in the solid-phase crystallization process.

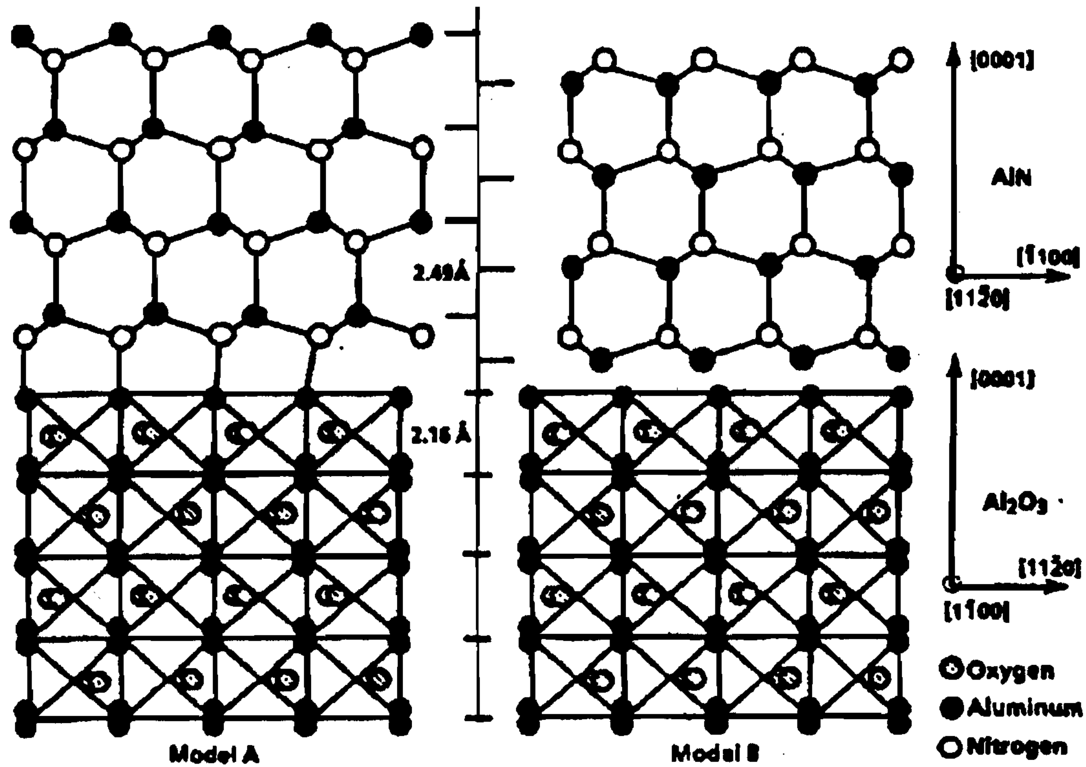

Figure 6. Two possible models of the AlN/ Al_2O_3 interface. The AlN film in model A is in the (0001) orientation with Al on the top of the basal plane, and in model B in the (000-1) orientation with N on the top of the basal plane.

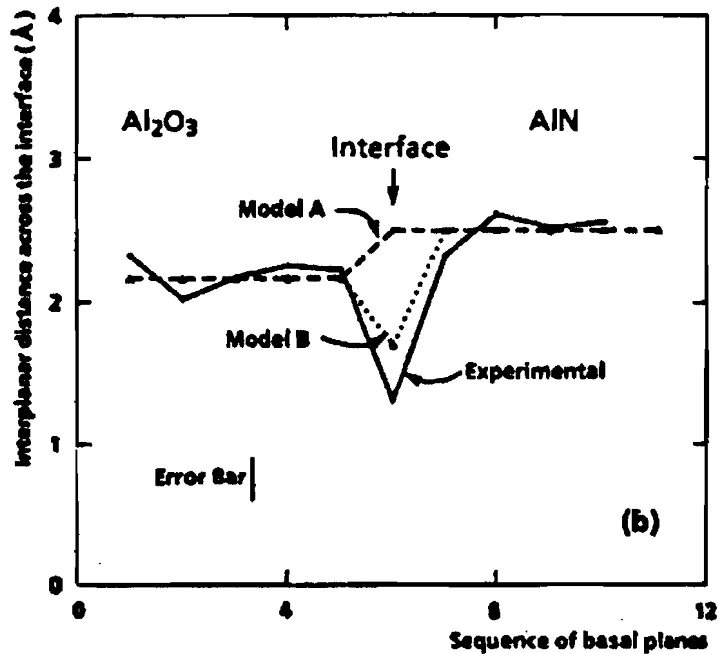

Figure 7. Interplanar separation across the Al_2O_3/AlN interface.

Milestone 4

- **Initiate studies of InGaN growth in "B" reactor.**
  University of Texas at Austin

  We have initiated studies of InGaN growth in B reactor. Thin films of InGaN have been grown by MOCVD on GaN buffer layers grown on (0001) Al_2O_3. These films have been examined by X-ray diffraction rocking curve measurements. A FWHM value as low as 145 arc sec have been measured for an InGaN film ~0.1 micron thick.

Milestone 5

- **Metal Contacts for n-type GaN Films**
  Hewlett-Packard, SDL

  Both institutions have verified that Ti/Al as a core technology works well for n-type GaN.

  The literature shows that the best metal contact for n-type GaN is 20 nm of Ti followed by a thick Al layer for good wire bonding yield. We deposited evaporated Ti/Al films through

resistance-heated boat evaporation. The Ti/Al n-type contacts were tested on n-type GaN samples with two different doping levels, $3.0x10^{18}/cm^3$ and $1.2x10^{19}/cm^3$. Wafer dot-to-dot I-V curves are attached for the as-deposited metal contacts, as well as after annealing at 400, 500 and 600°C for one minute, and after annealing at 600°C for five minutes. All of the annealing experiments were performed in a Heatpulse 210 rapid thermal annealer manufactured by AG Associates.

All of the films made ohmic contacts to the highly doped Si:GaN wafer, with lower resistance seen for increaingly more intense anneal conditions, as expected. It was not possible to make ohmic contact to the $3.0x10^{18}/cm^3$ Si:GaN film prior to annealing. The evaporated Ti/Al contact gave the lowest resistance, followed by the sputtered TiW/Al.

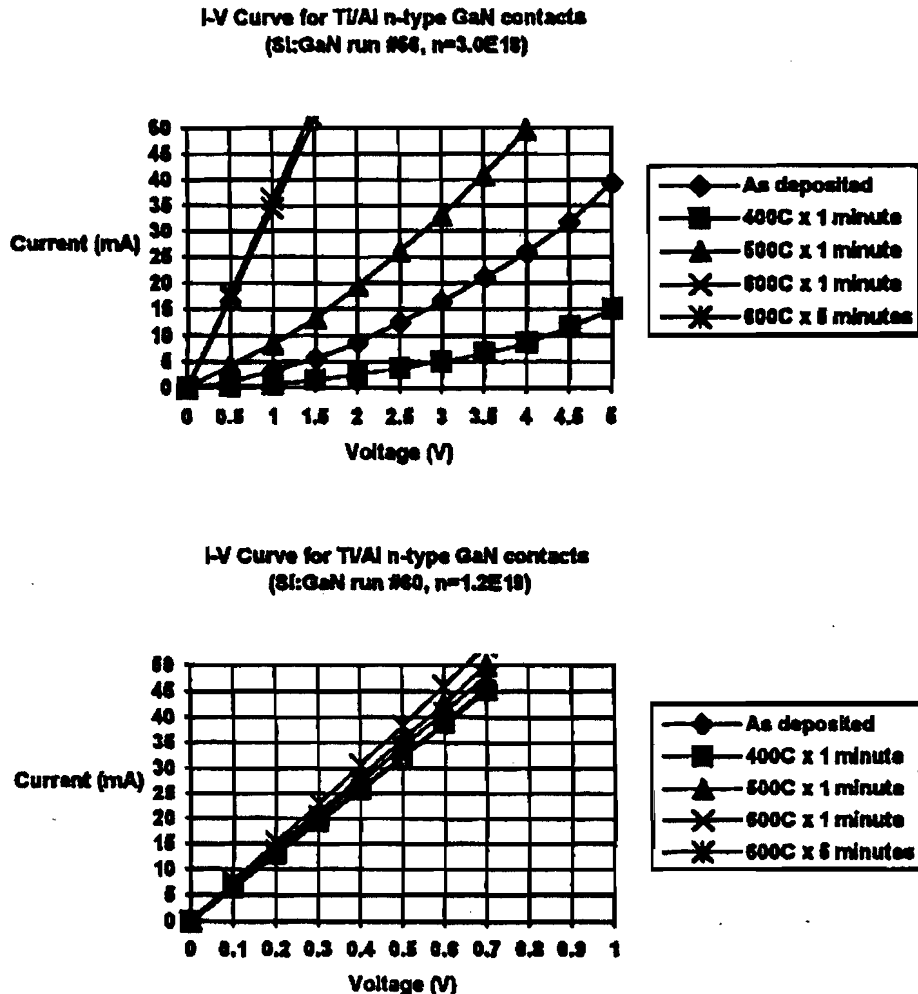

Figure 8 IV curves for Ti/Al contact for n doping levels of $3x10^{18}$and $1.2x10^{19}$ cm^{-3}.

Contact resistance was measured by a standard TLM technique. We used 2.5 mm thick GaN film on sapphire substrate. Electron concentration in the film was n = 1◊10^{18} cm^{-3} and mobility m = 180 cm^{2} V^{-1} s^{-1}. Pairs of rectangular contact pads 250 mm by 100 mm with the spacing between pads varying in the nominal range of 5-25 mm were patterned by a lift-off procedure. A titanium layer with a thickness of 40 nm was first deposited by RF sputtering in Ar at the pressure of 10^{-3} Torr followed by aluminum layer 200 nm thick deposited by thermal evaporation. After the lift-off procedure, contacts were annealed in an RTA in an argon/hydrogen atmosphere. An annealing cycle consisted of the 30 second temperature ramp to 650°C, 30 second hold at this temperature and 1 min cooling to the room temperature. An actual spacing between contact pads after annealing was measured in a

scanning electron microscope. A typical dependence of the resistance between pads on the spacing for Ti/Al contacts annealed at 650°C is shown in Figure 9. An extrapolation to zero spacing gives a resistance value of 0.7W, which in turn yields a value of 8◊10^{-5}Wcm^{3} for a specific contact resistance. An annealing at higher temperature (up to 850°C) did not result in significantly lower values of the specific resistance.

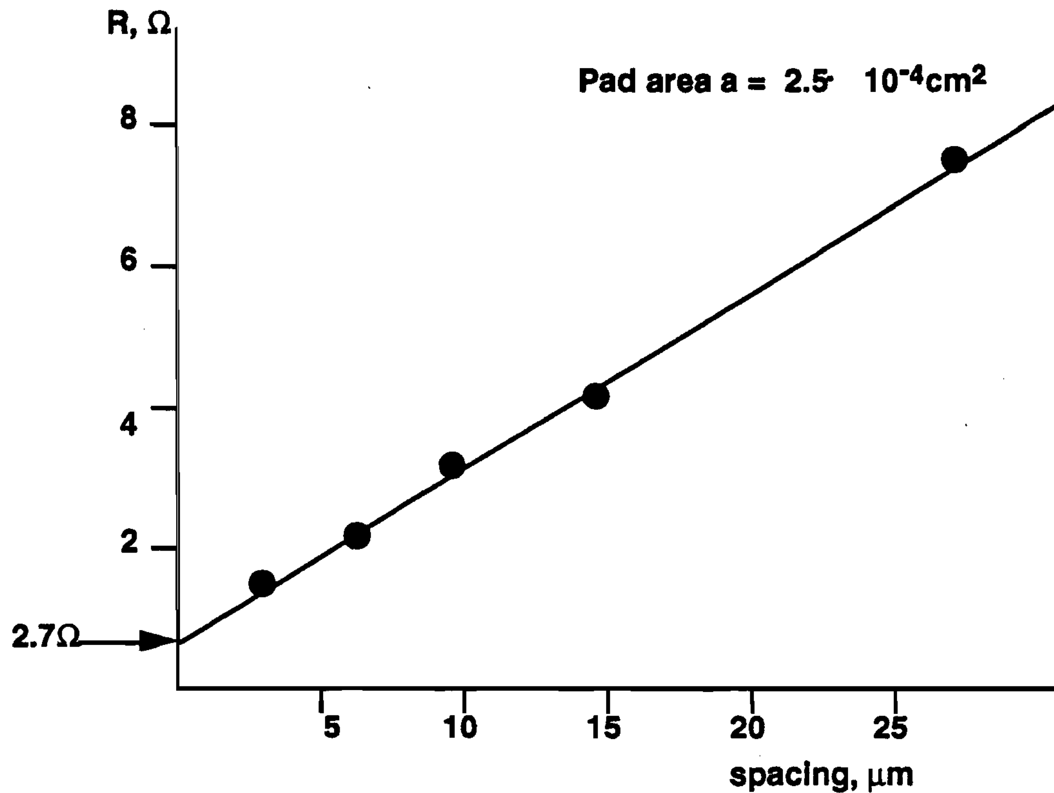

Figure 9

- **Deliver GaN with n-type impurities to Xerox for materials characterization.**

SDL, HP

Both SDL and HP have delivered n-type (Si-doped) samples to Xerox for analysis. The analysis of these materials follows.

Initiate Electrical Characterization of GaN

Xerox

We have initiated electrical characterization of GaN thin films grown on sapphire c-plane subtrates. The variable temperature Hall effect measurement is a well-established and suitable tool to study the electronic properties of impurities or native defects, investigate scattering mechanisms that limit the carrier mobility, and determine the concentration of compensating centers present in the GaN epi layers. This information is essential for the growth of electronic-grade material that can be used in light emitting diodes (LEDs) or laser diodes(LDs).

The Hall effect measurements were enabled by using a Van der Pauw geometry for the Ohmic contacts. The contacts were fabricated by vacuum deposition of first Ti (200Å) and then Au (2000Å) in the four corners of 5 x 5 mm^2 samples. These contacts exhibited Ohmic current-voltage characteristic over the entire temperature range of the Hall effect measurements (80K - 500K).

For n-type films, the Hall effect data result in electron concentrations (Hall scattering factor is assumed to be of unity value) and electron Hall mobilities as functions of the sample temperature. With this data, activation energies for donors, their concentration and the concentration of the compensation can be estimated.

The samples investigated are listed in Table I:

Table I: GaN samples investigated with variable temperature Hall effect measurements

Supplied by	Sample #	doped/undoped
SDL	B906N	undoped
SDL	B938N	undoped
HP	15	undoped
HP	19	Si-doped
HP	50331a	undoped

In addition to the Hall measurements, some samples were also characterized by room temperature (2K) photoluminescence (PL) spectroscopy. PL measurements reveal the presence of electronic states in the bandgap of semiconductors which may act as efficient recombination centers in LEDs or LDs. These electronic states may be useful in LEDs but need to be eliminated in LDs. In both cases characterization of these levels and the relation of their appearance to growth conditions is extremely important.

A. Hall effect results

Hall effect data obtained from unintentionally doped, n-type GaN films are presented in Figure 1 (# 50331a) and 11 (#B938N). Figures 10a and 11a show electron concentrations as a function of the temperature. The solid squares refer to the experimental data while the solid lines are results of fitting the charge neutrality equation to the experimental data. The fits show evidence of the presence of two independent donors in both samples. The activation energies for the donors, their concentration and the concentration of compensating acceptors are summarized in Table II.

Figure 10b and 11b show the mobility measured with Hall effect as a function of sample temperature. The mobility at room temperature (300K) is 568 cm^2/Vs and

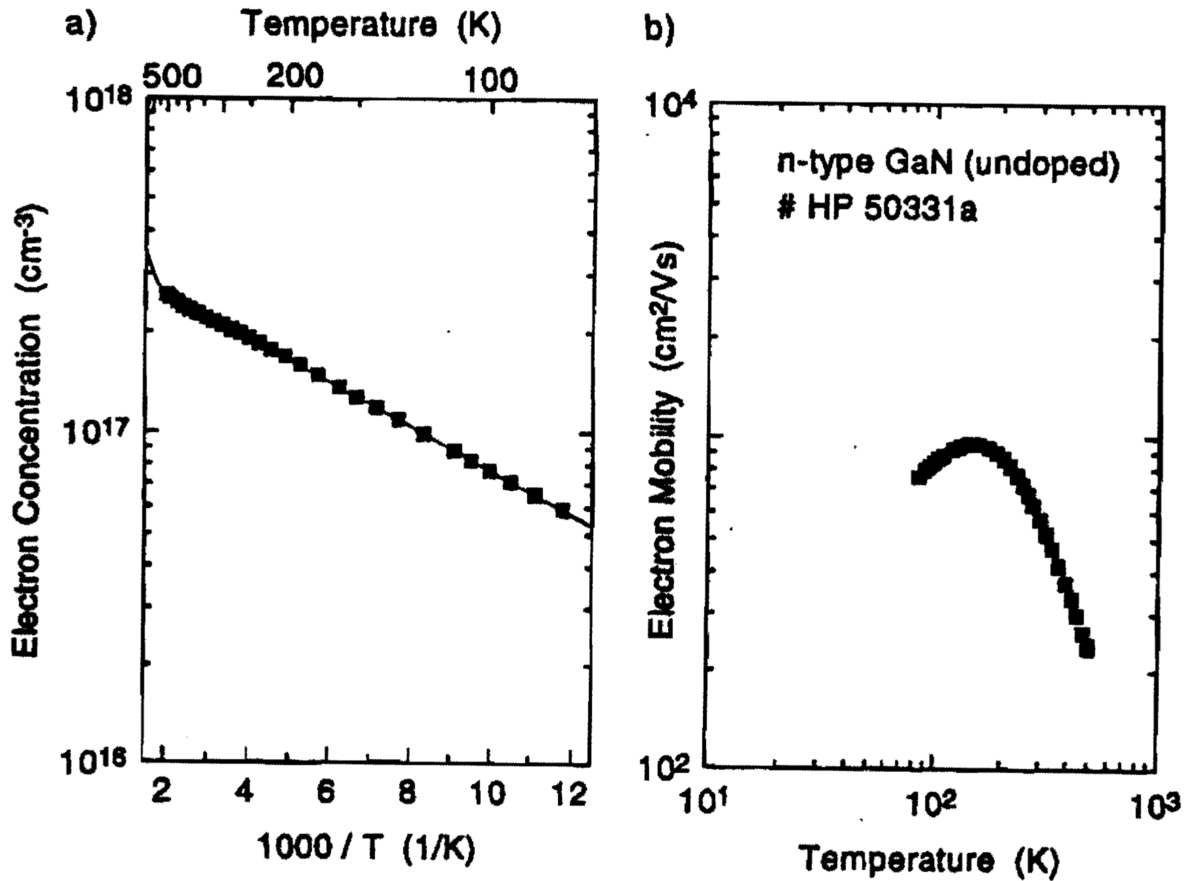

Figure 10: Electron concentration vs reciprocal temperature (a) and electron mobility vs temperature (b) measured with Hall effect from an unintentionally doped GaN film. The solid squares refer to the experimental data. The solid line in Figure 10A results from a fit of the charge neutrality equation to the experimental data.

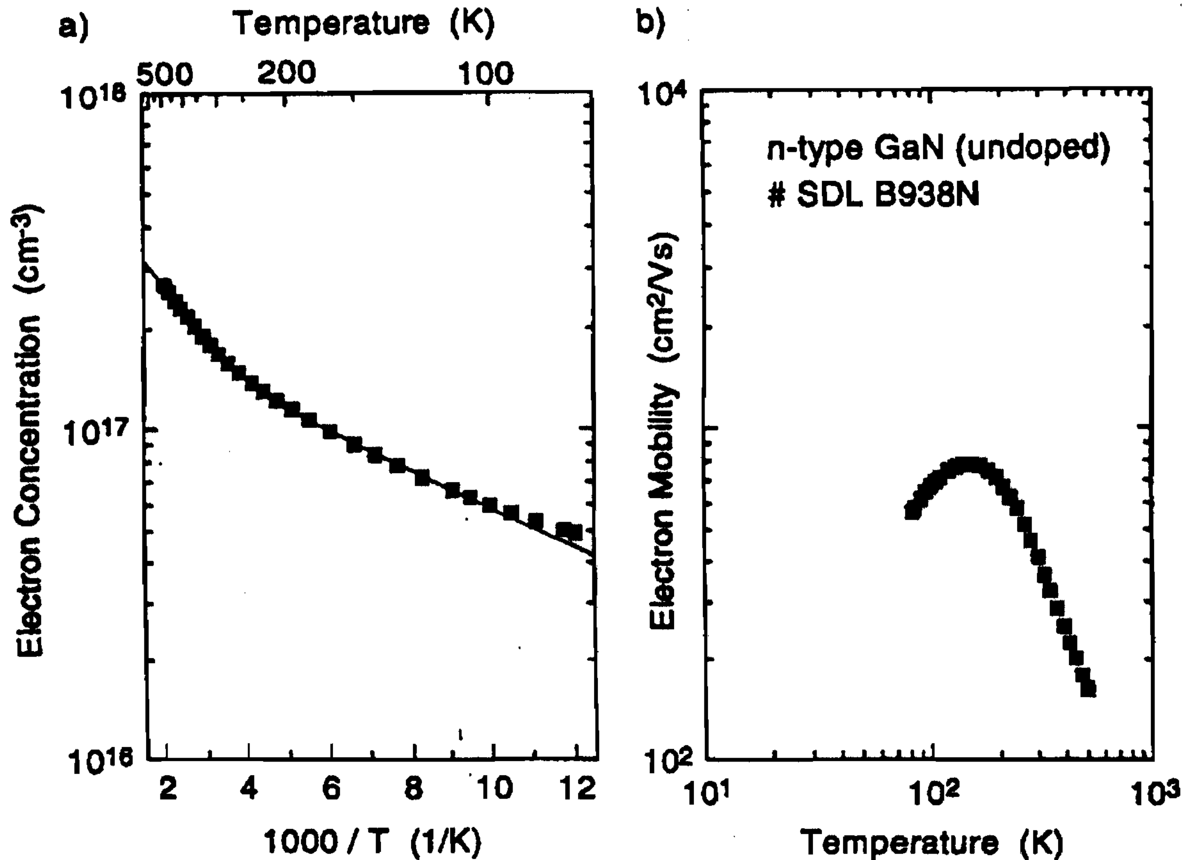

Figure 11: Electron concentration vs reciprocal temperature (a) and electron mobility vs temperature (b) measured with hall effect from an unintentionally doped GaN film. The solid squares refer to the experimental data. The solid line in Figure 11a results from a fit of the charge neutrality equation to the experimental data.

410 cm^2Vs and the maximum mobility is 950 cm^2/Vs at 150K and 776 cm^2/Vs at 150 K for sample # 50331a and # B938N, respectively.

In Figure 12, similar results as in Figure 10 and 11 are shown for a GaN sample (#19) which was intentionally doped with Si. The electron mobilities measured in this sample are 501 cm^2/Vs and 764 cm^2/Vs at room temperature and at 160 K, respectively. Results obtained with the fit of the charge neutrality equation to the experimental n vs. 1/T data for sample # 19 are also summarized in Table II.

Table II lists activation energies and concentrations of donors and compensation evaluated from variable temperature Hall effect measurements of the GaN samples available in the time period of this report. In addition, room temperature and maximum electron mobilities are shown. The data show the presence of a shallow donor with an activation energy ~ 15 meV to be present in all the GaN samples. This donor is likely to be the "autodoping" center that is responsible for the n-type conductivity of unintentionally doped GaN films. Its chemical or structural nature is still unknown but Si, O or nitrogen vacancies are likely candidates.

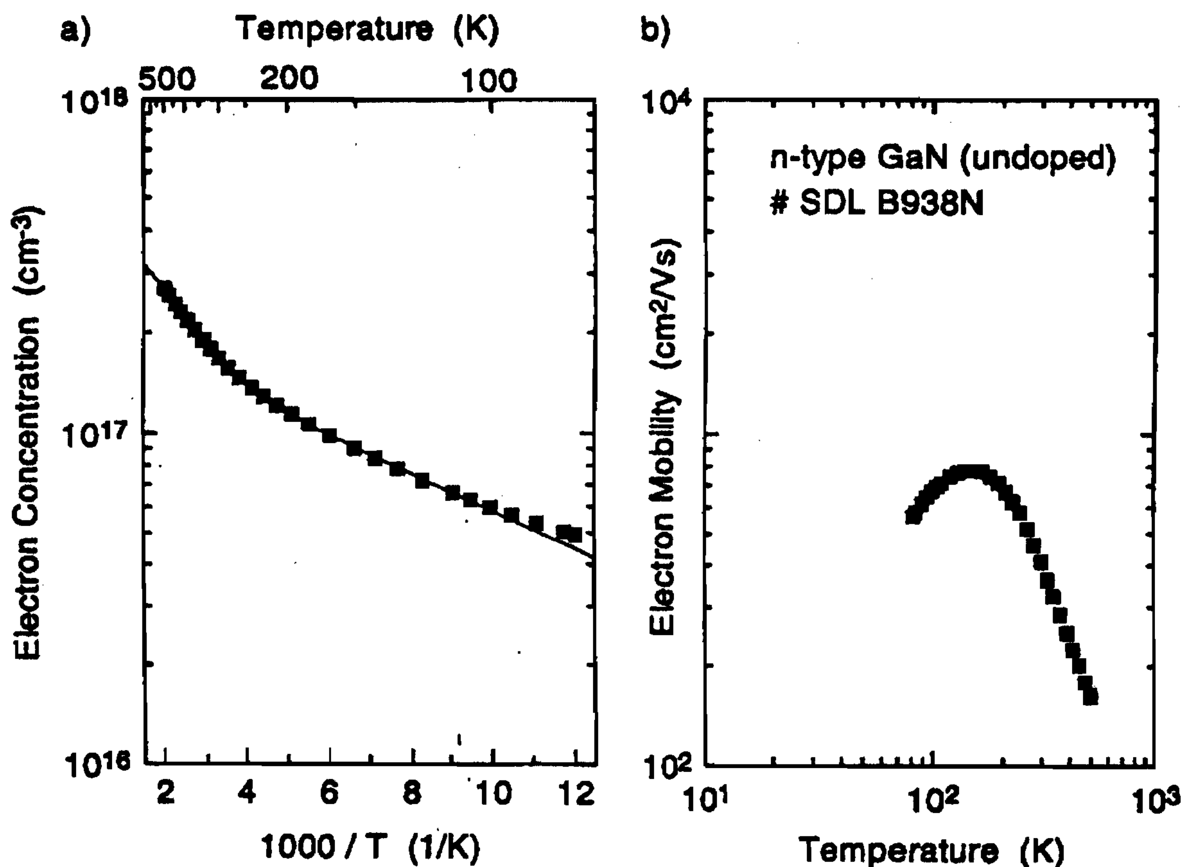

Figure 12: Electron concentration vs reciprocal temperature (a) and electron mobility vs temperature (b) measured with Hall effect from a Si-doped GaN film. The solid squares refer to the experimental data. The solid line in Figure 12a results from a fit of the charge neutrality equation to the experimental data.

There is also evidence of a second donor species in the investigated GaN films. films grown at SDL show a second donor with an activation energy of ~90 meV, while sample grown in the EMCORE reactor (# 15, # 19) at HP exhibits a second donor with an activation energy of ~30 meV. Sample # 50331a which was also grown at HP but in a horizontal MOCVD reactor shows evidence of a deep donor level with an activation energy of ~400 meV. These second donor levels are likely to be related to impurities.

Table II. A summary of test results.

Sample #	N_1 (cm^{-3})	N_1 (cm^{-3})	DE_2 (meV)	N_2 (cm^{-3})	N_{comp} (cm^{-3})	m (300 K) (cm^2/Vs)	m (max) (cm^2/Vs)
B906N	10	$1.6x10^{17}$	96	$2.5x10^{16}$	$1x10^{17}$	20	21
B938N	16	$1.6x10^{17}$	89	$2.4x10^{17}$	$4x10^{16}$	410	776
15	15	$1.1x10^{17}$	37	$3.9x10^{16}$	$3x10^{16}$	370	582
19	13	$2.0x10^{17}$	29	$1.1x10^{17}$	$5x10^{16}$	501	764
50331a	18	$2.9x10^{17}$	400	$8x10^{18}$	$5x10^{16}$	568	950

B. Pl spectroscopy

Three of the samples listed in Table I (# 15, # 19, and # 50331a) were characterized with room temperature and low temperature (2 K) PL spectroscopy. As an example a PL spectrum taken at 2 K from sample # 50331a is shown in Figure 13. The PL was excited with the 325 nm line of a HeCd laser and the spectra were recorded in the wavelength range from 300 nm to 750 nm. The spectra shown in

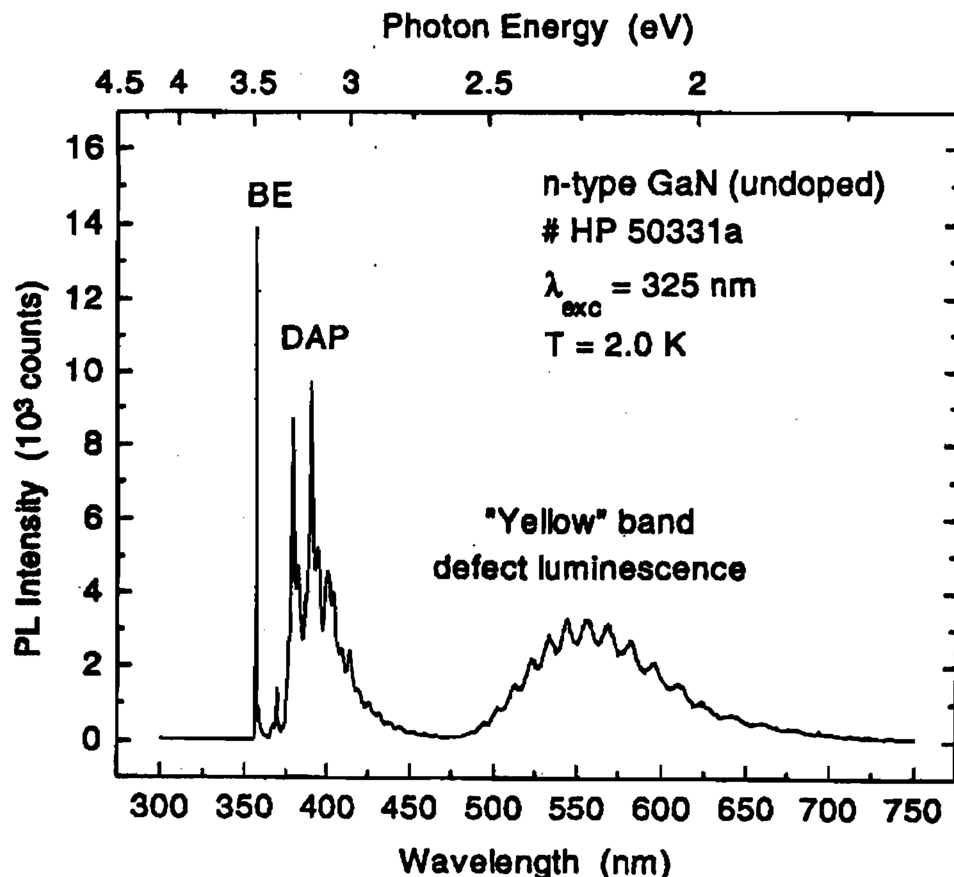

Figure 13: PL spectrum taken at 2K from an unintentionally doped GaN film. The PL lines are identified by labels.

Figure 13 exhibits a narrow peak at 357 nm (3.476 eV) which is related to the recombination of a donor-bound exciton. The full width at half maximum of this line is 2.4 meV. This narrow line width of the BE exciton lines is evidence for the high crystalline quality of film # 50336a. The spectrum also exhibits recombination between shallow donor and acceptor levels (zero phonon lines at 379 nm and 382.4 nm) and the yellow luminescence band centered at ~ 550 nm.

- **Theoretically Investigate Native Defects in GaN**

Xerox

Defect levels and formation energies of native defects are important to understand the doping properties of GaN. We have used state-of-the-art total energy methods to calculate formation energies, atomic geometry, and electronic structure of all native defects for all relevant charge states. The calculations employ density-functional theory and soft Troullier-Martins

pseudopotentials which take the Ga $3d$ electrons explicitly into account. Atomic relaxation was fully taken into account. Details of the method can be found in Ref. [1].

The calculations were performed both for GaN in the wurtzite structure (which is the stable phase for bulk GaN) and for GaN in the zincblende structure (which can be stabilized in epitaxial growth). Our results show nearly equivalent formation energies and only minor differences in the defect levels indicating very similar defect properties in both structures. The main difference is a small splitting of the p-like defect states in the wurtzite structure caused by the reduced symmetry of the wurtzite structure.

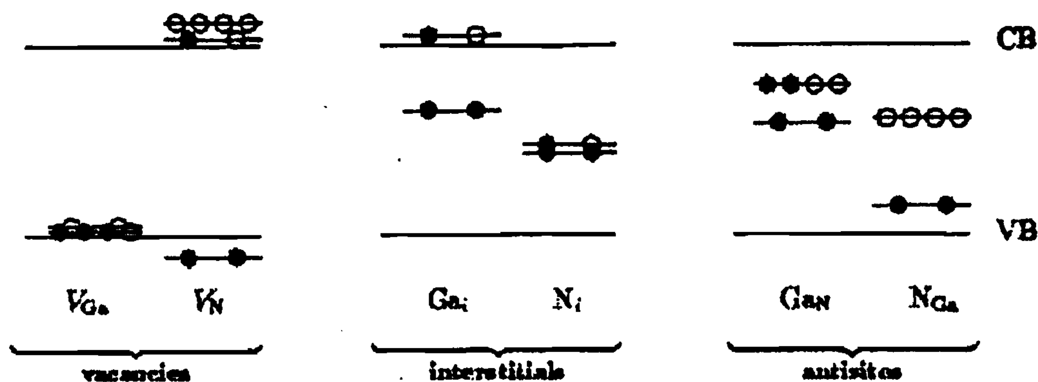

Figure 14: Schematic representation of the defect levels in GaN. The occupations are shown for the neutral charge state, filled circles indicate electrons, open circles indicate holes.

Figure 14 shows the positions of the defect levels for the neutral charge state. From these results we can immediately classify the defects into donors, acceptors, and amphoteric defects. The nitrogen vacancy and the gallium antisite are donors, the gallium vacancy an acceptor and the nitrogen interstitial and both antisites are amphoteric.

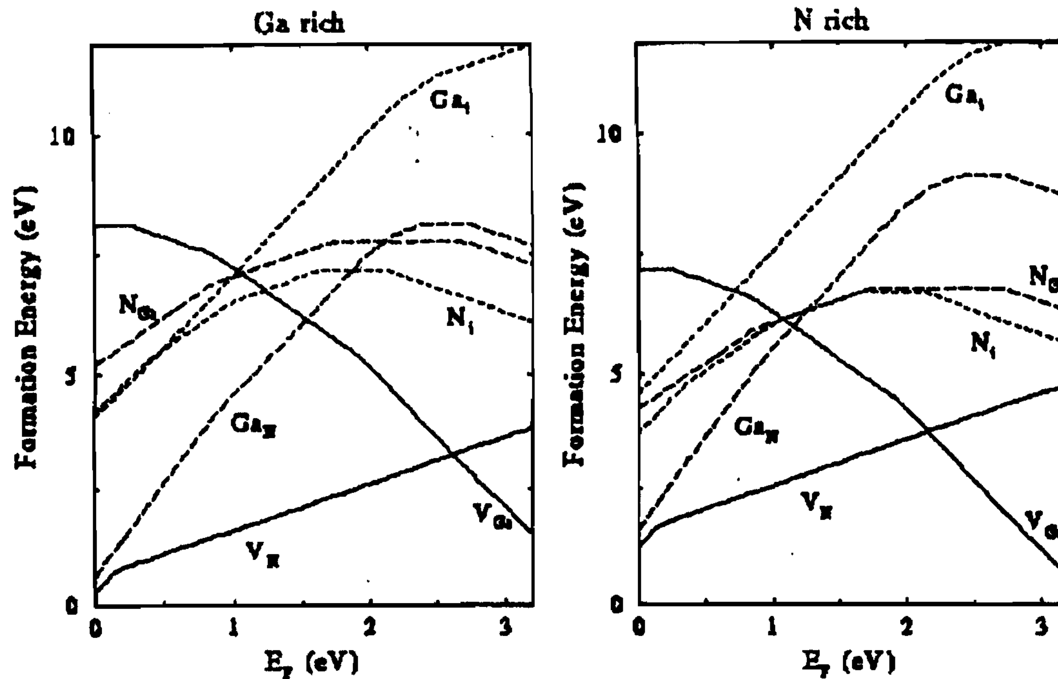

Figure 15: Defect formation energy as a function of the Fermi energy for vacancies (solid lines), antisites (long-dashed lines), and interstitials (dashed lines). Ga rich conditions (left) and N-rich conditions (right) are assumed.

We have further calculated the formation energy (as function of the Fermi energy and of the chemical potential) for all native defects. The results are displayed in Fig. 15 for both Ga-rich conditions (which appear to be common in experimental growth conditions) and N-rich conditions. The most striking feature is the high formation energy of the self-interstitials and antisite defects. The defects with the lowest formation energy are the vacancies: under *p*-type conditions the nitrogen vacancy has a very low formation energy, while under *n*-type conditions the Ga vacancy has a low energy.

The kinks in the formation energy are caused by a change in the defect charge state; increasing the Fermi level makes charge states with a higher filling more favorable. Both the sign and the value of the slope identify the charge state: a positive slope indicates a positive charge state, a negative slope a negative charge state. The position of the Fermi level at which the slope changes, i.e., the position of the kink, identifies the transition level.

These results also shed light on the issue of whether the nitrogen vacancy is the source of the n-type conductivity typically observed in as-grown GaN. Under n-type condition the formation energy of the nitrogen vacancy is quite high. In thermodynamic equilibrium, the

concentration of nitrogen vacancies should therefore be quite low, and they should not be responsible for the *n*-type conductivity. However, we note that the nitrogen vacancy in *p*-type material and the gallium vacancy in *n*-type material may act as compensating centers.

Milestone 6

- **Development of undoped GaN films on 6H-SiC, introduce n and p dopants. Deliver to Xerox.**

Boston University

I Introduction

Boston University's responsibility within the consortium is to investigate the effect of substrate type and quality upon the growth of AlGaInN. During the first quarter we investigated the growth and doping of GaN on 6H-SiC substrates. Some work was also initiated on the growth of GaN on single crystal ZnO substrates, however this work will be discussed in a later report.

II Growth of GaN on 6H-Sic

The substrates used in this study were purchased from CREE Research and are research grade heavily doped n-type.

a) cleaning procedures:

The substrate were first degreased, subjected to the RCA etching procedure and passivated by immersing them in buffered HF. This cleaning procedure led to surfaces which give excellent RHEED diffraction patterns (with good Kikuchi lines). We therefore found that the recommended in-situ- cleaning procedure involving H_2 plasma may not be necessary.

b) Growth of undoped GaN on 6H-SiC

A number of GaN films were grown on 6H-SiC. Some of the films were grown with a low temperature AlN buffer while others were grown without any buffer.

i) Properties of films 6H-SiC/AlN/GaN

- XRD studies indicate that the FWHM of about 1m thick films is about 17-18 min.

- Hall effect measurements indicate that the films are n-type with carrier concentration varying from 10^{19} to 10^{21} cm^{-3} and electron mobilities from 200 to 10 $cm^2\ V^{-1}\ s^{-1}$ respectively and resistivity of 10^{-4} ohm cm^{-1}. Thus these films appear to be excellent n-type doped for device development. However, these measurements assumed that the AlN buffer is an insulator and isolates the contribution from the substrate. We intend to do further measurements to verify this supposition.
- Typical room temperature photoluminescence data for such films are shown in figure 16. These data indicate that most of the recombination occurs across the gap (3.40 eV) and some photoluminescence through centers in the gap.
- SEM surface morphology of such films reveal roughness of approximately 1000 A.

ii) Properties of films 6H-SiC/GaN

- XRD studies indicate that the FWHM of about 0.5 mm thick films is 9 min. However this should be considered as the upper limit since the resolution of our graphite monochrometer is 9 min.
- Hall effect measurements on these samples could not be performed due to the direct contact with the conducting substrate.
- typical photoluminescence at 78 K for such samples are shown in figure 7. The recombination occurs across the gap (3.45 eV). The peak at 2.70 eV is due to luminescence from the SiC substrate.
- SEM surface morphology of such films indicates atomically smooth films. Furthermore the RHEED studies of such films indicate 2x3 surface reconstruction.

In conclusion it appears from these studies that the low temperature AlN buffer when one grown on 6H-SiC may not be necessary since films grown without such a buffer appear to have superior structural and electronic properties.

c) Growth of p-type GaN films on 6H-SiC

The GaN films were doped p-type by coevaporating Mg during the growth of the films. All p-type films were grown directly on the 6H-SiC without an AlN or GaN buffer.

- The conductivity type on these films was confirmed by the hot probe method.
- XRD data indicate that the FWHM of the rocking curve of such films is larger (15 min.) from the undoped films.
- Photoluminescence spectra fro a Mg doped is shown in figure 18. The recombination is dominated by D-A transitions at ~3.20 eV.
- SEM surface morphology is atomically smooth.

d) Growth of n-type GaN films on 6H-SiC

- XRD of heavily Si-doped GaN film is 16 min.

- Hall effect measurements could not be performed since both the film and the substrate are heavily doped n-type.
- Photoluminescence measurements for this is shown in figure 19. These data indicate both transitions across the gap 3.46 eV as well as D-A recombinations. We propose that part of the Si may have incorporated into N2 sites due to the amfoteric nature of Si -impurity.
- SEM studies show atomically smooth surfaces.

III Deliverables

1) One undoped GaN film (GaN304) grown on 6H-SiC and one undoped GaN film (GaN298) grown on sapphire (0001) were delivered to Xerox on July 6, 1995. (See letter to Noble Johnson). These two samples will be used for electron microscopy studies. 2) One p-type Mg doped and one n-type Si-doped films grown on 6H-SiC substrates are being delivered to Xerox simultaneously with this report.

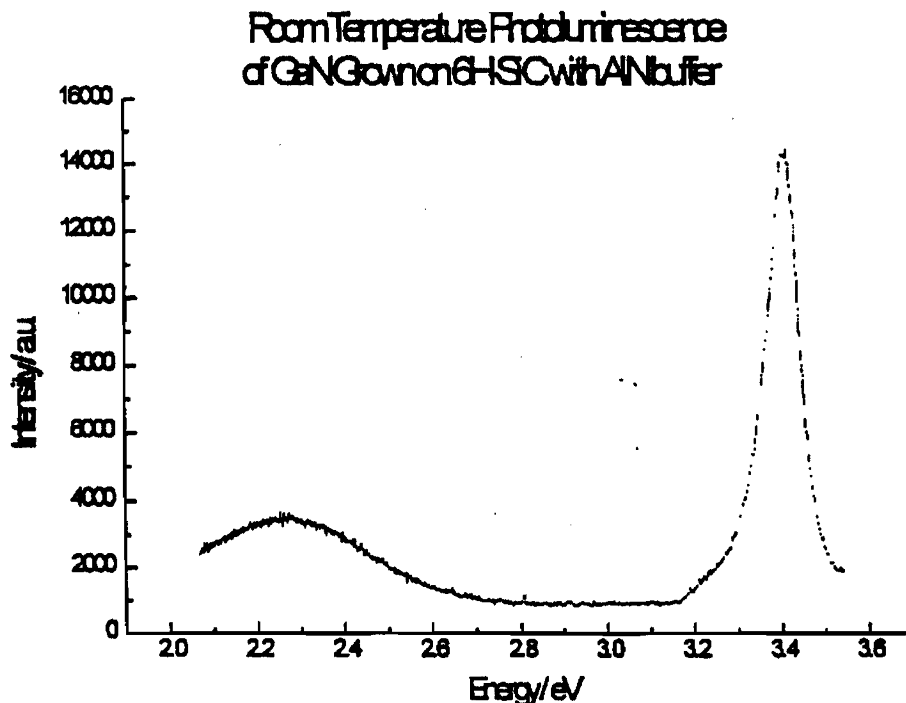

Figure 16 Room Temperature Photoluminescense of GaN Grown on 6HSiC with AlN buffer.

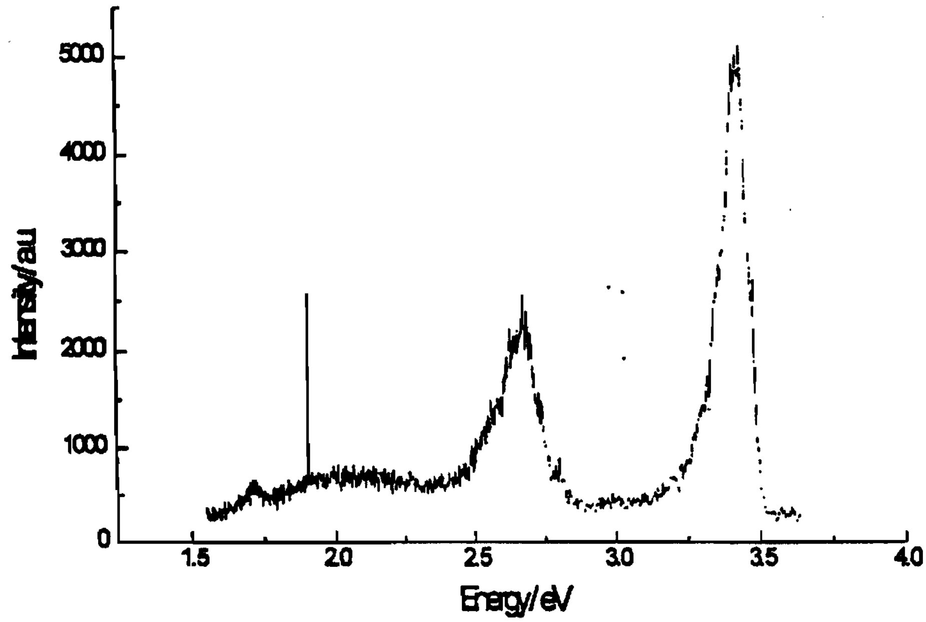

Figure 17 Photoluminescence of GaN Grown SiC without AlN Buffer.

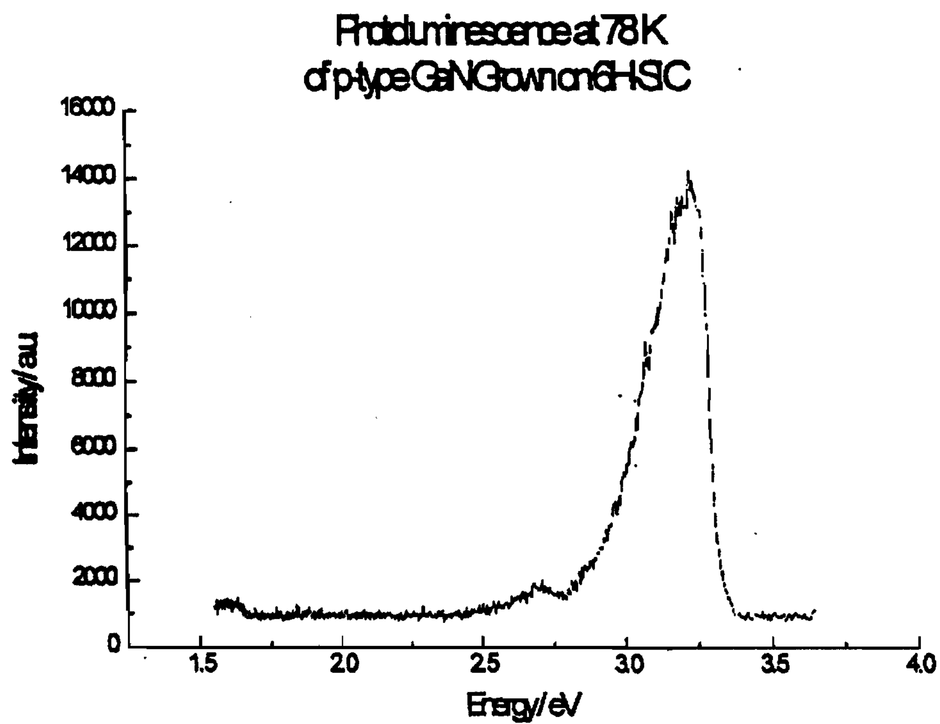

Figure 18 Photoluminescence at 78K of p-tykpe GaN Grown on 6HSiC.

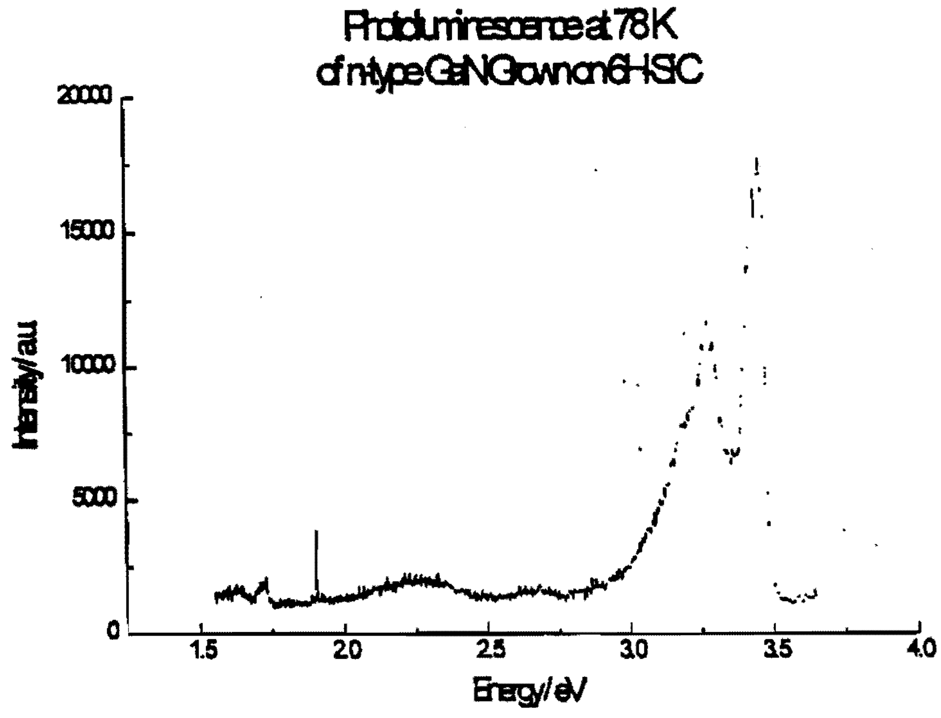

Figure 19 Photoluminescence at 78K of n-type GaN Grown on 6HSiC.

Boston University

College of Engineering
44 Cummington Street
Boston, Massachusetts 02215
617/353-2811

Electrical, Computer and Systems Engineering

July 6, 1995

Dr. N.M. Johnson
Xerox
Palo Alto Research Center
Palo Alto, CA 94304

Dear Noble,

Enclosed please find two samples to be considered as deliverables for the ARPA grant.

1. GaN-304 grown on 6H-SiC
2. GaN-298 grown on C-plane sapphire

I discussed with Ponse and he wants to perform electron microscopy on these samples.

Also, my student R. Singh has sent two samples of GaN grown on ZnO substrates.

1. GaN-306 grown on C-plane ZnO
2. GaN-306 grown on Prism plane of ZnO

We also sent photoluminescence data of these two samples performed with a He-Cd laser at liquid nitrogen as well as the photoluminescence spectrum of the ZnO substrate. The photoluminescence data of the GaN indicates a broad peak at 3.17eV consistent with doping of the films with Zn. (These three graphs are attached for your review)

Best regards.

Sincerely yours,

Ted

T.D. Moustakas

Letter to Noble Johnson

- **Characterization of Reactor for GaN growth**
  Advanced Technology Materials
  The GaN reactor is now fully constructed. The entire system, including supply lines, gas manifold and reactor have been leakchecked. The temperature profile has been measured and initial growths will take place in the next reporting period.

- **Deliver 2 mm scale GaN single-crystal substrates to consortium for study.**
  America Xtal Technology
  The mm scale GaN samples which were delivered to AXT cover a range of growth modes of the crystal ranging from rod-like structures to smooth platelets. One platelet (SN 0065), as per AXT's SOW, with a smooth surface was delivered to XEROX-PARC for characterization, the smooth face is atomically flat and epi-ready; however, the sample probably needs cleaning and HPRC has not been able to establish entirely satisfactory cleaning procedures. The other face of the sample grows in 20-40 angstrom steps and is not suitable for epi growth.

  At a meeting with XEROX on 19 July 1995, XEROX showed data on PL and CL spectra of the sample as well as photo-micrographs of the sample. XEROX plans to use a proprietary technique for polishing the sample prior to growing MOCVD epi on it.

  AXT has initiated a purchase order for ductile diamond grinding of ultra-hard materials with Horizon Technology Group. Work at NIST has produced <6 nM surface finish with hard diamond wheels on sapphire and silicon nitride. Hard wheels with precision grinding equipment are not practical for volume production. HTG will polish sapphire samples with loose diamond grit and various laps to verify the lap requirements for ductile grinding of ultra-hard materials. Preliminary tests show that loose diamond can ductile-grind ultra-hard materials.

References:
[1] R. Stumpf and M. Scheffler, Comp. Phys. Commun. 79, 447 (1994).

BLUE BAND

Blue Light and Ultra-Violet Emitters, the Bay Area Nitride Consortium
Report for Month 6
Contract: MDA972-95-3-0008

DISTRIBUTION: SDL, HP, Xerox, AXT, ATM, Boston University, the University of Texas at Austin, D. Scifres, J. Endriz, R. Craig, J. Johnson, and R&D	**To:** Distribution **From:** Jo S. Major **Date:** 1.16.96

Distribution authorized to U.S. Government agencies only to protect information not owned by the U.S. Government and protected by a contractor's "limited rights" statement, or received with the understanding that it not be routinely transmitted outside the U.S. Government. Other requests for this document shall be referred to ARPA Security and Intelligence Office.

Summary: Milestones 7-11 have been completed.

Milestone #7 (UT, HP, Xerox), Milestone Complete

- **Milestone #7: UT:** Complete installation of new Emcore HT "D" Reactor. Demonstrate GaN and AlGaN growth in D reactor. Deliver samples to Xerox. **HP:** Scanning PL operational. Whole wafer scans of member's GaN available. **XE:** Structural characterization of the GaN/SiC interface.

- **Summary:**

UT: The Emcore HT "D" Reactor is now installed and is operational. It has been used to grow GaN and AlGaN films. Some of these films have been sent to HP for characterization. UT has begun to study the growth of GaN in the new EMCORE "D" reactor. Parameters for the growth of the buffer layer and the high-temperature layer have been varied. At this time, X-ray rocking curves with FWHM values of ~700 arc sec have reproducible been obtained for lilms ~1.4 μm thick. AlGaN growth has been initiated. Samples have been sent to HP for characterization before sending them to Xerox for further analysis.

HP: A room-temperature photoluminescence wafer mapping system has been designed and assembled which is capable of measuring hundreds of points per wafer in under 10 minutes. The purpose of this tool is to provide detailed information on epitaxial layer uniformity, which can be used to provide rapid feedback to the epi growers about the effect of process changes on the wafer uniformity. The PL mapping system uses a 100 mW HeCd laser pump beam and f1.4 collection optics to image the spectrum onto a multi-

Distribution authorized to U.S. Government agencies only to protect information not owned by the U.S. Government and protected by a contractor's "limited rights" statement, or received with the understanding that it not be routinely transmitted outside the U.S. Government. Other requests for this document shall be referred to ARPA Security and Intelligence Office.

channel detector. The software is designed to calculate the peak wavelength and emitted "power" (actually integrated area under the PL spectrum) at each point, and provides output in the form of color-coded and automatically scaled contour plots. Examples of the peak wavelength and PL "power" maps for an InGaN layer are shown in Figures 1 and 2 below.

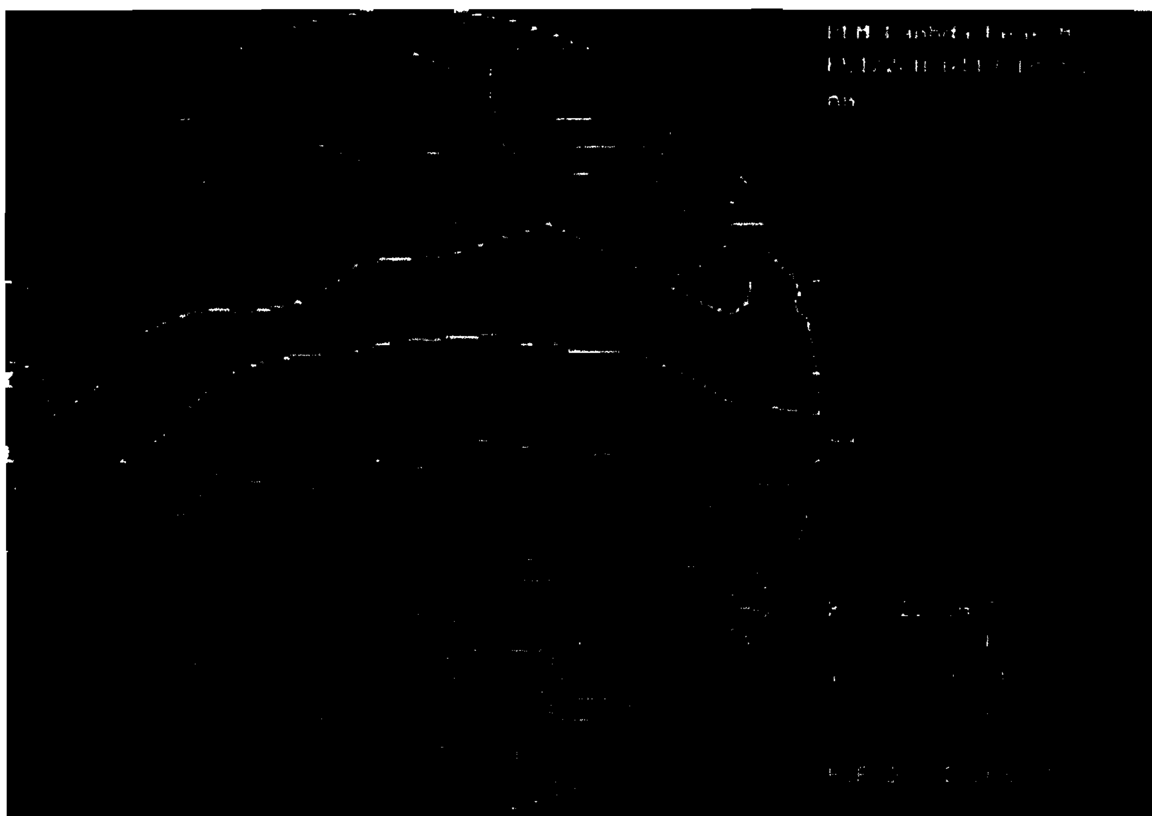

Figure 1: PL peak wavelength map of InGaN test wafer.

Distribution authorized to U.S. Government agencies only to protect information not owned by the U.S. Government and protected by a contractor's "limited rights" statement, or received with the understanding that it not be routinely transmitted outside the U.S. Government. Other requests for this document shall be referred to ARPA Security and Intelligence Office.

Figure 2: PL "power" map of InGaN test wafer.

Xerox: Electron Microscopy of the GaN/AlN/SiC Epitaxy. The AlN/SiC interface has been studied using high resolution transmission electron microscopy. Cross section lattice images of the AlN/SiC interface have been analyzed to establish the connection between image contrast and the atomic positions in the lattice. Assuming atomically abrupt and planar AlN/SiC interfaces, four possible atomic bonding configurations are taken into account for SiC substrates with the (0001)Si orientation. Image simulations of these four interface models are compared with the experimental images. Considering variations at the interface of the image contrast, the basal-plane distance, and the projected charge density, it is shown that the C-Al and Si-N bonds are in agreement with the experimental images and are not distinguishable under our experimental conditions. The other two possiblilities, involving C-N and Si-Al bonds, are not consistent with our observations.

There is much current interest in the growth of epitaxial thin films of the group III nitrides. The bandgap of the AlGaInN system ranges from 1.89 to 6.2 eV at room temperature, extending from the red to the ultraviolet region of the electromagnetic spectrum. Recently, epitaxial thin films based on GaN have been successfully used in the fabrication of high efficiency light emitting diodes in the range between yellow and blue (Nakamura, 1995). This has been achieved by metalorganic chemical vapor deposition (MOCVD) of $In_{1-x}Ga_xN$ thin films on sapphire substrates at temperatures above 1000°C. The growth of these films requires the use of low temperature buffer layers, the most widely used being AlN (Amano et al, 1986) and GaN (Nakamura, 1991). Transmission electron microscopy (TEM) of actual high efficiency devices shows that GaN grown epitaxially on sapphire contains a surprisingly high density of dislocations at the 10^{10} cm^{-2} level (Lester et al. 1995). On the other hand, high resolution TEM of the AlN/Al2O3 interface shows that it can be relatively free of defects

Distribution authorized to U.S. Government agencies only to protect information not owned by the U.S. Government and protected by a contractor's "limited rights" statement, or received with the understanding that it not be routinely transmitted outside the U.S. Government. Other requests for this document shall be referred to ARPA Security and Intelligence Office.

Compound	C-N	Si-N	Si-C	Al-N	Al-C	Si-Al
Actual	1.16	1.71-1.76	1.88	1.89	1.90-2.22	-
Sum of atomic radii	1.47	1.87	1.94	1.96	2.03	2.43

in spite of the large lattice mismatch between both materials (Ponce, 1994). It is believed that lowering the defect density should improve the quality of the materials and provide improved device performance. From the point of view of lattice matching, a-6H SiC is thought to be an improvement over sapphire, and some significant progress has already been done in producing material approaching the performance of epitaxy on sapphire (see e.g., Zubrilov et al., 1995).

One of the key aspects in heteroepitaxy occurs at the interface between the film and the substrate, since it is there that the differences in crystalline structure and in chemical bonding between epilayer and substrate are resolved. The resulting atomic arrangement at the interface will determine the degree of perfection of the epitaxial layer. The lattice structures and lattice parameters of the film and the substrate play a significant role, especially in the case of coherent interfaces, where a periodic array of misfit dislocations is desired in order to retain the local coherency at the junction. In addition, the nature of the chemical bond at the interface will determine the atomic bonding coordination, and therefore the orientation and structural stability of the epilayer.

The similarities between the lattice structures of a-6H SiC and the group III nitrides provide a number of advantages. The 6H and wurtzite (2H) structures are tetrahedrally coordinated, with a nearest neighbor configuration similar to the zinc-blende structure. In particular, the lattice parameter of SiC is within 1% of the AlN value, and the values of the thermal expansion coefficient along the basal plane are nearly identical (See Table I). This close match at the basal planes is expected to facilitate the formation of highly coherent interfaces. The resulting atomic arrangement should determine the stable growth configurations as well as the polarity of growth of the AlN epilayer.

The focus of the present paper is the determination of the atomic arrangement at the interface between AlN and SiC by high resolution transmission electron microscopy (HRTEM). Lattice images of the interface region, taken at various defocus values, are used to determine the specimen thickness and the objective lens defocus values. Assuming atomically abrupt interfaces, the four possible interface atomic structures are considered. Calculated images corresponding to these atomic models are compared with the experimental images. Two models involving C-N and Si-Al bonds are found to be inconsistent with the observations. Models involving Si-N and C-Al bonds are shown to be indistinguishable and consistent with the HRTEM observations.

The epitaxial layers were grown by MOCVD on the Si-face of (0001) a-6H SiC, following the technique of Sasaki and Matsuoka (1988). An AlN buffer layer was first deposited,

Distribution authorized to U.S. Government agencies only to protect information not owned by the U.S. Government and protected by a contractor's "limited rights" statement, or received with the understanding that it not be routinely transmitted outside the U.S. Government. Other requests for this document shall be referred to ARPA Security and Intelligence Office.

followed by growth of GaN at 1050°C. The microstructure of such films has been recently reported (Ponce, Krusor, et al, 1995). The specimen was oriented by x-ray diffraction and cut along bars for observation on the <11-20> SiC projection. The specimens were mechanically thinned to about 20mm and subsequently ion milled with Ar+ at 4 kV to electron transparency. High resolution TEM was performed at the Atomic Resolution Microscope at Berkeley (operating at 800kV accelerating potential, C_s= 2.0mm, C_c = 1.5mm), with an instrumental point resolution of less than 1.5 Å. Sample thickness was determined by linear extrapolation to the first extinction distance. Objective defocus values were obtained by callibrated increments from the Gaussian (minimum contrast) value. Image calculations were performed using the MacTempas simulation programs (Kilaas 1995).

High resolution TEM of the AlN/SiC Interface

Figure 3 shows micrographs corresponding to a through-focus-series of the AlN/SiC interface, taken at intervals of 12nm in the objective lens defocus(Df) values. These images indicate parallel epitaxy with [002]AlN //[002]SiC, and [11-20]AlN// [11-20]SiC. A schematic diagram showing the atomic positions in this projection is shown in Fig. 4. Figure 3 shows a larger area micrograph for Df = -105nm from the same series as in Fig. 1. The SiC lattice is viewed in the <11-20> projection, with the basal (0006) and a {1-100} plane appearing in horizontal and vertical projections, respectively. The AlN layer is observed in its <11-20> projection, where the horizontal corresponds to the basal (0002) plane and the vertical to a {1-100} plane. The respective interplanar separations are shown in Table 1.

Measurements of the AlN lattice dimensions using the SiC as reference indicate no measurable strain present in the epitaxial layer. The position of the interface can be observed by noticing the change in the direction of the oblique planes. The position of the lattice spots in the SiC follows a zig-zag with a period of 6 basal planes (cf. the ball and stick model of the AlN/SiC interface in Fig. 2). In the AlN, the atomic positions have a period of 2 planes in the direction normal to the basal planes, a characteristic of the wurtzite structure. Thus, the 6H/2H interface is easily observed to be atomically abrupt and parallel to the basal planes.

The electron-optical parameters affecting the high resolution images were carefully determined following a method similar to the one described by Spence (1981). In Fig. 3, the increments in the defocus values are known from callibration of the electron microscope (performed by analysis of the diffuse scattering in an optical transform of an amorphous/crystalline interface). The absolute defocus value was determined by observation of the minimum contrast value (Gaussian focus). The specimen thickness of the region in Fig. 3 was determined by interpolation to the first extinction distance in a wedge sample to be around 8.5nm. In order to determine the relationship between the lattice images and the actual atomic structure, image simulations were performed for the range of possible electron optical parameters. The variation of the image characteristics

Distribution authorized to U.S. Government agencies only to protect information not owned by the U.S. Government and protected by a contractor's "limited rights" statement, or received with the understanding that it not be routinely transmitted outside the U.S. Government. Other requests for this document shall be referred to ARPA Security and Intelligence Office.

(e.g. location and shape of bright spots) in both AlN and SiC lattices is consistent with a specimen thickness of 8.5 nm.

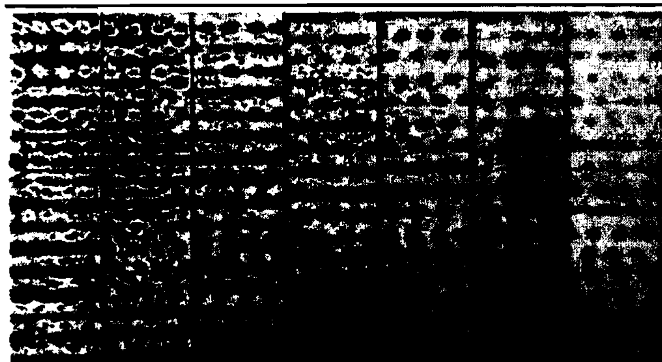

Figure 3. Lattice images in a through-focus series of the AlN/SiC interface. The defocus values are (a) -42.5nm, (b) -55nm, (c) -67.5nm, (d) -80nm, (e) -92.5nm, (f) -105nm, and (g) -117.5 nm.

Atomic bonding at abrupt-planar AlN/SiC interfaces

The detailed atomic arrangement at the interface, shown schematically in Fig. 4 with questions marks, is the subject of this article. For the silicon face of a (0001) SiC substrate, there are four possible, atomically planar and abrupt, interface bonding configurations as shown in Figure 6. Models A and C consists of Al-C and N-C bonds, respectively, which are oblique to the interface plane. The N-Si and Al-Si bonds in models B and D, respectively, are normal to the interface plane. In models A and B, the AlN lattice is oriented in the (0001) direction with Al at the top position of the basal plane. Similarly, in models C and D, AlN is oriented in the (000-1) direction with N at the top position.

Distribution authorized to U.S. Government agencies only to protect information not owned by the U.S. Government and protected by a contractor's "limited rights" statement, or received with the understanding that it not be routinely transmitted outside the U.S. Government. Other requests for this document shall be referred to ARPA Security and Intelligence Office.

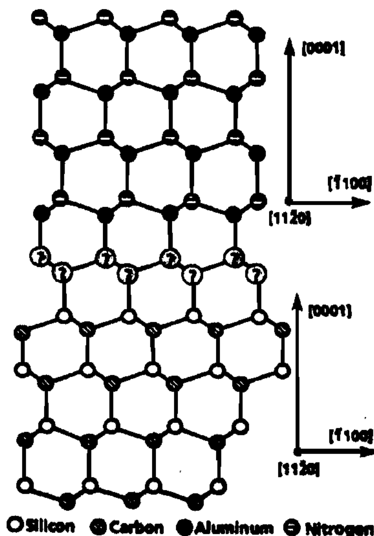

Figure 4. Schematic diagram of the interface between SiC and AlN discussed in this work.

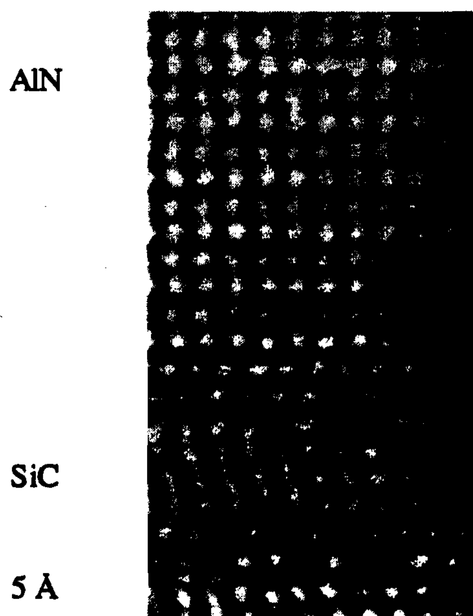

Figure 5. Lattice image of the AlN/SiC interface, for objective lens defocus of -105nm and specimen thickness of 8.5nm.

The intensity of lattice images for thin TEM specimens (less than 12nm for SiC and AlN) have been shown to follow the projected charge density approximation (PCD) (Spence, 1981) where the image intensity I is proportional to the projected charge density of the

Distribution authorized to U.S. Government agencies only to protect information not owned by the U.S. Government and protected by a contractor's "limited rights" statement, or received with the understanding that it not be routinely transmitted outside the U.S. Government. Other requests for this document shall be referred to ARPA Security and Intelligence Office.

atomic columns r_p: I (x,y) = 1 + A r_p(x,y). A is a constant proportional to the value of image defocus and to the electron wavelength. Thus, the variation in I (x,y) at a fixed thickness is linearly proportional to the sum of the atomic numbers of the elemental constitutents of the atomic columns. The atomic numbers and the corresponding sum are shown to the right of each of the interface models in Fig. 6. In both AlN and SiC the resolved atomic columns correspond to dumbbells consisting of double columns of the elemental components, with a total sum of 20 for both of these materials, with 13 + 7 for Al + N, and 14 + 6 for Si + C, respectively. This is the reason for the nearly identical spot intensities in the AlN and SiC regions in Figs. 3 and 5. The fact that the interface plane itself has a similar intensity means that its interface plane should have a sum of atomic numbers close to 20.

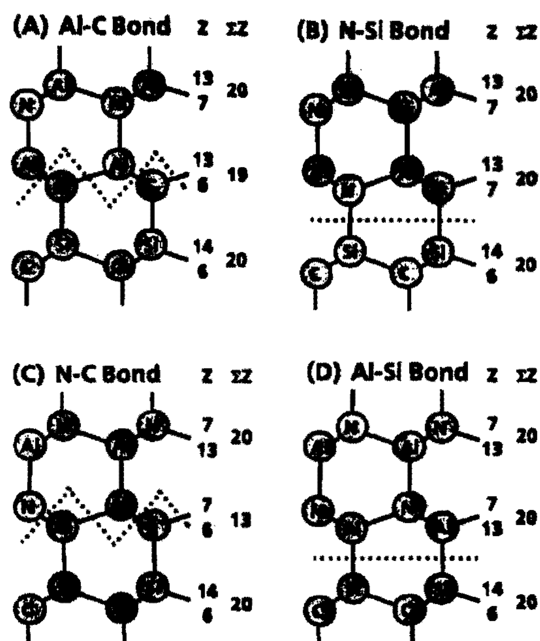

Figure 6. Four possible bonding configurations for atomically abrupt planar interfaces corresponding to the (0001)Si surface of SiC.

The chemical bond lengths for these atomic species are shown in Table 2, and the characteristics of the atomic bonds relevant to the AlN/SiC interface models in Fig. 2 are shown in Table 3. It is interesting to note that the N-C bond is much shorter than the other bonds, while the Al-Si bond is much larger. Also, the N-C bond has a sum of Z equal to 13, much lower than the rest; while the Al-Si bond has a sum of Z of 27, much larger than the rest.

Distribution authorized to U.S. Government agencies only to protect information not owned by the U.S. Government and protected by a contractor's "limited rights" statement, or received with the understanding that it not be routinely transmitted outside the U.S. Government. Other requests for this document shall be referred to ARPA Security and Intelligence Office.

Bond	Sum of Z	Avg. Bond Length	Δ in Bond Length	Orientation of Bond	Interplanar Distance
N-C	13	1.47	-0.41	tilted	2.35
Al-C	19	2.06	+0.18	tilted	2.55
Al-Si	27	2.43	+0.55	normal	3.06
N-Si	21	1.74	-0.13	normal	2.38
Al-N	20	1.89	+0.01	both	2.49
Si-C	20	1.88	-	both	2.516

Image simulation of atomically-abrupt AlN/SiC interfaces

Figure 7 shows the contrast transfer function for an objective-lens defocus of -105nm. The interplanar separations of SiC and AlN are shown for the relevant planes. The favorable position of the pass-band region in the contrast transfer function at spatial frequencies around 4 nm^{-1} is particularly favorable for white atom lattice structure images involving the relevant periodicities found in AlN and SiC, specifically the (0002), (11-20) and (1-100) reflections.

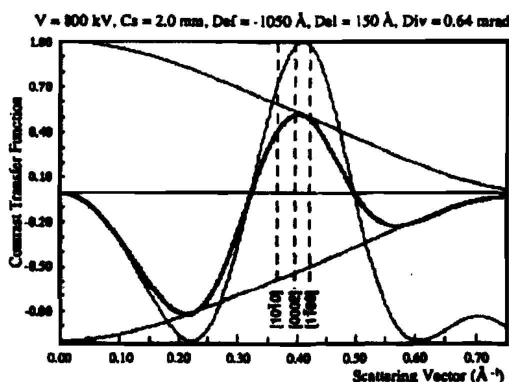

Figure 7. Contrast transfer function of microscope, for -105 nm defocus. Note that the relevant information in the range d ~ 2.3-2.6 Å transfers strongly with the same phase.

Figure 8 shows a montage of calculated images corresponding to a defocus of -105nm for various specimen thicknesses, calculated for the four models discussed in the preceding section. The projected potential density (PPD) indicating the position of the atomic sites is also shown. The position of the abrupt interface is marked with arrows in the left and right margins. At -105nm defocus the characteristics of the image do not change significantly with specimen thickness. These calculations show that models A and B are not distinguishable at our experimental conditions. On the other hand, models C and D show distinct interface features. Model C exhibits a bright row of spots at the interface coinciding with the C-N plane in Fig. 6c. Model D shows a broad, symmetric interface associated with the longer Si-Al atomic bonding configuration.

Distribution authorized to U.S. Government agencies only to protect information not owned by the U.S. Government and protected by a contractor's "limited rights" statement, or received with the understanding that it not be routinely transmitted outside the U.S. Government. Other requests for this document shall be referred to ARPA Security and Intelligence Office.

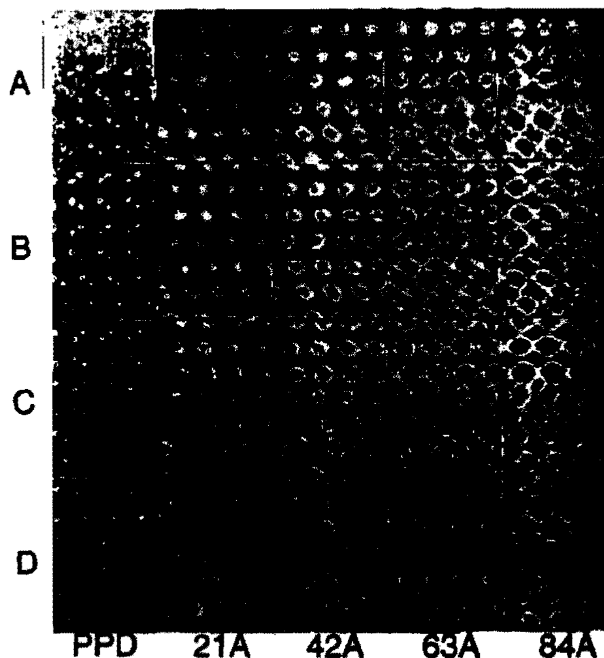

Figure 8. Specimen thickness dependence in simulated images of interface structures corresponding to the four configurations in Fig. 6, at -105 nm defocus.

Figure 9 shows the variation of lattice images with defocus values for the four AlN/SiC interface models. These calculated images correspond to a specimen thickness of 8.5nm. The strong dependence of the image characteristics with defocus indicates the particular benefit of choosing Df = -105nm, where the image is closely related to the actual structure image corresponding to white spots at atomic positions.

Distribution authorized to U.S. Government agencies only to protect information not owned by the U.S. Government and protected by a contractor's "limited rights" statement, or received with the understanding that it not be routinely transmitted outside the U.S. Government. Other requests for this document shall be referred to ARPA Security and Intelligence Office.

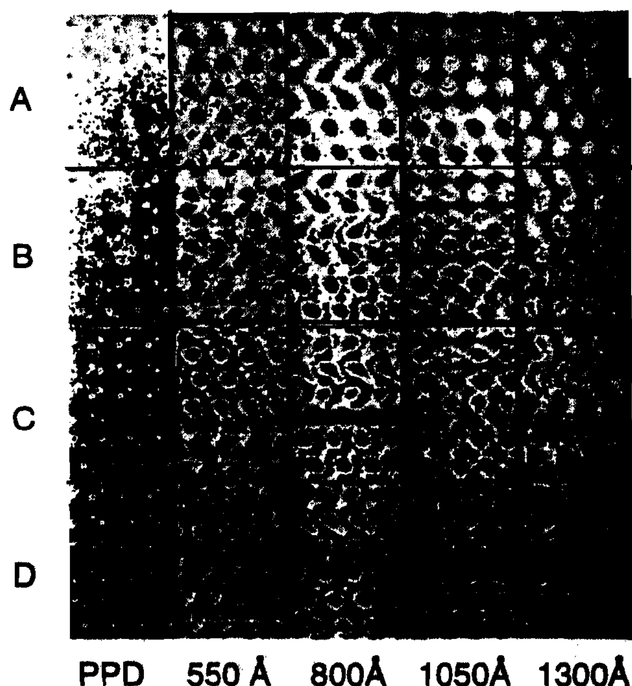

Figure 9. Objective-lens defocus dependence in simulated images of interface structures corresponding to the four configurations in Fig. 6, at a specimen thickness of 8.5 nm.

Structure determination of the AlN/SiC interface

The next step in our study is to determine the extent to which the atomic bonding arrangement at the AlN/SiC interface can be deduced by comparing calculated and experimental images. From the preceding discussion, the lattice image in Fig. 5 (for sample thickness of 8.5nm and Df = -105nm) resembles very closely the real structure image. For a narrow range of thickness and defocus centered around these values, bright spots correspond to the atomic dumbbells of the basal planes in Fig. 4.

Some quantitative characteristics of the lattice image in Fig. 5 are plotted in Fig. 10. These plots were obtained by digitizing Fig. 5 and integrating the image intensity in the horizontal direction. The intensity variation of the maxima corresponding to the basal planes is shown in Fig. 10a. The intensities of the basal planes at the interface are virtually identical. This indicates that the total atomic number of the dumbells at the interface must be very close to 20 (which, as already mentioned previously, is the value for both AlN and SiC). Fig. 10b shows the distance between basal planes in Fig. 3. Although there is some variation in the SiC values due to its high sensitivity to tilt, no significant variations are observed in the AlN. The width of the interface (or equivalently the interplanar separation at the interface) is 2.5 Å, and closely resembles the mean values of AlN and SiC of 2.49 Å and 2.52 Å, respectively. For comparison, the values corresponding to the C-N and Si-Al bonds, from Table 3, are shown. The basal-plane integrated-intensity variations along the c-direction

Distribution authorized to U.S. Government agencies only to protect information not owned by the U.S. Government and protected by a contractor's "limited rights" statement, or received with the understanding that it not be routinely transmitted outside the U.S. Government. Other requests for this document shall be referred to ARPA Security and Intelligence Office.

for the calculated and the experimental images are shown in Figure 11. Note the similarity between the experimental image (E) and models A and B. As previously mentioned, models C and D have unique characteristics at the interface which are not observed in the experimental images.

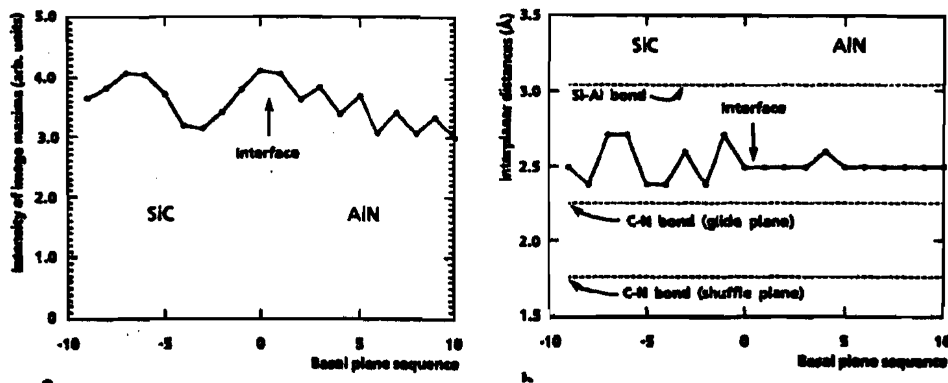

Figure 10. Characteristics of the lattice image in Fig. 3. (a) Integrated image intensity maxima of basal planes. (b) Interplanar separation accross the interface plane.

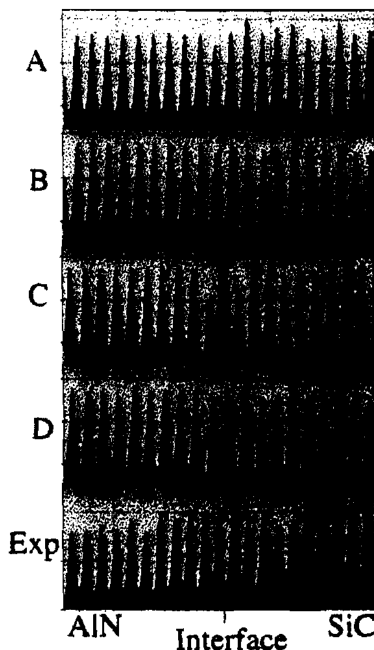

Figure 11. Image intensities integrated along the basal planes, corresponding to specimen thickness of 8.5nm and objective lens defocus of -105nm, corresponding to the four models (A-D) in Fig. 4, and the experimental image (E) in figure 3.

• DISCUSSION

Distribution authorized to U.S. Government agencies only to protect information not owned by the U.S. Government and protected by a contractor's "limited rights" statement, or received with the understanding that it not be routinely transmitted outside the U.S. Government. Other requests for this document shall be referred to ARPA Security and Intelligence Office.

The AlN/SiC interface has some interesting features which make it an ideal subject for characterization by HRTEM. The interface can easily be identified by the change in the stacking sequence from 6H to 2H. The fact that the Al-N and Si-C pairs have identical sums of atomic numbers and very similar lattice parameters, provides a uniform background against which the interface bonding arrangement can be evaluated. Based on the observation of abrupt interfaces, we use in this paper the assumption of atomically planar and abrupt interfaces, and we have clearly identified two atomic bonding configurations which are consistent with the experimental observations. One conclusion that is reached is that silicon terminated SiC surfaces generate epitaxy with Al in the top position of the basal plane. This result is consistent with electronegativity considerations. Al,Si, C, and N have electronegativity values of 1.5, 1.8, 2.5 and 3.0, respectively. Thus, Al and Si behave as cations in the presence of C and N. A proper anion-cation sequence at the interface would imply the presence of Si-N and Al-C bonds, and would void the C-N and Si-Al possibilities, in agreement with our deduction from HRTEM observations.

The images presented in this work correspond to the predominant flat areas in the specimen. In general, the SiC surfaces exhibited a large degree of roughness which added complications to the defect structure of the film. These effects are considered to be artifacts of surface preparation. The planar regions, on the other hand, represent the intrinsic features of the interface, and all such regions showed the same characteristics as described here.

The difference in the electronic nature of AlN and SiC (III-V and IV-IV compounds, respectively), introduces the possibility of a charge-dipole at the interface (Harrison, 1978) and the consequent Coulomb instability. This topic will be discussed in more detail elsewhere (Ponce, Northrup and Van de Walle, 1995).

• CONCLUSIONS

The atomic arrangement at the AlN/SiC interface has been studied using HRTEM. Lattice images were obtained in the <1-100> projection of thin epilayers. The imaging parameters have been determined experimentally and by image calculations. Calculated images of the four possible combinations corresponding to atomically planar and abrupt interfaces indicate that these models are characterized by unique signatures in the basal-plane integrated intensity distribution in the c-direction. By comparing calculated images with the experimental image, it is determined that C-N and Si-Al bonds are not present. The Si-N and C-Al bonding configurations cannot be resolved under the experimental conditions and both are consistent with the experimental results.

REFERENCES

AMANO, H., SAWAKI, N., AKASAKI, I., AND TOYODA, Y., 1986, Appl. Phys. Lett. 48, 353.

HARRISON, W. A., KRAUT, E. A., WALDROP, J. R., AND R. W. GRANT, 1978, Phys. Rev. B 18, 4402.

Distribution authorized to U.S. Government agencies only to protect information not owned by the U.S. Government and protected by a contractor's "limited rights" statement, or received with the understanding that it not be routinely transmitted outside the U.S. Government. Other requests for this document shall be referred to ARPA Security and Intelligence Office.

KILAAS, R., *MacTempas and CrystalKit*, Total Resolution, 20 Florida Ave., Berkeley, CA 94707.

KITTEL, C., *Introduction to Solid State Physics*, 1971, 4th ed. (Wiley, New York), p. 129.

LESTER, S. D., PONCE, F. A., CRAFORD, M. G., AND STEIGERWALD, D. A., 1995, Appl. Phys. Lett. 66, 1249.

NAKAMURA, S., SENOH, M., IWASA, N., AND NAGAHAMA S., 1995, Jpn. J. Appl. Phys. 34, L797.

NAKAMURA, S., 1991, Jpn. J. Appl. Phys. 30, L 1705.

PONCE, F. A., MAJOR, J. S., PLANO, W. E., AND WELCH, D. F., 1994, Appl. Phys. Lett., 65, 2303.

PONCE, F. A., KRUSOR, B. S., MAJOR, J. S., PLANO, W. E., AND WELCH, D. F., 1995, Appl. Phys. Lett. 67, 410.

PONCE, F. A., VAN DE WALLE, C. G., AND NORTHRUP, J. E., 1996 Phys. Rev. B, in press.

RALLS, K. M., COURTNEY, T. H., AND WULFF, J., 1976, *Introduction to Materials Science and Engineering* (Wiley, New York), p. 55.

SASAKI, T., AND MATSUOKA, T., 1988, J. Appl. Phys. 64, 4531.

SPENCE, J. C. H., 1981, *Experimental High-Resolution Electron Microscopy* (Clarendon Press, Oxford), pp. 136-138.

WELLS, A. F., 1962, *Structural Inorganic Chemistry* (Oxford, London), pp. 720-722.

WYCKOFF, R. W. G., 1960, *Crystal Structures* (Interscience, Wiley, New York), Vol. 2, pp. 157-164.

ZUBRILOV, A. S., NIKOLAEV, V. I., TSVETKOV, D. V., DMITRIEV, V. A., IRVINE, K. G., EDMOND, J. A., AND CARTER, JR., C. H., 1995, Appl. Phys. Lett. 67, 533.

Milestone #8 (HP, SDL), Milestone Complete

- **Milestone #7: HP,SDL:** AlGaN heterostructures demonstrated. Deliver Samples to Xerox.

- **Summary:** AlGaN has been grown over the entire composition range. SDL has observed that the aluminum content of the film is not linear with the ratio $Flow_{Al}/(Flow_{Al}+Flow_{Ga})$. HP has observed difficulty in growing AlN at atmospheric pressure and that the in variable pressure experiments the Al content of the AlGaN film decreases with increasing pressure. These experiments indicate parasitic reactions between the Al source and NH_3.Samples of heterostructures have been delivered to Xerox PARC for characterization.

HP: The growth of GaN, AlN and AlGaN using organometallic vapor phase epitaxy (OMVPE) has been studied as a function of reactor temperature and pressure. At atmosheric pressure, GaN with growth efficiency comparable to that of GaAs in the same reactor is obtained. In addition, the GaN growth efficiency changes little at different reactor pressures. These results indicate that parasitic reactions between TMGa and NH3

Distribution authorized to U.S. Government agencies only to protect information not owned by the U.S. Government and protected by a contractor's "limited rights" statement, or received with the understanding that it not be routinely transmitted outside the U.S. Government. Other requests for this document shall be referred to ARPA Security and Intelligence Office.

are not substantial. In contrast, the growth of AlN at atmosperic pressure has not been possible. By lowering the reactor pressure below 250 torr, AlN deposition can be achieved. However, the growth efficiency decreases at higher reactor pressures and higher growth temperatures, indicating that a strong parasitic reaction occurs between TMAl and NH3.

AlGaN epilayers have also been grown at different reactor pressures with a growth temperature of 1075 °C. In Figure 17, the Al solid composition, as measured by Rutherford Backscattering, is plotted as a function of reactor pressure. The experimental results are shown as points, and are compared to the theoretical result, shown as a solid line, which is calculated by assuming that parasitic reactions occur between TMAl and NH_3. A maximum of 16% Al was incorporated in the AlGaN layer at a pressure of 30 torr.

Finally, AlGaN/GaN heterostrucures have been grown at different pressures and a fixed temperature of 1075 °C. The X-ray rocking curves are shown in Figure 13 for AlGaN/GaN heterostructures grown at different reactor pressures. The spectra have been aligned to the GaN peak in order to show the Al composition in AlGaN. It can be seen that at a reactor pressure of 30 torr, the AlGaN peak is well separated from the GaN peak. As the reactor pressure is increased, the AlGaN peak moves closer to the GaN peak, indicating that less Al is incorporated at higher reactor pressure. At 250 torr, no distinctive AlGaN peak is seen. It is clear that the decrease in Al incorporation into AlGaN at higher reactor pressure is due to the parasitic reaction of TMAl with NH_3.

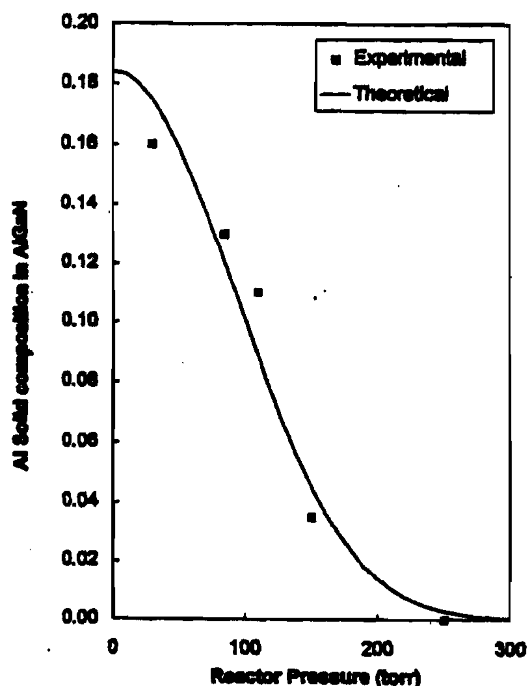

Figure 12: %Al in AlGaN vs reactor pressure at T_g = 1075 °C.

Distribution authorized to U.S. Government agencies only to protect information not owned by the U.S. Government and protected by a contractor's "limited rights" statement, or received with the understanding that it not be routinely transmitted outside the U.S. Government. Other requests for this document shall be referred to ARPA Security and Intelligence Office.

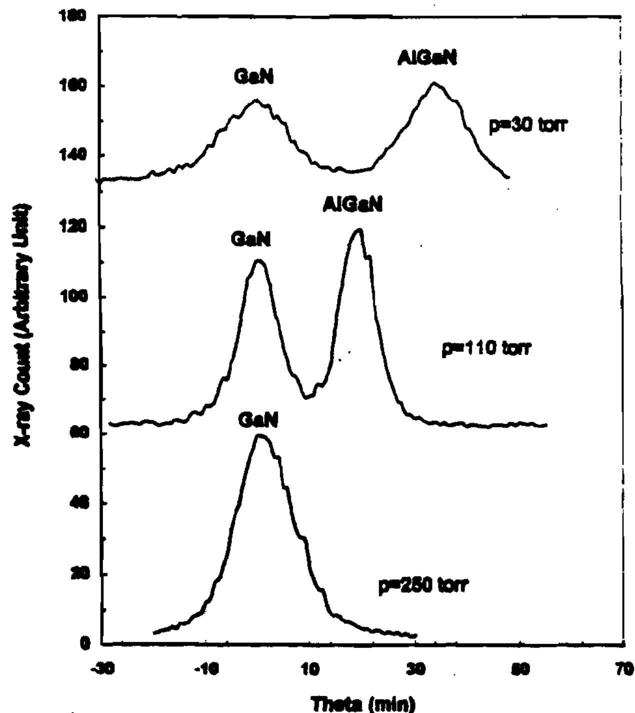

Figure 13: X-ray rocking curves for AlGaN/GaN heterostructures vs reactor pressure.

SDL:

The majority of work at SDL has focussed upon the growth of AlGaN with compositions less than $Al_{0.2}Ga_{0.8}N$ for two reasons. First, this composition range is sufficient for both electrical and optical confinement and second, the p-doping of materials with aluminum composition higher than 20% has been problematic for other groups.

Figure 14 shows the aluminum concentration versus the figure of merit $Flow_{Al}/(Flow_{Ga} + Flow_{Al})$. The Al composition is measured by X-ray diffraction using the peak associated with the GaN as a reference. For samples with Al composition less than ~35%, the films are smooth and specular. The single point at ~60% Al is from a film with low growth rate and roughened surface morphology.

An undoped doubled heterostructure of $Al_{0.1}Ga_{0.9}N/GaN/Al_{0.1}Ga_{0.9}N$ has been fabricated and sent to Xerox for characterization. The heterostructure has been designed to confine light and produce a ~40° far-field. The broadening of the GaN reference is due to the fact that the GaN layer is both thin and buried under an AlGaN layer.

Distribution authorized to U.S. Government agencies only to protect information not owned by the U.S. Government and protected by a contractor's "limited rights" statement, or received with the understanding that it not be routinely transmitted outside the U.S. Government. Other requests for this document shall be referred to ARPA Security and Intelligence Office.

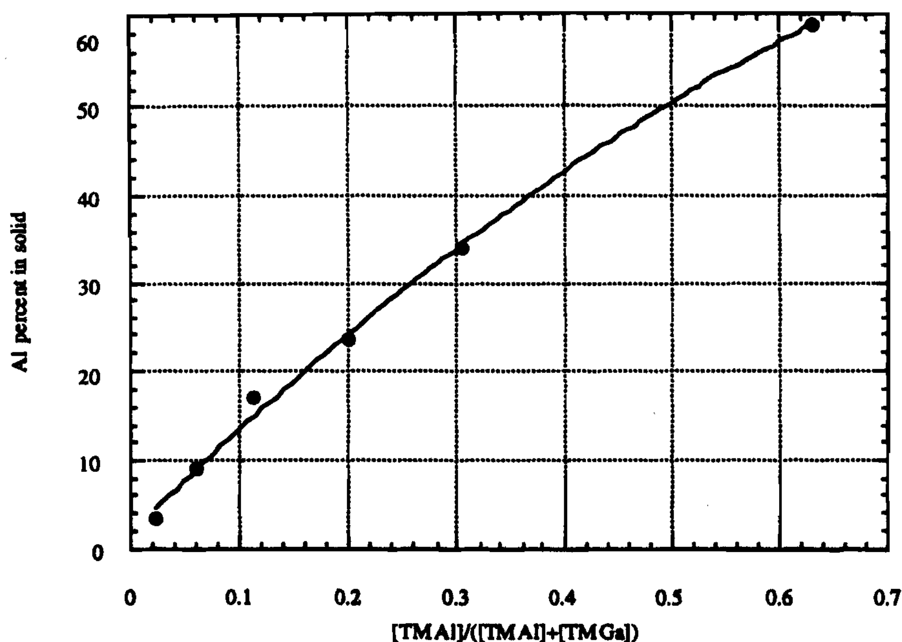

Figure 14: A plot of Al composition versus Al percentage in the gas stream.

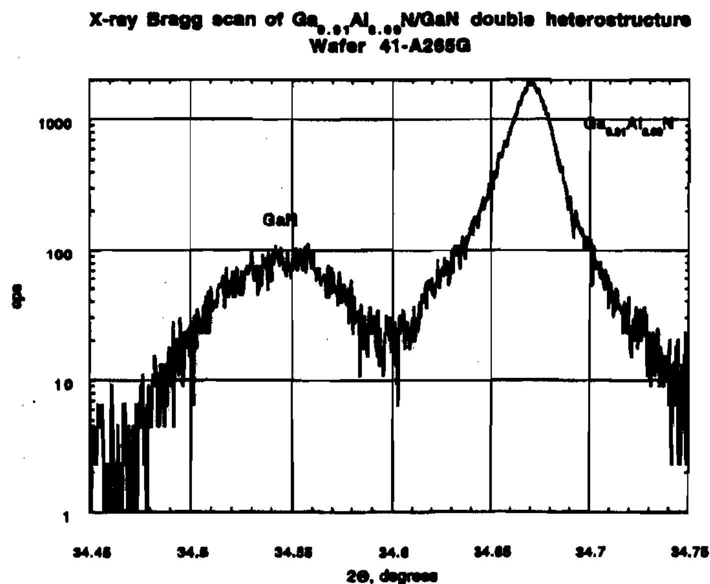

Figure 15: A theta-two theta scan of the double heterostructure sent to Xerox. The Al composition, determined by X-ray, is about 9%.

Milestone #9 (HP, SDL, Xerox), Milestone Complete

Distribution authorized to U.S. Government agencies only to protect information not owned by the U.S. Government and protected by a contractor's "limited rights" statement, or received with the understanding that it not be routinely transmitted outside the U.S. Government. Other requests for this document shall be referred to ARPA Security and Intelligence Office.

- **Milestone #7: HP,SDL,Xerox:** Controllable n-type doping in GaN demonstrated, with dping levels between 2 x 10^{17} and 5 x 10^{18} cm^{-3}. Deliver GaN with p-type impurities to Xerox. Electrical characterization of donor-doped n-type GaN. Calculate properties of p-type dopants (Mg and Zn) in GaN.

- **Summary:** Both SDL and HP have demonstrated good control of n-type doping levels throughout the aforementioned range. The mobility values are comparable with the literature. Due to the desire for highly conductive material considerable effort has been expended on highly doped films. The lowest values of resistivity for n-type GaN achieved are 3.47 x 10^{-3} Ohm-cm (sample doped 1.2 x 10^{19} cm^3, mobility of 150 cm2/Vs) and 5.79 x 10^{-3} Ohm-cm (sample doped 5.4 x 10^{18} cm^3, the upper limit our SDL current flow capacity, mobility of 200) for HP and SDL, respectively. The doping level versus flow is well controlled throughout the range of interest. Both SDL and HP are currently concentrating on p-type doping levels. Both groups have achieved active p-type doping and p-n junctions. P-type samples have been, and will continue to be, delivered to Xerox for characterization. In the next quarterly report, the results of Mg-doping experiments will be detailed. Xerox has completed a thorough evaluation of the behavior of Si in GaN and n-type samples in general. The properties of Mg and Zn in GaN have been modelled theoretically.

HP, SDL: Silicon doping of GaN is well-controlled across the range spanning 2 x 10^{17} to 5 x 10^{18} cm^{-3}. We begin by showing, in Fig. 16, the linearity of the doping level as a function of Silane dopant flow (SDL). These doping values cover the useful range of the flow controller currently employed at SDL. The high degree of linearity shows the good degree of control of doping level. Similarly, HP shows, in table form, data on a variety of samples doped with silicon.

Distribution authorized to U.S. Government agencies only to protect information not owned by the U.S. Government and protected by a contractor's "limited rights" statement, or received with the understanding that it not be routinely transmitted outside the U.S. Government. Other requests for this document shall be referred to ARPA Security and Intelligence Office.

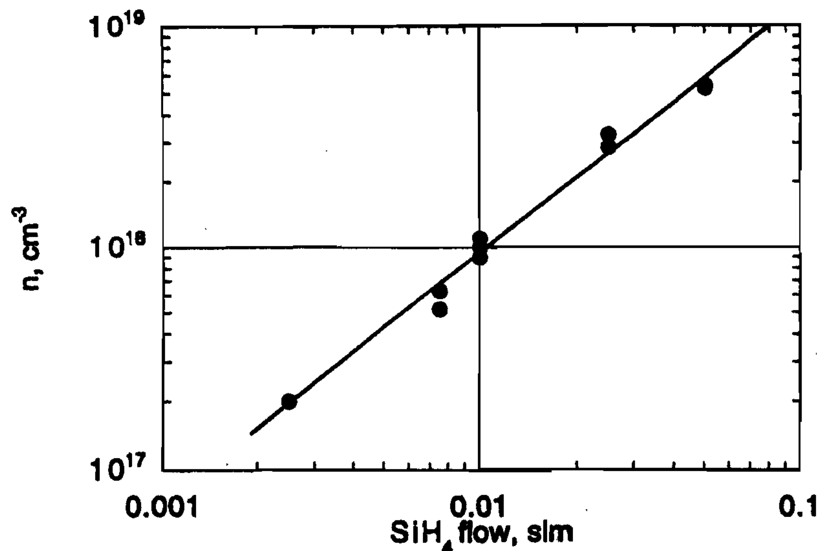

Fig. 16 The electron carrier concentration of versus silane flow in GaN.

The results of a study of Si doping to produce n-type GaN.

Run Number	Doping	Thickness (μm)	Carriers (n)	Mobility (μ) (cm^2/V-s)
15	"undoped"	2.90	8.6E16	413
16	Si	3.05	2.9E17	471
17	Si	2.88	3.8E17	469
18	Si	3.15	2.1E17	481
19	Si	3.02	1.9E17	463
20	Si	1.58	4.2E17	416
21	Si	1.57	4.2E17	421
23	Si	1.75	5.9E18	216
24	"undoped"	1.74	2.1E16	77
25	"undoped"	1.81	4.9E16	385
26	"undoped"	—	2.7E16	272
56	Si	2.78	3.0E18	232
60	Si	2.70	1.2E19	150

Distribution authorized to U.S. Government agencies only to protect information not owned by the U.S. Government and protected by a contractor's "limited rights" statement, or received with the understanding that it not be routinely transmitted outside the U.S. Government. Other requests for this document shall be referred to ARPA Security and Intelligence Office.

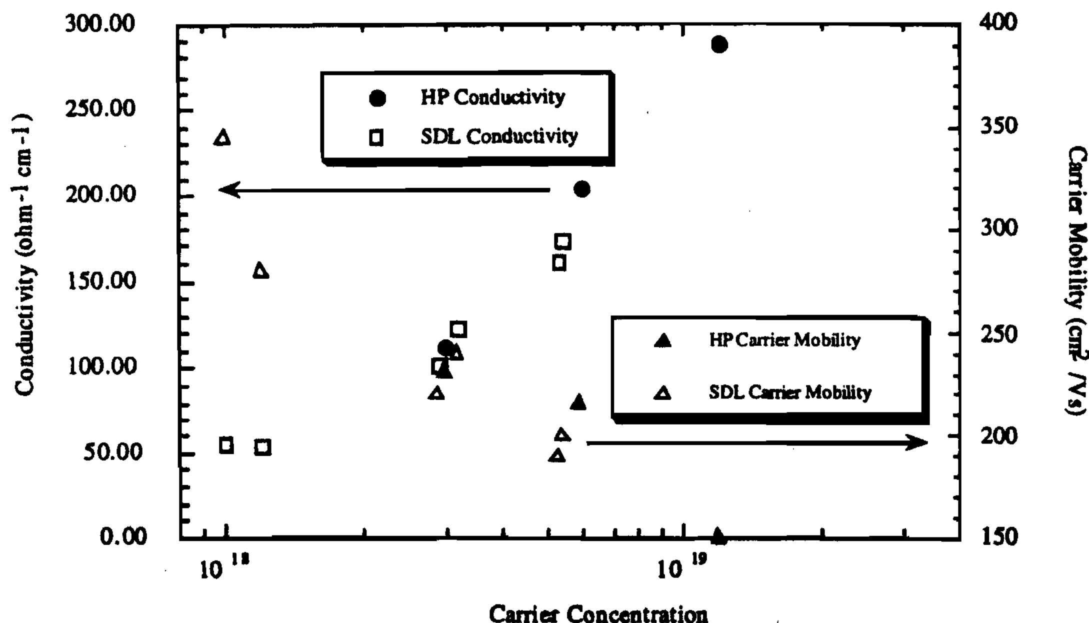

To illustrate the current conductivity of SDL and HP n-type GaN, Figure 17 shows the resistivity of GaN materials and mobility versus carrier concentration for heavily (> 10^{18} cm^{-3}) Si-doped GaN.

Fig. 17 The mobility and conductivity of heavily Si-doped materials grown at HP and SDL.

Xerox: The realization of light emitting (LED) or laser diodes (LD) requires the fabrication of contact and cladding layers with low electrical resistivity. Especially LDs are operated with high current densities to reach threshold for lasing. To avoid heating, the voltage drop across the device must be minimized and, therefore, any series resistance avoided. This is especially challenging for III-V nitrides, since carrier mobilities are relatively low, as compared with other device grade semiconductors. Shallow n- and p-type dopants are required which are sufficiently ionized at the temperature at which the device operates.

Si has successfully been used as a donor impurity in GaN and AlGaN for the fabrication of LEDs and transistors. However, quantitative information on the electronic properties of Si donors is not available. We have investigated Si-doped GaN films grown by metal-organic chemical vapor deposition (MOCVD) by variable temperature Hall effect measurements and low-temperature (2 K) photoluminescence (PL) spectroscopy. The thermal activation energy for ionization of Si donors and the position of the donor ground-state level in the bandgap of GaN were determined.

The Hall effect measurements were enabled by using a Van der Pauw geometry for the Ohmic contacts. These contacts exhibited Ohmic current-voltage characteristic over the

Distribution authorized to U.S. Government agencies only to protect information not owned by the U.S. Government and protected by a contractor's "limited rights" statement, or received with the understanding that it not be routinely transmitted outside the U.S. Government. Other requests for this document shall be referred to ARPA Security and Intelligence Office.

$$n + N_{comp} = \sum_{i=1}^{M} \frac{N_{Di}}{1 + \frac{g_i n}{N_c} exp\left(\frac{\Delta E_{Di}}{kT}\right)}, \quad (1)$$

entire temperature range of the Hall effect measurements (80 K - 500 K). An isotropic and temperature independent Hall scattering factor of unity value was assumed to derive electron concentrations from the measured Hall constants.

The samples investigated are listed in Table I:

Table I: GaN samples investigated with variable temperature Hall effect measurements

Supplied by	Sample #	doping
HP	50331a	undoped
HP	15	undoped
HP	19	Si-doped
HP	26	Si-doped
HP	52	Si-doped
HP	60	Si-doped

In addition to the Hall measurements, some of the samples were also characterized by room temperature and low temperature (2 K) photoluminescence (PL) spectroscopy. PL measurements reveal the presence of electronic states in the bandgap of semiconductors which may act as efficient recombination centers in LEDs or LDs. These electronic states may be useful in LEDs but need to be eliminated in LDs. In both cases characterization of these levels and the relation of their appearance to growth conditions is extremely important.

A. Hall effect results

Hall effect data obtained from unintentionally and Si-doped, n-type GaN films are presented in Fig. 18. Figure 18a shows electron concentrations as a function of the temperature. The experimental data are represented by symbols. The SiH_4 flux during growth was gradually increased from sample # 15, 19, 52 to 60. Consequently, the electron concentrations increased accordingly as determined by the Hall effect measurements.

To obtain information about the donors which determine the electron freeze-out behavior of our n-type GaN, we performed a least-squares fit of the charge neutrality equation to the experimental data. The charge neutrality equation for n-type, wide bandgap semiconductors (intrinsic carriers are neglected) with M independent donors is given by

where the index i refers to the i-th donor; NDi is its concentration, gi the degeneracy of its electronic state in the band gap, and ΔEDi the thermal activation energy of the donor

Distribution authorized to U.S. Government agencies only to protect information not owned by the U.S. Government and protected by a contractor's "limited rights" statement, or received with the understanding that it not be routinely transmitted outside the U.S. Government. Other requests for this document shall be referred to ARPA Security and Intelligence Office.

electrons. Ncomp is the concentration of compensating acceptors and NC is the conduction band effective density of states; k is the Boltzman constant and T the sample temperature. For the fits shown in Fig. 18a an effective electron mass of $0.2m_0$ (m_0 = mass of a free electron) was assumed. The calculated electron concentration as a function of the sample temperature is indicated by the solid straight line. For these fits, two independent donor levels had to be employed. Defect parameters are summarized in Table II. The temperature dependence of the electron concentration of sample # 52 at temperatures below 250 K indicates defect band conduction leading to a deviation of the fitted curve from the experimental data. For sample # 52 only data above 250 K was used for the fit. The electron concentration of sample # 60 does not vary with the sample temperature indicating a doping level above the degeneracy limit. The charge neutrality condition as given in Eq. (1) does not describe the temperature dependence of the electron concentration for a degenerately doped semiconductor and, therefore, no fit was attempted. The room temperature and the peak mobilities of the n-type GaN samples depend on the Si content (Fig. 1b). Sample # 15, which has the lowest Si content, has a room temperature (300 K) mobility of 370 cm^2 / Vs and a peak mobility at 150 K of 582 cm^2 / Vs. The highest mobilities for Si-doped material are measured in sample # 19 with values of 501 cm^2 / Vs (300 K) and 764 cm^2 / Vs (160 K). In sample # 52 the mobilities are 369 cm^2 / Vs and 459 cm^2 / Vs (190 K). For sample # 60 the peak mobility is measured at 300 K with 135 cm^2 / Vs. The temperature dependence of the mobilities at temperatures higher than the peak mobilities is well approximated by a power dependence ~T-1.5 for all Si -doped GaN films shown in Fig. 18b (except sample # 60).

Distribution authorized to U.S. Government agencies only to protect information not owned by the U.S. Government and protected by a contractor's "limited rights" statement, or received with the understanding that it not be routinely transmitted outside the U.S. Government. Other requests for this document shall be referred to ARPA Security and Intelligence Office.

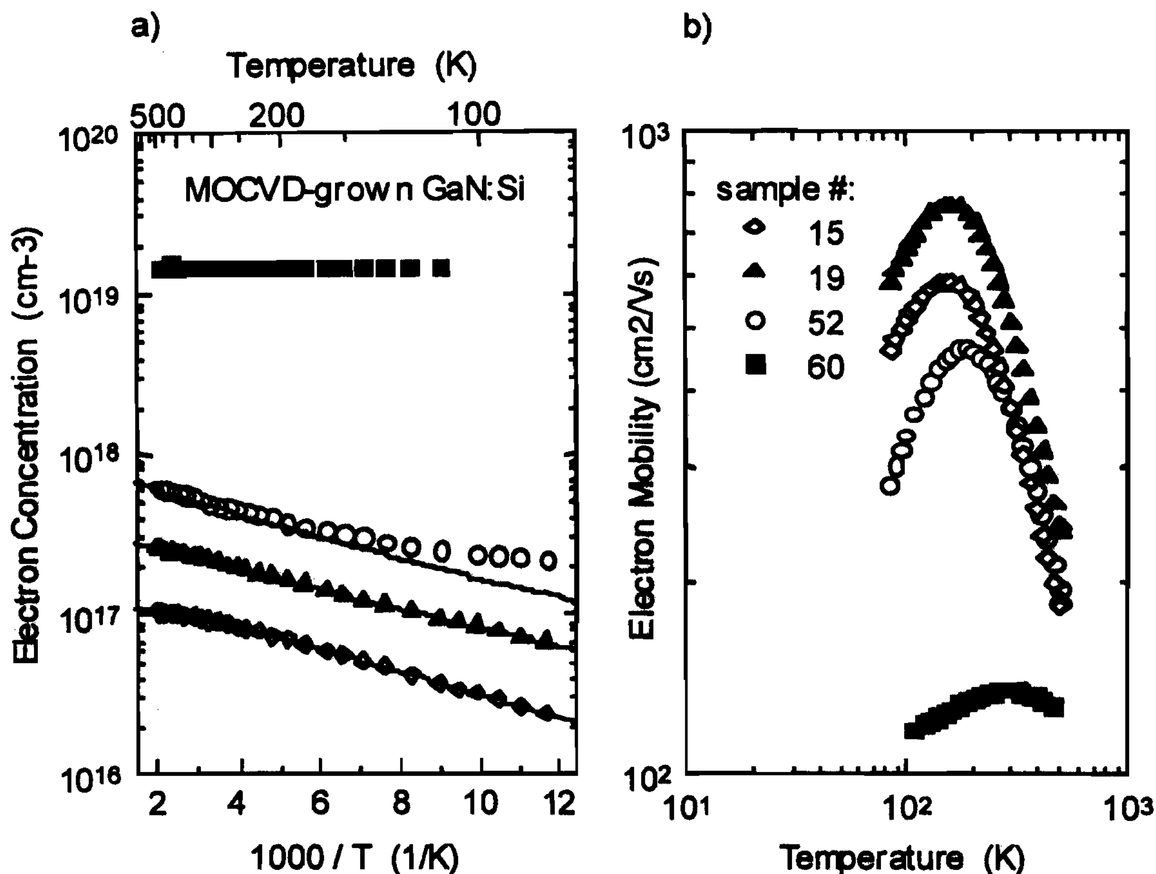

Fig. 18. Electron concentration vs reciprocal temperature (a) and Hall mobility vs temperature (b) for Si-doped GaN. The symbols refer to the experimental data. The solid lines in Fig. 1a result from least squares fits to the experimental data. The fits yield parameters for shallow donors which are summarized in Table II.

Table II also shows results from secondary ion mass spectrometry (SIMS) for samples # 15, 19, 52 and 60. The concentration of atomic Si [Si] was obtained by using an implantation standard. The Si concentration follows the amount of SiH4 flow which was increased from sample # 15, 19, 52 to 60. The comparison with the donor concentrations as obtained from the analysis of the Hall effect data leads to the conclusion that the donor labeled D1 is associated with Si incorporation in GaN. Its concentration N_{D1} in samples # 15, 19, 52 and 60 increases according to the SiH_4 flow and is, within the errors of the Hall and SIMS measurements, equal to the atomic Si concentration in the samples. Therefore, it seems reasonable to conclude that the shallow donor level with an activation energy (ΔE_{D1}) in the range between 12 meV and 15 meV is due to Si incorporation into GaN. Also, a donor with a similar activation energy (17 meV) dominates the n-type conductivity in our unintentionally doped GaN films. Results from the Hall effect (donor D1) and SIMS ([Si])

Distribution authorized to U.S. Government agencies only to protect information not owned by the U.S. Government and protected by a contractor's "limited rights" statement, or received with the understanding that it not be routinely transmitted outside the U.S. Government. Other requests for this document shall be referred to ARPA Security and Intelligence Office.

analysis of an unintentionally doped n-type GaN film (# 50331a) are presented in Table II and demonstrate that the dominant donor in this film is Si.

Table II: Parameters for shallow donors as determined from least-squares fits of the charge neutrality equation to the experimental Hall effect data and results from secondary ion mass spectrometry (SIMS) for n-type GaN samples (column one). The parameter set includes donor electron activation energies (ΔE_{Di}, column two and four) and concentration of shallow donors (N_{Di}, column three and five) for two independent donors. Also given is the concentration of compensating acceptors (N_{comp}, column six). SIMS results for the Si content are summarized in column seven.

	Hall effect					SIMS
sample #	ΔE_{D1} (meV)	N_{D1} (cm^{-3})	ΔE_{D2} (meV)	N_{D2} (cm^{-3})	N_{comp} (cm^{-3})	[Si] (cm^{-3})
HP50331a	17	3.1×10^{17}			no	4×10^{17}
HP15	15	1.1×10^{17}	37	3.9×10^{16}	3.2×10^{16}	2×10^{17}
HP19	14	2.3×10^{17}	34	6.9×10^{16}	no	5×10^{17}
HP52	12	7.4×10^{17}	32	6×10^{16}	no	9×10^{17}
HP60						2×10^{19}

A second donor level (D2) with an activation energy of ~ 34 meV (ΔE_{D2}) is present in the GaN films # 15, 19 and 52, as determined from the Hall effect analysis. We tentatively assign this donor level to the unintentional incorporation of oxygen in these GaN. O substituting for N in the GaN lattice may act as a donor and is a common impurity during MOCVD growth.

B. PL spectroscopy

A PL spectrum for sample # 50331a is shown in Fig. 19. Sample # 50331 contains 4x1017 cm-3 of Si (SIMS, Table II). The spectrum taken at 2 K, exhibits features which are generally observed for n-type GaN. The strongest line (BX) appears at 357.0 nm (3.473 eV) with a FWHM of ~2.2 meV. This emission line is due to the annihilation of excitons bound to neutral shallow donors. At lower phonon energies a series of lines labeled "DAP" is present in the spectrum. In the literature, they are usually referred to as due to donor-acceptor recombinations. The yellow luminescence band centered at ~2.2 eV is also present in our material. The inset in Fig. 19 magnifies the high energy portion of the PL spectrum. PL emission lines are labeled and indicated by arrows. The zero-phonon lines (ZPL) are indicated by solid lines and their first LO-phonon replicas by dotted lines.

Distribution authorized to U.S. Government agencies only to protect information not owned by the U.S. Government and protected by a contractor's "limited rights" statement, or received with the understanding that it not be routinely transmitted outside the U.S. Government. Other requests for this document shall be referred to ARPA Security and Intelligence Office.

The PL line labeled L1 is positioned at 358.6 nm (3.458 eV) is likely to be an acceptor bound exciton. The lines L2 and L3 at 369.7 nm (3.353 eV) and 376.7 nm (3.292 eV), respectively, indicate Mg contamination since these lines usually appear in our Mg-doped GaN; their origin is unknown. The emission lines labeled DAP1 and DAP2 are associated with donor acceptor pair recombinations and are positioned at 379.0 nm (3.272 eV) and 390.0 nm (3.179eV), respectively. A broad PL line at (376.4±0.4) nm ((3.294±0.004) eV) is labeled "CB".

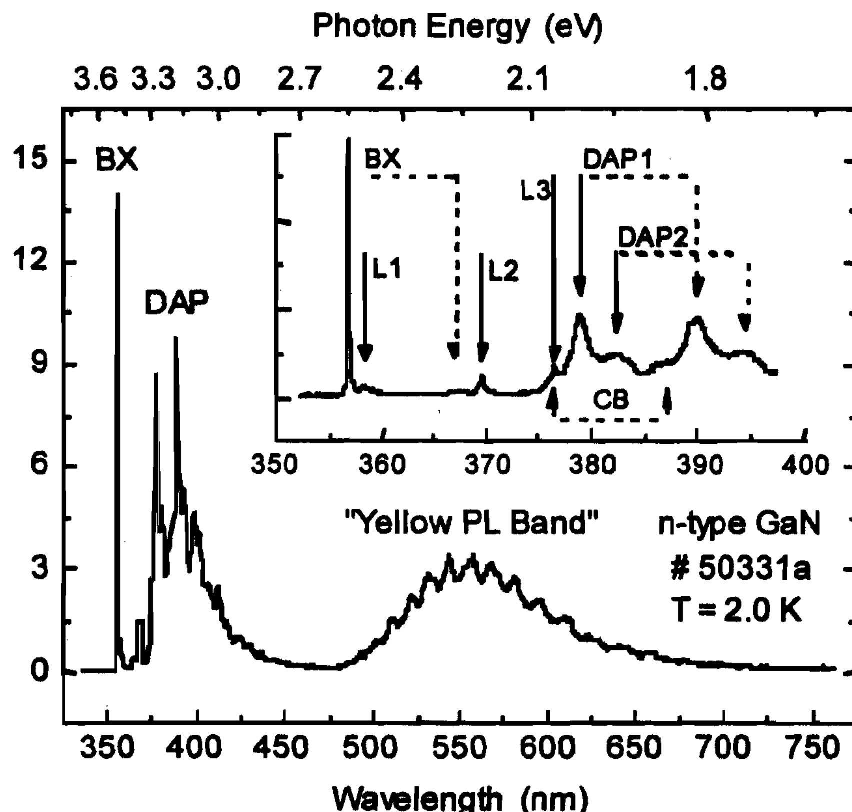

Fig. 19. PL spectrum for sample # 50331a. PL emission lines are labeled "BX","DAP", and "yellow PL band". The inset magnifies the high energy portion of the spectrum. Zero-phonon lines are indicated by arrows with solid lines and their first LO-phonon replicas by arrows with doted lines. The arrows labeled "CB" indicate a recombination process that may involve the conduction band as the initial state.

In the following, we use the PL emission lines CB and DAP1 to determine the position of the optical donor level of Si donors at 2 K. DAP1 is the highest energy line and therefore should involve the shallowest donors and acceptors, namely Si and Mg. We assume that the broad line "CB" is due to the same radiative transition, however, with the initial state

Distribution authorized to U.S. Government agencies only to protect information not owned by the U.S. Government and protected by a contractor's "limited rights" statement, or received with the understanding that it not be routinely transmitted outside the U.S. Government. Other requests for this document shall be referred to ARPA Security and Intelligence Office.

being the conduction band edge. The energy difference between the CB and the DAP1 line yields the position of the optical level in the GaN band gap at EC - (22±4) meV.

Due to its electronic properties (low thermal activation energy for ionization, efficient incorporation and high electron mobility of Si-doped GaN films) Si is well suited as a donor dopant for the growth of light emitting devices.

Xerox PARC: Properties of p-type dopants (Mg, Zn) in GaN

We have studied the properties of Mg and Zn acceptors in GaN employing state-of-the-art first-principles calculations. Based on these results we identify the mechanisms which limit the achievable hole concentration. In particular, we investigate the following doping limiting mechanisms: (i) solubility issues, (ii) compensation or passivation by native defects or impurities, and (iii) the incorporation of the acceptors on other sites.

Solubility:

We have calculated a phase diagram for the incorporation of Mg and Zn acceptors in GaN assuming thermodynamic equilibrium. Acceptor incorporation may be limited by the formation of bulk Mg or Zn. However, our calculations show that an even more stable configuration is Mg_3N_2 (for Mg doping) and Zn_3N_2 (for Zn doping). Thus, the formation of these compounds is a lower limit for the Mg_{Ga} and Zn_{Ga} formation energy providing an upper limit for the solubility of Mg and Zn in GaN.

Compensation by native defects:

The incorporation of acceptors dramatically changes the position of the Fermi level which may enhance the formation of native defects acting as compensating centers. In order to address this issue we combined the results about acceptor formation energies with our previous results about native defects.

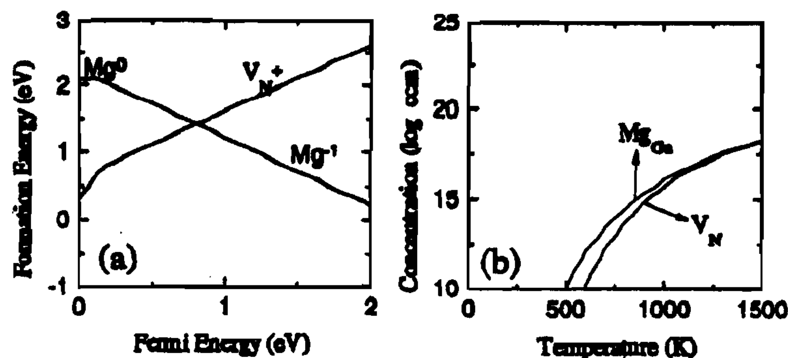

Figure 20: Formation energy vs. Fermi level for the Mg_{Ga} acceptor and the native defects. The corresponding equilibrium concentrations are

Distribution authorized to U.S. Government agencies only to protect information not owned by the U.S. Government and protected by a contractor's "limited rights" statement, or received with the understanding that it not be routinely transmitted outside the U.S. Government. Other requests for this document shall be referred to ARPA Security and Intelligence Office.

given in (b). Ga-rich conditions are assumed. A high formation energy indicates that it is hard to incorporate the impurity or defect on a particular site, resulting in a low concentration.

The results are shown in Fig. 20 where the formation energy of the Mg_{Ga} acceptor and the dominant native defect under p-type conditions (the nitrogen vacancy) are shown. Using the calculated formation energies and taking charge neutrality into account we can calculate the equilibrium concentration of the Mg acceptors and the native defects (Fig. 1b). The results show that the Mg concentration, as expected, increases with the growth temperature. The only native defect which occurs in relevant concentrations is the nitrogen vacancy. At temperatures exceeding 1000 K the Mg acceptors become increasingly compensated by the N vacancies. Compensation by native defects is therefore potentially a major concern for high-temperature growth techniques. We note however, that in most high temperature growth techniques (MOCVD, HVPE) hydrogen is highly abundant which may reduce the compensation by native defects. Growth at low temperatures as characteristic for MBE may suffer less from this problem since non-equilibrium conditions probably apply. This may explain why p-type GaN without post-growth treatment was successful in MBE.

Incorporation on other sites:

Another mechanism that may limit the hole concentration, is self compensation of the Mg or Zn acceptor: instead of being incorporated on the Ga substitutional site the acceptor may be built in on other sites where it is electrically inactive or even becomes a donor. As possible configurations we have investigated the N substitutional site and several interstitial configurations.

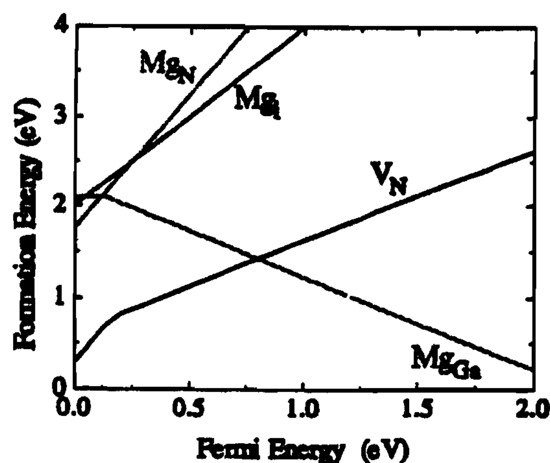

Figure 21: Formation energy as a function of the Fermi level for Mg in different configurations (Mg_{Ga}, Mg_i, Mg_N). Also included are the dominant native defects (nitrogen vacancy V_N).

Distribution authorized to U.S. Government agencies only to protect information not owned by the U.S. Government and protected by a contractor's "limited rights" statement, or received with the understanding that it not be routinely transmitted outside the U.S. Government. Other requests for this document shall be referred to ARPA Security and Intelligence Office.

The calculated formation energies for Mg are displayed in Fig. 21. The positive slope in the formation energy indicates that Mg in both configurations acts as a donor: Mg_i as a double donor, Mg_N as a triple donor. Figure 2 shows that the formation energies of Mg_i and Mg_N are negligible; they become comparable with Mg_{Ga} only under extreme p-type conditions. We further find that the N vacancy is the dominant donor: its formation energy is lower for all Fermi energies. We therefore conclude that Mg will always prefer the Ga substitutional site: for Mg, incorporation on other sites can be ruled out. For other possible acceptors (particularly elements with a small ionic radius), such effects may be important.

Milestone #10 (AXT, BU, ATM), Milestone Complete

- **Milestone #10:** AXT: Deliver 5 mm scale GaN single crystal substrates to the consortium for epitaxial growth. BU: Development of GaN substrates by the VPE method. Such substrates will be grown on ZnO coated sapphire substrates. ATM: Characterization of GaN on growth template.

- **Summary:** AXT has delivered four 5-mm-scale substrates to Xerox PARC for growth and characterization. BU has constructed two operational VPE machines and has grown GaN films on ZnO-coated sapphire substrates. ATMI has grown GaN both on sapphire substrates and on the growth template.

AXT: Four (4) 5 mm-scale platelet substrates were delivered to Xerox for characterization and epitaxial growth. These samples were labelled M3-BB-1, M3-BB-2, M3-BB-3 and L3-BB-5. The samples were a significant improvement in size and quality over the previous delivery. All samples appear clear and yellow to orange in color. On face is flat and the other has the usual step structure. Xerox has polished samples and grown MOCVD epitaxy on both faces. The epitaxial quality appears to be very good.

The results of loose diamond grinding show that with the appropriate lap selection an electronic quality surface can be produced on sapphire very rapidly when compared to the standard sapphire polishing technology. AXT will verify this technology on GaN materials.

AXT recently visited HPRC and the most recent crystals are completely clear and glass-like. They have found the proper growth conditions for high quality GaN crystals. HPRC projects that the new, larger growth system wil be substantially completed in January 1996. Growth in this system will start shortly thereafter.

Boston University: We designed and constructed two different halide VPE reactors and we are in the process of studying their relative merits.

React A is schematically illustrated in Fig. 22 and is based on the original design proposed by Maruska [1]. The system is made of clear fused quartz and it consists of two chambers separated by a large bore stopcock. The system employs a 3-zone high-temperature funace

Distribution authorized to U.S. Government agencies only to protect information not owned by the U.S. Government and protected by a contractor's "limited rights" statement, or received with the understanding that it not be routinely transmitted outside the U.S. Government. Other requests for this document shall be referred to ARPA Security and Intelligence Office.

leading to a temperature profile as shown in Fig. 23. The advantage of this design is that the growth chamber is not exposed to the atmosphere during the introduction and removal of the substrate. Furthermore, the samples can be moved in the load lock chamber for cooling down in a ammonia atmosphere. The disadvantage of this design is the employment of vacuum grease as a sealant in the stopcock and the endcaps used for the injection of reactive and inert gases. We observed that the grease reacts with the byproducts of the process and forms powdery deposits. A number of GaN samples were grown on this reactor at atmospheric pressure.

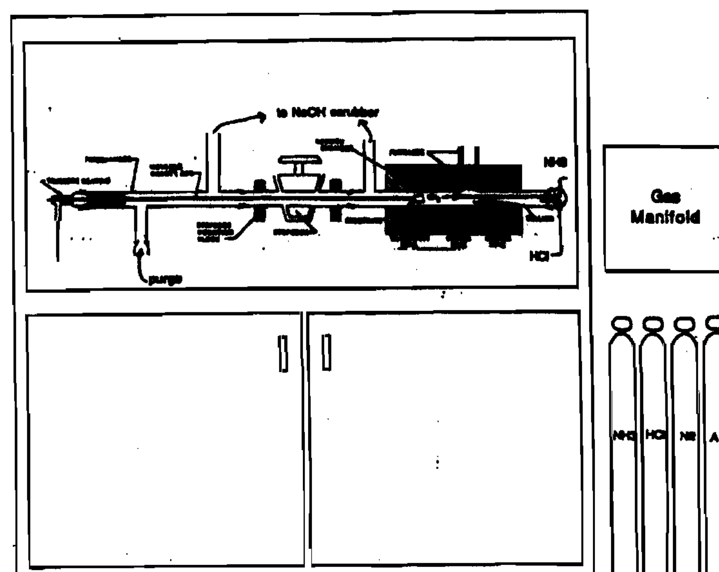

Fig. 22 HVPE GaN Reactor A.

Distribution authorized to U.S. Government agencies only to protect information not owned by the U.S. Government and protected by a contractor's "limited rights" statement, or received with the understanding that it not be routinely transmitted outside the U.S. Government. Other requests for this document shall be referred to ARPA Security and Intelligence Office.

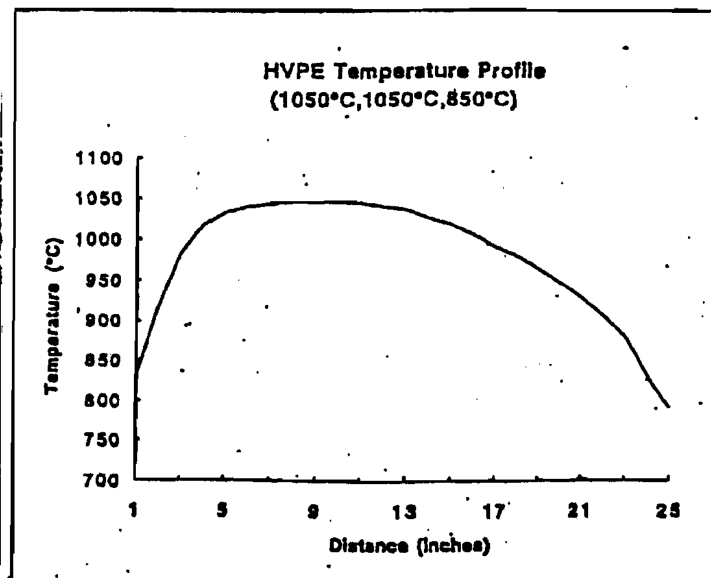

Fig. 23 Temperature profile of Reactor A.

Reactor B is schematically illustrated in Fig. 24. The novelty in this reactor is the physical separation of the Ga-chamber and the growth chamber. A number of samples were grown in this reactor at atmospheric pressure.

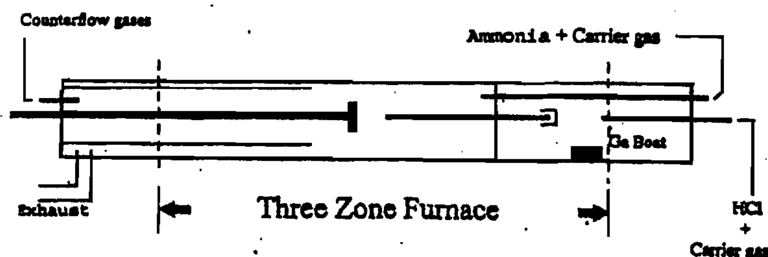

Fig. 24 HVPE GaN Reactor B.

Since the beginning of the program, we have grown 54 samples in the two reactors. Tehj second reactor is still under development. A number of deposition parameters were investigated. The most important parameters studied included the ratio NH3/HCL and the nature of the carrier gas (nitrogen, hydrogen, or helium). The films were evaluated by XRD, SEM and photoluminescence measurements. The XRD rocking curve for films 10-15 μm thick tends to be between 17-30 arcmin. Fig. 25 shows the rocking curve of one of the samples.

Distribution authorized to U.S. Government agencies only to protect information not owned by the U.S. Government and protected by a contractor's "limited rights" statement, or received with the understanding that it not be routinely transmitted outside the U.S. Government. Other requests for this document shall be referred to ARPA Security and Intelligence Office.

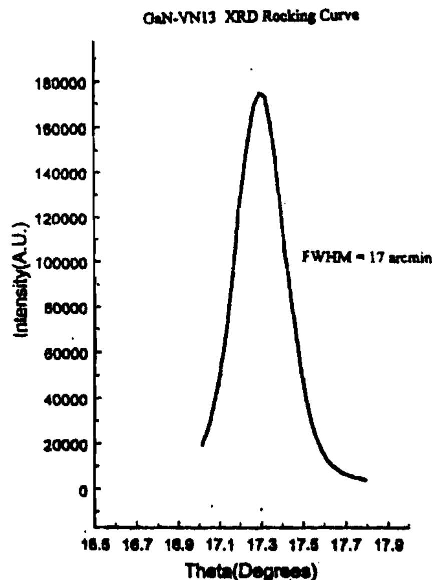

Fig. 4: XRD rocking curve of a GaN sample.

Fig. 25 A rocking curve of a GaN film grown by HVPE.

SEM morphology indicates that the films grown at ratios of NH3/HCL of about 10-30 tend to be smooth. However, this conclusion is stil tentative and further studies will be conducted during the next quarter. An example of such SEM surface and cross-section morphology is shown in Fig. 26. This sample was grown at NH3/HCL = 13 at a growth rate of 15 μm/hour.

Fig. 26 An SEM image of GaN grown via HVPE at BU.

Distribution authorized to U.S. Government agencies only to protect information not owned by the U.S. Government and protected by a contractor's "limited rights" statement, or received with the understanding that it not be routinely transmitted outside the U.S. Government. Other requests for this document shall be referred to ARPA Security and Intelligence Office.

The PL data show features either at 3.48 eV or close to 3.28 eV. A specific example showing both of these features is shown in Fig. 27.

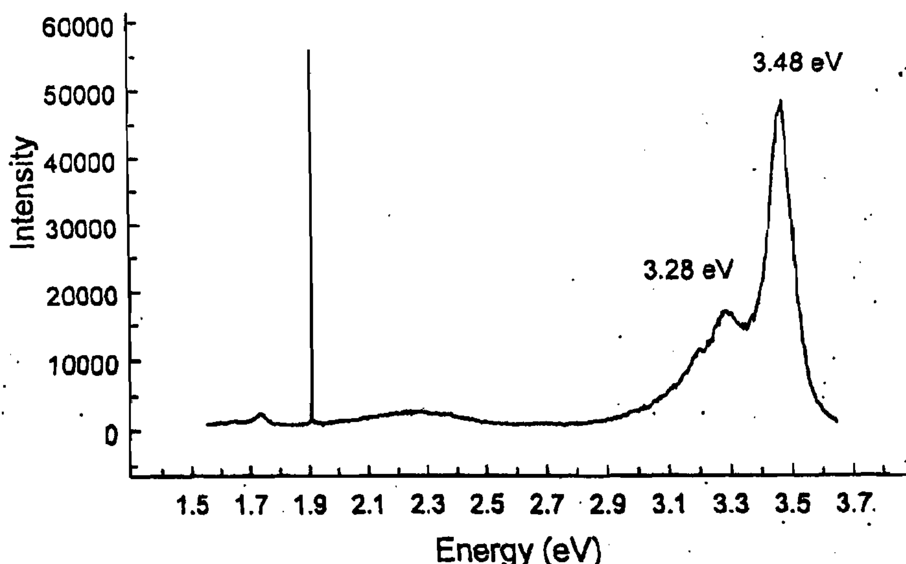

Fig. 27 Typical PL spectra of HVPE GaN.

Boston University has purchased two sputtering targets for the development of ZnO coating on sapphire substrates by the method of sputtering. One target consists of elemental Zn and the formation of ZnO will involve the reactive sputtering in an oxygen atmosphere. The second target in ZnO and formation of ZnO films will involve sputtering in an Ar-atmosphere. There are conflicting reports as to which is the better method of forming good crystalline quality ZnO. The development of ZnO coatings on sapphire will continue during the next quarter and GaN films will be formed on such coatings by the VPE method.

ATM: Our objectives for this period were to produce and analyze GaN on the growth template. In order to meet these goals, we initially established a baseline for the reactor by growing GaN on sapphire substrates, and then proceeded to grow GaN on the removable growth template.

High quality GaN was grown on (0001) sapphire substrates at growth rates in excess of 50 μm/hr. The crystal quality is excellent, as demonstrated by the narrow double crystal x-ray rocking curve (best FWHM = 184 arcsec.) shown in Figure 28. The room temperature photoluminescence (PL) spectrum (Figure 29) obtained from the same sample is dominated by near band edge emission at 3620Å, with a FWHM of 47 Å. The surface morphology is slightly rough, as shown in the Normarski optical microscope photographs of Figure 30. Additional work will be done to optimize the surface morphology. In general, these characteristics are comparable to high quality GaN grown by any method.

Distribution authorized to U.S. Government agencies only to protect information not owned by the U.S. Government and protected by a contractor's "limited rights" statement, or received with the understanding that it not be routinely transmitted outside the U.S. Government. Other requests for this document shall be referred to ARPA Security and Intelligence Office.

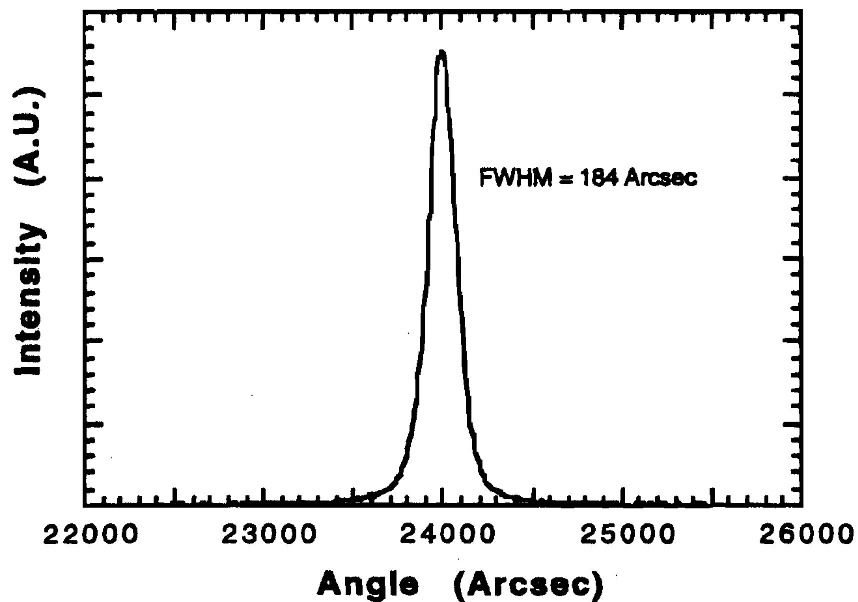

Figure 28. Double crystal x-ray rocking curve for a GaN layer grown on (0001) Sapphire.

Distribution authorized to U.S. Government agencies only to protect information not owned by the U.S. Government and protected by a contractor's "limited rights" statement, or received with the understanding that it not be routinely transmitted outside the U.S. Government. Other requests for this document shall be referred to ARPA Security and Intelligence Office.

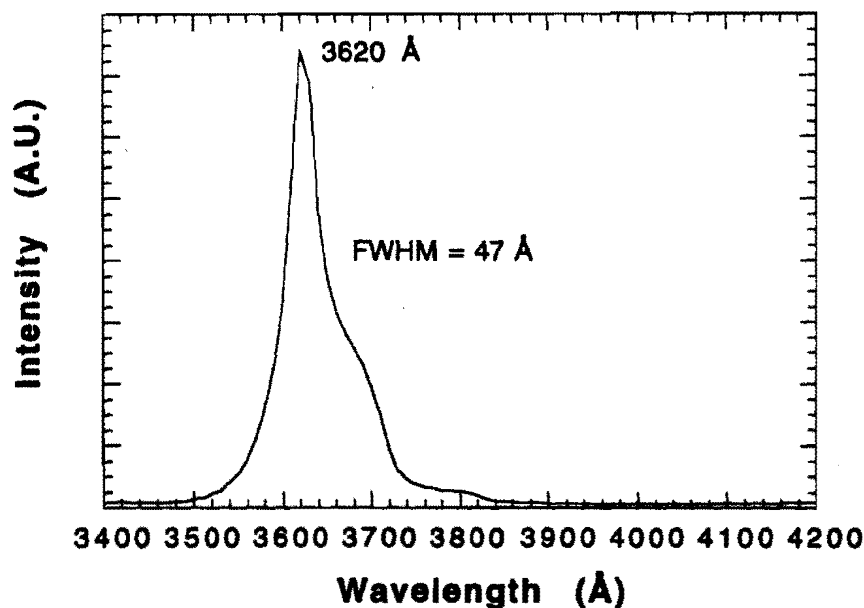

Figure 29. Room temperature photoluminescence spectrum obtained from a GaN sample grown on (0001) sapphire.

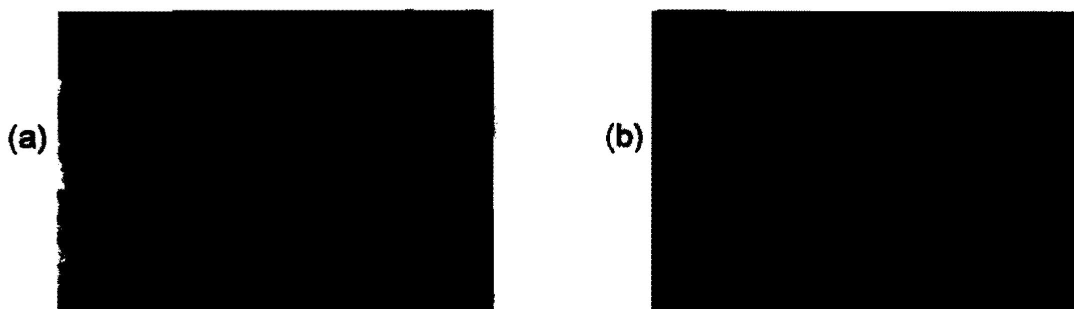

Figure 30. Normarksi contrast interference microscope images of the surface of a GaN sample grown on (0001) sapphire, at magnifications of (a) 255 X and (b) 645 X.

The results obtained in the growth of GaN on sapphire provided a baseline for the growth reactor, but it would be difficult to remove the sapphire to leave a free standing GaN substrate. Thus, we initiated growth on a removable growth template. Initial GaN layers on the growth template were discontinuous and polycrystalline. Figure 31 demonstrates the lack of surface coverage that was obtained in some of the initial films, as the grown layer did not adequately "wet" the template surface. By adjusting growth parameters, continuous, single crystal GaN was obtained. The surface morphology of these layers is shown in the high magnification Normarski contrast interference microscope image of

Distribution authorized to U.S. Government agencies only to protect information not owned by the U.S. Government and protected by a contractor's "limited rights" statement, or received with the understanding that it not be routinely transmitted outside the U.S. Government. Other requests for this document shall be referred to ARPA Security and Intelligence Office.

Figure 32. The surface contains many hexagonal pits and is cracked. Θ-2Θ scans demonstrate that the GaN films are single crystal. The FWHM of the rocking curve of the (0002) peak is approximately 2 arcmin for these films. In addition, intense PL emission is measured from these GaN samples grown on the growth template. As shown in Figure 33, the emission is dominated by near band edge emission at 3645 Å, and no deep level emission was observed. In conclusion, very high quality GaN has been grown on sapphire substrates, and single crystal GaN has been grown on the growth template.

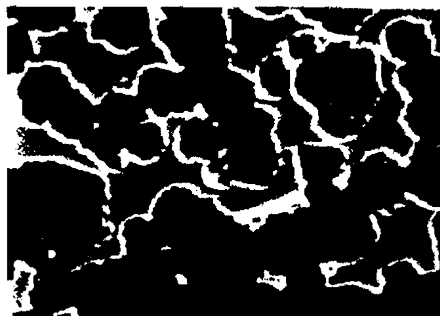

Figure 31. Normarksi contrast interference microscope images of the surface of an initial GaN sample grown on the growth template at a magnification of 65 X.

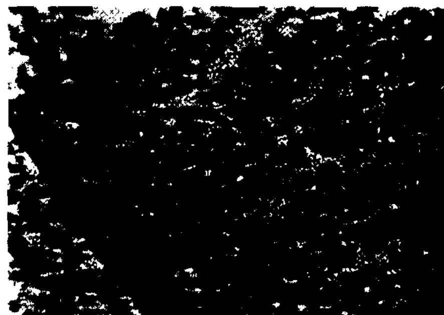

Figure 32. Normarksi contrast interference microscope images of the surface of an improved GaN sample grown on the growth template at a higher magnification of 645 X.

Distribution authorized to U.S. Government agencies only to protect information not owned by the U.S. Government and protected by a contractor's "limited rights" statement, or received with the understanding that it not be routinely transmitted outside the U.S. Government. Other requests for this document shall be referred to ARPA Security and Intelligence Office.

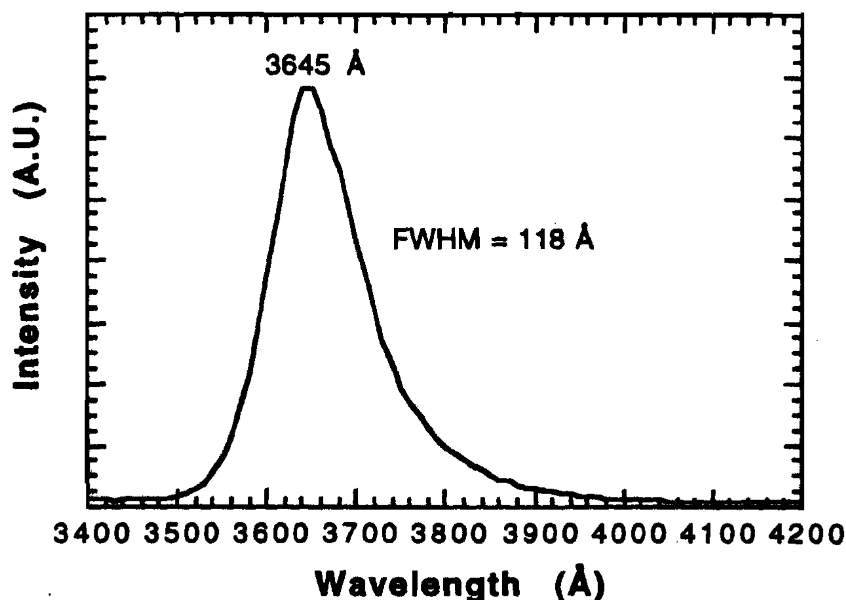

Figure 33. Room temperature photoluminescence spectrum obtained from a GaN sample grown on the growth template.

In the next reporting period we will focus on improving the surface morphology of GaN grown on sapphire, improving the overall quality of the GaN films grown on the growth template and delivering GaN samples to the consortium for growth and characterization.

Milestone #11 (HP), Milestone Complete

- **Milestone #10:** HP: RIE etching of GaN films demonstrated.

- **Summary:**

GaN, InGaN and AlGaN films have been etched using reactive ion etching (RIE). Several different plasma chemistries have been investigated including various combinations of chlorine compounds, argon and methane/hydrogen. We are currently using a $SiCl_4/Cl_2$ gas mixture to define the mesas in our LED device fabrication process. Under standard conditions, the etch rate is approximately 50 nm/minute; the typical 1.5 micron tall mesas are etched in 30 minutes using SiO_2 and thick photoresist as the masking materials. Figure 34 is a SEM micrograph of an array of mesas with n- and p-contacts after removal of the mask material. The uniformity is excellent over a 2" wafer. Figure 35 is a higher

Distribution authorized to U.S. Government agencies only to protect information not owned by the U.S. Government and protected by a contractor's "limited rights" statement, or received with the understanding that it not be routinely transmitted outside the U.S. Government. Other requests for this document shall be referred to ARPA Security and Intelligence Office.

magnification view showing the smooth sidewalls and etched n-GaN surface at the corner of a single mesa.

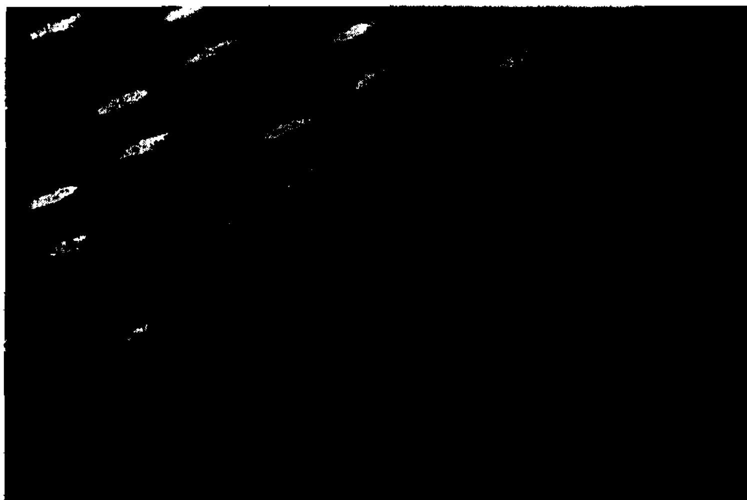

Figure 34: An array of RIE-etched GaN/InGaN/GaN mesas.

Figure 35: Edge of a single mesa etched via RIE.

Distribution authorized to U.S. Government agencies only to protect information not owned by the U.S. Government and protected by a contractor's "limited rights" statement, or received with the understanding that it not be routinely transmitted outside the U.S. Government. Other requests for this document shall be referred to ARPA Security and Intelligence Office.

BLUE BAND

Blue Light and Ultra-Violet Emitters, the Bay Area Nitride Consortium

Report for Month 12

Contract: MDA972-95-3-0008

DISTRIBUTION: SDL, HP, Xerox, AXT, ATM, Boston University, the University of Texas at Austin, D. Scifres, J. Endriz, R. Craig, J. Johnson, and R&D

To: Distribution
From: Jo S. Major
Date: 8.14.96

Distribution authorized to U.S. Government agencies only to protect information not owned by the U.S. Government and protected by a contractor's "limited rights" statement, or received with the understanding that it not be routinely transmitted outside the U.S. Government. Other requests for this document shall be referred to ARPA Security and Intelligence Office.

Overview:

The BlueBand program is changing focus from materials-related issues to increasingly device related milestones. In the first year of the program, basic materials issues such as n- and p-type doping, AlGaN and InGaN growth, native defect behavior, basic crystallography have been addressed. Homojunction, heterostructure and quantum well diodes have been constructed. At the point of writing of this report, HP has demonstrated a blue LED with ~70% of the optical intensity of the Nichia quantum well device.

In the coming year, the milestones, particularly of HP and SDL, become increasingly device driven. Upcoming milestones of this type include high-brightness LEDs, single mode waveguides, facet construction and the achievement of a pulsed injection laser in the nitrides.

The consortium met during this quarter and decided the issue of substrate vendor downselect. Based upon both technical and financial reasoning, the BlueBand consortium has decided to continue into the second year with ATMI as the continuing substrate vendor.

Summary: Milestones 17 through 21 are completed.

Milestone #17

Microstructure of undoped and highly doped GaN epilayers

The microstructure of highly doped GaN layers grown epitaxially by MOCVD at Xerox PARC has been characterized using transmission electron microscopy. High purity GaN was used as reference. In all cases, a columnar structure is evident, with column diameters between 0.2 and 1.0 mm. The characteristics of the columnar structure are reflected in the x-ray diffraction rocking curves (XRRC). A distribution of tilt of the c-axis of ~5 arcmin and a distribution in the rotation of the c-axis of ~8 arcmin is characteristic of some high quality materials. The addition of silicon for medium level carrier concentrations

(mid $10^{17}cm^{-3}$) does not seem to affect the columnar structure. Higher carrier concentration (about 10^{19} cm^{-3}) produces significant changes in the XRRCs and in the measured lattice parameter (cf work by Brent Krusor on HP samples). Similarly, the addition of magnesium does not affect significantly the microstructure for low/medium doping levels. Energy dispersive x-ray analysis supports the concept of Mg_3N_2 precipitates for Mg concentrations above 10^{19} cm^{-3}. The nature of dislocations does not appear to change noticeably when crossing a p-n junction between highly doped materials. This has been observed in Nichia LEDs as well as in a number of other samples. A few differences are observed with the use of other complementary techniques.

(a) Undoped GaN: The columnar structure of high purity material is easily observed with cathodoluminescence (CL). The near bandedge emission appears to be associated with the center of the column, and the yellow-region with dislocated regions [1]. Dislocations have burgers vectors of **a**, **a+c** and **c** [2]. Nanotubes and inversion domains have been identified in certain regions of the sample. Most of the nanopipes are associated with screw dislocations with a burgers vector of **c** [3]. One issue which is very stimulating is that the lattice of GaN/sapphire seems to be fully relaxed from the thermal stresses expected from this system. Lattice parameter measurements indicate that for device quality materials there is very little difference between bulk and heteroepitaxial lattice parameters. We have proposed a model for the relaxation of the thermal stresses based on the dislocation geometry [4].

(b) Highly Si- and Mg-doped films: The CL is uniform spatially for high-luminescence wavelengths. The disappearance of the columnar structure (in the CL images, but not in the TEM images) is intriguing. We have found that Raman scattering can be used to image the spatial variation of donors in the material, and images of donor distribution in hexagonal hillocks have been obtained [5]. As grown Mg-doped films give a particular Raman signal at 519 cm^{-1} which vanished after the thermal anneals used for acceptor activation [6]. We are in the process of establishing the connection between CL, Raman, and the microstructure. We need to be able to quantify the strain associated with dislocations. We suspect that dislocations getter some of the dopants and as a result of dopant reaction with the core the dislocation strain is relaxed.

References:

[1] F. A. Ponce, D. P. Bour, W. Goetz, P. J. Wright, Appl. Phys. Lett. **68**, 57 (1996).

[2] F. A. Ponce, D. Cherns, W. Young, and J. W. Steeds, Appl. Phys. Lett. 69 (6) in press (1996).

[3] F. A. Ponce, D. Cherns, W. Young, and J. W. Steeds, and S. Nakamura, submitted to Appl. Phys. Lett.

[4] F. A. Ponce, B. S. Krusor, F. Ross, and S. Nakamura, 1st Europ. Workshop on GaN. To be published.

[5] F. A. Ponce, J. W. Steeds, C. Dyer, and D. Pitt, submitted to Appl. Phys. Lett.

[6] F. A. Ponce, J. W. Steeds, C. Dyer, D. Pitt, and S. Nakamura, submitted to Appl. Phys. Lett.

Milestone #18

Heterojunction growth for fundamental bandoffset studies.

UT Austin has successfully grown InGaN/GaN and AlGaN/GaN heterojunctions and samples are being studied using low-temperature PL and will be supplied to the Consortium members for further study.

Milestone #19

Fabrication of p/n AlGaN/GaN heterojunction. Turn-on voltage goal specification is less than 4.4 V.

An $Al_{0.08}Ga_{0.92}N$/GaN heterojunction was grown which showed diode behavior similar to the GaN/GaN homojunctions that we have produced. I-V and L-I curves for both junction types are shown in Figures 1 and 2. Light output for the heterojunction device is one-third that of the homojunction device. V characteristics are nearly identical, with a 20 mA Vf of 7.6 to 7.7 volts. Peak wavelength is 471 nm for the $Al_{0.08}Ga_{0.92}N$/GaN device and 465.4 nm for the GaN/GaN device. The forward voltage is greatly improved to a value of 4.4 volts by increasing the Mg concentration in the p-GaN layer, facilitating ohmic contact formation. UT Austin has recently achieved p-type doping and has now demonstrated a working p-n GaN homojunction. This LED is now under characterization.

Electrical characterization of p-n homojunctions

The ability to dope GaN n- and p-type by employing Si as a donor and Mg as an acceptor leads to the fabrication of p-n^+ junction devices. The diodes were grown on sapphire substrates and the p and n^+ layers were ~5 μm and 0.56 μm thick, respectively. The acceptors were activated with a standard postgrowth furnace anneal. Reactive ion etching was employed to fabricate mesa structures with a diameter of 0.5 mm. Ohmic metal

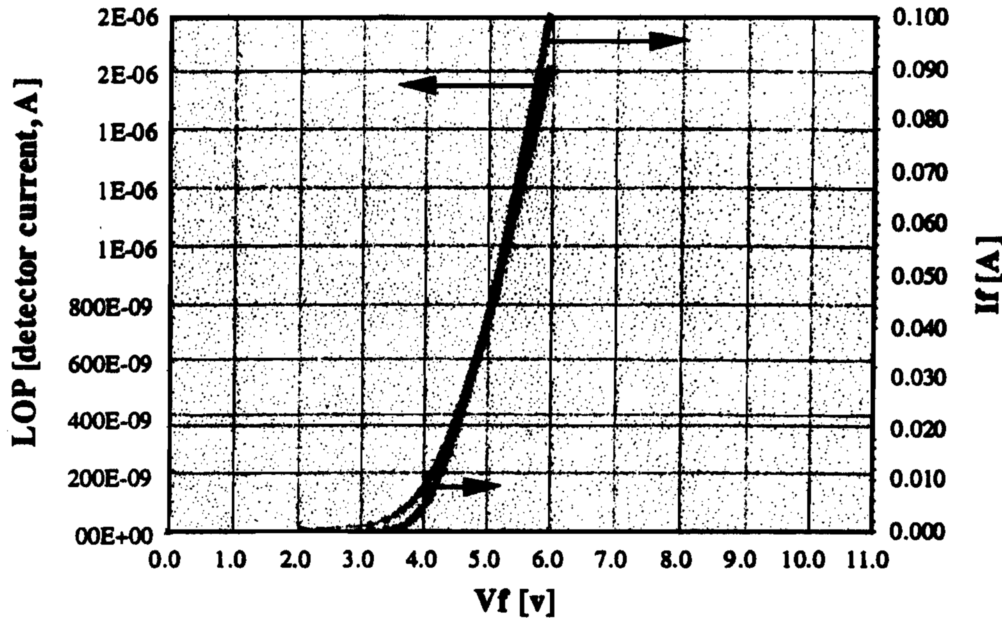

An AlGaN/GaN heterojunction LED. The turn-on voltage is 4 volts with the 20 mA operating current reached at a voltage of 4.4 volts.

contacts were deposited on the n^+ and p-layers. The performance of the diodes was tested with current-voltage (I-V) and capacitance-voltage (C-V) measurements. Results are shown below.

The analysis of the C-V data reveals an effective acceptor concentration (NA-ND) of ~2×1018 cm-3 uniformly distributed over the depth of the capacitance measurement. In the case of acceptors in Mg-doped GaN the C-V measurement determines the acceptor concentration (minus the concentration of donors) rather than the hole concentration. The I-V characteristic of a representative diode is shown in the inset (above). The leakage current at a reverse bias of -4 V is -2.1 μA.

The diodes were utilized in deep level transient spectroscopy (DLTS) measurements to

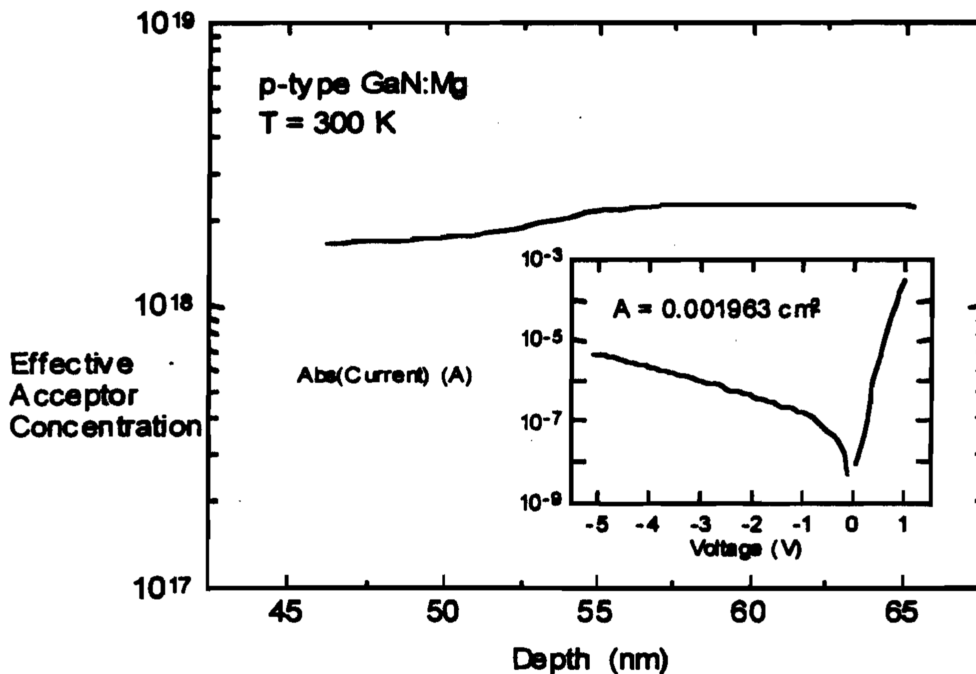

Effective acceptor concentration vs. depth of the depletion region for p-type, Mg-doped GaN. The inset shows the current through the p-n+ junction diode as a function of applied bias. Negative voltage corresponds to a reverse bias.

investigate deep level defects in p-type GaN for the first time. The diodes were well suited for these measurements which use a 1 MHz test-signal to measure the differential capacitance. The analysis of the DLTS data yielded deep levels with activation energies for hole emission to the valance band of (0.21 ± 0.03) eV (ET(DLP1)), (0.30 ± 0.11) eV (ET(DLP2)), and (0.45 ± 0.10) eV (ET(DLP3)). The concentrations of the deep levels (NT) were found to be (3.9 ± 2.3)×1014 cm-3 (NT(DLP1)), (5.0 ± 2.0)×1014 cm-3 (NT(DLP2)), and (8.6 ± 1.4)×1014 cm-3 (NT(DLP3)).

The identification of deep levels in GaN and the ability to control their concentrations are important issues for the fabrication of light emitters with III-V nitrides since deep level

defects may act as efficient recombination centers and influence the efficiency of LEDs or the threshold power for injection lasers.

Publications submitted:

1 *A donor-like deep level defect in $Al_{0.12}Ga_{0.88}N$ characterized by capacitance transient spectroscopies*

W, Götz, N.M. Johnson, M.D. Bremser, and R.F. Davis, Appl. Phys. Lett. (1996)

2 *Activation of acceptors in Mg-doped, p-type GaN*

W. Götz, N.M. Johnson, J. Walker, D.P. Bour

Symposium E of the 1996 Spring Meeting of the Materials Research Society, April 8-12,

1996, San Francisco, CA

Publications appeared:

1 *Activation Energies of Si Donors in GaN*

W, Götz, N.M. Johnson, C. Chen, H. Liu, C. Kuo, and W. Imler, Appl. Phys. Lett. **68**, 3144 (1996)

2 *Deep level defects in Mg-doped, p-type GaN grown by metalorganic chemical vapor deposition*

W, Götz, N.M. Johnson, and D.P. Bour, Appl. Phys. Lett. **68**, 3470 (1996)

Milestone #20

Substrates: Evaluate SiC vs. Al_2O_3, MBE growth of GaN films on M-plane sapphire, program plans for AXT and ATMI.

All companies within the consortium have grown on SiC, along with the more common C-plane sapphire. At present the consortium members are not planning to put significant emphasis on SiC, due primarily to the high cost of SiC substrates. Growth on micropipe-free SiC is more forgiving to process variations, however, no significant performance advantage in terms of mobility, diode performance, etc., has been found.

GaN films were grown by the MBE method on the M-plane (1010) of sapphire, with or without a low temperature buffer. The structure and the opto-electronic properties of these films are summarized as follows.

A. <u>Films grown without a low temperature buffer.</u>

The only cleaning procedure of the substrates was heating in molecular hydrogen to 700°C. Films approximately 1μm thick were grown at this temperature and doped with the Si-cell at 1375°C.

- <u>SEM examination</u> reveals relatively smooth surface morphology but with micropores about 1000Å in diameter.
- <u>XRD examination</u> reveals two reflections, a strong one with Miller indices (1122) and a weaker one with Miller indices (1010).
- <u>Hall effect measurements</u> show that the material is heavily doped with carrier concentration 3-4 x 10^{18} cm^{-3}, electron mobility $60cm^2$/V-sec and resistivity 3 x 10^{-2} ohm-cm.
- <u>Photoluminescence measurements</u> with a 10mW He-Cd laser show a strong luminescence across the gap (365nm) with no observable yellow luminescence.

B. Films grown with a low temperature buffer.

In this series of films the substrate was first nitridated at 750°C, then cooled to 500°C for the growth of a 250Å thick GaN buffer and heated to 750°C for the growth of about 1μm thick film. The temperature of the Si-cell was at 1350°C.

- <u>SEM examination</u> reveals very smooth surface morphology.
- <u>XRD examination</u> reveals again two reflections with indices (1122) and (1010) as in the previous case.
- <u>Conductivity measurements</u> show that the material has a resistivity 130 ohms, which is 4.3 x 10^3 times larger than the resistivity of the samples grown without a buffer.
- <u>Photoluminescence measurements</u> show a sharp photoluminescence peak at room temperature (FWHM = 79meV) occurring at 365nm. The intensity is one order of magnitude weaker than in the previous sample. These samples do not show yellow luminescence as well.

Conclusions:

The main conclusions from this study can be summarized as follows:

1. The low temperature buffer promotes two dimensional growth leading to smoother surface morphologies. This result is similar to growth on the c-plane.

2. The investigated conditions lead to the growth of (1122) and (1010) planes. However, these planes are not well matched to the M-plane sapphire. The plane we want is the (1013), in which the mismatch with the sapphire (1010) lattice in he two perpendicular axes is the minimum. (The mismatch is 2.6% in GaN [1210]/sapphire [0001] direction and 1.9% in GaN [3031]/sapphire [2110] direction). Further work is required to identify conditions for the epitaxial growth of the (1013) plane.

3. The films without a low temperature buffer dope far more efficiently with silicon than the films with the buffer. The evidence suggests that the films with the buffer are more strained and this probably affects the incorporation of silicon in the sites.

4. The photoluminescence intensity is reduced as the carrier concentration is reduced. However, no yellow luminescence is observed even at low doping levels. This is generally opposite to GaN on the c-plane which shows yellow luminescence at low doping levels.

AXT and HPRC have made dramatic progress in crystal growth. The most recent crystals are nearly 1 cm in scale (~8 mm by ~ 8 mm). They are quite clear and have smooth surfaces. Since the beginning of the program, the crystal area has been scaled up by a factor of two every three to four months. At the current rate of development, the crystals will reach 2-2.5 cm diameter in approximately 12 months. MBE epitaxial growth at the University of Ulm shows the narrowest exciton lines for any GaN material. The FWHM of the lines is on the order of 0.5 meV. In addition, exciton lifetime studies at HPRC show that the lifetime of the GaN on GaN epitaxy is an order of magnitude greater than that of GaN on sapphire. This is a clear indication of the superior quality of the GaN on GaN epitaxial films.

A reactor design was carried out for the growth of 2-2.5 cm scale crystals. This design shows that the reactor for manufacturing commercializable substrates comparable to that for other crystal growth systems. The estimated cost, if built in Poland, is competitive with other technologies.

The polishing tests resulted in about a 6 Å RMS surface finish. This is still not as good as shown by XEROX and further refinement of the technique is required.

Future Plans

AXT participated in the downselect meeting hosted by HP on 13 June 1996. The Blue Band Consortium decided against continuing support of bulk crystal development. Given the high quality of the epitaxy which has been demonstrated by the Blue Band and others on GaN substrates, AXT expects that a true UV or blue laser will be demonstrated

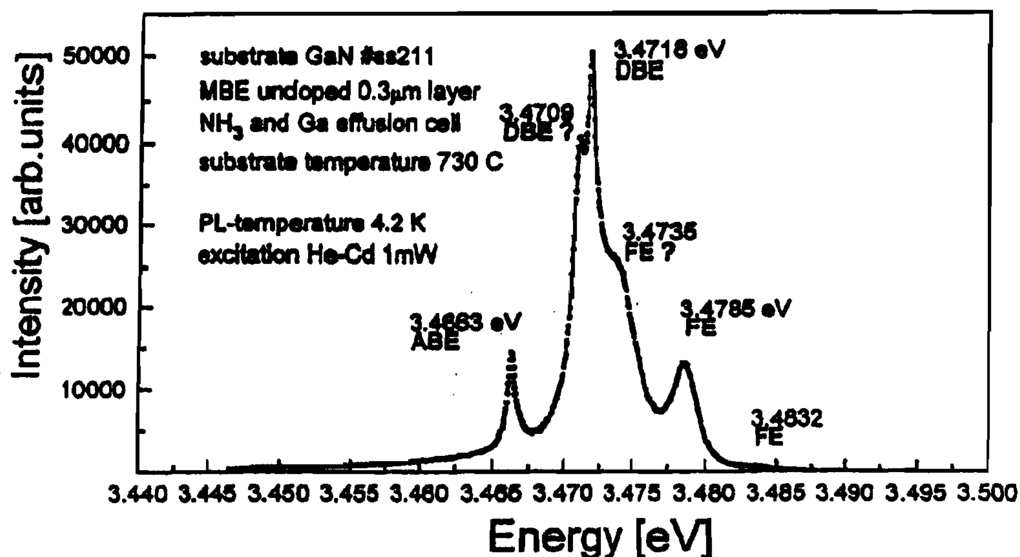

The low temperature PL of a GaN film, grown by MBE, on a GaN substrate.

successfully on the GaN substrates.

ATMI:

During this work period, we have further improved the uniformity and quality of GaN grown on sapphire by HVPE. In addition, we directly addressed the components needed to make free-standing GaN, namely:

- Improved the quality of GaN on the template substrate by HVPE
- Reconfigured the HVPE reactor to allow for backside template etching
- Demonstrated Si template etching at large etch rates

Several samples have been delivered to the Consortium for epi-layer growth and characterization:

- 3- 2" wafers of GaN grown on Sapphire
- A small piece of free-standing GaN

- GaN grown on the template substrate

Plans for Second Year:

We have demonstrated all the components needed to make GaN substrates by the method which we proposed in this program. These will be combined to remove the silicon template from crack-free GaN on silicon to produce free-standing GaN substrates. In addition, there is potential for other removable template materials which could act as a substrate for GaN growth. Among the candidates which are of interest are:

- Lithium Gallium Oxide (LGO)
- Lithium Aluminum Oxide (LAO)
- Zinc Oxide

Finally ATMI has worked at predicting the wafer cost for a 2" GaN wafer grown via HVPE. The cost curve is $1500 @ 100 wafers/month (w/m), $400 @ 1000 w/m, and $250 @ 10000 w/m.

Milestone #21

GaN LED Demonstration

Materials and modeling parameters that critically influence LED operation

Numerical device simulations can greatly aid the optimization of LED (as well as laser diode) structures. The ability to perform such simulations is currently hampered by incomplete knowledge of a number of basic materials parameters in the nitrides. We have surveyed the literature to obtain state-of-the-art values for the key parameters, and identify areas where first-principles calculations can provide new or more accurate information. Here we focus on parameters describing the band structure of the component materials.

For ternary alloys, linear interpolation between the values for the constituent binary compounds often provides adequate parameter values. However, some parameters exhibit nonlinear behavior as a function of alloy composition. The prime example is the bowing of the band gap. Our first-principles calculations have produced values of b=0.5 for AlGaN and b=1.0 for InGaN; these results are very close to those obtained by A. F. Wright and J. S. Nelson [Appl. Phys. Lett. **66**, 3051 (1995)]. It is expected that refractive indices will also exhibit a nonlinear dependence on composition.

The band structure of the component materials is not only a function of alloy composition, but also of strain induced by lattice mismatch. The effect of strain on the band structure can be described in terms of deformation potentials. We have calculated the following values (in eV, Pikus-Bir notation):

	AlN	GaN	InN
a (hydrostatic)	-9.1	-8.0	-5.0
b (100 strain)	-1.5	-1.7	-1.2
d (111 strain)	-4.5	-4.2	-3.0

Finally, we point out that heterojunction band offsets may be the most crucial parameters determining optoelectronic device behavior. Measured values of band offsets in the nitride system exhibit a great deal of scatter right now, which is at least in part due to improper inclusion of the effects of strain. First-principles calculations of the band lineups, including strain effects, are in progress.

Published:

"Defects, impurities and doping levels in wide-band-gap semiconductors", C. G. Van de Walle and J. Neugebauer, Braz. J. Phys. 25, 163 (1996).

"Native defects and impurities in GaN", J. Neugebauer and C. G. Van de Walle, Festkörperprobleme/Advances in Solid State Physics 35, 163 (1996).

Accepted for publication:

"Gallium vacancies and the yellow luminescence in GaN", J. Neugebauer and C. G. Van de Walle (Applied Physics Letters, July 22 1996).

Submitted:

"Role of hydrogen and hydrogen complexes in doping of GaN", J. Neugebauer and C. G. Van de Walle, MRS Symposia Proceedings Vol. 423 (MRS, Pittsburgh, PA).

BLUE BAND

Blue Light and Ultra-Violet Emitters, the Bay Area Nitride Consortium

Report for Month 9

Contract: MDA972-95-3-0008

DISTRIBUTION: SDL, HP, Xerox, AXT, ATM,	**To:**	Distribution
Boston University, the University of Texas at Austin,	**From:**	Jo S. Major
D. Scifres, J. Endriz, R. Craig, J. Johnson, and R&D	**Date:**	5.2.96

Distribution authorized to U.S. Government agencies only to protect information not owned by the U.S. Government and protected by a contractor's "limited rights" statement, or received with the understanding that it not be routinely transmitted outside the U.S. Government. Other requests for this document shall be referred to ARPA Security and Intelligence Office.

Summary: Milestones 12-16 have been completed.

Milestone #12, Milestone Complete

- **Milestone #12:** Photopumping set-up completed; PL studies initiated

The PL systems are now installed and are operational. UT Austin how has a Coherent Radiation "Saber" CW UV laser operating at 244 nm; and a Laser Photonics pulsed N_2 laser

Milestone #13, Complete

- **Milestone #13:** Structural characterization of AlGaN layers.

The microstructure of AlGaN layers grown epitaxially by MOCVD at SDL has been characterized using transmission electron microscopy. AlN buffer layers were first deposited on (0001) sapphire substrates at about 550°C followed by growth of a 0.5 µm thick $Al_{0.5}Ga_{0.5}N$ film at 1050°C. Figure 1 is a TEM immage showing the associated microstructure. Misfit dislocations are obsrved at the substrate/buffer layer interface with a separation of about 20.3Å. The buffer-layer/AlGaN interface shows a misfit dislocation arrangement with a period of 226Å. These values are consistent with the 12.5% lattice mismatch between AlN and Al_2O_3, and the 1.19% mismatch between $Al_{0.5}Ga_{0.5}N$ and AlN. The buffer layer leads to a film microstructure which can be

Distribution authorized to U.S. Government agencies only to protect information not owned by the U.S. Government and protected by a contractor's "limited rights" statement, or received with the understanding that it not be routinely transmitted outside the U.S. Government. Other requests for this document shall be referred to ARPA Security and Intelligence Office.

described as a columnar structure with a distribution of tilt and twist orientations. Materials with best electronic properties have a distribution of 5 arcmin for tilt, and about twice as much for twist. Threading dislocations observed in these materials are the result of these low angle grain boundaries.

Fig. 1 TEM micrograph of the AlGaN film: (a) and (b) misfit dislocations at the AlN/Al2O3 and AlGaN/AlN interfaces; (c) and (d) stacking faults along basal planes.

Milestone #14 Milestone Complete

- Milestone #14: Controllable p-type doping in GaN demonstrated between 10^{17} and 10^{18} cm^{-3}. Demonstration of p/n homojunction, w/goal specs of turn-on voltage less than 4.5 V and reverse breakdown voltage greater than 10 V. Deliver sample to Xerox. Metal contacts for p-type GaN films. Deliver heavily n-doped samples to Xerox for material study. Electrical characterization of acceptor-doped GaN. Calculate properties of n-type dopants (SI, O, C) in GaN. Studies of passivation in nitride films initiated. Doping demonstrated for p- and n-type GaN in D system.

Distribution authorized to U.S. Government agencies only to protect information not owned by the U.S. Government and protected by a contractor's "limited rights" statement, or received with the understanding that it not be routinely transmitted outside the U.S. Government. Other requests for this document shall be referred to ARPA Security and Intelligence Office.

Bio-Rad Microscience HL5500 Hall System
Measured on 3/15/96 at 3:40 PM

SPECIMEN	MEASURING CONDITIONS
Wafer ID: 694 pt 700C	I-meas: 3.9 uA DC
Batch ID:	Temperature: AMB
Material: GaN	Field: 0.320 Tesla
Description:	
Thickness: 2.000 um	Targ.Vr: 20 mV

RESULTS SUMMARY

Rs:	1.75e+04 ohm/sq	RHs:	+1.86 m²/C	Ns:	+3.35e+14 /cm²
R :	3.49 ohm-cm	Mob:	1.07 cm²/V-s	N :	+1.68e+18 /cm3

CONTACT CHECK

Pair	K-ohms
12	22
23	24
34	27
41	21
13	30
24	25

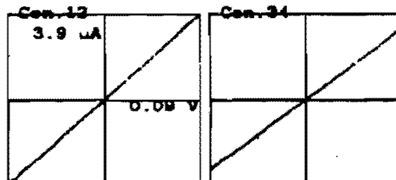

RESISTIVITY

Meas	+++	Vm ---	Sym	Factor	R-sheet
43	1.89e-02	-1.89e-02	1.61	0.98	1.75e+04
41	1.17e-02	-1.18e-02	1.61	0.98	1.75e+04
21	1.90e-02	-1.89e-02	1.61	0.98	1.75e+04
23	1.18e-02	-1.17e-02	1.61	0.98	1.75e+04

HALL MEASUREMENTS	+++ 24	---	+++ 13	---
Misalignment	+7.30e-03	-7.12e-03	-7.15e-03	+7.21e-03
Offset applied	-7.42e-03		+7.42e-03	
V-hall North	-3.56e-04	+5.31e-04	+5.08e-04	-4.36e-04
V-hall South	-3.64e-04	+5.41e-04	+5.10e-04	-4.36e-04
V-hall (mean)	+4.49e-06		+1.56e-07	
V-hall (over all cycles)	+2.32e-06			

Figure 2: The Hall data of $Al_{0.05}Ga_{0.95}N$ grown at SDL

P-type doping has been demonstrated to a doping level of ~2 x 10^{18} cm^{-3}. Figure 2 shows the room-temperature hole concentration and mobility. Figure 3 shows the hole concentration vs temperature. The composition of the sample is $Al_{0.05}Ga_{0..95}N$. Doping levels exceeding 10^{17} cm^{-3} have been achieved in $Al_{0.15}Ga_{0..85}N$. HP, SDL (and Xerox) have all demonstrated good p-n junction operation. Figures 4 and 5 show the I-V characteristics of junctions fabricated at HP and SDL, respectively. The turn-on voltage of the p-n junction is ~3V with small leakage currents observed in reverse-biased operation.

Distribution authorized to U.S. Government agencies only to protect information not owned by the U.S. Government and protected by a contractor's "limited rights" statement, or received with the understanding that it not be routinely transmitted outside the U.S. Government. Other requests for this document shall be referred to ARPA Security and Intelligence Office.

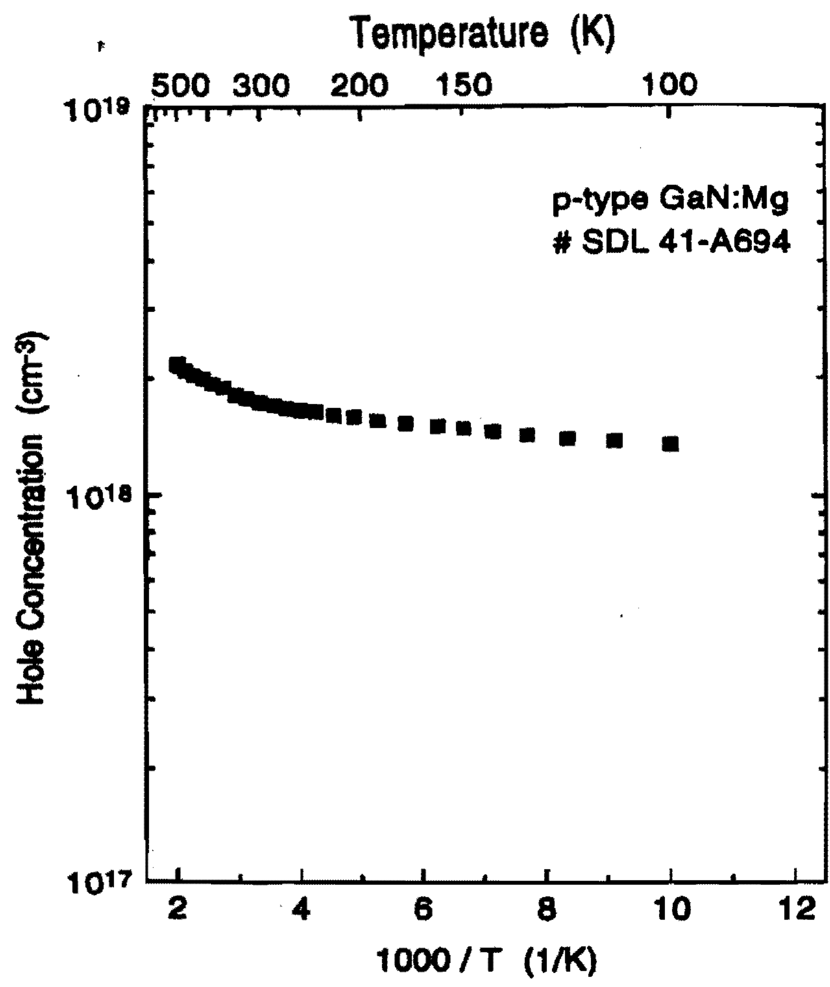

Figure 3: The doping concentration versus temperature for $Al_{0.05}Ga_{0.95}N:Mg$ grown at SDL

Distribution authorized to U.S. Government agencies only to protect information not owned by the U.S. Government and protected by a contractor's "limited rights" statement, or received with the understanding that it not be routinely transmitted outside the U.S. Government. Other requests for this document shall be referred to ARPA Security and Intelligence Office.

GaN P/N Homojunction I-V

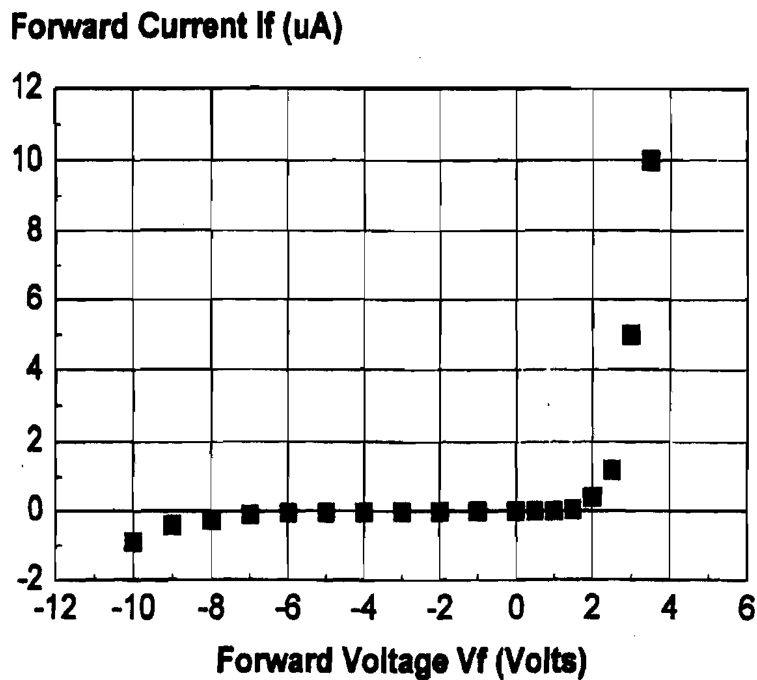

Figure 4: The I-V of H-P's GaN Homojunction

Distribution authorized to U.S. Government agencies only to protect information not owned by the U.S. Government and protected by a contractor's "limited rights" statement, or received with the understanding that it not be routinely transmitted outside the U.S. Government. Other requests for this document shall be referred to ARPA Security and Intelligence Office.

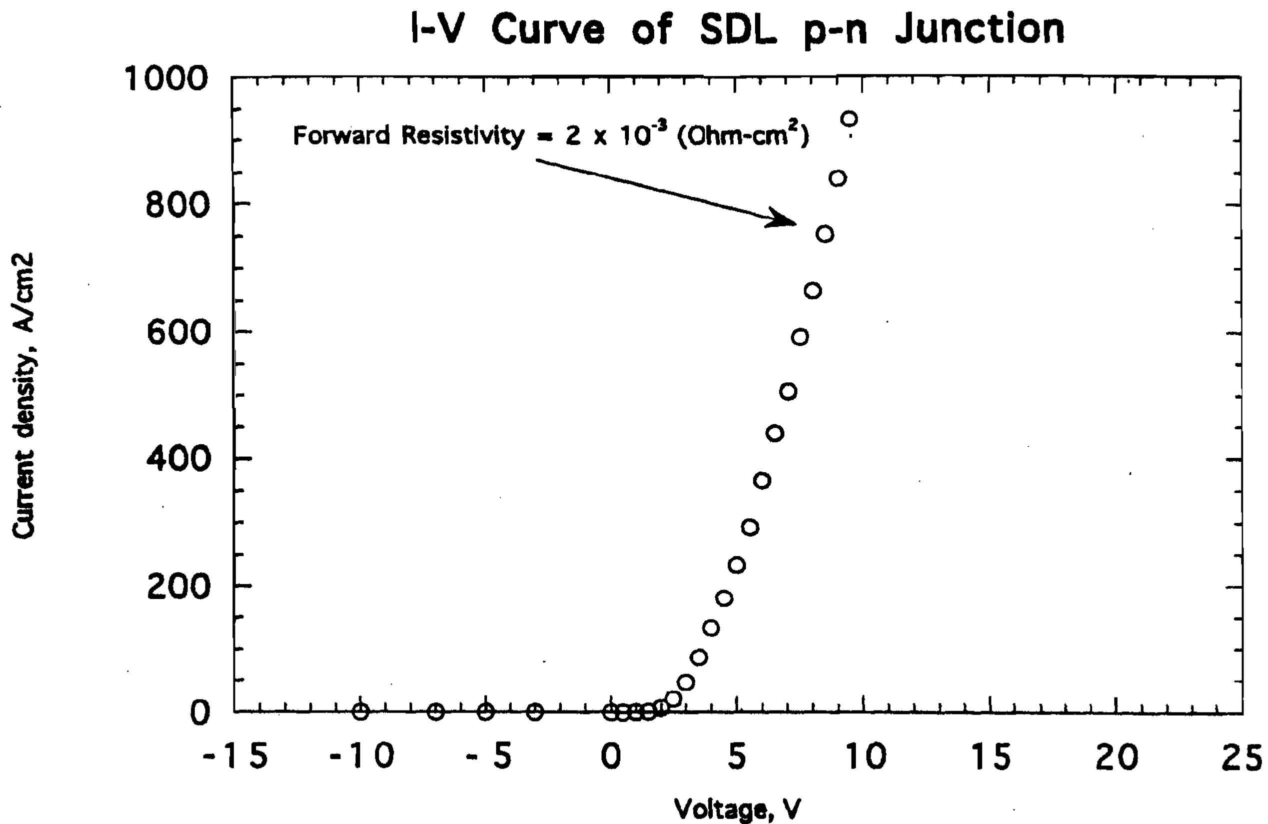

Figure 5: I-V Curve of SDL p-n Junction

Both SDL and HP have examined p-metals. The experimental work done to date shows that the dominant p-metal of the literature, NiAu, is an acceptable contact metal for p-type GaN. HP has investigated NiV/AuZn and AuPd. The results of this investigation at HP is shown in Figure 6. The AuPd contact is linear following a contact anneal (upper panel). The NiV/AuZn contact is not ohmic even after the metal anneal.

Distribution authorized to U.S. Government agencies only to protect information not owned by the U.S. Government and protected by a contractor's "limited rights" statement, or received with the understanding that it not be routinely transmitted outside the U.S. Government. Other requests for this document shall be referred to ARPA Security and Intelligence Office.

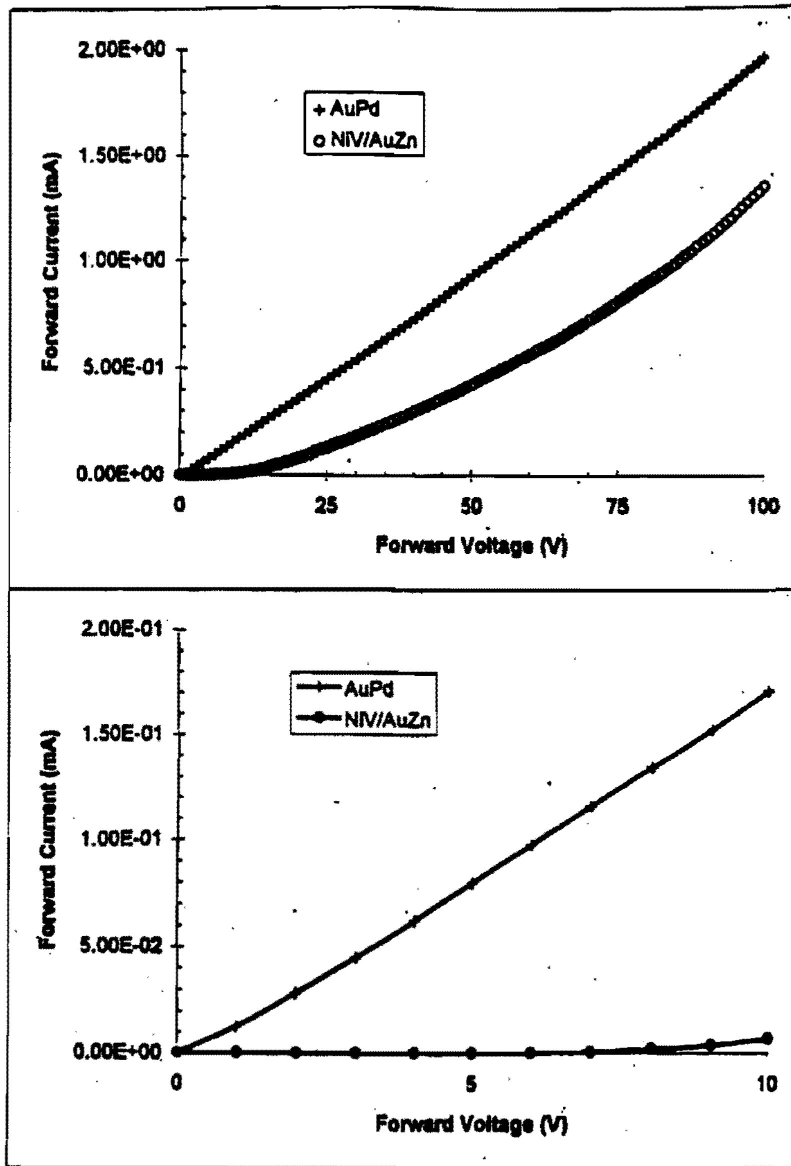

Figure 6: I-V's of AuPd and NiV/AuZn. The measurement is simply taken from pad to pad.

Distribution authorized to U.S. Government agencies only to protect information not owned by the U.S. Government and protected by a contractor's "limited rights" statement, or received with the understanding that it not be routinely transmitted outside the U.S. Government. Other requests for this document shall be referred to ARPA Security and Intelligence Office.

HP and SDL have delivered both n- and p-type samples to Xerox for characterization. In fact, the p-type characterization shown in Figures 1 and 2 are the result of such collaborative efforts with the data of Figure 1 being generated at SDL while the data of Figure 2 has been measured at Xerox.

SDL's investigation of p-metal contacts includes the following elemental metals – Ti, An, Pd, Pt, Ni – and the following combinations – NiAu, TiAu, TiPd, and PtPd. Currently our work has indicated that Pd is the best metallic contact to GaN:Mg and that of the metal combinations PtPd has good contact properties coupled with excellent thermal stability.

One of the difficulties associated with doping GaN p-type with Mg is the relatively high activation energy for ionization of the acceptors. Thus only ~1% of the active acceptors are ionized at room temperature and contribute holes to the valence band for the p-type concentrations of Mg atoms are required to obtain sufficiently high hole concentrations at room temperature. The presence of many acceptor states leads to impurity band conduction.

To illustrate these problems, in Figure 7, we show results from variable temperature Hall measurements (symbols) obtained from three Mg-doped GaN samples. The acceptor dopant was activated for all the samples shown in Figure 6. Figure 6a shows hole

Distribution authorized to U.S. Government agencies only to protect information not owned by the U.S. Government and protected by a contractor's "limited rights" statement, or received with the understanding that it not be routinely transmitted outside the U.S. Government. Other requests for this document shall be referred to ARPA Security and Intelligence Office.

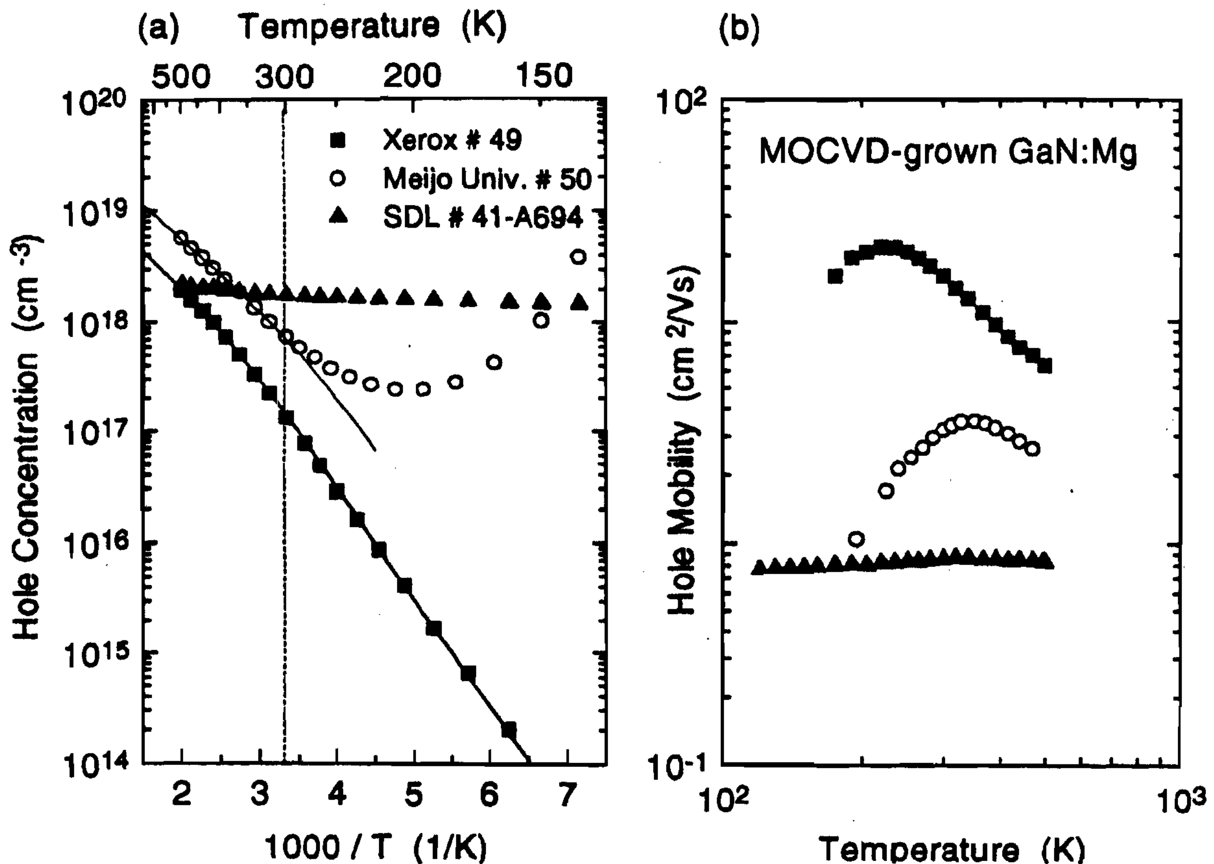

Figure 7. Hole concentration vs. reciprocal temperature (a) and mobility vs. temperature (b) for three Mg-doped, p-type GaN samples. The symbols refer to the experimental data. The solid lines in Figure 6a result from least-squares fits assuming a single acceptor and donor compensation to the experimental data.

concentrations as a function of the reciprocal temperature; the Hall scattering factor was assumed to be temperature independent and of unity value. The temperature dependence of the hole concentration measured for sample Xerox # 49 is dominated by the ionization of a single acceptor. The Activation energy for ionization and the concentration of this acceptor were determined from at least-squares fit (solid line) of the charge neutrality equation to the experimental data. The activation energy is ~170 meV and the acceptor concentration is 2 x 10^{19} cm^{-3}. Our analysis of the Hall effect data also provides the concentration of any donors present in Mg-doped GaN samples. for the Xerox sample this concentration is ~2 x 10^{18}. An activation energy in the range between ~160 meV and ~185 meV is usually observed for Mg-doped GaN. The second sample shown in figure 7 was grown at Meijo University in Japan (#50) and is shown here as a reference. The results for the activation energy,, the acceptor concentration, and the concentration of the compensation are ~165 meV, 8 x 10^{19} cm^{-3}, and 4 x 10^{18} cm^{-3}, respectively. the third sample was grown at SDL (#41-A694). This sample exhibits hole concentrations of

Distribution authorized to U.S. Government agencies only to protect information not owned by the U.S. Government and protected by a contractor's "limited rights" statement, or received with the understanding that it not be routinely transmitted outside the U.S. Government. Other requests for this document shall be referred to ARPA Security and Intelligence Office.

~2 x 10^{18} cm^{-3} which are independent of the sample temperature. This behavior is indicative of impurity band conduction. As a consequence the SDL sample has the highest hole concentration at room temperature (300K) as indicated by the vertical dashed line in Figure 6a. Hole mobilities for the three samples are shown in Figure 6b. Hole mobilities for the three samples are shown in Figure 6b. The Xerox sample exhibits the highest hole mobility, which corresponds to the lowest acceptor concentration. The sample which is dominated by impurity band conduction (SDL # 41-A694) shows the lowest hole mobility. Consequently, the resistivities of the p-type layers turn out to be nearly identical (~3Ωcm at 300K).

Published:

1. *Electronic and Structural Properties of GaN Grown by Hydrid Vapor Phase Epitaxy,* W. Götz, L.T. Romano, B.S. Krusor, N.M. Johnson, and R.J. Molnar, Appl. Phys. Lett. (1996)

2. *Activation Energies of Si donors in GaN,* W. Götz, N.M. Johnson, C. Chen, H. Liu, C. Kuo, and W. Imler, Appl. Phys. Lett. (1996)

3. *Deep Level Defects in Mg-doped p-type GaN grown by Metalorganic Chemical Vapor deposition,* W. Götz, N.M. Johnson, D.P. Bour, Appl. Phys. Lett. (1996)

4. *Shallow dopants and the Role of Hydrogen in Epitaxial Layers of Gallium Nitride (GaN),* W. Götz, N.M. Johnson, D.P. Bour, C. Chen, H. Liu, C. Kuo, and W. Imler, Proceedings of the 189th Meeting of the Electrochemical Society, Los Angeles, CA, May 5 – 10, 1996

Submitted:

1. *Activation of Acceptors in Mg-doped GaN grown by metal organic chemical vapor deposition,* W. Götz, N.M. Johnson, J. Walker, D.B. Bour, and R.A. Street, Appl. Phys. Lett. **68** (5), 667 (1996)

We have studied the properties of various donor impurities in GaN, based on state-of-the-art first-principles calculations. We arrive at the following conclusions: (a) Carbon is unlikely to incorporate on the Gasite, where it would act as a donor; it prefers to incorporate on the N site, where it acts as an acceptor. (b) Silicon and oxygen are both shallow donors in GaN, and can be incorporated in high concentrations. The solubility of Si is limited by formation of Si_3N_4; the solubility of O is limited by formation of Ga_2O_3. We propose that incorporation of Si and O as unintentional impurities is responsible for the observed *n*-type conductivity as-grown GaN. (c) The dominant native defect in *n*-type GaN is the gallium vacancy. Its concentration is low enough not to cause significant compensation; we propose, however, that the gallium vacancy is responsible for the infamous "yellow luminescence."

Distribution authorized to U.S. Government agencies only to protect information not owned by the U.S. Government and protected by a contractor's "limited rights" statement, or received with the understanding that it not be routinely transmitted outside the U.S. Government. Other requests for this document shall be referred to ARPA Security and Intelligence Office.

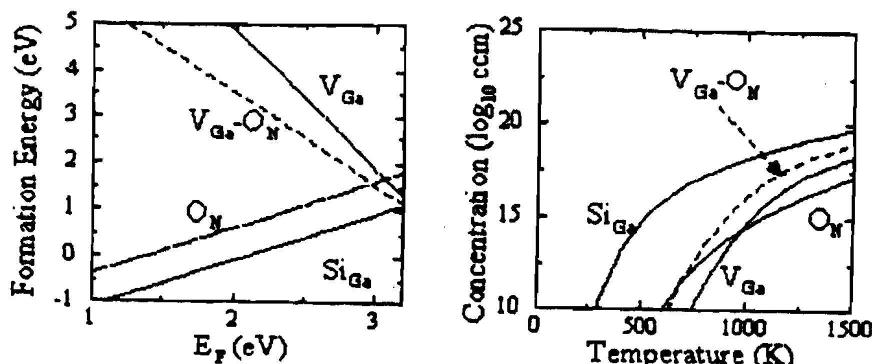

Figure 8: Formation energy vs. Fermi energy and equilibrium concentrations vs. temperature for donor impurities and native defects in GaN. Si and O can be incorporated in high concentrations. The concentration of the gallium vacancy is enhanced by formation of a complex with the oxygen donor.

Published:

1. "Hydrogen in GaN: Novel aspects of a common impurity", J. Neugebauer and C.G. Van de Walle, Phys. Rev. Lett. **75**, 4452 (1995).

2. "Role of hydrogen in doping of GaN", J. Neugebauer and C.G. Van de Walle, Appl. Phys. Lett. **68**, 1829 (1996).

Submitted:

1. Gallium vacancies and yellow luminescence in GaN", J. Neugebauer and C.G. Van de Walle (Applied Physics Letters).

At the University of Texas at Austin studies of H passivation in nitride films have been initiated. We have begun to study the incorporation of H in GaN in the new EMCORE D125 reactor. Parameters for the growth of the buffer layer and the high-temperature layer have been varied. Samples are being grown under a variety of conditions and will be sent to HP for characterization and then to Xerox for further analysis.

At the University of Texas at Austin, doping has been demonstrated for p- and n-type GaN in D system. We have grown n-type films using SiH_4 as a dopant source and have established growth conditions for n-type films with n~1E17 to 2E19 cm^{-3} concentrations. P-type doing studies using Mg as an acceptor atom are underway at time. We have not yet demonstrated good activation of Mg acceptors. Mg-doped GaN films have low

Distribution authorized to U.S. Government agencies only to protect information not owned by the U.S. Government and protected by a contractor's "limited rights" statement, or received with the understanding that it not be routinely transmitted outside the U.S. Government. Other requests for this document shall be referred to ARPA Security and Intelligence Office.

conductivities and the doping concentrations are not measurable but are believed to be p-type from thermal probe tests.

Milestone #15, Milestone Complete

- **Milestone #15:** Development of GaN films on single crystalline ZnO substrates. Deliver GaN samples for Consortium growth and characterization. Deliver 1 cm scale GaN single crystal substrates to Consortium for evaluation.

- **Summary:**

During this quarter GaN films were grown both on bare and ZnO coated (0001) sapphire substrates by the VPE method at growth rates varying from 20-100 μm/hour. Conditions and luminescence properties are similar to those produced by MBE and MOCVD.

A large number of thick (20-150μm) GaN samples were grown on bare (0001) sapphire substrates in order to optimize the deposition parameter space. The deposition rates were varied from 20-100 μm/hour by adjusting the flow rate of HCl. The films were characterized by studying their surface morphology and cross-sectional views using SEM, their structure using XRD and their electronic properties by room temperature and low temperature (77K) photoluminescence spectroscopy. The optimized films show XRD curves of ~9 min., a substantial improvement over last quarter's 17 min. figure and have featureless, smooth surfaces.

ZnO films were grown on sapphire substrates by sputtering either from a ZnO target or a Zn target. Films grown at above 300° C were found to be crystalline with their (0001) axis perpendicular to the substrate. The surface morphology of these films is relatively smooth. GaN films (about 10 μm thick) grown on a ZnO-coated (0001) sapphire substrate show very dense cross-sectional views but rather rough surface morphology.

Conclusions:

Films grown directly on (0001) sapphire by the VPE method were found to have smooth surface morphologies if the growth rate is less than 50 μm/hour. ZnO thin films with good crystallinity and surface morphology were grown on (0001) sapphire by reactively sputtering either from ZnO or Zn targets. GaN films were grown on such substrates and show dense cross sectional view but rougher surfaces.

References:

1. T.D. Moustakas, *Mat. Res. Soc. Proc.* vol. 395 (1996).

Distribution authorized to U.S. Government agencies only to protect information not owned by the U.S. Government and protected by a contractor's "limited rights" statement, or received with the understanding that it not be routinely transmitted outside the U.S. Government. Other requests for this document shall be referred to ARPA Security and Intelligence Office.

AXT

Two (2) samples and micrographs delivered to AXT by HPRC. AXT has delivered these samples, of maximum dimension of 5-6 mm to XEROX-PARC.

Four (4) 5 mm-scale platelet substrates were delivered to XEROX-PARC for characterization and epitaxial growth. XEROX polished both sides of two samples and grew MOCVD epitaxy on both faces. The epitaxial quality was very good and the results were reported in a paper at the Boston MRS fall meeting. TEM measurements did not locate any dislocation defects on the good side (Ga side) of the crystals thus placing the upper limit of the dislocation defect density at less than $10^6/cm^2$. This is about two orders of magnitude lower than the lower limit of the best GaN epitaxy on SiC. On the poor side (N side) a high density ($10^8/cm^{-2}$) of dislocation loops apparently originating at gallium inclusions was seen. The PL and CL show that the quality of the MOCVD films is better than films grown on sapphire or SiC. The FWHM of the lines was <2meV.

A variety of processing errors with the remaining two crystals resulted in structures of poor quality. After review with Xerox of the procedures to be used in processing the GaN crystals AXT has supplied a fifth (5) 5 mm-scale crystals to Xerox for structure growth.

Xerox has demonstrated that their polishing process which was developed for polishing facets for structures gown on sapphire works well for polishing the single crystal GaN substrates from Poland. AXT has also been exploring the polishing of GaN using loose diamond slurry. We are currently exploring the effects of changing grit size, lap properties, pressure and speed on obtaining a growth-ready surface on GaN; however, this process is not ready for preparing the crystals for epitaxial growth.

HPRC has installed a 20 mm diameter crucible. This is scaled up from their mm crucible. Currently they are in the process of optimizing growth in this larger crucible. Since the size of the crystals is limited by the scale size of the crucible, it should be possible to grow 1.5 to 2 cm scale crystals. Also, HPRC has received a 60 mm diameter high pressure furnace. This will be able to hold 30-35 mm diameter crucibles which is projected to permit the growth of 2-2.5 cm scale crystals. This work would be completed in Phase II.

Since the size of the crystals is limited by the scale size of the crucible, it should be possible to grow 1.5 to 2 cm scale crystals. Also, HPRC has received a 60 mm diameter high pressure furnace. This will be able to hold 30-35 mm diameter crucibles which is projected to permit the growth of 2-2.5 cm scale crystals. This work would be completed in Phase II.

During the course of this program, HPRC has shown dramatic improvement in the quality of the GaN single crystals. The first crystals which were delivered to us were 2

Distribution authorized to U.S. Government agencies only to protect information not owned by the U.S. Government and protected by a contractor's "limited rights" statement, or received with the understanding that it not be routinely transmitted outside the U.S. Government. Other requests for this document shall be referred to ARPA Security and Intelligence Office.

MM scale and dark brown, almost opaque. The next lot of 5 mm scale crystals were a clear yellow to orange color and much better in appearance. The 1 cm scale crystals are almost colorless and transparent. When AXT visited HPRC last October, we were shown 5 mm scale crystals which were completely colorless and transparent. HPRC believes that the large crucibles will permit the transfer of this quality to proportionately larger crystals.

HPRC has completed the crystal deliverables for this program. They will prepare a plan for Phase II during which we expect to obtain crystals of 2-2.5 cm size. In the meantime, HPRC is proceeding with their optimization of the larger crucibles. During Phase I, HPRC met all of the program objectives ahead of schedule and has shown excellent progress.

We believe that a demonstration of a III-Nitride laser on a homosubstrate is important for the success of our program as well as a key accomplishment for the Blue Band Consortium.

We are continuing with the polishing studies. Initially, we are looking at purely mechanical polishing processes with various diamond grits in a loose slurry. One of the difficulties in polishing the small samples is that the Ga side grows slowly and the N side appears to grow more rapidly. Excessive polishing of the Ga side can lead to breaking into the poor morphology of the N side. The crystals also grow with stepped layers. If the surface alignment of the crystals is not carefully maintained the resulting surface can be badly misoriented. Epitaxial growth at Xerox demonstrated that badly misoriented surfaces nucleate hexagonal structures and the morphology is poor. Since the crystals are still quite small, care needs to be taken when mounting the crystals onto the polishing fixture to ensure that they are properly aligned.

ATMI

a. Technical Objectives for this Period

Grow, characterize and deliver GaN samples for consortium growth and characterization.

b. Work Carried Out

Out objectives for this period were to improve the surface morphology and film uniformity of GaN and deliver GaN samples to the consortium members for evaluation.

The surface morphology of GaN layers has been improved as compared to previous GaN layers grown by HVPE. A Normarski interference contrast microscope image, at 255x, of the surface of a GaN layer grown by HVPE on (0001) sapphire shows only slight texturing. The surface is smooth and specular to the eye.

Distribution authorized to U.S. Government agencies only to protect information not owned by the U.S. Government and protected by a contractor's "limited rights" statement, or received with the understanding that it not be routinely transmitted outside the U.S. Government. Other requests for this document shall be referred to ARPA Security and Intelligence Office.

The electrical characteristics of the GaN layers have been measured. Room temperature Hall effect measurements determined the layers to be n-type as grown with a background carrier concentration of 1^{18} cm^{-3} and mobility of 90 cm^2/V-s.

The uniformity of the GaN on sapphire samples has not been optimized. At present, the variation in thickness across a 2 inch wafer, shown in figure 9, varies by approximately 50%. We are confident that changes we are planning in the system configuration and growth conditions will further improve the thickness uniformity. Note that the average growth rate by this technique is greater than 100 µm/hr for high quality GaN.

The uniformity of structural quality was also measured. In figure 10, the FWHM of double crystal x-ray rocking curves taken across a 2 inch wafer is plotted on a contour map. A large part of the film is very uniform, but there is as much as a 30% increase in FWHM as you approach the edge of the wafer.

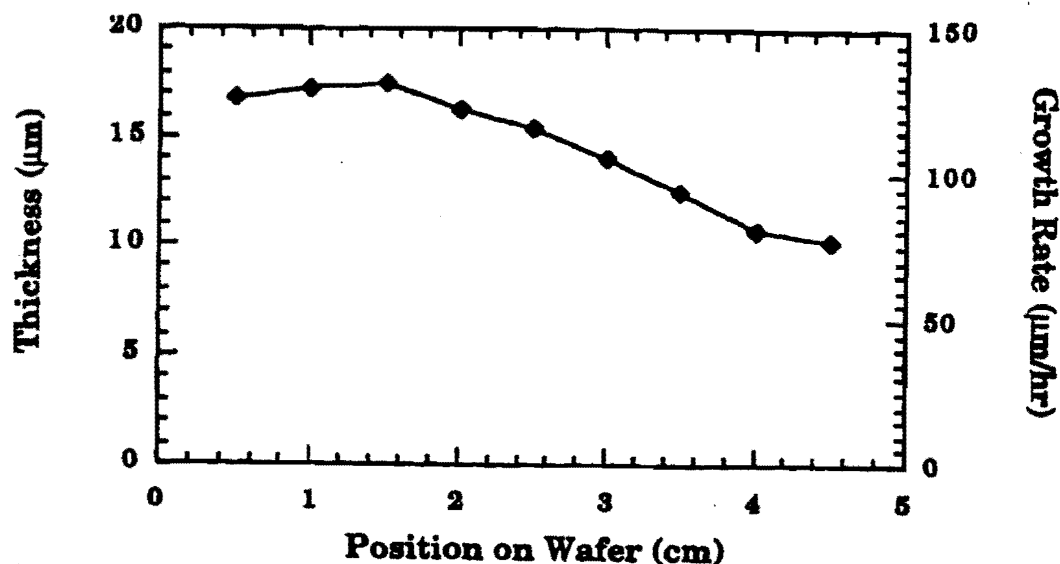

Figure 9. GaN film thickness and growth rate across a 2 inch wafer of GaN grown on (0001) sapphire by HVPE.

Distribution authorized to U.S. Government agencies only to protect information not owned by the U.S. Government and protected by a contractor's "limited rights" statement, or received with the understanding that it not be routinely transmitted outside the U.S. Government. Other requests for this document shall be referred to ARPA Security and Intelligence Office.

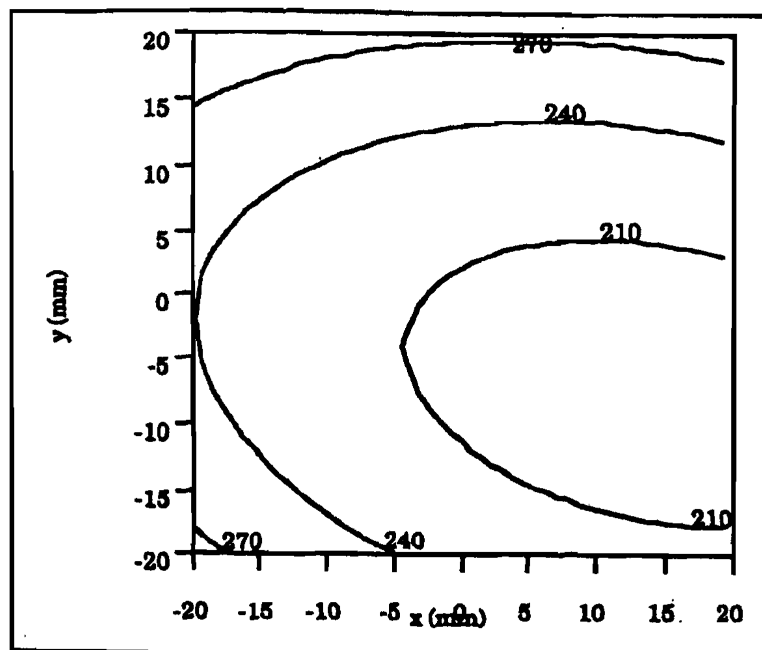

Figure 10. Contour map of the FWHM of double crystal x-ray rocking curve across a 2 inch wafer of GaN grown on (0001) sapphire by HVPE.

Accompanying this report is one 2 inch wafer of GaN (-10 µm thick) on (0001) sapphire grown by HVPE. The surface morphology and DCXRC map for this sample is shown in figures 1 and 3 above. A small piece (several mm across and -20 µm thick) of free standing GaN is also being delivered at this time. Additional samples on sapphire will follow soon.

c. Plans for Forthcoming Reporting Period

A suitable baseline for GaN growth by HVPE has now been established and will be extended to growth of GaN on the growth template. In the next reporting period, we will develop a plan for the second year of this program.

Distribution authorized to U.S. Government agencies only to protect information not owned by the U.S. Government and protected by a contractor's "limited rights" statement, or received with the understanding that it not be routinely transmitted outside the U.S. Government. Other requests for this document shall be referred to ARPA Security and Intelligence Office.

Milestone 16, Milestone Complete

- **Milestone 16:** First LED chip configuration and processing designed. N- and p-type GaN film etching.

Several different chip configurations and LED fabrication processes have been investigated. The two-mask EV process is used for daily routine processing of device structures, and was used to fabricate the LED samples delivered to Anis in February. Mesa structures have been patterned in both n- and p-type GaN using RIE: the n-type material was found to etch more slowly than p-type as shown in Fig. 11.

Distribution authorized to U.S. Government agencies only to protect information not owned by the U.S. Government and protected by a contractor's "limited rights" statement, or received with the understanding that it not be routinely transmitted outside the U.S. Government. Other requests for this document shall be referred to ARPA Security and Intelligence Office.

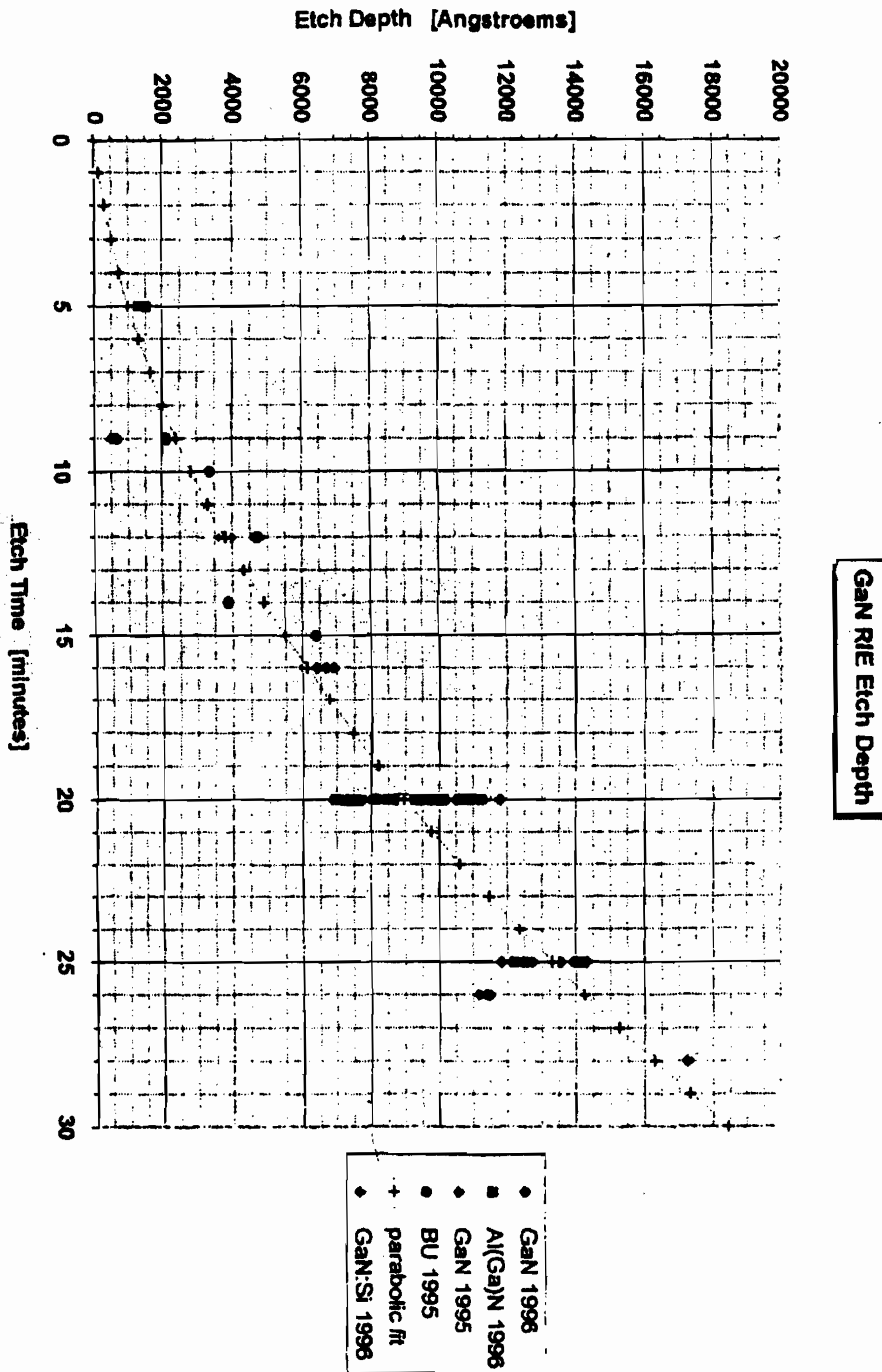

Figure 11: GaN RIE Etch Depth

Distribution authorized to U.S. Government agencies only to protect information not owned by the U.S. Government and protected by a contractor's "limited rights" statement, or received with the understanding that it not be routinely transmitted outside the U.S. Government. Other requests for this document shall be referred to ARPA Security and Intelligence Office.

BLUE BAND

Blue Light and Ultra-Violet Emitters, the Bay Area Nitride Consortium

Report for Month 12

Contract: MDA972-95-3-0008

DISTRIBUTION: SDL, HP, Xerox, AXT, ATM, Boston University, the University of Texas at Austin, D. Scifres, J. Endriz, R. Craig, J. Johnson, and R&D

To: Distribution
From: Jo S. Major
Date: 8.14.96

Distribution authorized to U.S. Government agencies only to protect information not owned by the U.S. Government and protected by a contractor's "limited rights" statement, or received with the understanding that it not be routinely transmitted outside the U.S. Government. Other requests for this document shall be referred to ARPA Security and Intelligence Office.

Overview:

The BlueBand program is changing focus from materials-related issues to increasingly device related milestones. In the first year of the program, basic materials issues such as n- and p-type doping, AlGaN and InGaN growth, native defect behavior, basic crystallography have been addressed. Homojunction, heterostructure and quantum well diodes have been constructed. At the point of writing of this report, HP has demonstrated a blue LED with ~70% of the optical intensity of the Nichia quantum well device.

In the coming year, the milestones, particularly of HP and SDL, become increasingly device driven. Upcoming milestones of this type include high-brightness LEDs, single mode waveguides, facet construction and the achievement of a pulsed injection laser in the nitrides.

The consortium met during this quarter and decided the issue of substrate vendor downselect. Based upon both technical and financial reasoning, the BlueBand consortium has decided to continue into the second year with ATMI as the continuing substrate vendor.

Summary: Milestones 17 through 21 are completed.

Milestone #17

Microstructure of undoped and highly doped GaN epilayers

The microstructure of highly doped GaN layers grown epitaxially by MOCVD at Xerox PARC has been characterized using transmission electron microscopy. High purity GaN was used as reference. In all cases, a columnar structure is evident, with column diameters between 0.2 and 1.0 mm. The characteristics of the columnar structure are reflected in the x-ray diffraction rocking curves (XRRC). A distribution of tilt of the c-axis of ~5 arcmin and a distribution in the rotation of the c-axis of ~8 arcmin is characteristic of some high quality materials. The addition of silicon for medium level carrier concentrations

(mid $10^{17}cm^{-3}$) does not seem to affect the columnar structure. Higher carrier concentration (about 10^{19} cm^{-3}) produces significant changes in the XRRCs and in the measured lattice parameter (cf work by Brent Krusor on HP samples). Similarly, the addition of magnesium does not affect significantly the microstructure for low/medium doping levels. Energy dispersive x-ray analysis supports the concept of Mg_3N_2 precipitates for Mg concentrations above 10^{19} cm^{-3}. The nature of dislocations does not appear to change noticeably when crossing a p-n junction between highly doped materials. This has been observed in Nichia LEDs as well as in a number of other samples. A few differences are observed with the use of other complementary techniques.

(a) Undoped GaN: The columnar structure of high purity material is easily observed with cathodoluminescence (CL). The near bandedge emission appears to be associated with the center of the column, and the yellow-region with dislocated regions [1]. Dislocations have burgers vectors of **a**, **a+c** and **c** [2]. Nanotubes and inversion domains have been identified in certain regions of the sample. Most of the nanopipes are associated with screw dislocations with a burgers vector of **c** [3]. One issue which is very stimulating is that the lattice of GaN/sapphire seems to be fully relaxed from the thermal stresses expected from this system. Lattice parameter measurements indicate that for device quality materials there is very little difference between bulk and heteroepitaxial lattice parameters. We have proposed a model for the relaxation of the thermal stresses based on the dislocation geometry [4].

(b) Highly Si- and Mg-doped films: The CL is uniform spatially for high-luminescence wavelengths. The disappearance of the columnar structure (in the CL images, but not in the TEM images) is intriguing. We have found that Raman scattering can be used to image the spatial variation of donors in the material, and images of donor distribution in hexagonal hillocks have been obtained [5]. As grown Mg-doped films give a particular Raman signal at 519 cm^{-1} which vanished after the thermal anneals used for acceptor activation [6]. We are in the process of establishing the connection between CL, Raman, and the microstructure. We need to be able to quantify the strain associated with dislocations. We suspect that dislocations getter some of the dopants and as a result of dopant reaction with the core the dislocation strain is relaxed.

References:

[1] F. A. Ponce, D. P. Bour, W. Goetz, P. J. Wright, Appl. Phys. Lett. **68**, 57 (1996).

[2] F. A. Ponce, D. Cherns, W. Young, and J. W. Steeds, Appl. Phys. Lett. 69 (6) in press (1996).

[3] F. A. Ponce, D. Cherns, W. Young, and J. W. Steeds, and S. Nakamura, submitted to Appl. Phys. Lett.

[4] F. A. Ponce, B. S. Krusor, F. Ross, and S. Nakamura, 1st Europ. Workshop on GaN. To be published.

[5] F. A. Ponce, J. W. Steeds, C. Dyer, and D. Pitt, submitted to Appl. Phys. Lett.

[6] F. A. Ponce, J. W. Steeds, C. Dyer, D. Pitt, and S. Nakamura, submitted to Appl. Phys. Lett.

Milestone #18

Heterojunction growth for fundamental bandoffset studies.

UT Austin has successfully grown InGaN/GaN and AlGaN/GaN heterojunctions and samples are being studied using low-temperature PL and will be supplied to the Consortium members for further study.

Milestone #19

Fabrication of p/n AlGaN/GaN heterojunction. Turn-on voltage goal specification is less than 4.4 V.

An $Al_{0.08}Ga_{0.92}N$/GaN heterojunction was grown which showed diode behavior similar to the GaN/GaN homojunctions that we have produced. I-V and L-I curves for both junction types are shown in Figures 1 and 2. Light output for the heterojunction device is one-third that of the homojunction device. V characteristics are nearly identical, with a 20 mA Vf of 7.6 to 7.7 volts. Peak wavelength is 471 nm for the $Al_{0.08}Ga_{0.92}N$/GaN device and 465.4 nm for the GaN/GaN device. The forward voltage is greatly improved to a value of 4.4 volts by increasing the Mg concentration in the p-GaN layer, facilitating ohmic contact formation. UT Austin has recently achieved p-type doping and has now demonstrated a working p-n GaN homojunction. This LED is now under characterization.

Electrical characterization of p-n homojunctions

The ability to dope GaN n- and p-type by employing Si as a donor and Mg as an acceptor leads to the fabrication of p-n$^+$ junction devices. The diodes were grown on sapphire substrates and the p and n$^+$ layers were ~5 μm and 0.56 μm thick, respectively. The acceptors were activated with a standard postgrowth furnace anneal. Reactive ion etching was employed to fabricate mesa structures with a diameter of 0.5 mm. Ohmic metal

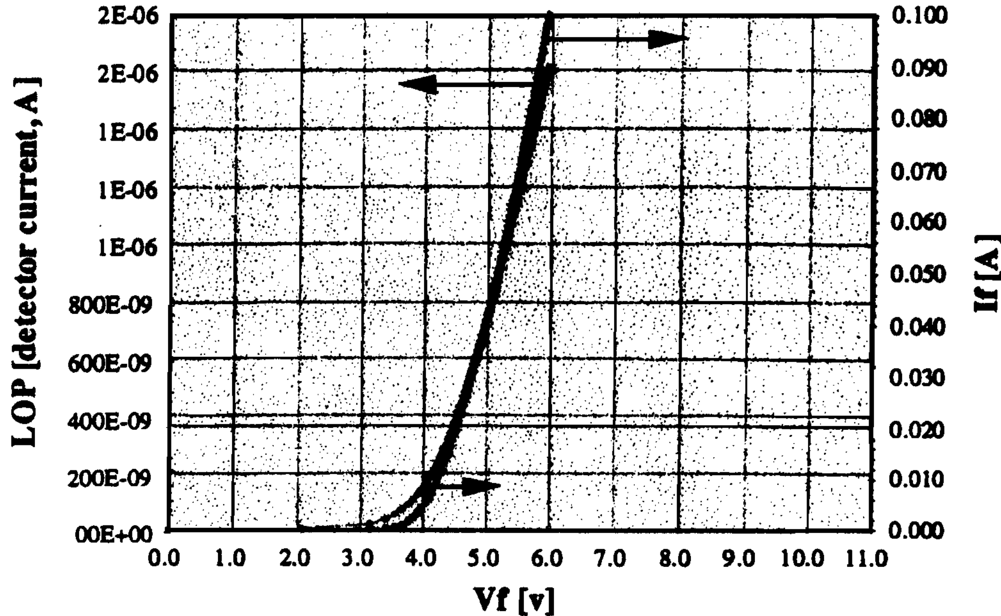

An AlGaN/GaN heterojunction LED. The turn-on voltage is 4 volts with the 20 mA operating current reached at a voltage of 4.4 volts.

contacts were deposited on the n$^+$ and p-layers. The performance of the diodes was tested with current-voltage (I-V) and capacitance-voltage (C-V) measurements. Results are shown below.

The analysis of the C-V data reveals an effective acceptor concentration (NA-ND) of ~2×1018 cm-3 uniformly distributed over the depth of the capacitance measurement. In the case of acceptors in Mg-doped GaN the C-V measurement determines the acceptor concentration (minus the concentration of donors) rather than the hole concentration. The I-V characteristic of a representative diode is shown in the inset (above). The leakage current at a reverse bias of -4 V is -2.1 μA.

The diodes were utilized in deep level transient spectroscopy (DLTS) measurements to

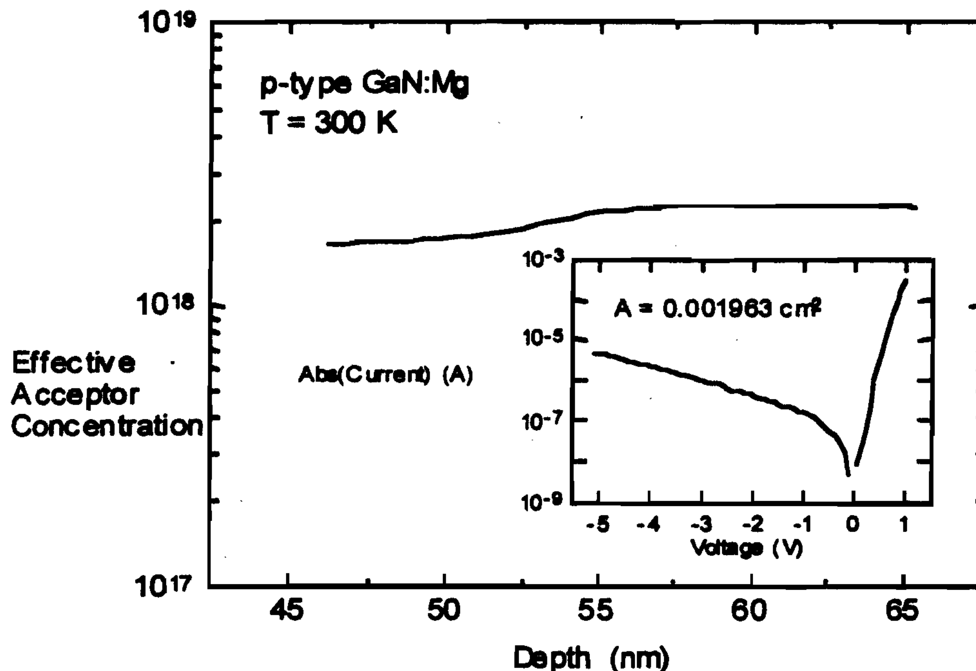

Effective acceptor concentration vs. depth of the depletion region for p-type, Mg-doped GaN. The inset shows the current through the p-n+ junction diode as a function of applied bias. Negative voltage corresponds to a reverse bias.

investigate deep level defects in p-type GaN for the first time. The diodes were well suited for these measurements which use a 1 MHz test-signal to measure the differential capacitance. The analysis of the DLTS data yielded deep levels with activation energies for hole emission to the valance band of (0.21 ± 0.03) eV (ET(DLP1)), (0.30 ± 0.11) eV (ET(DLP2)), and (0.45 ± 0.10) eV (ET(DLP3)). The concentrations of the deep levels (NT) were found to be (3.9 ± 2.3)×1014 cm-3 (NT(DLP1)), (5.0 ± 2.0)×1014 cm-3 (NT(DLP2)), and (8.6 ± 1.4)×1014 cm-3 (NT(DLP3)).

The identification of deep levels in GaN and the ability to control their concentrations are important issues for the fabrication of light emitters with III-V nitrides since deep level

defects may act as efficient recombination centers and influence the efficiency of LEDs or the threshold power for injection lasers.

Publications submitted:

1 *A donor-like deep level defect in $Al_{0.12}Ga_{0.88}N$ characterized by capacitance transient spectroscopies*

W, Götz, N.M. Johnson, M.D. Bremser, and R.F. Davis, Appl. Phys. Lett. (1996)

2 *Activation of acceptors in Mg-doped, p-type GaN*

W. Götz, N.M. Johnson, J. Walker, D.P. Bour

Symposium E of the 1996 Spring Meeting of the Materials Research Society, April 8-12,

1996, San Francisco, CA

Publications appeared:

1 *Activation Energies of Si Donors in GaN*

W, Götz, N.M. Johnson, C. Chen, H. Liu, C. Kuo, and W. Imler, Appl. Phys. Lett. **68**, 3144 (1996)

2 *Deep level defects in Mg-doped, p-type GaN grown by metalorganic chemical vapor deposition*

W, Götz, N.M. Johnson, and D.P. Bour, Appl. Phys. Lett. **68**, 3470 (1996)

Milestone #20

Substrates: Evaluate SiC vs. Al_2O_3, MBE growth of GaN films on M-plane sapphire, program plans for AXT and ATMI.

All companies within the consortium have grown on SiC, along with the more common C-plane sapphire. At present the consortium members are not planning to put significant emphasis on SiC, due primarily to the high cost of SiC substrates. Growth on micropipe-free SiC is more forgiving to process variations, however, no significant performance advantage in terms of mobility, diode performance, etc., has been found.

GaN films were grown by the MBE method on the M-plane (1010) of sapphire, with or without a low temperature buffer. The structure and the opto-electronic properties of these films are summarized as follows.

A. <u>Films grown without a low temperature buffer.</u>

The only cleaning procedure of the substrates was heating in molecular hydrogen to 700°C. Films approximately 1μm thick were grown at this temperature and doped with the Si-cell at 1375°C.

- SEM examination reveals relatively smooth surface morphology but with micropores about 1000Å in diameter.
- XRD examination reveals two reflections, a strong one with Miller indices (1122) and a weaker one with Miller indices (1010).
- Hall effect measurements show that the material is heavily doped with carrier concentration 3-4 x 10^{18} cm^{-3}, electron mobility $60cm^2$ /V-sec and resistivity 3 x10^{-2} ohm-cm.
- Photoluminescence measurements with a 10mW He-Cd laser show a strong luminescence across the gap (365nm) with no observable yellow luminescence.

B. Films grown with a low temperature buffer.

In this series of films the substrate was first nitridated at 750°C, then cooled to 500°C for the growth of a 250Å thick GaN buffer and heated to 750°C for the growth of about 1μm thick film. The temperature of the Si-cell was at 1350°C.

- SEM examination reveals very smooth surface morphology.
- XRD examination reveals again two reflections with indices (1122) and (1010) as in the previous case.
- Conductivity measurements show that the material has a resistivity 130 ohms, which is 4.3 x 10^3 times larger than the resistivity of the samples grown without a buffer.
- Photoluminescence measurements show a sharp photoluminescence peak at room temperature (FWHM = 79meV) occurring at 365nm. The intensity is one order of magnitude weaker than in the previous sample. These samples do not show yellow luminescence as well.

Conclusions:

The main conclusions from this study can be summarized as follows:

1. The low temperature buffer promotes two dimensional growth leading to smoother surface morphologies. This result is similar to growth on the c-plane.

2. The investigated conditions lead to the growth of (1122) and (1010) planes. However, these planes are not well matched to the M-plane sapphire. The plane we want is the (1013), in which the mismatch with the sapphire (1010) lattice in he two perpendicular axes is the minimum. (The mismatch is 2.6% in GaN [1210]/sapphire [0001] direction and 1.9% in GaN [3031]/sapphire [2110] direction). Further work is required to identify conditions for the epitaxial growth of the (1013) plane.

3. The films without a low temperature buffer dope far more efficiently with silicon than the films with the buffer. The evidence suggests that the films with the buffer are more strained and this probably affects the incorporation of silicon in the sites.

4. The photoluminescence intensity is reduced as the carrier concentration is reduced. However, no yellow luminescence is observed even at low doping levels. This is generally opposite to GaN on the c-plane which shows yellow luminescence at low doping levels.

AXT and HPRC have made dramatic progress in crystal growth. The most recent crystals are nearly 1 cm in scale (~8 mm by ~ 8 mm). They are quite clear and have smooth surfaces. Since the beginning of the program, the crystal area has been scaled up by a factor of two every three to four months. At the current rate of development, the crystals will reach 2-2.5 cm diameter in approximately 12 months. MBE epitaxial growth at the University of Ulm shows the narrowest exciton lines for any GaN material. The FWHM of the lines is on the order of 0.5 meV. In addition, exciton lifetime studies at HPRC show that the lifetime of the GaN on GaN epitaxy is an order of magnitude greater than that of GaN on sapphire. This is a clear indication of the superior quality of the GaN on GaN epitaxial films.

A reactor design was carried out for the growth of 2-2.5 cm scale crystals. This design shows that the reactor for manufacturing commercializable substrates comparable to that for other crystal growth systems. The estimated cost, if built in Poland, is competitive with other technologies.

The polishing tests resulted in about a 6 Å RMS surface finish. This is still not as good as shown by XEROX and further refinement of the technique is required.

Future Plans

AXT participated in the downselect meeting hosted by HP on 13 June 1996. The Blue Band Consortium decided against continuing support of bulk crystal development. Given the high quality of the epitaxy which has been demonstrated by the Blue Band and others on GaN substrates, AXT expects that a true UV or blue laser will be demonstrated

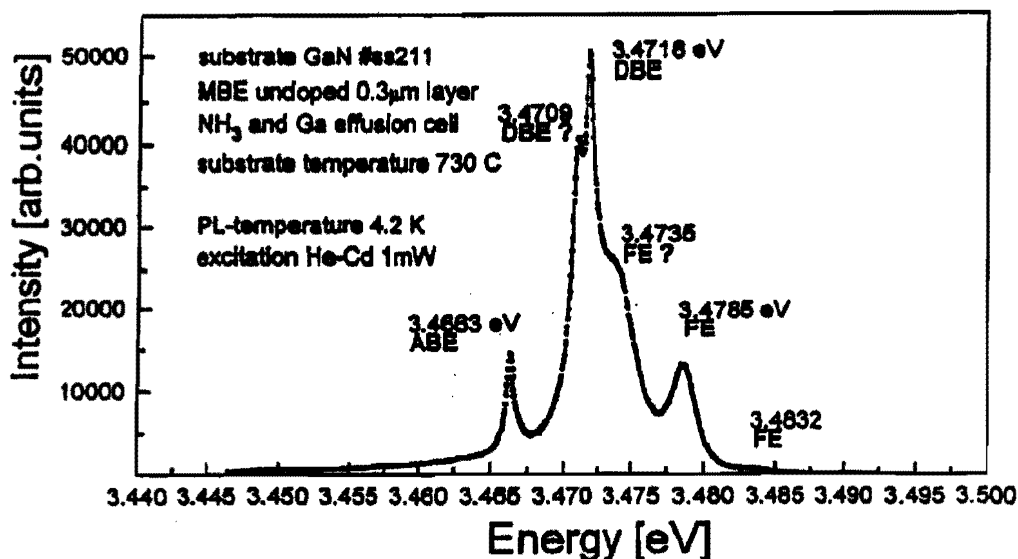

The low temperature PL of a GaN film, grown by MBE, on a GaN substrate.

successfully on the GaN substrates.

ATMI:

During this work period, we have further improved the uniformity and quality of GaN grown on sapphire by HVPE. In addition, we directly addressed the components needed to make free-standing GaN, namely:

- Improved the quality of GaN on the template substrate by HVPE
- Reconfigured the HVPE reactor to allow for backside template etching
- Demonstrated Si template etching at large etch rates

Several samples have been delivered to the Consortium for epi-layer growth and characterization:

- 3- 2" wafers of GaN grown on Sapphire
- A small piece of free-standing GaN

- GaN grown on the template substrate

Plans for Second Year:

We have demonstrated all the components needed to make GaN substrates by the method which we proposed in this program. These will be combined to remove the silicon template from crack-free GaN on silicon to produce free-standing GaN substrates. In addition, there is potential for other removable template materials which could act as a substrate for GaN growth. Among the candidates which are of interest are:

- Lithium Gallium Oxide (LGO)
- Lithium Aluminum Oxide (LAO)
- Zinc Oxide

Finally ATMI has worked at predicting the wafer cost for a 2" GaN wafer grown via HVPE. The cost curve is $1500 @ 100 wafers/month (w/m), $400 @ 1000 w/m, and $250 @ 10000 w/m.

Milestone #21

GaN LED Demonstration

Materials and modeling parameters that critically influence LED operation

Numerical device simulations can greatly aid the optimization of LED (as well as laser diode) structures. The ability to perform such simulations is currently hampered by incomplete knowledge of a number of basic materials parameters in the nitrides. We have surveyed the literature to obtain state-of-the-art values for the key parameters, and identify areas where first-principles calculations can provide new or more accurate information. Here we focus on parameters describing the band structure of the component materials.

For ternary alloys, linear interpolation between the values for the constituent binary compounds often provides adequate parameter values. However, some parameters exhibit nonlinear behavior as a function of alloy composition. The prime example is the bowing of the band gap. Our first-principles calculations have produced values of b=0.5 for AlGaN and b=1.0 for InGaN; these results are very close to those obtained by A. F. Wright and J. S. Nelson [Appl. Phys. Lett. **66**, 3051 (1995)]. It is expected that refractive indices will also exhibit a nonlinear dependence on composition.

The band structure of the component materials is not only a function of alloy composition, but also of strain induced by lattice mismatch. The effect of strain on the band structure can be described in terms of deformation potentials. We have calculated the following values (in eV, Pikus-Bir notation):

	AlN	GaN	InN
a (hydrostatic)	-9.1	-8.0	-5.0
b (100 strain)	-1.5	-1.7	-1.2
d (111 strain)	-4.5	-4.2	-3.0

Finally, we point out that heterojunction band offsets may be the most crucial parameters determining optoelectronic device behavior. Measured values of band offsets in the nitride system exhibit a great deal of scatter right now, which is at least in part due to improper inclusion of the effects of strain. First-principles calculations of the band lineups, including strain effects, are in progress.

Published:

"Defects, impurities and doping levels in wide-band-gap semiconductors", C. G. Van de Walle and J. Neugebauer, Braz. J. Phys. **25**, 163 (1996).

"Native defects and impurities in GaN", J. Neugebauer and C. G. Van de Walle, Festkörperprobleme/Advances in Solid State Physics **35**, 163 (1996).

Accepted for publication:

"Gallium vacancies and the yellow luminescence in GaN", J. Neugebauer and C. G. Van de Walle (Applied Physics Letters, July 22 1996).

Submitted:

"Role of hydrogen and hydrogen complexes in doping of GaN", J. Neugebauer and C. G. Van de Walle, MRS Symposia Proceedings Vol. 423 (MRS, Pittsburgh, PA).

BLUE BAND

Blue Light and Ultra-Violet Emitters, the Bay Area Nitride Consortium
Report for Month 15
Contract: MDA972-95-3-0008

DISTRIBUTION: SDL, HP, Xerox, ATM, Boston University, the University of Texas at Austin, D. Scifres, J. Endriz, R. Craig, J. Johnson, and R&D

To: Distribution
From: Jo S. Major
Date: 11.07.96

Distribution authorized to U.S. Government agencies only to protect information not owned by the U.S. Government and protected by a contractor's "limited rights" statement, or received with the understanding that it not be routinely transmitted outside the U.S. Government. Other requests for this document shall be referred to ARPA Security and Intelligence Office.

Overview:

Device-related work is now the focus of BlueBand. Topics discussed within this report include the fabrication of facets, wire-bonding to LED chips, and the scaling of the ATMI's growth machinery to accommodate 2" wafers.
Materials studies include TEM characterization of heterostructures, modeling of bandstructure offsets, and a DLTS study of defect states.
Upcoming milestones include high-brightness LEDs, single mode waveguides, and the achievement of a pulsed injection laser in the nitrides.
The consortium presented results in Florida for the semi-annual DARPA review.

Summary: Milestones 22 through 26 are completed.

Milestone #22

Structural characterization of AlGaN/GaN heterojunctions. InGaN film growth demonstrated. InGaN/GaN structures delivered to Xerox for study. Theoretically investigate the band offsets of the AlGaInN material system.

Structural Characterization of AlGaN/GaN Heterojunctions

AlGaN/GaN heterojunctions are used for cladding layers in light emitting diodes and in diode lasers. Unlike the arsenides, the materials parameters of these nitrides vary significantly with the group III composition. In the extreme case of AlN/GaN, the lattice mismatch of 2.4% requires a critical thickness for plastic relaxation of about 3 to 10nm (depending of the model used); and the thermal expansion difference is equivalent to up to 0.15% of lattice mismatch when cooling from the growth temperature. It is important to understand the mechanism of relaxation of the stress associated with the lattice mismatch in this system. We have performed microscopy on samples containing heterojunctions with various Al contents. We have successfully imaged misfit dislocations at interfaces containing Al-Ga variations ≥50%. Fig. 1 shows a misfit dislocation at the $AlN/Al_{0.5}Ga_{0.5}N$ interface corresponding to a lattice mismatch of 1.19%. An extra atomic plane on the top half of the sample compensates for the difference in lattice spacings of the two materials. These misfit dislocations have a Burgers vector of magnitude $1/3[1\bar{2}10]$ corresponding to displacements on the basal plane. The separation of misfit dislocations is about 23nm.

AlGaN/GaN heterojunctions are used for cladding layers in light emitting diodes and in diode lasers. Unlike the arsenides, the materials parameters of these nitrides vary significantly with the group III composition. In the extreme case of AlN/GaN, the lattice mismatch of 2.4% requires a critical thickness for plastic relaxation of about 3 to 10nm (depending of the model used); and the thermal expansion difference is equivalent to up to 0.15% of lattice mismatch when cooling from the growth temperature. It is important to understand the mechanism of relaxation of the stress associated with the lattice mismatch in this system. We have performed microscopy on samples containing heterojunctions with various Al contents. We have successfully imaged misfit dislocations at interfaces containing Al-Ga variations ≥50%. Fig. 1 shows a misfit dislocation at the $AlN/Al_{0.5}Ga_{0.5}N$ interface corresponding to a lattice mismatch of 1.19%. An extra atomic plane on the top half of the sample compensates for the difference in lattice spacings of the two materials. These misfit dislocations have a Burgers vector of magnitude $1/3[1\bar{2}10]$ corresponding to displacements on the basal plane. The separation of misfit dislocations is about 23nm.

For lower compositional variations, the expected dislocation separation rapidly increases, exceeding 0.1mm for 10%, and 0.4 mm for 1%. In addition, the critical thickness for plastic relaxation (introduction of misfit dislocations) also increases rapidly, greater than 20nm and 0.2 mm for 50% and 10% variation of Al content, respectively. These separations are comparable to those observed in the dislocation network resulting from the columnar structure of these materials, with lateral dimensions ranging from 0.2 mm to 0.5 mm. Using the model of a low-angle tilt domain structure, and the critical thickness model of People and Bean, it is believed that for compositional variations of less than 50%, the critical thickness and the misfit dislocation separation will exceed the average lateral dimensions of the columns, lattice mismatch strain will not be relieved inside the columns, and the long range strains will be relieved at the domain boundaries.

TEM observations of cladding layers with Al compositions of the order of 10% are consistent with these considerations: such interfaces do not exhibit dislocations nor stacking faults. This seems to be one of the beneficial features of the columnar nature of the III-V nitride thin films.

Fig. 1. Lattice image of a $AlN/Al_{0.5}Ga_{0.5}N$ interface showing misfit dislocation on the basal plane with Burgers vector $1/3[1\bar{2}10]$.

Publications submitted:

[1] *Direct imaging of impurity-induced Raman scattering in GaN*
F. A. Ponce, J. W. Steeds, C. Dyer, and D. Pitt, Appl. Phys. Lett. (in press).

[2] *Observation of nanopipes and inversion domains in high quality GaN epitaxial layers*
F. A. Ponce, D. Cherns, W. Young, and J. W. Steeds, and S. Nakamura, submitted to Appl. Phys. Lett. (1996).

[3] *Observation of coreless dislocations in GaN*
D. Cherns, W. T. Young, J. W. Steeds, F. A. Ponce, and S. Nakamura, Journal of Crystal Growth (1996)

[4] *Determination of the atomic structure of inversion domain boundaries in GaN by transmission electron microscopy*
D. Cherns, W. T. Young, M. Saunders, F. A. Ponce, and S. Nakamura, Philosophical Magazine (1996).

[5] *Microstructure of Epitaxial III-V Nitride Thin Films*
F. A. Ponce, Chapter 6, in "GaN and Related Materials, S. Pearton, Ed. (1996) in press.

Publications appeared:

[1] *Determination of lattice polarity for growth of GaN bulk single crystals and epitaxial layers*
F. A. Ponce, D. P. Bour, W. T. Young, M. Saunders, and J. W. Steeds, Appl. Phys. Lett. 69 (3), 337-339 (1996)

[2] *Characterization of dislocations in GaN by transmission electron diffraction and microscopy techniques*
F. A. Ponce, D. Cherns, W. Young, and J. W. Steeds, Appl. Phys. Lett. 69 (6), 770-772 (1996).

[3] *Transmission electron microscopy of the AlN-SiC interface*
F. A. Ponce, M. A. O'Keefe, E. C. Nelson, Phil. Mag. A 74 (3) 777-789 (1996).

InGaN film growth demonstrated. InGaN/GaN structures delivered to Xerox for study.

Numerous InGaN quantum well structures have been grown and characterized. The In composition in the wells has been varied to produce emission wavelengths from 420 to 540 nm using the test structure illustrated in Fig. 2

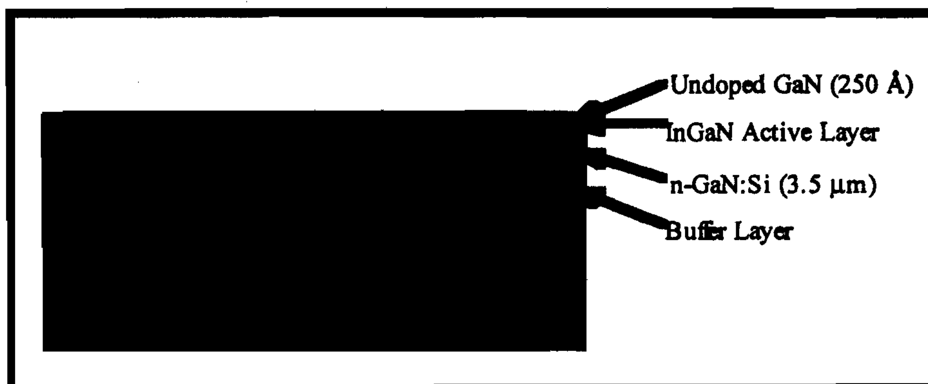

Fig. 2. InGaN quantum well test structure for In incorporation studies.

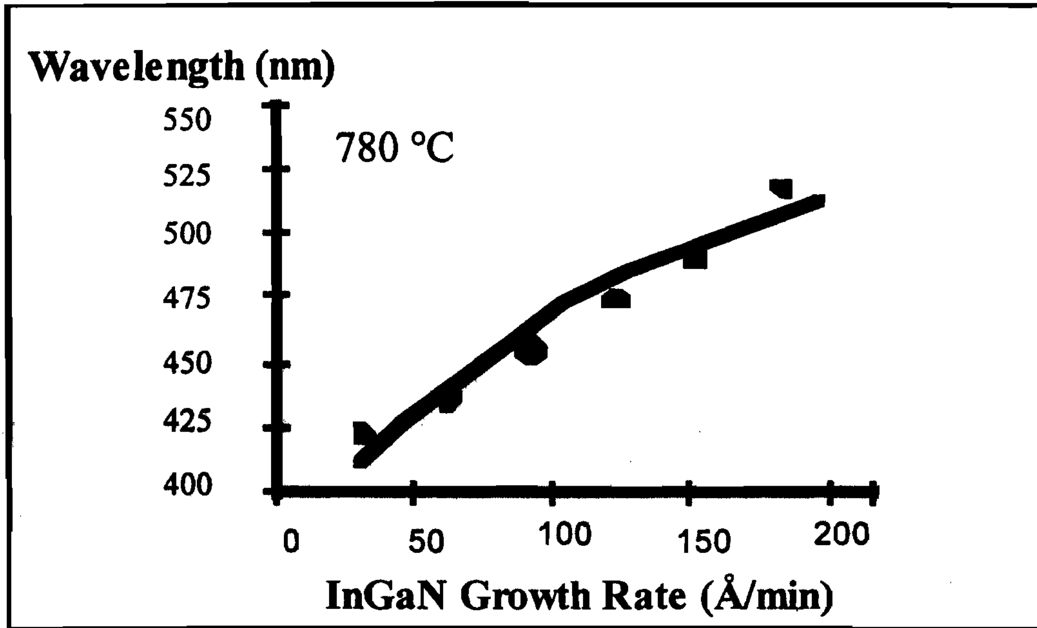

Fig. 3. Effect of growth rate on In incorporation.

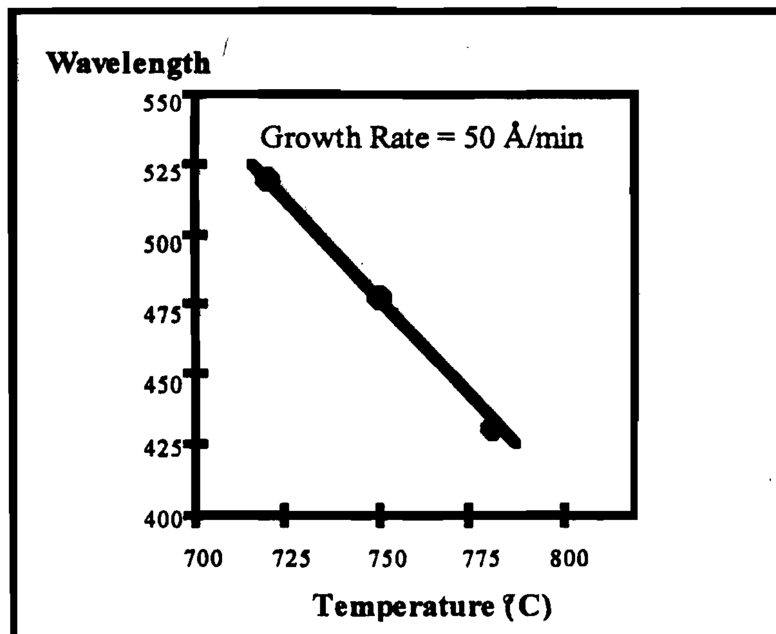

Fig. 4. Effect of growth temperature on In incorporation.

The effect of varying the growth rate while keeping the growth temperature constant is shown in Fig. 3. Fig. 4 shows the effect of varying the growth temperature while keeping the growth rate constant. These results demonstrate the means of improving indium incorporation by reducing the desorption of indium species from the growth surface, which is the key for growth of high-indium-containing InGaN material.

One design of InGaN/AlGaN lasers is based on the use of multiple InGaN quantum well structures. Such structures were grown to characterize crystalline and optical quality of InGaN quantum wells. High-resolution X-ray Bragg scan of InGaN/GaN multiple quantum well structure (MQW) is shown in Fig.5. The appearance of clearly visible satellite peaks around the principal diffraction peak of the MQW substantiates the excellent crystalline quality of the structure. The angular distance between the main (0th order) and satellite (+1 or -1 order) peaks gives the period of the MQW as 50 nm.

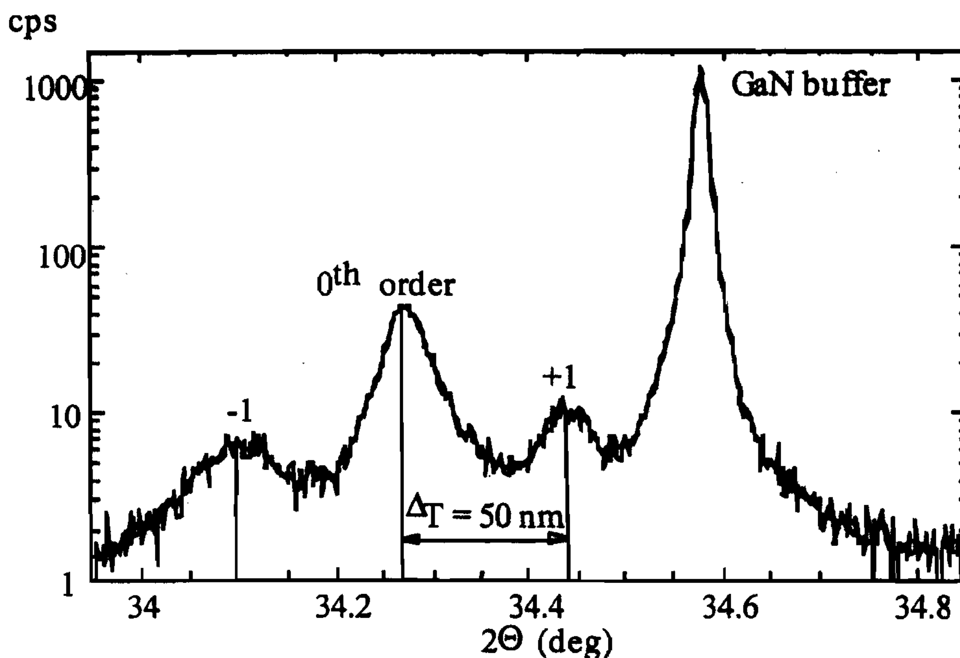

Fig.5. XRD Bragg scan of 10 period InGaN/GaN MQW structure

Samples of quantum well structures with GaInN wells have been delivered to Xerox for further characterization. Temperature dependent Hall measurements and low temperature photoluminescence have been performed, and results are being evaluated.

Theoretically investigate the band offsets of the AlGaInN system

Knowledge of the band discontinuities between AlN, GaN, and InN (and their alloys) is essential for designing optoelectronic devices. Experimental numbers for the offsets currently display wide scatter; these variations are at least in part attributable to the role played by strain at the heterojunction between these strongly-mismatched materials. We have performed first-principles density-functional-pseudopotential calculations to determine the band offsets, with particular attention to the role of strain. This approach has previously been successfully applied to a wide variety of semiconductor heterojunctions. To avoid complications associated with polar interfaces, we have first addressed the offsets for the nonpolar zincblende interfaces; however, we have strong reasons to believe that the results for other interface orientations and for the wurtzite structure will not differ by more than a few 0.1 eV.

Because of the importance of strain, it is most convenient to express the band lineups in terms of a hypothetical *unstrained offset*, and then use deformation potentials to describe the effects of strain. *Absolute* deformation potentials a_v describing changes in valence-band positions under hydrostatic strain are listed in the Table 22.1. Combined with the deformation potentials appropriate for uniaxial strains (reported in Milestone #21) these parameters allow determination of the valence-band offset for any strain situation.

Table 1: *Absolute* deformation potentials

	AlN	GaN	InN
a_v	3.5	2.8	2.5

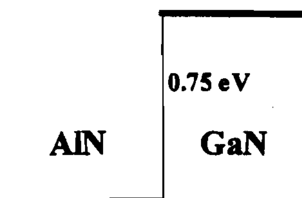

Fig. 6. Unstrained valence-band offset between GaN and AlN.

The crucial values then are the *unstrained* valence-band offsets, illustrated in Fig. 22.1. For AlN/GaN, we find an offset of 0.75 eV, in good agreement with previous theoretical work, and with some of the experimental determinations. Calculations for GaN/InN are in progress. In all cases we find that proper inclusion of atomic relaxation near the interface is essential.

Published:

"Hydrogen diffusion and complex formation in GaN", J. Neugebauer, W. Goetz, and C. G. Van de Walle, in *Proceedings of the 6th International Conference on SiC and Related Materials*, Kyoto, 1995, edited by S. Nakashima, H. Matsunami, S. Yoshida, and H. Harima, Inst. Phys. Conf. Ser. No 142 (IOP Publishing, Bristol, 1996), p. 1035.

"Gallium vacancies and the yellow luminescence in GaN", J. Neugebauer and C. G. Van de Walle, Appl. Phys. Lett., **69**, 503 (1996).

Accepted for publication:

"Role of defects and impurities in doping of GaN", J. Neugebauer and C. G. Van de Walle, in *Proceedings of the 23rd International Conference on the Physics of Semiconductors*, Berlin, 1996, edited by M. Scheffler and R. Zimmermann (World Scientific Publishing Co Pte Ltd., Singapore, 1996).

Milestone #23

Electronic characterization and PL study of defects in n-type GaN

Defects which introduce electronic levels into the band gap of semiconductors can be characterized by capacitance transient techniques. For example, deep level transient spectroscopy (DLTS) is a sensitive spectroscopic tool to detect and characterize deep level defects in III-V nitrides.

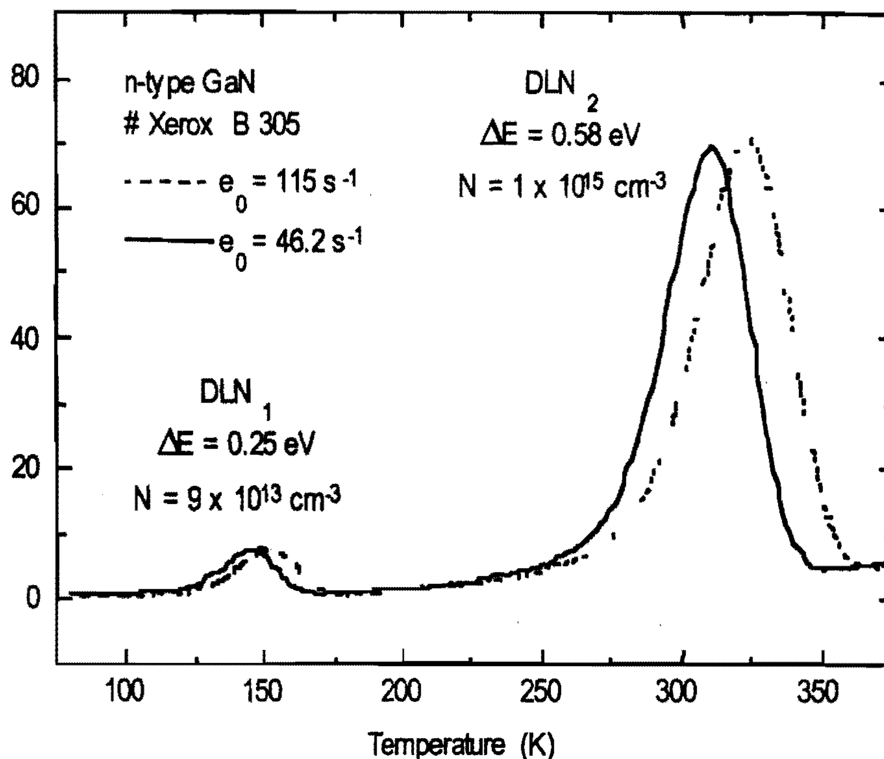

Fig. 7. DLTS spectrum for unintentionally doped, n-type GaN grown by MOCVD. The DLTS signal is shown for two different emission rates e_0 vs. sample temperature. Two peaks - labeled DLN_1 and DLN_2 - reveal the presence of two deep levels within the sensitivity range of our DLTS measurements. The peaks are labeled with the corresponding thermal activation energy for electron emission (ΔE) and the concentration of the deep level (N).

We have investigated n-type (undoped and Si-doped) GaN with DLTS using Schottky diodes. A typical DLTS spectrum is displayed in Fig. 1 for two different instrument-determined emission rates e_0. In a DLTS spectrum, the DLTS signal is shown as a function of the sample temperature and each peak in the spectrum is related to a discrete deep level. The spectrum shown in Fig. 1 reveals two discrete deep levels located in the upper half of the GaN band gap. They are labeled DLN_1 and DLN_2. Parameters for DLN_1 and DLN_2 are depicted in the figure.

To date, the chemical or structural nature of the deep levels DLN_1 and DLN_2 are unknown. However, they seem to be present in all n-type GaN samples we have investigated with DLTS. Furthermore, DLN_1 and DLN_2 were also detected in n-type GaN grown by hydride vapor phase epitaxy (HVPE). Since both growth techniques use different group III precursors but the same group V precursor (NH_3) common impurities in NH_3 or native defects may be responsible for DLN_1 and DLN_2.

In general, deep levels are present in MOCVD grown GaN in concentrations below 10^{15} cm^{-3}. Therefore, deep levels cannot play a significant role as compensation for shallow donors or acceptors. Further studies are underway, to reveal the chemical nature of the

common deep levels and to determine their significance as recombination centers in active regions of light emitting diodes.

Publications submitted:

1. *Characterization of the electrical properties of GaN Grown by Hydride Vapor Phase Epitaxy* , W. Jets, L.T. Roman, N.M. Johnson, and R.J. Molar, Proceedings of the ICPS-96, Berlin, Germany (1996)

2. *Local Vibrational Modes of the Mg-H Acceptor Complex in GaN*, W. Götz, N.M. Johnson, M.D. McCluskey, and E.E. Haller, Appl. Phys. Lett. (1996)

Publications appeared:

1 *Electronic and Structural Properties of GaN Grown by Hydrid Vapor Phase Epitaxy* , W. Götz, L.T. Romano, B.S. Krusor, N.M. Johnson, and R. J. Molnar, Appl. Phys. Lett. 69 (2), 242 (1996)

2 *Shallow Dopants and the Role of Hydrogen in Epitaxial Layers of Gallium Nitride (GaN),* W. Götz, N.M. Johnson, D.P. Bour, C. Chen, H. Liu, C. Kuo, and W. Imler, Electrochemical Society Proceedings, Vol. 96-11, 87 (1996)

Milestone #24

Scale-up of growth system to 2" substrates. Comparison of GaN devices on sapphire and SiC substrates. Development of n-type and p-type AlGaInN on 6H-SiC substrates.

Scale-up of growth system to 2" substrates

The HVPE reactor at ATMI has repeatedly demonstrated growth and etching with 2 inch diameter wafers, thus achieving the goals of the current reporting period. We have grown on both 2 inch diameter sapphire and 2 inch diameter Si wafers. We have achieved a steady improvement in crystallinity of the 2 inch diameter GaN/sapphire, demonstrated by a decrease in the FWHM of double crystal x-ray rocking curve (DCXRC) with time. This trend is shown in figure 8. We can now reproducibly achieve FWHM of DCXRC below 300 arc sec across an entire 2 inch wafer of GaN/sapphire. A similar trend is seen for the growth of GaN on the removable Si template. A DCXRC obtained from the best GaN sample grown on a 2 inch diameter Si template is shown in Figure 9. These x-ray diffraction results indicate that the material is single crystal with a FWHM = 793 arc sec. The crystallinity of the HVPE GaN on the removable template is continually improving.

We have continued to investigate the *in situ* backside etching of Si templates at the growth temperature. We have achieved Si etch rates in excess of 25 µm/min. for a 2 inch diameter wafer and full removal of a 250 µm thick Si wafer in less than 10 minutes. Thus, both growth and etching of 2 inch wafers in the ATMI reactor has been achieved

The uniformity across a 2 inch wafer has also been improved. As an example of the improved uniformity, figure 10 shows the room temperature photoluminescence spectra obtained at several points across the diameter of a 2 inch wafer of GaN on sapphire. Notice, that not only is the intensity and width of the 361 nm peak relatively constant across the wafer, but there is also a consistent lack of the 550 nm defect peak. The FWHM of the 361 nm peak varies from 42.6 to 44.6 Å

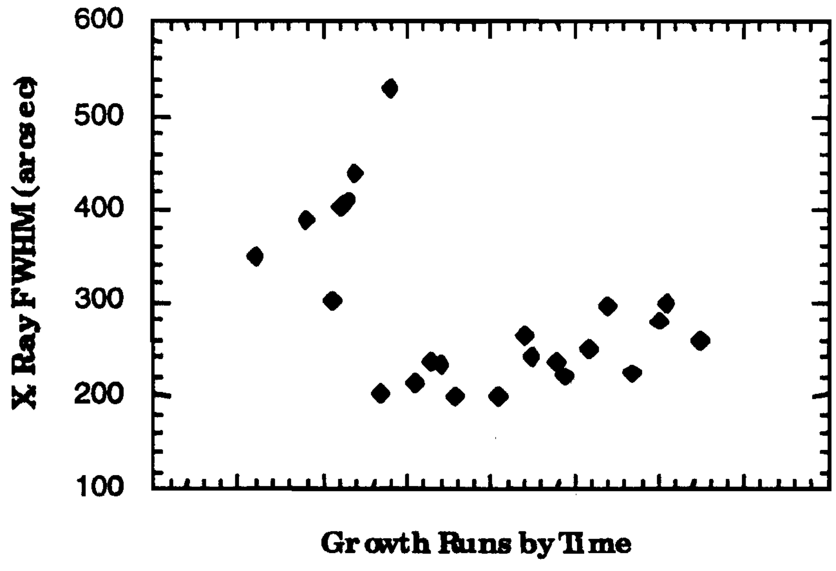

Figure 8. FWHM of double crystal x-ray rocking curves obtained from GaN samples grown on sapphire as function of time.

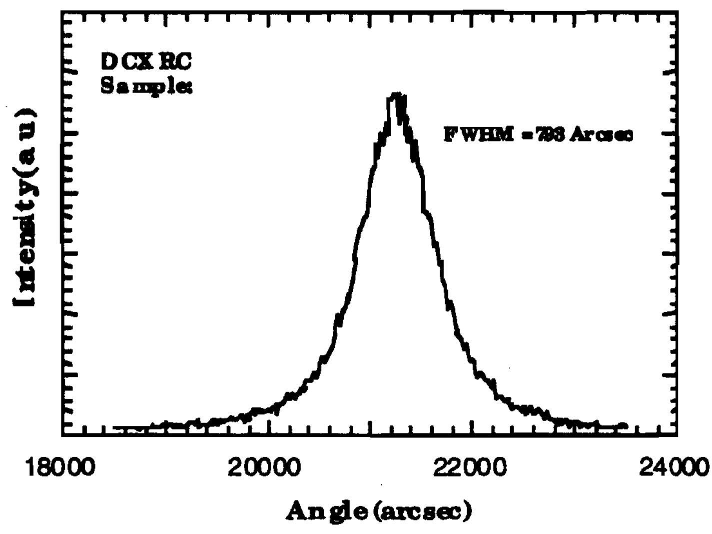

Figure 9. Double crystal x-ray rocking curve for a GaN sample grown on the silicon template.

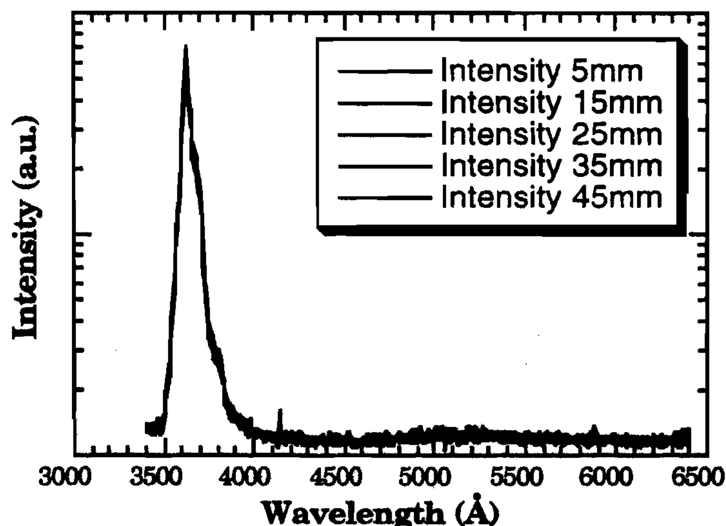

Figure 10. Room temperature photoluminescence spectra obtained from a HVPE GaN sample grown on a 2 inch sapphire wafer. The spectra were obtained at 10 mm intervals across the diameter of the wafer.

Comparison of GaN devices on sapphire and SiC substrates.

We have successfully grown InGaN/GaN and AlGaN/GaN heterojunctions on (0001) sapphire substrates. We have also grown, fabricated, and tested InGaN/GaN MQW heterostructure *p-n* junction LED's on sapphire substrates. The comparison of structures grown on SiC substrates has been initiated with the growth of similar heterostructures on vicinal (0001) 6H-SiC wafers.

Development of n-type and p-type AlGaN on 6H-SiC substrates

AlGaN alloys have been grown on 6H-SiC substrates without the employment of a buffer, which is the usual mode of heteroepitaxial growth of this class of materials. Alloys with Al concentration up to 60 percent were fabricated. Films with low Al-content were found to be of high structural equality, with 0002 rocking curve having FWHM of 9-Arc min. The films were doped n-type with silicon and p-type with magnesium. In both cases, the conductivity of the films for constant Al concentration was found to scale with the vapor pressure of the two elements. The conductivity of both the undoped and the Si-doped AlGaN alloys decreases with Al-concentration. Specifically, the conductivity of the Si-doped films decreases from $3x10^2$ to $4x10^{-4}$ by varying the Al concentration from zero percent to 60 percent. The evidence suggests that Si becomes a deeper donor as the Al concentration increases. In AlGaN alloys, photoluminescence occurs across the gap. For comparison similar studies were conducted on AlGaN alloys grown on (0001) sapphire substrates.

One of the advantages of 6H-SiC as a potential substrate for III-V nitrides is that vertical devices can be fabricated with the SiC as an active part. However, this requires that one should be able to deposit the III-V nitrides directly on the SiC substrate without a low

temperature buffer, which is the usual mode of heteroepitaxial growth for these materials. In this report, we describe the growth and doping of AlGaN films on 6H-SiC with Al concentration up to 60 percent. Samples were also grown on (0001) sapphire for comparison.

The various AlGaN alloys were deposited at 750°C by adjusting the beam equivalent pressures of Al and Ga. The films were doped n-type with Si and p-type with Mg. The concentration of Al in the films was determined from XRD assuming Veragd's Law. The structure of the films was determined by measuring the rocking curve of the (0002) peak. The sample with 5 percent Al (approximately 1μm thick) was found to have a rocking curve for the (0002) peak with FWHM of 9 Arc min. The FWHM of the same peak in the θ-2θ scan was found to be about 3 arc min. and the FWHM of the (0004) peak in the θ-2θ scan was found to be about 4 arc min., Fig. 11 is indicating very little inhomogeneous strain.

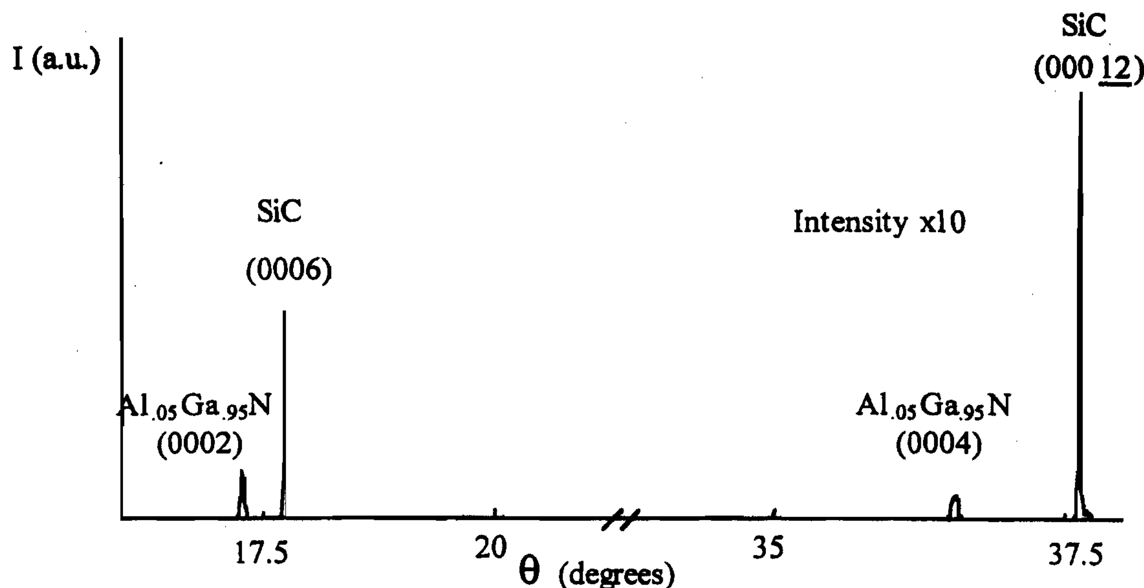

Figure 11. Theta-Two Theta scan of $Al_{.05}Ga_{.95}N$ grown directly on 6H-SiC. FWHM of (0002) peak is 3 arc min., and of (0004) peak 4 arc min.

The n- and p-type doping of these alloys was evaluated by measuring the conductivity of the films using pressure contacts. Fig. 12 shows the conductivity of undoped AlGaN and Si-doped alloys. For comparison a number of Si-doped samples were grown under identical conditions on sapphire substrates. Upon doping the conductivity increased by 4-5 orders of magnitude. However, the conductivity of the films decreases with the Al-concentration. Our initial transport studies suggest that Si becomes a deeper donor as the Al concentration increases.

A number of AlGaN alloys with fixed Al concentration and variable amount of Si or Mg were also grown. Fig. 13 shows the dependence of the conductivity for both the n-type and p-type films as a function of the vapor pressure of both the Si and Mg. The best

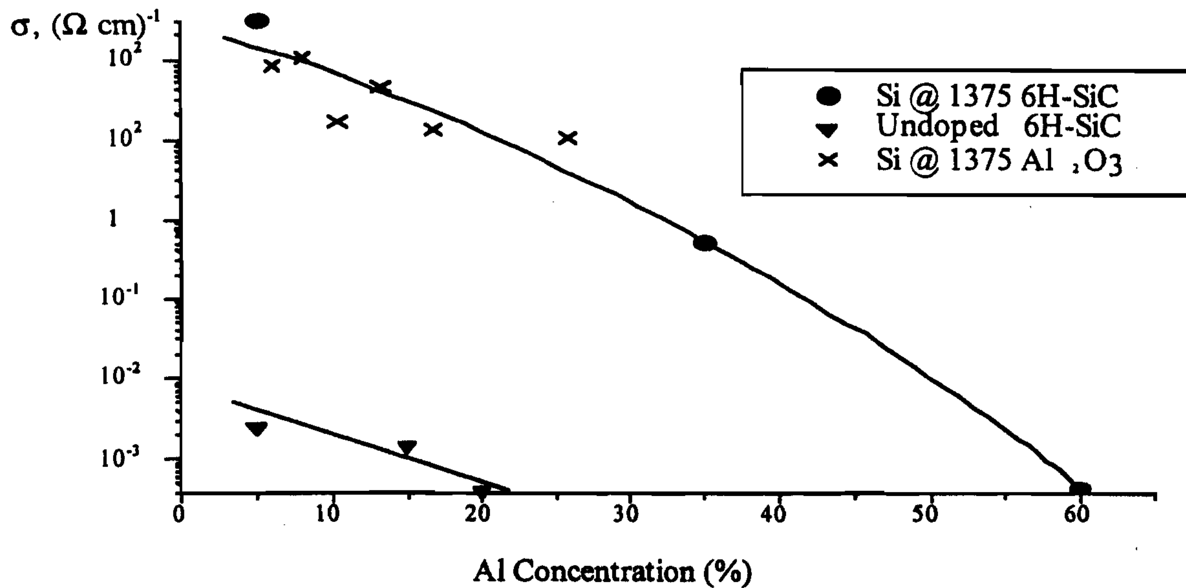

Figure 12: Effect of AlN mole fraction on the conductivity of undoped and Si doped $Al_xGa_{1-x}N$ alloys. The doped films were grown both on 6H-SiC and Al_2O_3 substrates for comparison and doped with the Si cell at 1375 °C

n-type doped films have conductivity of $3x10^2$ $(Ohm.cm)^{-1}$ and p-type films have conductivity 10^{-1} $(Ohm.cm)^{-1}$. The films were p-type without post-growth annealing.

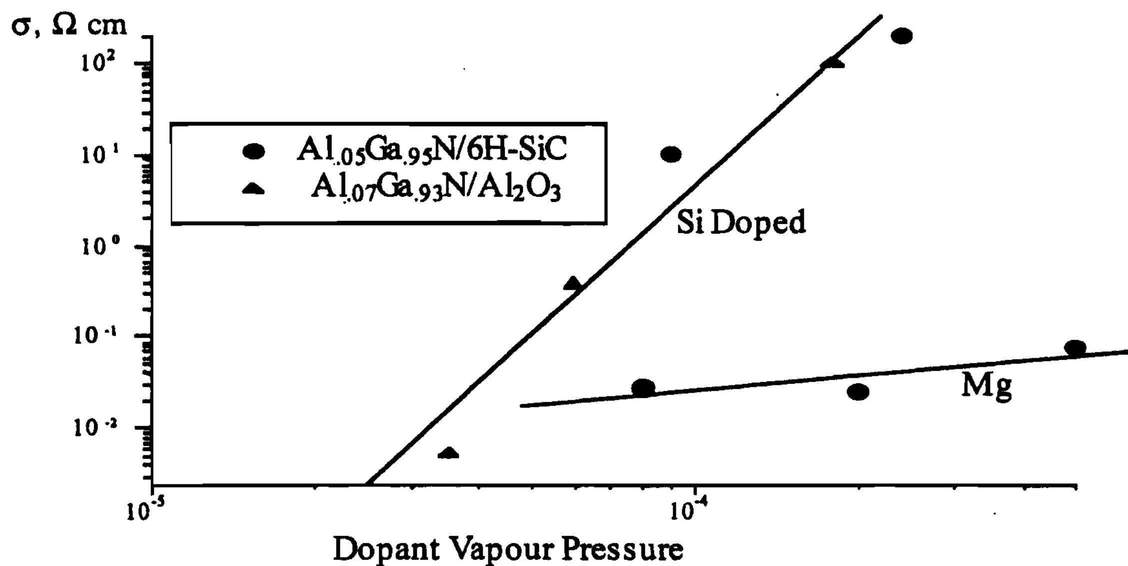

Figure 13. The electrical conductivity of $Al_xGa_{1-x}N$ films grown on 6H-SiC or sapphire (for comparison) vs. the equilibrium vapor pressure inside the Si and Mg effusion cells. This direct dependence between conductivity and vapor pressure indicates efficient incorporation of the dopants.

Photoluminescence in some films was investigated with a He-Cd laser. The data for a sample with 5 percent Al, doped with silicon, is shown in Fig. 14. The main

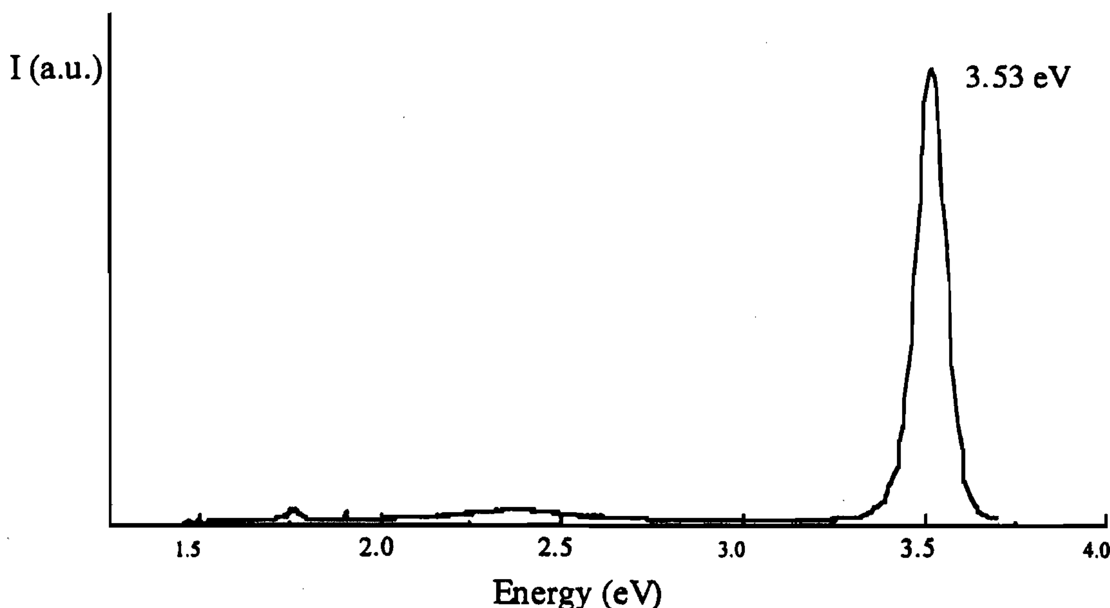

Figure 14. Room temperature photoluminescence spectra of $Al_{.05}Ga_{.95}N$ film doped with Si at the level of about $5x10^{17}$ cm^{-3}.

luminescence peak occurs at 3.53eV which is 10 meV below the gap of the semiconductor (3.54eV)

AlGaN films with Al content up to 60 percent were grown on 6H-SiC and (0001) sapphire substrates. The growth on 6H-SiC substrates took place without the employment of any kind of buffer. The films were doped n-type with Si and p-type with Mg to maximum conductivity of $3x10^2$ ($Ohm^{-1}. cm^{-1}$) and 10^{-1} ($Ohm^{-1}. cm^{-1}$). The conductivity of the n-type films decreases with Al concentration suggesting that Si becomes a deeper donor. The Mg doped films were p-type as grown without any post-growth annealing.

Milestone #25

Bonding to simple devices demonstrated.

LED devices have been fabricated and diced for bonding on headers and in lamp packages. A typical die attached and wire bonded device under forward bias is illustrated in Fig. 16. Viewed from the top, the etched mesa emitting region is visible in the center and glows more brightly than the rest of the chip. One ball bond is in the upper left hand corner of the mesa; the other ball bond is off the mesa at the lower right. The entire chip glows blue, but there is wave guiding along the top surface of the chip which makes the edges of the chip brighter and appear white in the photograph.

Fig. 15 is an SEM image of a similar chip and shows the wire bonds in more detail. This particular chip has some contamination on the upper surface as a result of the epi-side-down dicing process. Recent improvements at the dicing step have eliminated such contamination.

Fig. 15. SEM image of a typical wire bonded GaInN LED.

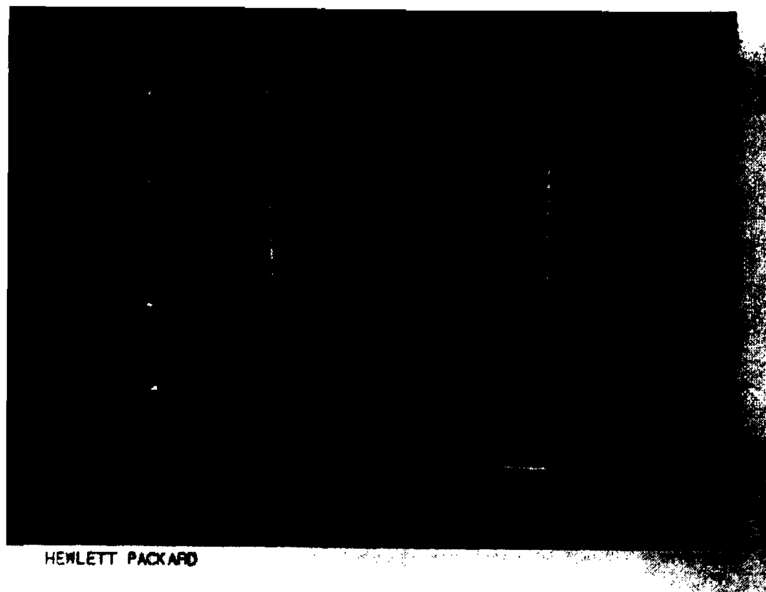

Fig. 16. GaInN LED under forward bias.

Milestone #26

Development of facet formation technologies, including polishing, dry etching and cleaving.

Samples of AlGaN/GaN heterostructures grown on c-plane sapphire were sawn into bars of 1mm width, mounted in the fixture facet up and polished on diamond polishing pad. An SEM image of the polished facet is shown in Fig.17.

Fig.17. Polished facet of GaN/AlGaN heterostructure grown on c-plane sapphire

It can be seen that although smooth fragments could be found, the chipping and delamination of the grown film predominantly occurs during mechanical facet polishing.

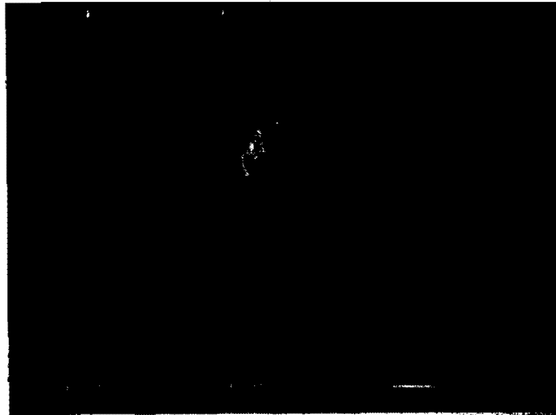

Fig.17. SEM image of CAIBE etched GaN/AlGaN heterostructure.

Preliminary experiments with dry etching of GaN/AlGaN heterostructures has been performed on a Technics Plasma GMBH chemically-assisted ion beam etching machine (CAIBE). As can be seen from Fig. 18 further work is needed in order to optimize facet smoothness and etching angle. Both SDL and Xerox have orders with Technics for similar machines and expect dry-etching capability to be in place by January 1, 1997. Preliminary inspection of the machines has been accomplished.

Facet formation by cleaving seems to give satisfactory results for GaN/AlGaN heterostructures grown both on c-plane and A-plane sapphire as demonstrated in Figs. 18 and 19.

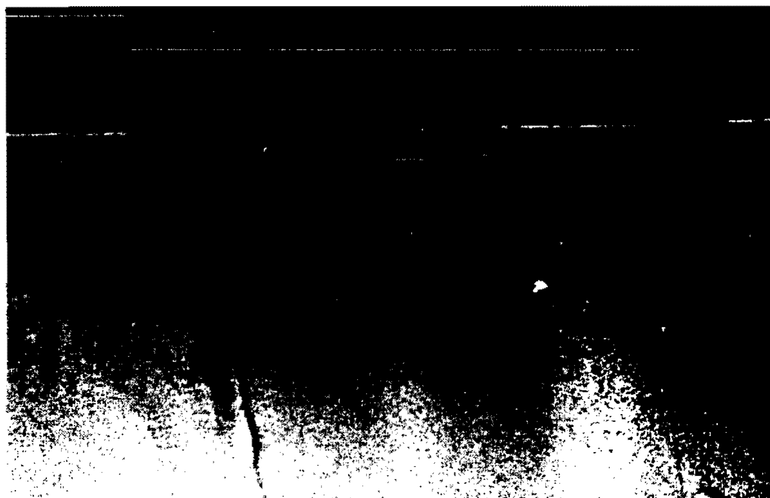

Fig. 18. SEM micrograph showing cleaved facet of GaN/AlGaN heterostructure on c-plane sapphire.

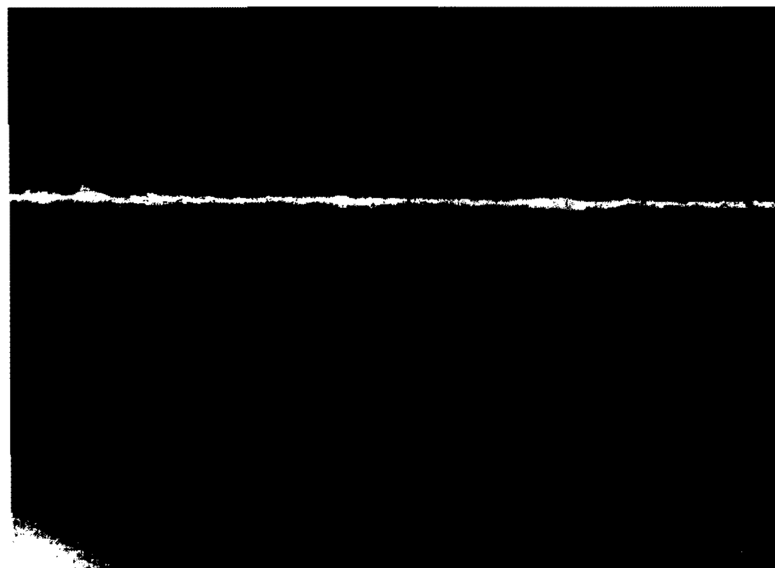

Fig. 19. SEM micrograph showing cleaved facet of GaN/AlGaN heterostructure on A-plane sapphire.

BLUE BAND

Blue Light and Ultra-Violet Emitters, the Bay Area Nitride Consortium
Report for Month 24
Contract: MDA972-95-3-0008

DISTRIBUTION: SDL, HP, Xerox, AXT, ATM, Boston University, the University of Texas at Austin, D. Scifres, J. Endriz, R. Craig, J. Johnson, and R&D

To: Distribution
From: Richard H. Miles
Date: 8.26.97

Distribution authorized to U.S. Government agencies only to protect information not owned by the U.S. Government and protected by a contractor's "limited rights" statement, or received with the understanding that it not be routinely transmitted outside the U.S. Government. Other requests for this document shall be referred to ARPA Security and Intelligence Office.

Overview:

BlueBand has now concluded with a final report describing issues addressed under the program, key results, conclusions, and recommendations for future work.
Technical topics discussed within this quarterly report include characterizations of the best current LED technology and of AlGaInN diode laser structures.
Materials studies include analyses of ZnO and HVPE GaN substrates, electrical characterization of nitride heterojunctions, a structural study of pits, and calculations of the electronic and atomic structure of native defects and impurities.

Summary: Milestones 38 through 43 are completed.

Milestone #38

Structural characterization of pits at the surface of GaN diode heterostructures

Pits at the surface of homogeneous GaN layers and on InGaN/GaN diode heterostructures have been observed in material grown by MOCVD from several independent research groups. These surface defects are likely to adversely affect the electrical characteristics and introduce optical scattering centers in laser diodes.

In the present study the pits were characterized by transmission electron microscopy (TEM) and atomic force microscopy (AFM) in $In_xGa_{1-x}N$ SQW and MQW LEDs and laser diode structures grown on sapphire. The pits are hexagonal at the surface with pyramidal sidewalls that extend into the QWs. The size and the density of pits depends on the well thickness, the number of wells, and the In composition. For $x > 0.40$, pits were found in both SQW and MQW LED structures with well thickness of 3nm. At lower In compositions ($x \sim 0.20$), the pits occur after the growth of ~ 5 QWs for the same well thickness. Once the pits form, they extend into the subsequently-deposited QW layers. Typically either AlGaN or GaN layers were deposited above the QWs. The pits were found to extend into these overlayers, to the surface of the device, if the first overlayer was GaN with a thickness < 200nm. However, we have limited results indicating that if a 10nm AlGaN layer is grown on the QWs, followed by a 200nm layer of GaN, the pits became planarized and therefore do not extend to the surface.

Figures 1 and 2 are AFM and TEM cross sectional (XTEM) images, respectively, of a 5QW $In_{0.45}Ga_{0.55}N$/GaN optically-pumped laser device structure. In this case, the pits are found to extend to the surface of the device. The structure consists of a thick GaN

underlayer, followed by 5QWs with a well/barrier thickness of 3nm/6nm, and GaN and AlGaN overlayers. The AFM image is taken from the surface of the device. The pits were found by AFM to range in size from 20-500 nm with a density of $10^8/cm^2$. The XTEM image shows a pit that initiated at the bottom of the QWs. The opening of the pit at the top surface is 300nm.

One possible manifestation of pitting has arisen in photopumping studies of heterostructures. We have performed Fourier transforms of the emission spectra from optically pumped GaN heterostructures which reveal subcavity reflections. These intracavity reflections may be due to microstructural defects within the diode and therefore represent optical scattering centers.

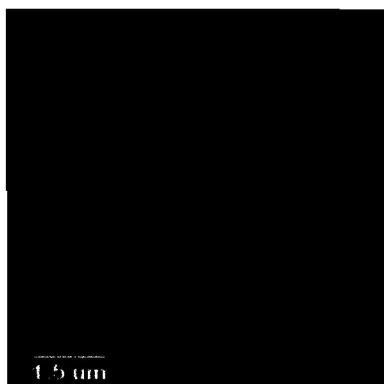

Figure 1. AFM image showing pits at the surface of an $In_{0.45}Ga_{0.55}N/GaN$ MQW device.

Figure 2. XTEM image of a pit in an $In_{0.45}Ga_{0.55}N/GaN$ MQW device.

Publications

1. R. J. Singh, D. Doppalapudi, T. D. Moustakas, L. T. Romano, "Phase Separation InGaN thick films and formation of InGaN/GaN double heterostructures in the entire alloy composition range," Appl. Phys. Lett. **70**, 1089 (1997).

2. D. Hofstetter, L.T. Romano, R.L. Thornton, D.P. Bour, and N.M. Johnson, "Characterization of intra-cavity reflections by Fourier transforming spectral data of optically pumped InGaN laser", submitted to Appl. Phys. Lett.

Milestone #39

Calculate formation energies of selected native defects and dopant impurities in AlN and InN. Electrical characterization of a doped AlGaN/GaN single heterojunction.

Calculate formation energies of selected native defects and dopant impurities in AlN and InN

Following up on our comprehensive first-principles studies of defects and impurities in GaN, we have now also investigated the electronic and atomic structure of native defects and impurities in AlN and InN, based on pseudopotential-density-functional theory. Among our key results are the *formation energies* of native defects, since these determine the abundance of the defect species. Our results for AlN are summarized in Fig. 3. We find that the nitrogen vacancy, V_N^{3+}, and aluminum interstitial, Al_i^{3+}, have the lowest formation energies in *p*-type material. These defects act as compensating centers. We anticipate that this tendency to compensate acceptors will start appearing in $Al_xGa_{1-x}N$ alloys and become progressively worse as *x* increases. This type of compensation is likely responsible for the diminished doping efficiency of Mg in AlGaN; indeed, our calculations of Mg in AlN do not reveal any qualitative difference in its ionization energy or solubility compared to GaN. Figure 3 shows that the aluminum vacancy, V_{Al}^{3-}, has the lowest formation energy in *n*-type material. This defect will be responsible for compensation of donors, and for deep-level luminescence in AlGaN.

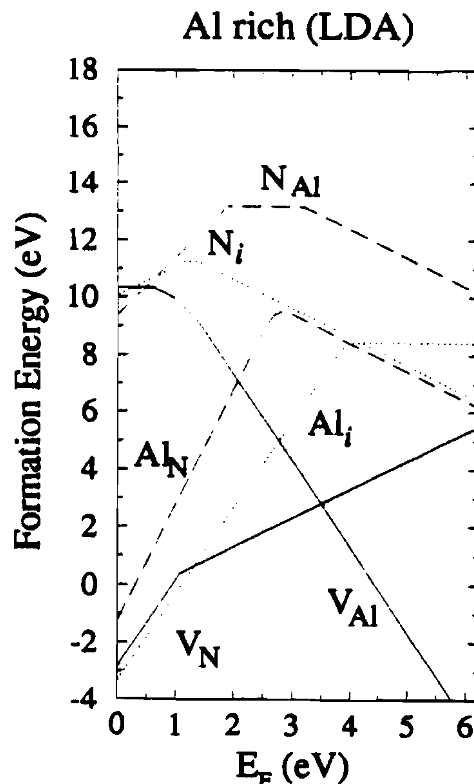

Figure 3. Formation energy as a function of Fermi level for all native defects, in all possible charge states, in AlN. E_F=0 corresponds to the top of the valence band. Al-rich conditions are chosen.

In InN, we find that the nitrogen vacancy has the lowest formation energy in *p*-type material; in *n*-type material, all defect formation energies are rather high. We note that in *n*-

type AlN as well as InN the formation energies of the nitrogen vacancies are high, indicating that these defects will not occur in high concentrations and cannot be responsible for unintentional *n*-type conductivity, strengthening the conclusion we reached previously for GaN.

Finally, we have carried out extensive studies of oxygen and silicon donors in AlN. We find that oxygen undergoes a so-called *DX* transition from a shallow to a deep state as the Al content of AlGaN is increased. Silicon does not exhibit this transition. We also find that the deep-center formation occurs only in the wurtzite phase, not in the zinc-blende phase.

Publication

1. "Hydrogen interactions with native defects in GaN", C. G. Van de Walle, submitted to Physical Review B.

Electrical characterization of a doped AlGaN/GaN single heterojunction.

The AlGaN layer is an essential component in heterostructures fabricated from III-V nitrides for both light emitting diodes (LEDs) and injection laser diodes (Lds). In LEDs, AlGaN is incorporated as a thin layer above the active region and serves mainly as a blocking layer to avoid spill-over of electrons. In LDs, AlGaN layers are utilized to form index wave guiding layers and are positioned both below and above the active region. In both of these types of diodes, the AlGaN layer must be electrically conducting, either the n- or p-type, since it is situated in the conduction path adjacent to the active (light generating) region of the diode.

The quality of the AlGaN layer and its conductivity are therefore important for diode performance due to its essential function and proximity to the active region. For the range of Al compositions currently being utilized for LEDs and LDs (e.g, <15%), controlled n-type conductivity in the range of 10^{18} cm^{-3} is readily achieved with silicon donors. Consequently, our studies of doping of AlGaN have focused on p-type conductivity, with Mg acceptors. The results presented below are for an AlGaN on GaN heterostructure grown at HP.

Variable temperature Hall-effect measurements were used to characterize the electrical properties of AlGaN layers on GaN. The heterostructure was chosen to simulate the structure in an LED, with the AlGaN layer is grown on GaN. The composite structure, shown in the inset in Fig. 4(b), was grown by MOCVD on sapphire and consisted of a low-temperature buffer layer followed first by a 1 μm, undoped semi-insulating GaN layer and then a 1.8 μm AlGaN top layer. The AlGaN layer had an Al composition of ~7% and was doped with Mg. The growth conditions were optimized for acceptor incorporation, and the Mg was activated with an RTA at 850°C.

Results from the variable temperature Hall-effect measurements are shown in Fig. 4. The temperature dependence of the hole concentration in Fig. 4(a) was analyzed with a single-acceptor model which allowed for donor compensation. The fit of the model to the experimental data yields the acceptor concentration N_A, the concentration of compensating donors N_{comp}, and the activation energy for acceptor ionization ΔE_A. In Fig. 4(a) the fit is shown as a solid line and the fitting parameters are listed. Even though the acceptor concentration of 1×10^{20} cm^{-3} is comparable to that achieved in GaN:Mg, the room-temperature hole concentration is only 5×10^{16} cm^{-3}, an order of magnitude lower than that in GaN, because of the larger acceptor ionization energy (207 meV vs ~160 meV in GaN). Also shown in Fig. 4(b) is the temperature dependence of the hole mobility, with a room-temperature mobility of ~3 cm^2/V-s.

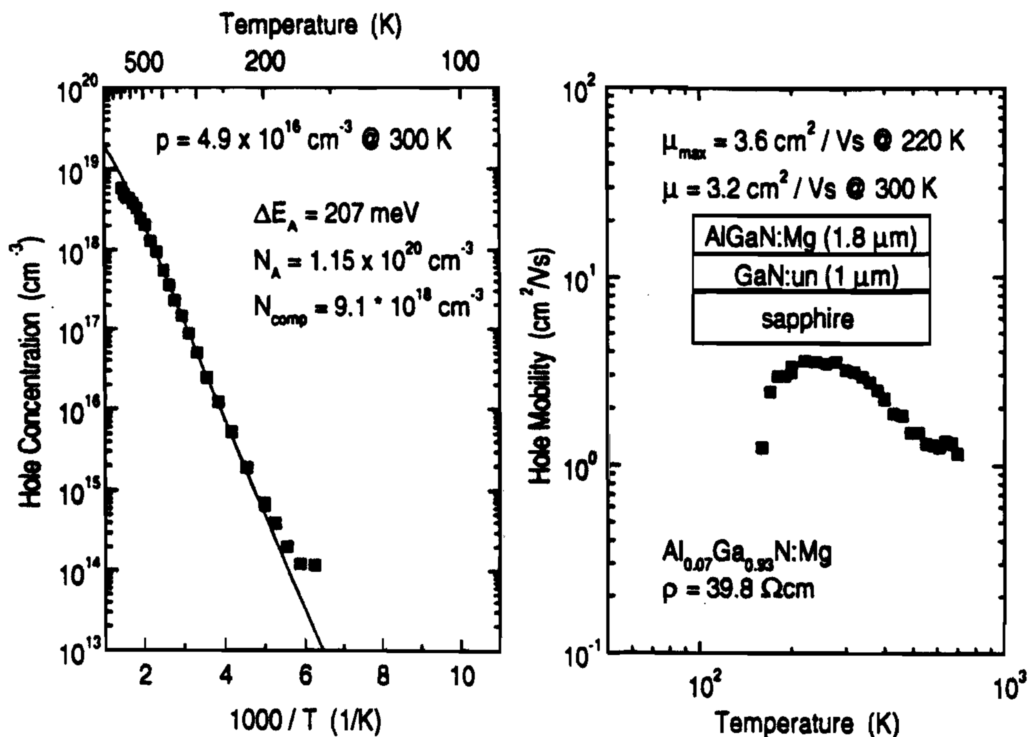

Figure 4. Hole concentration vs reciprocal temperature (a) and mobility vs temperature (b) for AlGaN:Mg (7% Al) on GaN. The symbols refer to the experimental data. The solid line in (a) is from a model fit with a single acceptor level of concentration N_A and compensating donors of concentration N_D. The fit also yields the thermal activation energy for acceptor ionization ΔE_A.

Publications

1. "Spectroscopic Identification of the Acceptor-hydrogen Complex in Mg-doped GaN Grown by MOCVD," W. Gotz, M. D. McCluskey, N. M. Johnson, and D. B. Bour, Mater. Res. Soc. Symp. Proc., Vol. 468 (1997).

2. "Characterization of Dopants and Deep Level Defects in Gallium Nitride," W. Gotz and N. M. Johnson, eds. J. Pankove and T. D. Moustakas, Academic Press, Inc.

Milestone #40

Deliver substrates grown in new reactor to consortium members. Development of AlGaInN alloys on single crystal ZnO substrates.

Deliver substrates grown in new reactor to consortium members

We have extended the results of the last reporting period by further increasing the conductivity of HVPE-grown GaN by Si-doping. We have also improved our understanding of the electrical properties of HVPE GaN by further characterization and modeling.

As we have previously discussed, there is a difference between Hall effect and capacitance-voltage (C-V) measurement of the electrical properties of HVPE GaN-on-sapphire. The

fundamental reason for this difference stems from the high interfacial charge density at the GaN/sapphire interface. C-V measurements at low bias are sensitive to only the top few microns of GaN, while Hall effect measurements average the full thickness. Thus, Hall effect measurements consistently measure a higher reading for electron concentration than the C-V technique.

A two layer model can be used to describe these electrical properties. The full thickness of the undoped HVPE GaN was modeled as (1) a thin n^+ layer at the interface and (2) a thick n^- layer on top. Based on C-V and Hall measurements on varied thickness HVPE GaN films on sapphire, the thin layer was assumed to have a thickness (t_1) of 200 nm, $n_1/t_1 \approx 5\times10^{20}$ cm^{-3}, and $\mu_1 \approx 35$ cm^2/V-s, while the n^- top layer was assumed have $n_2/t_2 \approx 2\times10^{16}$ cm^{-3} and $\mu_2 \approx 300$ cm^2/V-s. The effective electron concentration (n) and electron mobility (μ) of the two layers combined are given by[i]:

$$n = \frac{\left(n_1\mu_1 + n_2\mu_2\right)^2}{n_1\mu_1^2 + n_2\mu_2^2}$$

$$\mu = \frac{n_1\mu_1^2 + n_2\mu_2^2}{n_1\mu_1 + n_2\mu_2}$$

respectively. These equations and the assumed values for the individual layers were compared with the Hall-measured electron concentration and electron mobility versus GaN thickness shown in Figure 5. In reality, the electron concentration is more likely to vary gradually down to 2×10^{16} cm^{-3}, and thus assumptions of an abrupt change decrease the accuracy of the model. Nonetheless, the two layer model appears to provide a reasonable estimate of the electrical behavior of the HVPE GaN grown on sapphire.

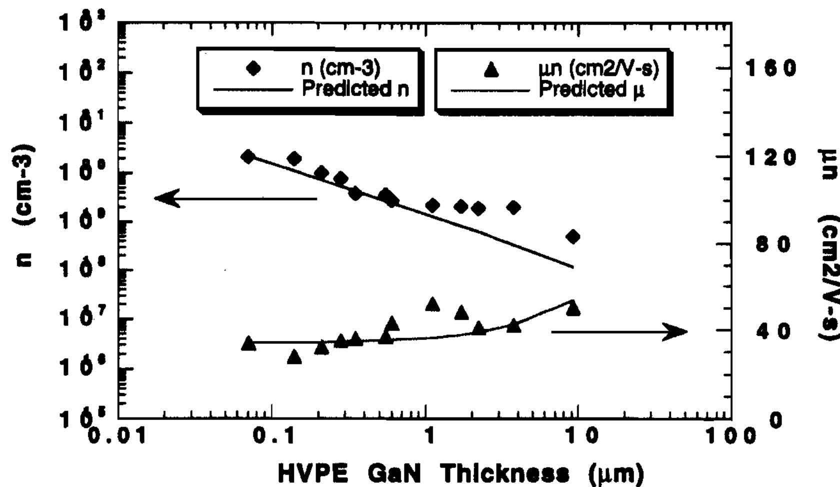

Figure 5. Electron concentration and electron mobility versus HVPE GaN thickness grown on sapphire. The two layer model predicts the general reduction in electron concentration and increase in mobility with increased film thickness.

---

[i] W. Gotz, et al, MRS Symp. Proc. 449 (1997) 525.

Although the HVPE GaN was electrically conductive as grown, the conductivity was further increased for optoelectronic devices by doping with silane. The undoped HVPE GaN grown on sapphire was conductive, mainly due to the interfacial region just described, however, the bulk of the material is lightly doped. We have intentionally Si-doped the HVPE GaN with SiH_4 over the range of $5x10^{16}$ to $8x10^{18}$ cm^{-3}. Figure 5 shows both C-V (when obtainable) and Hall effect measurements of the electron and donor concentrations as a function of Si/Ga ratio. Notice that the electron concentration continued to increase with Si/Ga ratio and did not saturate within the parameter space investigated. Electron concentrations as high as $8x10^{18}$ cm^{-3} were achieved. The electron mobility of all of the Si-doped wafers was higher than undoped HVPE GaN. At $n = 8x10^{18}$ cm^{-3}, the room temperature electron mobility was 160 cm^2/V-s (*cf.* mobility of undoped HVPE GaN $\approx$ 50-70 cm^2/V-s at a similar thickness). This enhancement in mobility can be explained as a gradual increase in the conductivity of the bulk layer with increased doping, which pulls the current path away from the low mobility interface region described above. Secondary ion mass spectroscopy (SIMS) was employed to examine the concentration of Si in some of the highly doped samples shown. Even for the highest doped sample, all of the Si is electrically active. The sheet resistance of these samples was also measured. Two-dimensional representations of the sheet resistance versus position on the wafer are shown in Figure 6 for representative 10 μm thick undoped and the highest Si-doped GaN-on-sapphire wafers. For a representative undoped GaN wafer (Figure 6a), the average sheet resistance was ~29 Ω/sq., while the sheet resistance was lowered by more than a factor of 5 by Si-doping. The uniformity of the sheet resistance was also improved by Si-doping. Non-uniformity of sheet resistance is indicative of variations in film thickness as well as resistivity of the material. These measurements demonstrate the usefulness of HVPE GaN:Si layers for reducing the series resistance in lateral geometry LEDs and laser diodes.

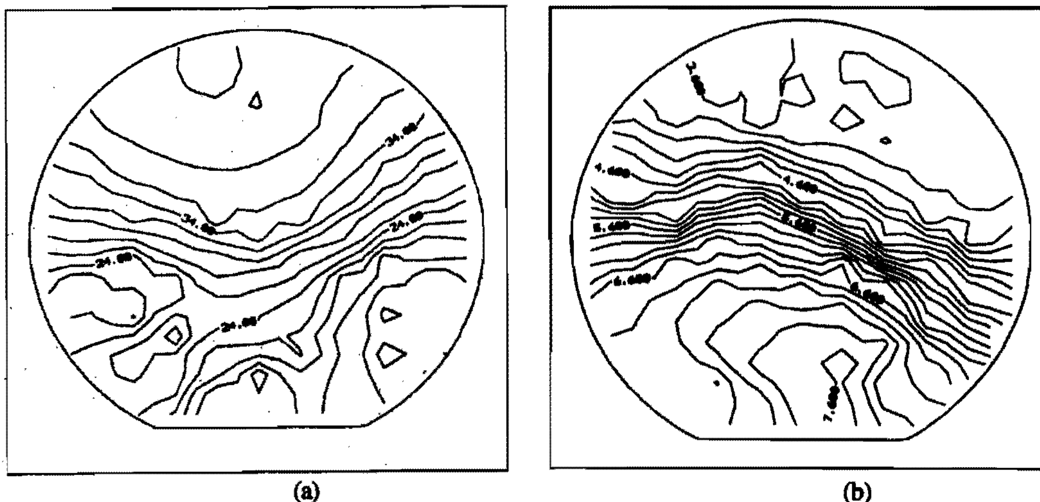

Figure 6. 2D maps of sheet resistance vs. position measured across 2" diameter wafers of (a) undoped (ave: 29 Ω/sq.) and (b) Si-doped (ave: 5.5 Ω/sq.) HVPE GaN-on-sapphire grown by HVPE.

Development of AlGaInN alloys on single crystal ZnO substrates

The advantage of ZnO as a potential substrate for the growth of III-V nitrides is that one can develop lattice matched heterostructures of InGaAlN materials having composition which correspond to a lattice constant of 3.25Å. Such heterostructures span the spectral region from 2.8 to 4.5 eV. Ideally, one would like to carry out the heteroepitaxial studies of III-V nitrides on single crystalline ZnO substrates. However, such substrates are not available at reasonable sizes and cost. We therefore deposited a number of GaN and

((

InGaN alloys on sputtered ZnO thin films. Such films were either produced in our laboratory by RF sputtering from a ZnO target in an atmosphere of $Ar+O_2$, or at Rome Laboratories using a propriatory sputtering method. These films were found to have (0002) XRD rocking curve with a FWHM of 450-850 Arcsec and an RMS roughness between 2.2 and 5.6 µm. The ZnO films produced by both methods are polycrystalline with (0001) preferred orientation.

Some nitride samples were grown on the ZnO substrate without any prior treatment. Others were grown after the substrate was exposed to a nitrogen plasma or after the growth of a low temperature nitride-buffer.

It was observed that the ZnO substrate had a streaky RHEED pattern when it was examined at a temperature below 400°C. However, the RHEED pattern deteriorated as the substrate was heated to growth temperature of about 650°C. Specifically, the diffraction pattern because spotty and weak, suggesting surface degradation due to dissociation of the compound. Deposition of InGaN alloys on such surfaces led to films with rough surfaces and poor optical (photoluminescence) and transport properties. The InGaN films grown on nitrided ZnO layers also had poor properties. We concluded from these studies that ZnO needs to be encapsulated by a low temperature buffer to prevent this dissociation. Similar observations were also reported by other workers. (1) Two types of buffers were investigated on ZnO layers sputtered in our laboratories. Thin layers (~200 µm) of AlN or GaN were deposited at 400°C prior to growth of InGaN at 650°C. Evidence from both RHEED patterns and SEM studies indicate that these buffer layers prevented dissociation of ZnO. InGaN films grown on such GaN buffer layers had fairly smooth surface and good optical properties. Photoluminescence spectra were similar to those obtained from InGaN films grown on sapphire. We also observed that annealing the buffer at 750°C prior to growth considerably improved the quality of the epitaxial layer. The films grown with AlN buffer were very rough presumably due to the larger lattice mismatch between AlN and ZnO or due to poor crystallization of the AlN-buffer.

We observed that the ZnO films grown by the Rome Laboratories were stable even up to 550°C. RHEED patterns indicated that these films had better crystalline structure than those grown by our own sputtering method. On these films, we deposited AlN and GaN buffers at 550°C followed by GaN growth at around 775°C. The resulting films were characterized by SEM, XRD, and Hall Effect measurements and were found to have good structural, electrical and photoluminescence properties. However, the epitaxial layers had spalled partially. SEM studies showed the cracks were initiated at the sapphire/ZnO interface in the case of films grown on GaN buffer and at the ZnO/AlN interface in the case of AlN buffer. We believe that the thermal mismatch stresses between the various layers lead to this kind of spalling. We also investigated the use of InGaN buffer at 550°C, followed by growth at temperatures of 630°C - 660°C. *In situ* RHEED studies indicated that the films were very smooth, with good epitaxial orientation. Photoluminescence studies show a similar spectra as are obtained generally from InGaN films grown on sapphire, without a ZnO layer. SEM micrographs show that the growth is very columnar, with very smooth surfaces at the top. This is due to the non-uniform wetting of the surface by the InGaN layer at 550°C. Further optimization of these layers is needed to obtain good quality films.In conclusion, the growth of III-V nitrides on sputtered ZnO thin films requires a low temperature III-V nitride buffer to prevent the decomposition of the ZnO which occurs at about 400°C - 500°C. This requirement makes the use of such substrates less attractive than previously has been suggested.

References:

1) T. Shirasawa et al. Mat. Res. Soc. Proc. **449**, 373 (1997)

Milestone #41

Characterization of best current LED technology

The best current LED technology at Hewlett-Packard is represented by the following three samples, along with their peak emission wavelengths at 20 mA forward current.

Sample Number	Peak Wavelength
E70312D4	468 nm
E70313A3	484 nm
E70310B1	503 nm

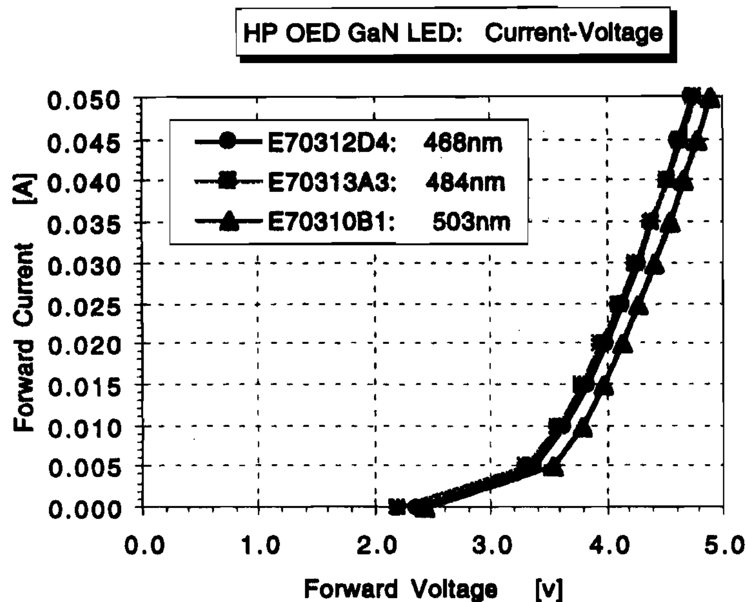

Figure 7. Current-voltage characteristics for HP OED GaN LEDs

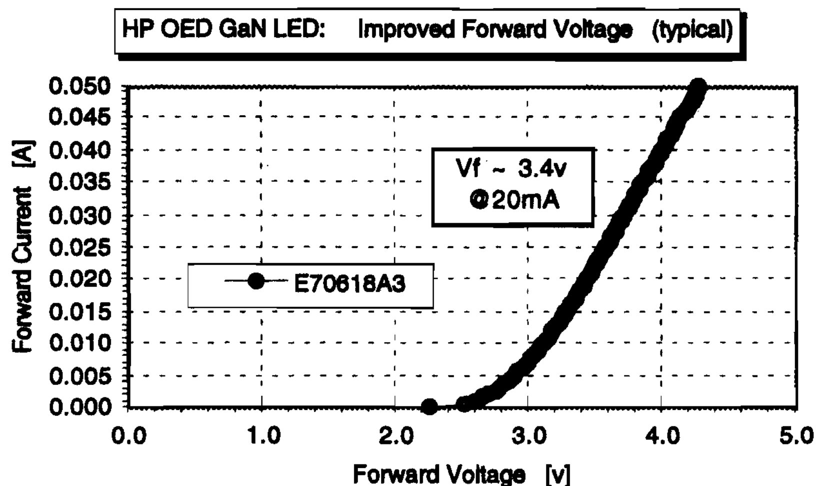

Figure 8. An improved wafer fabrication process reduces the typical forward voltage on a blue HP LED to approximately 3.4 Volts at 20 mA, with a series resistance of 28Ω.

The current-voltage characteristics of these devices are shown in Figure 7. At a typical current rating of 20 mA, the forward (operating) voltage ranges from 3.9 Volts for the short wavelength samples to 4.1 Volts for the 503 nm sample. Recently, an improved wafer fabrication process has been implemented which results in a substantial reduction of the forward voltage. Figure 8 shows a typical blue device fabricated using this new process, in which the forward voltage at 20 mA has been reduced to approximately 3.4 Volts and which has a series resistance of 28Ω.

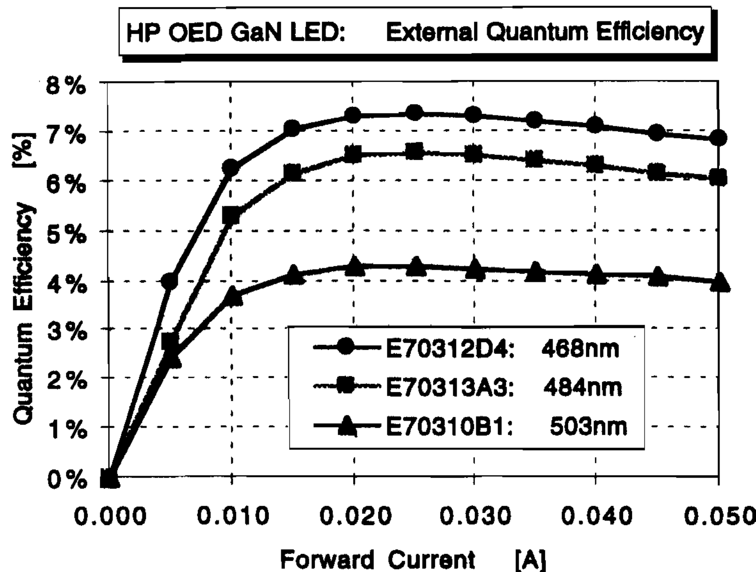

Figure 9. External quantum efficiency versus forward current. Peak quantum efficiencies are obtained at approximately 25 mA for all three devices.

Figure 9 shows the external quantum efficiency of the 468, 484 and 503 nm samples as a function of forward current. The peak quantum efficiency for all three devices is obtained at a drive current of 25 mA. At this current, the peak external quantum efficiencies are 7.34% for the 468 nm sample, 6.55% for the 484 nm sample and 4.28% for the 503 nm sample. At the typical 20 mA operation points the efficiency drops slightly to 7.31%, 6.50% and 4.27% respectively.

Luminous flux as a function of forward current for the three samples is shown in Figure 10. Peak luminous performance in lumens/amp (lumens/watt) for the three samples is 14.65 l/A (3.90 l/W) for the 468 nm sample, 26.60 l/A (7.02 l/W) for the 484 nm sample and 40.21 l/A (9.41 l/W) for the 503 nm sample.

Figure 11 is a normalized plot of typical electroluminescence spectra for blue and green devices when operated at 50 mA. The actual devices measured to obtain the data in this figure are not identical to those for the previous figures, although they are from the same wafers. However, we always observe a blue shift in peak EL wavelength as the drive current is increased, which is opposite to the shift seen for other types of LED materials where junction heating reduces the bandgap. In the InGaN devices, increasing the drive from 20 to 50 mA typically shifts the wavelength by -5 nm at 470 nm and -15 nm at 520 nm. The reason for the blue shift and the wavelength dependence on the shift is not understood at this time.

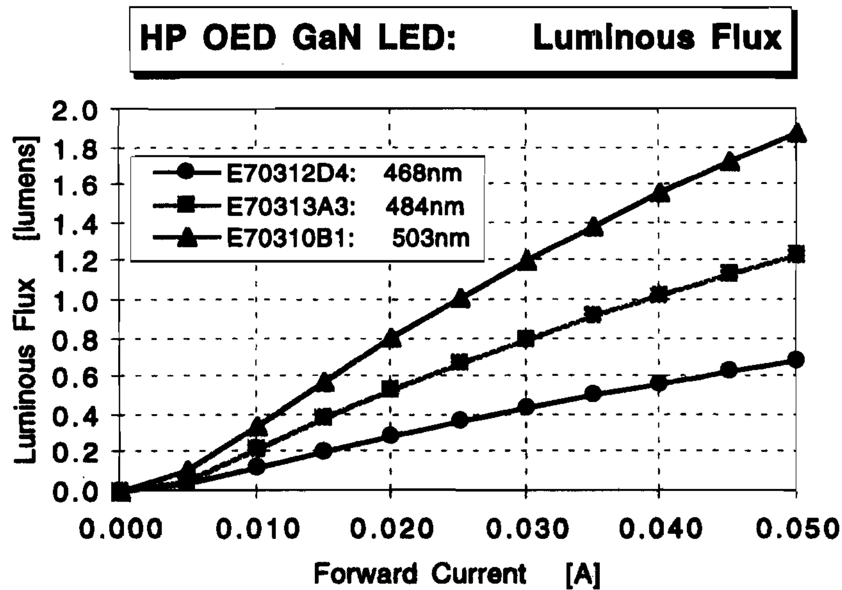

Figure 10. Luminous flux versus forward current for LEDs emitting between 468-503nm. Peak luminous performance is 14.65 l/A (3.90 l/W) for the 468nm sample, 26.60 l/A (7.02 l/W) for the 484nm sample, and 40.21 l/A (9.41 l/W) for the 503nm sample.

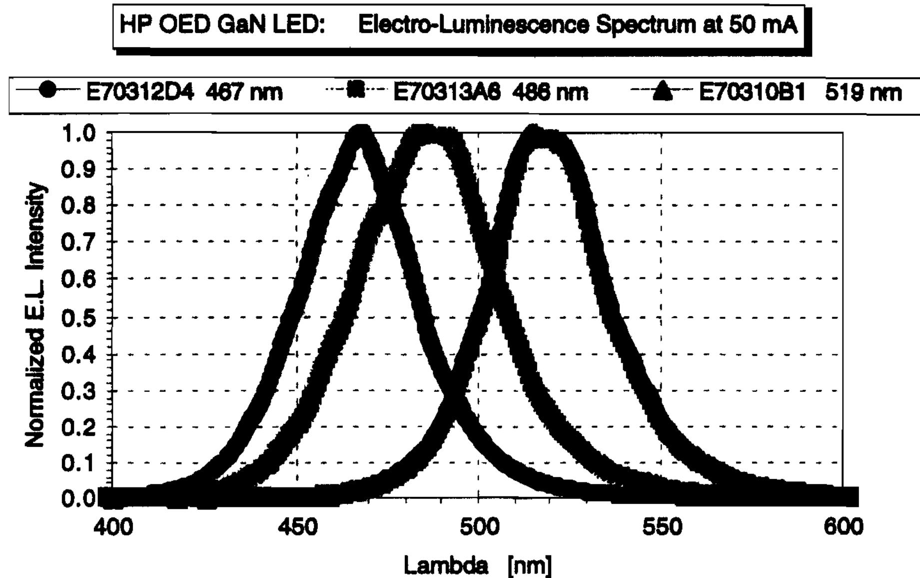

Figure 11. Typical electroluminescence spectra for blue and green LEDs at 50 mA. Increasing the drive from 20 to 50 mA typically shifts the wavelength by -5 nm at 470 nm and -15 nm at 520 nm.

((

Milestone #42

Demonstration of AlGaInN ridge waveguide p/n junction under cw electrical excitation. The goal specification is cw laser action with an emission wavelength in the blue or near-ultraviolet portion of the electromagnetic spectrum. Characterization of AlGaN/InGaN QW diode laser structure.

Demonstration of AlGaInN ridge waveguide p/n junction under cw electrical excitation. The goal specification is cw laser action with an emission wavelength in the blue or near-ultraviolet portion of the electromagnetic spectrum.

Multiquantum well separate confinement heterostructures similar to those previously employed in pulsed experiments were processed to examine emission under cw electrical excitation. The MOCVD-grown structures employed Si doped GaN buffer layers typically 3μm thick, grown on c-plane sapphire substrates. Lower and upper clads were 0.4μm Si- and Mg-doped $Ga_{0.94}Al_{0.06}N$ layers, respectively, while waveguides were typically 0.1μm thick GaN, also Si- or Mg-doped. Doping densities were in all cases approximately 10^{18} cm^{-3}. Active layers consisted of five undoped, 4nm InGaN quantum wells separated by 7nm, Si-doped GaN barriers. Structures were terminated with 0.05μm GaN:Mg contact layers.

As illustrated in Fig. 12, ridges 0.4μm high and 5μm wide were formed by chemically assisted ion beam etching (CAIBE) employing a photoresist mask. Facets and grooves to access n-type layers were likewise formed by CAIBE. Ti/Pt/Au and Ni/Au metallizations were employed for n- and p-type contacts, respectively. Individual diodes were made by scribing the back sides of thinned and polished sapphire substrates and breaking them first into bars along facet directions and subsequent scribing and breaking along the lines separating individual diodes. Widths of the bars varied between 350 and 950μm. Unbonded diodes were tested employing current probes attached to contact pads.

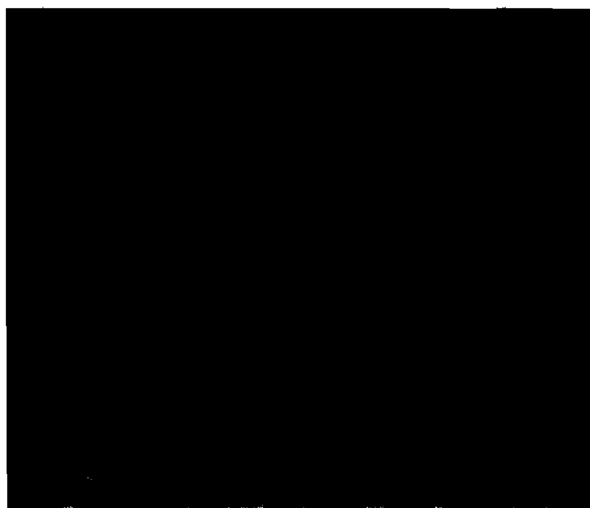

Figure 12. Scanning electron micrograph of a ridge waveguide heterostructure 5μm x 550μm in area, such as that described here. Ridge facets and channels were formed by CAIBE.

While pulsed injection levels as high as $50kA/cm^2$ have now been achieved experimentally, CW excitation above about $5kA/cm^2$ lead to appreciable device heating in the samples and

contacting scheme examined here. An L-I characteristic for excitation up to such densities is shown in Fig. 13. Emission peaked at 385nm. No evidence of stimulated emission was observed, which was to be expected as the facets were angled off normal in processing, owing to loss of temperature control of the CAIBE sample stage during processing. However, it remains possible that the excitation density was also insufficient to sustain lasing, although this is not yet clear. Ongoing work is directed to more reproducibly achieving good contacts, sometimes observed to be in the $10^{-5}\Omega/cm^2$ range. Problems of angled facets have been overcome with repair of the CAIBE.

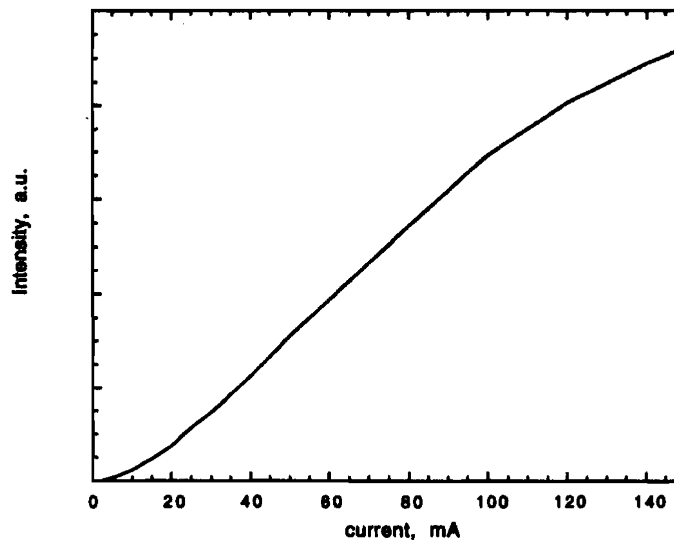

Figure 13. Intensity of electroluminescence versus injection current from a ridge waveguide heterostructure 5μm x 550μm in area. Heating upon cw injection above $5kA/cm^2$ and/or poor facets (angled due to failure of temperature control on CAIBE sample stage) precluded observation of stimulated emission.

Characterization of AlGaN/InGaN QW diode laser structure

We have grown, processed, and tested AlGaN/InGaN/GaN MQW diode structures (grown on sapphire substrates) which have been designed to support stimulated emission under forward-bias conditions. The growth of AlGaN films was studied for use in cladding layers for these injection laser structures. For this application, our interest is in alloys having Al mole fractions in the range $0 \leq x \leq 0.2$. We have grown AlGaN films throughout this range and have also achieved *n*- and *p*-type doping for AlGaN films. Shown below in Figure 14 are (0006) X-ray diffraction data for AlGaN films having different alloy compositions. From the 300K PL spectra and the relative lattice constant, we have determined the alloy composition for these films. These data have been used to grow AlGaN/InGaN double-heterostructure light-emitting diode structures on sapphire substrates.

Using these data, we have grown AlGaN/InGaN MQW heterostructures for X-ray and PL characterization. These structures consist of an InGaN/InGaN SL sandwiched between two AlGaN cladding layers grown on a GaN spacer layer. The X-ray data for one such

structure are shown below in Figure 15. From these data, we can determine the MQW period, average In composition, and the AlGaN composition.

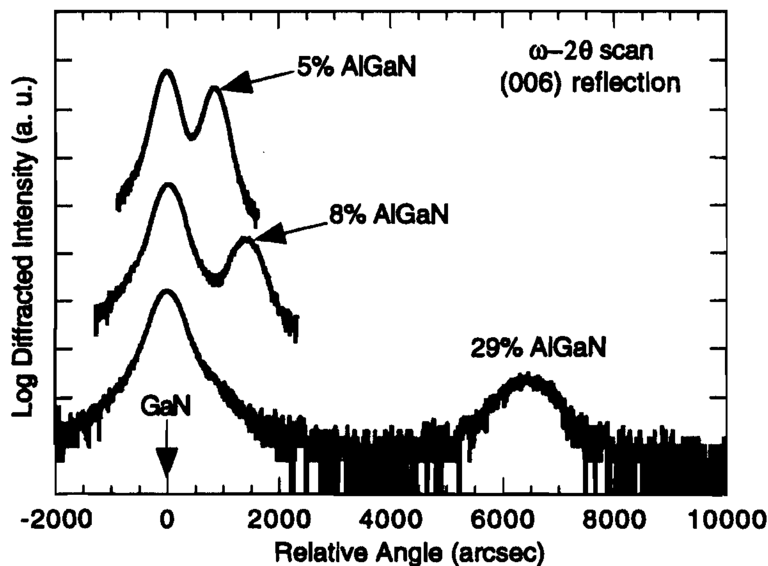

Figure 14. X-ray diffraction data for AlGaN/GaN films grown by MOCVD. The corresponding alloy compositions are indicated.

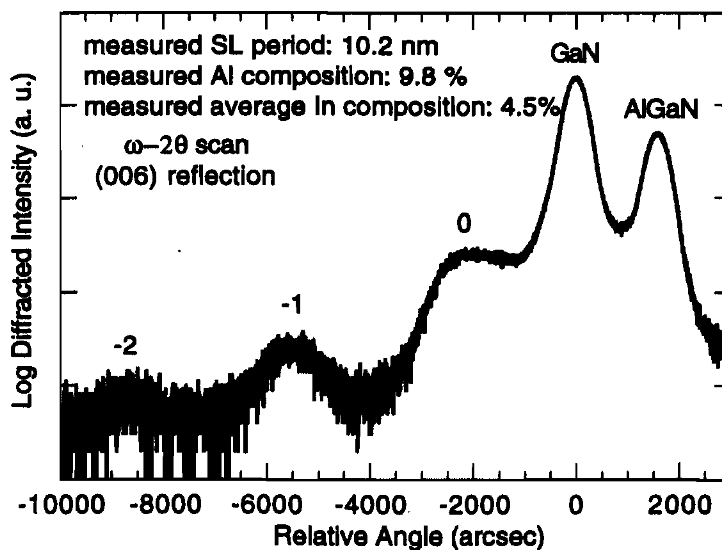

Figure 15. X-ray diffraction scan of an five-period InGaN MQW heterostructure with AlGaN (x~0.098) cladding layers grown on a GaN/sapphire wafer.

Using these undoped AlGaN/InGaN MQW structures, we have grown InAlGaN *p-n* heterojunction diodes. These structures are similar to the devices reported by Nichia. A schematic drawing of the energy gap variation in the device structure is shown below in Figure 16.

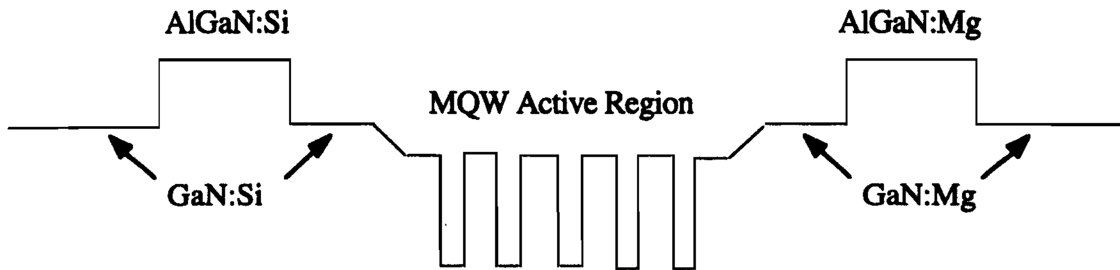

Figure 16. Schematic of the AlGaN/InGaN/GaN/sapphire diode structure.

These wafers were processed at UT-Austin using a mask set developed at UT for this purpose. We have developed the RIE etching process using BCl_3 as the reactive gas. Mesa etching has been developed for top-contact LED's and for injection laser structures. Ohmic contact metallization using Au-Ni for *p*-type contacts and Al-Si for *n*-type contacts has been developed. We have also studied the passivation of RIE-etched surfaces using SiO_2 layers deposited by plasma-enhanced CVD. For blue emission, we have fabricated AlGaN/InGaN MQW LED's having five InGaN wells and four InGaN barriers. The *I-V* characteristics of these devices are shown below in Figure 17. The Ohmic contacts employed are Ti/Al for *n*-type materials and Ni-Au for *p*-type layers.

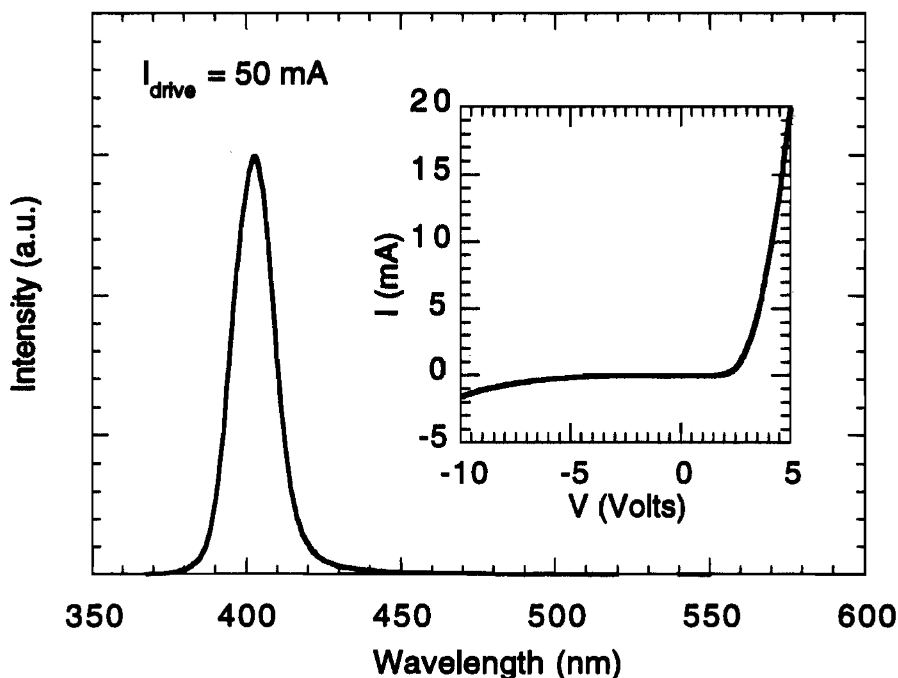

Figure 17. Electroluminescence spectrum and *I-V* plot (inset figure) for a heterostructure LED with an active region consisting of five periods of 35 Å $In_{0.13}Ga_{0.87}N$ quantum wells and 70 Å $In_{0.03}Ga_{0.97}N$ barriers, and containing $Al_{0.05}Ga_{0.95}N$ cladding layers.

We have obtained electroluminescence spectra from these diodes under CW and pulsed operation at room temperature. The devices exhibit a linear L-I characteristic for pulsed mode operation up to about 1.5A. Above this value, heating causes the light output to decrease. Since these device are not actively cooled, the CW operation is strongly affected above currents ~100 mA. We believe that further improvements to the conductivity of the p-type contact region and the improvement of the Ohmic contact performance will significantly improve the high-current performance of these devices. We plant to continue to work on this problem.

Milestone #43

Final Report

Attached.

DEVELOPMENT OF HIGH BANDGAP III-V MATERIALS AND OPTICAL DEVICES

BLUE BAND Consortium

Blue Light and UV Emitters, the Bay Area Nitride Development Consortium

SDL, Inc.	**Hewlett-Packard**	**Xerox PARC**
San Jose, CA	San Jose, CA	Palo Alto, CA

Prof. Russell D. Dupuis, University of Texas at Austin

Prof. Ted Moustakas, Boston University

ATMI, Danbury, CT

AXT, Dublin, CA

August 1997

Final Report

Other Transaction # MDA972-95-3-0008

June 1995 through August 1997

DEFENSE ADVANCED RESEARCH PROJECTS AGENCY

3701 North Fairfax Drive

Arlington, VA 22203-1714

Distribution authorized to U.S. Government agencies only to protect information not owned by the U.S. Government and protected by a contractor's "limited rights" statement, or received with the understanding that it not be routinely transmitted outside the U.S. Government. Other requests for this document shall be referred to DARPA Security and Intelligence Office.

CONTENTS

1 EXECUTIVE SUMMARY 3

2 KEY ISSUES 4

3 PRINCIPLE RESULTS 5

3.1 Materials Development 5

3.1.1 HVPE Substrates 5

3.1.2 Alternative Substrates 8

3.1.3 MOCVD Growth of GaN-based Epilayers 8

3.1.4 Materials Properties 10

3.2 Device Development 14

3.2.1 LEDs 14

3.2.2 Laser Diodes 15

4 CONCLUSIONS 16

4.1 Devices 16

4.2 Materials 16

5 RECOMMENDATIONS FOR FUTURE WORK 17

5.1 Substrates 17

5.2 Growth 18

5.3 Properties 18

5.4 Processing 19

5.5 Devices 19

1 Executive Summary

The goal of the Blue Band program was the development of nitride materials for the demonstration of visible LEDs and laser diodes spanning the near ultra-violet (UV) to yellow regions of the spectrum. The program teamed SDL, Inc.; Hewlett Packard (HP); Xerox; the University of Texas at Austin; Boston University; Advanced Technology Materials, Inc. (ATMI); and American Xtal Technology (AXT). Significant progress was made in all phases and aspects of the program, and all milestones were met.

Device highlights include the demonstration of single quantum well, blue nitride LEDs with over 7 mW of output power at 50mA and a maximum external quantum efficiency of 7.3% at 25 mA. These values are almost twice the original program goal. Further, critical elements of a low cost, high volume manufacturing process for nitride LEDs were also developed. In lasers, stimulated emission has now been observed in numerous optically pumped single and multi-quantum well structures. Delays in delivery of a custom dry etcher precluded demonstration of a laser diode, but all key elements of such a demonstration are now in place. Specifically, materials properties equal or exceed those of all competing efforts in all regards critical to demonstration of a laser diode, contacts displaying excellent adhesion and low resistivities have been developed, and a dry etching process yielding exceptionally controllable and smooth facets has now been demonstrated. Based on these results, realization of a high quality diode laser appears close.

Much of the Blue Band program was dedicated to developing underlying AlGaInN materials and analyzing intrinsic and extrinsic properties critical to device design, performance, and degradation. Significant strides were made in the MOCVD and MBE growth of nitride epilayers and in the development of alternate substrates, particularly HVPE-grown GaN. Record results include electroluminescence of exceptional spectral purity (*e.g.* 16nm for 450nm emission, 30nm for 500nm) in single quantum wells with quantum efficiencies of >2%. P-type doping in the 10^{18}'s cm^{-3} was routinely achieved, with crisp device turn-on voltages of 3-3.2V and differential contact resistivities appreciably lower than $10^{-4}\ \Omega/cm^2$.

The program contributed greatly to understanding of underlying structural, optical, and electronic characteristics of (Al,Ga,In)N alloys and heterostructures, which is likely to be critical to the continued development of competitive electronic and optoelectronic devices based on these materials. Considerable strides were made in elucidating both the energetics and microscopic mechanisms of doping, compensation, and formation of deep levels. Electronic properties such as band offsets and effects of strain were calculated. The classes and natures of structural defects were studied in detail, as were the intrinsic and extrinsic optical signatures of the materials. As degradation of even the best nitride-based laser diodes has been found to be intimately linked to microstructure, these studies are of particular practical importance. Each body of work has already guided both design of devices and development of improved growth processes.

The Blue Band program yielded significant technological and scientific advances, and has provided a sound foundation for future work. It is our belief that the progress underscores the merits of further pursuing several directions. Foremost amongst these are continued development of alternate substrates, particularly HVPE-grown GaN; refinements to epitaxial growth processes, aided by modeling where practical; further characterization of

the intrinsic and extrinsic nitride properties now known to influence device performance and degradation; refinement of processing techniques, particularly in the area of dry etching; and concerted efforts to develop surface emitting lasers and to improve the design and performance of edge emitters.

2 Key Issues

Key Blue Band goals were demonstration of efficient LEDs and optically and electrically pumped lasers. However, while devices were the primary goals, development of high quality GaN-based materials was the technical emphasis. The program addressed the crystal growth of GaN and related films by MOCVD; the fabrication and utility of candidate substrate materials; growth processes appropriate to achieving high quality buffer layers; materials characterization to determine crystallographic, electronic, and optical properties of GaN alloys; and calculations of underlying electronic properties.

Blue Band targeted the following specific issues germane to the demonstration of commercially viable, GaN-based visible emitters:

Growth of GaN-based materials. Realization of high performance emitters demands growth procedures yielding quantum-well heterostructures of high optical quality as well as low-resistivity p- and n-type epilayers. Issues of primary importance were demonstration of high p-type doping levels, fabrication of active layers with high quantum efficiencies and/or narrow spectral emission, and suppression of structural problems such as pitting and cracking.

Substrate fabrication and definition. Important to the growth of improved GaN films is the development of substrates crystallographically better matched to AlGaInN than conventional (0001) sapphire. Alternatives targeted under BlueBand were development of bulk GaN substrates as well as undoped and Si-doped GaN substrates grown by vapor phase epitaxy on sacrificial substrates. Utility of these substrates was examined by growing epilayers employing both molecular beam epitaxy and metalorganic chemical vapor deposition. M-plane sapphire, ZnO, and 6H-SiC substrates were similarly evaluated.

Advanced materials characteristics. Extensive theoretical and experimental investigations of structural, electrical, and photoelectric properties of nitrides were undertaken, largely at Xerox. Systematic studies of extended defects were performed, ranging from fundamental studies of film/substrate interfaces, to properties of dislocations and quantum wells, to analyses of defects related to growth and fabrication of diode heterostructures. Structural characteristics of both thin epilayers and thick, HVPE-grown films were studied. A comprehensive study of native defects, impurities (dopants and contaminants), and band structure of the III-V nitrides was undertaken at Xerox. At issue were doping limits, compensation, and related phenomena. The activation and properties of Mg acceptors were examined in particular detail, in accordance with the importance and difficulty of obtaining high densities of activated p-type dopants.

LED development. The primary issue addressed by HP was the development of a cost effective manufacturing process for high brightness blue and blue-green

nitride LEDs. This objective required the development of nitride MOCVD growth technology employing an EMCORE high volume production reactor, the establishment of routine characterization techniques for rapid feedback of information critical to the epi growth team, and the examination of various device designs to achieve the desired wavelengths and maximize light output. It was also necessary to develop new wafer fabrication, die fabrication and packaging technologies specifically for nitride LEDs, in order to initiate high volume manufacturing and investigate low-cost production technology. A goal of the program was to demonstrate double heterostructure blue LEDs with greater than 4 mW output and greater than 4% external quantum efficiency at 20 mA forward current.

Laser diode development. SDL was charted with developing GaN-based laser diodes. This demanded development of high structural quality AlGaN cladding and InGaN active layers; effective p- and n-type doping of clads; realization of efficient, spectrally narrow optical emission from quantum-well active regions; development of contacting and device definition processes; and design of appropriate device structures. Goals of the program were to demonstrate optically and electrically pumped blue or near-UV stimulated emission in ridge waveguide heterostructures.

3 Principle Results

3.1 Materials Development

3.1.1 HVPE Substrates

Both bulk GaN and GaN grown by hydride vapor phase epitaxy (HVPE) were explored under Blue Band. Based on the strength of ATMI's HVPE material, as judged largely by the optical, structural, and morphological quality of epilayers overgrown on their material, this approach alone was pursued for the latter half of the program.

HVPE GaN-on-sapphire

GaN layers were initially grown on sapphire wafers to establish a baseline for the HVPE process. The high quality of these layers warranted further investigation and evaluation beyond simple use as a baseline. Attractive characteristics of these layers included good crystallinity, low defect densities, high conductivities, and good uniformity. Homoepitaxy was found to be easy, proceeding without need of a low temperature buffer layer and without the introduction of additional defects at the MOVPE/HVPE interface. Slight texture of the HVPE surface was smoothed by MOVPE growth. Most importantly, LEDs fabricated by ATMI, HP, and Xerox employing these layers displayed both high brightness and excellent spectral purity.

Good crystallinity across 2" diameters was evidenced by typical double crystal x-ray rocking curve halfwidths < 300 arcsec, with best FWHM ≈ 184 arcsec, indicative of reduced strain compared with MOVPE GaN on sapphire. Typical defect densities of 10^9 cm^{-2} were measured, with the best wafers displaying $\approx 10^8$ cm^{-2}. Nominally undoped,

10μm thick GaN layers showed good electrical conductivity, with $n \approx 10^{18}$ cm^{-3} and μ_n=90 cm^2/V-s. Uniformity was ±10% in thickness across a 2 in. diameter wafer.

Figure 1 illustrates the high quality of an (Al,In,Ga)N MQW LED fabricated by Xerox on a 10 μm thick layer of HVPE GaN-on-sapphire. The excellent quality of the material grown on these substrates is indicated by the well-resolved InGaN/GaN superlattice, GaN and AlGaN x-ray features (a), as well as the very narrow room temperature EL peak at 420 nm (b).

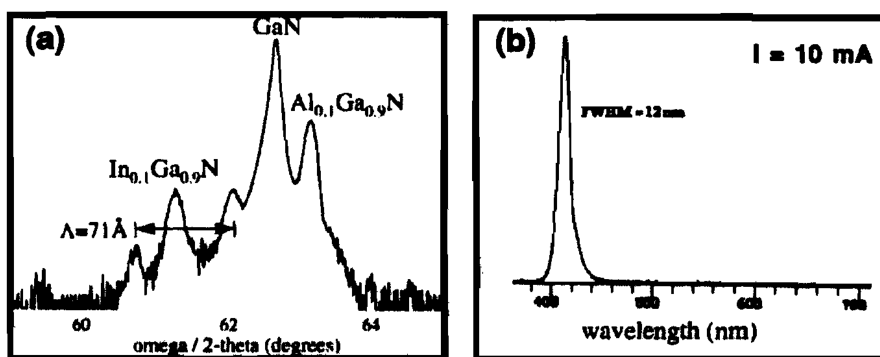

Figure 1. (a) X-ray diffraction and (b) room temperature electroluminescence from an AlGaInN MQW LED grown on HVPE GaN-on-sapphire substrates. The InGaN/GaN MQW active region is well resolved by XRD and the EL emission is exceptionally narrow.

A hydride VPE reactor was also designed and constructed at Boston University. The design stressed issues related to gas phase mixing, flow uniformity and minimization of parasitic reactions between the reactor and the growing film. GaN films grown on (0001) sapphire at rates of 10 - 100 μm/h were transparent and uniform, with smooth surface morphologies. Samples were generally heavily n-type doped (10^{19}-10^{20} cm^{-3}). Substrates were used for the MBE growth of GaN, InGaN and AlGaN. Best growth was obtained under Ga-rich conditions, at 700 to 750°C. The (0002) XRD rocking curve and the photoluminescence spectra of the GaN substrate and GaN films were found to be identical. Thick InGaN and AlGaN films were found to be transparent and smooth. The AlGaN films exhibited atomic long-range order, as evidenced by the appearance of otherwise forbidden (0001) and (0003) XRD peaks in θ-2θ.

Free-standing GaN

Considerable progress was made towards achieving free-standing GaN, at ATMI. The growth of high quality GaN on sacrificial Si templates was demonstrated, as was rapid etching of the Si template at the growth temperature.

The crystallinity, surface morphology, and optical characteristics of GaN grown on sacrificial Si wafers were significantly improved under this program. Each is now comparable to those of GaN on sapphire. Figure 2 compares double crystal x-ray diffraction characteristics of GaN grown on sapphire and Si. The FWHM obtained from a 2 μm thick GaN layer grown on Si was ~790 arcsec, which is comparable to that of GaN on sapphire grown to a similar thickness. The figure, as well as other work, suggests that

considerable improvements will be realized by growing thicker GaN on Si. Despite the excellent crystallinity of thin films such as these, to date it has not been possible to grow to thicknesses exceeding 2 μm, due to cracking during cooldown. Differences in the thermal expansion coefficients of GaN and Si result in sizable tensile stresses upon cooldown, bowing the GaN films and creating microcracks. However, as there is no evidence of cracking at the growth temperature, removal of the Si substrate at the growth temperature promises to eliminate these problems and permit growth of thicker, higher quality GaN.

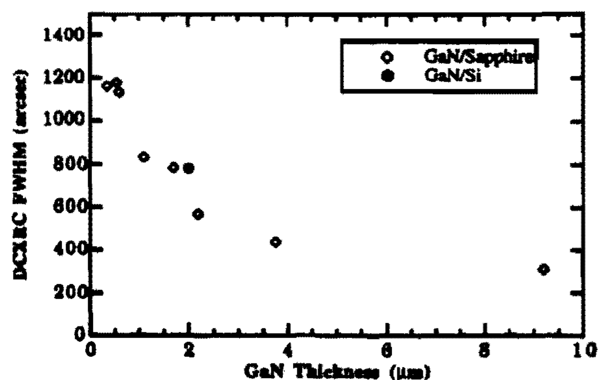

Figure 2. Comparison of the FWHM of double crystal x-ray rocking curves measured on HVPE GaN on sapphire and Si as a function of thickness. The crystallinity of GaN/Si is similar to that of GaN/sapphire for the same GaN thickness.

Feasibility of the GaN/Si template was demonstrated by etching Si at elevated temperatures to remove the substrates *in situ*. Backside etching with HCl was investigated for a variety of HCl partial pressures, yielding Si etch rates in excess of 25 μm/min. Complete removal of a Si wafer was achieved in less than 10 minutes. To make combined growth and etching practical, further attention must be given to isolating the growth and etch chambers from one another to prevent deleterious reactions. Nevertheless, the absence of cracking of the GaN at the growth temperature and the achievement of high Si etch rates demonstrates the feasibility of this approach.

Intentional Si-doping

Although the HVPE GaN was electrically conductive as grown, higher conductivities are desirable for devices relying on lateral transport. Nominally undoped HVPE GaN grown on sapphire is conductive, mainly due to a high density of charge at the GaN/sapphire interface. The bulk of the material is lightly doped ($N_d \approx 2x10^{16}$ cm^{-3}). Si-doping the HVPE GaN with silane (SiH_4) was demonstrated over the range $5x10^{16}$ to $8x10^{18}$ cm^{-3}. Comparison of SIMS and Hall results revealed that all of the Si is electrically active, even for the highest doping densities. Electron mobilities of the Si-doped samples was in all cases higher than for undoped HVPE GaN. At $n = 8\ x10^{18}$ cm^{-3}, the room temperature electron mobility was 160 cm^2/V-s (cf. mobility of undoped HVPE GaN $\approx$ 50-70 cm^2/V-s at a similar thickness). This enhancement in mobility is likely a consequence of transport away from the low mobility interface region. The ~5-fold decrease in sheet resistance afforded by this technique demonstrate the utility of HVPE GaN:Si layers in reducing the series resistances in lateral geometry LEDs and laser diodes.

3.1.2 Alternative Substrates

Growth by molecular beam epitaxy (MBE) of GaN and AlGaInN on 6H-SiC, ZnO, and M-plane sapphire was examined at Boston University. In the case of 6H-SiC substrates, high quality III-V nitride films could be grown without employing a low temperature buffer. GaN-films grown under Ga-rich conditions show a streaky RHEED pattern with (2x2) surface reconstruction. SEM examination of the surface morphology indicated an exceptionally smooth surface. XRD analysis yielded a FWHM of 3.5arcmin. TEM microscopy revealed an excellent epitaxial relationship between the substrate and film. Such films could be doped n-type to levels of 10^{19} cm^{-3} (with a room temperature mobility of 200 cm^2/V-s) to 10^{21} (mobility 10 cm^2/V-s and resistivity 10^{-4} Ω-cm). Such values are very high, suggesting a very low level of compensation. $Al_xGa_{1-x}N$ alloys were found to exhibit significant atomic long range order.

The advantage of ZnO as a potential substrate is that one can develop lattice matched heterostructures of InGaAlN in the spectral region from 2.8 to 4.5 eV. As single crystalline ZnO substrates are not available at reasonable sizes and cost, GaN and InGaN alloys were grown on sputtered ZnO thin films. It was observed that the ZnO substrate had a streaky RHEED pattern at a temperature below 400°C, but that the pattern deteriorated upon heating to the growth temperature of about 650°C. The diffraction pattern become spotty and weak, suggesting surface degradation due to dissociation of the substrate. We concluded from these studies that ZnO needs to be encapsulated by a low temperature buffer layer to prevent this dissociation. Films grown on such substrates were indeed found to have reasonable transport and optical properties.

GaN films were grown on M-plane (10-10) sapphire, with or without a low temperature buffer. The growth conditions explored led to (11-22) and (10-10) epilayers. These planes are not well matched to the M-plane sapphire; the desired plane to minimize mismatch with the sapphire (10-10) lattice in the two perpendicular axes is (10-13). (The mismatch is 2.6% in the GaN [1210]/sapphire [0001] direction and 1.9% in the GaN [3032]/sapphire [2110] direction). Further work is required to identify conditions for the epitaxial growth of the (10-13) plane.

3.1.3 MOCVD Growth of GaN-based Epilayers

At the University of Texas at Austin, a two-step MOCVD process was employed to grow heteroepitaxial InGaN/GaN and AlGaN/GaN films and quantum-well heterostructures on (0001) sapphire substrates. The epitaxial layers were grown in an EMCORE D125 vertical rotating-disk MOCVD reactor at a pressure of ~76 Torr using trimethylgallium (TMGa), trimethylindium (TMIn), trimethylaluminum (TMAl), and high-purity ammonia (NH_3) as sources. Dopant precursors employed are (bis)cyclopentadienylmagnesium (Cp_2Mg) for p-type doping and silane (SiH_4) for n-type doping. Typical precursor molar flow rates used in this study were: TMGa $\approx 3.7 \times 10^{-5}$ mole min^{-1}, TMIn $\approx 1.7 \times 10^{-5}$ mole min^{-1}, TMAl $\approx 2.0 \times 10^{-5}$ mole min^{-1}, and NH_3 $\approx 5.3 \times 10^{-2}$ mole min^{-1}. The heteroepitaxial InGaN and AlGaN films were deposited on GaN films grown on thin (~25 nm) low-temperature (~520°C) GaN buffer layers atop (0001)-oriented Al_2O_3 substrates. Growth temperatures were T_g = 760°C to 830°C for InGaN, and 1050°C-1080°C for GaN and AlGaN. The GaN and AlGaN films were grown in a H_2 ambient and the InGaN layers in a predominantly N_2

ambient. However, for all of the epitaxial layers in this study, H_2 was used as the alkyl source carrier gas. Typical growth rates were $R_g \approx 8$ nm/min (InGaN), 50 nm/min (GaN), and 14 nm/min (AlGaN).

Growth of GaN

A systematic study of the growth and photoluminescence (300K and 4.2K) characterization of unintentionally doped GaN on both exact and vicinal (0001) sapphire substrates was performed. A comparison of the 300K and 4.2K optical characteristics of the samples grown simultaneously on different substrates indicates that a higher photoluminescence intensity is measured for films on misoriented substrates.

A study of p- and n-type doping of GaN films using (bis)cyclopentadienylmagnesium and silane as dopants, respectively, was also completed. P-type films with 300K free hole concentrations $p \approx 3x10^{17}$ cm^{-3} were routinely grown. Recently, GaN:Mg films with hole concentrations $p \approx 2x10^{18}$ cm^{-3} at room temperature have also been successfully demonstrated.

Growth of AlGaN

Growth of AlGaN films was also studied. Alloys with Al mole fractions in the range $0 \leq x \leq 0.2$ were examined, consistent with our interest in candidate cladding layers for laser structures. AlGaN films were grown throughout this range, and both n- and p-type doping were achieved. Alloy compositions were determined from 300K PL spectra and relative lattice constant measurements. These data were used to grow AlGaN/InGaN double-heterostructure LED structures on sapphire substrates, as well as AlGaN/InGaN MQW heterostructures for X-ray and PL characterization. The latter structures consisted of an InGaN/InGaN SL sandwiched between two AlGaN cladding layers grown on a GaN spacer layer. Structures were analyzed to ascertain the MQW period, average In composition, and the AlGaN composition.

Growth of InGaN

The alloy composition of thick (80-200 nm) InGaN double-heterostructure films grown in this work was determined by 300K PL spectra as well as X-ray diffraction rocking curves and ω-2θ scans to determine the lattice parameter of the epitaxial film with respect to that of the thick GaN heteroepitaxial "substrate". We have studied 300K and 4.2K photoluminescence (PL) from these structures and have determined the relative PL intensities for MQWs having different periods, quantum well thicknesses, doping concentrations, and alloy compositions. We conclude that Si-doped MQW structures have higher PL intensities than undoped structures.

The high quality of these films is further indicated by demonstrations of lasing under optical excitation. Bulk InGaN films were optically pumped using a pulsed Ar-ion laser at 77K to determine the optical quality of the materials. Laser operation was achieved in a "front-to-back" (VCSEL) mode with optical feedback provided by the InGaN-air and InGaN-sapphire interfaces. Similarly, optically pumped laser operation of an InGaN MQW structure at 300K was obtained using pulsed N_2 laser excitation.

InAlGaN Diodes

The data contained on this page are subject to the restrictions outlined on page 1

The UT-Austin group has also grown, processed, and characterized GaN *p-n* junction LEDs, and AlGaN/InGaN MQW LEDs. We have developed an RIE etching process using BCl_3 as the reactive gas. Mesa etching was developed for top-contact LEDs and for injection laser structures. Ohmic contact metallization using Au-Ni for p-type contacts and Al-Si for n-type contacts was likewise developed. It was important to develop a process yielding smooth, vertical mesa side walls. Our lithographic process is well suited to this, providing a smooth mask which can withstand the RIE process.

For blue emission, we have fabricated InGaN MQW LED's having five InGaN wells and four InGaN barriers. We have characterized the *I-V* characteristics of the InGaN diodes and compared them to commercially available Nichia and Cree InGaN LEDs. Our devices compare favorably in terms of the reverse breakdown voltage and the forward turn-on voltage. The series resistance of our diodes is, however, somewhat higher than these commercial devices. We are working on improved Ohmic contacts and continuing to develop our device processing techniques.

3.1.4 Materials Properties

Microstructure of Nitride Semiconductors

Extensive transmission electron microscopy revealed a wide variety of extended structural defects in GaN-based epilayers. Limitations in the film quality were observed to result from differences in thermal expansion and lattice mismatch with available substrates; examples are the evolution of pits and the formation of cracks found in alloys containing In or having greater than 7-8% Al content. Thick films of GaN grown by HVPE were also studied as potential alternative substrates for devices.

Dislocations appear to be inherent in nitride heterostructures for light emitting diodes due to the lattice and thermal mismatches between films and currently available substrates. Typical defect densities range from 10^9 - 10^{10} dislocations/cm^2. Line dislocations were identified as having screw, edge, and mixed character. A fraction of c-dislocations were found to be coreless (nanopipes), with screw character.

Basal plane stacking faults are found in low-temperature GaN buffer layers grown on sapphire substrates. Appropriate buffer layer growth conditions can result in smooth films and affect the defect density. Inversion domain boundaries were observed in films grown by all techniques examined: MOCVD, MBE, and HVPE.

As illustrated in Fig. 3, pit defects were found in many InGaN/GaN multiquantum well structures. Pits form near dislocations, with a density which generally increases with In composition and quantum well thickness.

In keeping with the rich microstructure observed in nitride epilayers, spatial inhomogeneities in luminescence emission energy were observed in QWs with $x>0.20$. Cathodoluminescence studies indicate strong spatial variations in both intensity and wavelength with increasing indium composition.

The data contained on this page are subject to the restrictions outlined on page 1

Figure 3. Pits associated with dislocations in InGaN quantum well structures.

Atomic long-range ordering was observed for the first time in AlGaN alloys grown by MBE on sapphire, 6H-SiC and VPE-GaN. It was shown that the degree of ordering is greatest for approximately 50% Al, as expected theoretically. The degree was found to be sensitive to a number of kinetic factors such as the ratio of III-V fluxes or the presence of Si dopants. Such ordering may have implications in the design of devices since the ordered phase has a different energy gap than the random phase, changing the nature of AlGaN used as a well or as a barrier.

Analysis of HVPE grown GaN revealed defect densities to be less than $5x10^8$ dislocations/cm^2 for films 15μm or greater in thickness. Films as thick as 80μm were found to be crack-free. Any defect structure that was found at the top surface of HVPE GaN substrates was typically replicated in InGaN/GaN overlayers grown on these substrates for device applications.

Electrical Characterization of III-V Nitrides

Extensive electrical and photoelectric measurements were performed on III-V nitrides. Successful p-type doping is particularly problematic and critical in the nitrides, leading us to investigate in detail the activation and properties of Mg acceptors. Shallow donors and deep level defects were also characterized.

Mg acceptors were found to be passivated by hydrogen in GaN:Mg, as grown by MOCVD. As illustrated in Fig. 4, the bond-stretching mode for the Mg-H complex is at 3125 cm^{-1}, in good agreement with computational results. Rapid thermal annealing of GaN:Mg was found to dissociate the Mg-H complex, electrically activating the Mg acceptors. This dissociation is illustrated by the drop in the Mg-H infrared absorption peak in Fig. 4.

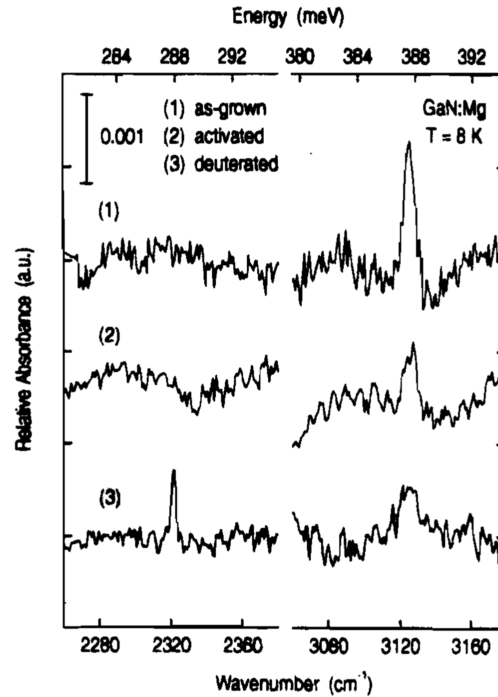

Figure 4. Infrared absorption spectra of Mg-H and Mg-D complexes in GaN:Mg.

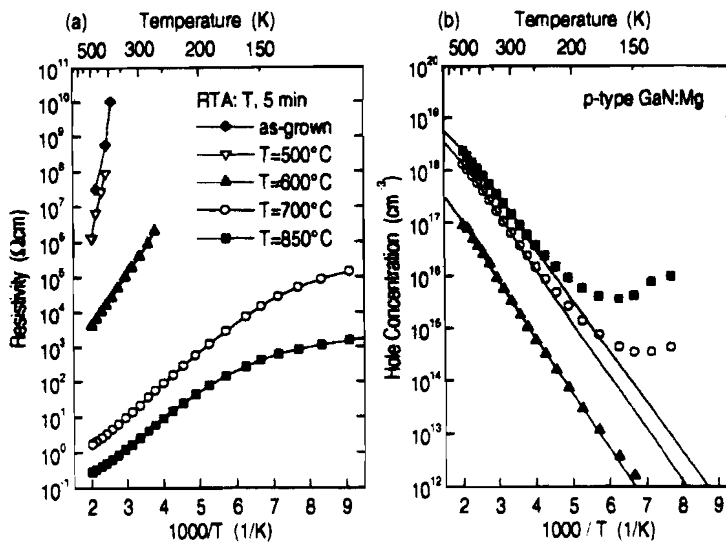

Figure 5. Variable-temperature Hall effect measurements for GaN:Mg processed by rapid thermal annealing for 5 min at different temperatures T: (a) resistivity and (b) hole concentration.

Fig. 5 illustrates results of variable-temperature Hall effect measurements on *p*-type GaN:Mg, which yield an acceptor ionization energy of ~170 meV. The figure also shows results of systematic annealing studies, which were used to optimize the activation of Mg

acceptors. Combining such Hall effect data with photoluminescence (PL) results, it was demonstrated that the generally observed red-shift of a prominent PL band upon thermal annealing of GaN:Mg is not directly due to activation of the Mg acceptors. Consequently, the magnitude of the red-shift (250 meV) does not relate to the acceptor ionization energy.

Deep level transient spectroscopy (DLTS) and optical-DLTS were performed on n-type and p-type GaN and on n-type AlGaN. In each case the energies and densities of detected discrete levels were catalogued. Detected deep level densities were $\lesssim 10^{16}$ cm^{-3} and therefore cannot be responsible for the high levels of compensation (e.g., 10%) generally found in activated Mg-doped GaN.

Correlated Hall effect and SIMS measurements were used to determine an ionization energy for silicon donors of ~18 meV and provided evidence that oxygen is a shallow donor in GaN with an ionization energy of ~32 meV. Oxygen is an important source of unintentional *n*-type doping.

Doping and Band-structure Engineering of III-V Nitrides

A comprehensive theoretical study of native defects, impurities (dopants and contaminants), and band structure of the III-V nitrides was performed at Xerox. A thermodynamic formalism used values calculated with the first-principles density-functional-pseudopotential approach to produce *formation energies* of defects and impurities, from which conclusions can be drawn about properties such as doping limits and compensation.

For the case of n-type material, nitrogen vacancies are found *not* to be responsible for n-type conductivity. Silicon and oxygen are shallow donors and can be incorporated in large concentrations. We ascribe n-type conductivity to unintentional incorporation of these impurities. These predictions have been confirmed by combined Hall effect and SIMS studies.

Oxygen (but not silicon) undergoes a transition from a shallow to a deep center in GaN under pressure, and in $Al_xGa_{1-x}N$ alloys. Gallium vacancies are the likely source of the yellow luminescence.

For the case of p-type material, the hole concentration is limited by Mg solubility; incorporation of Mg on other sites (interstitial, or N site) is energetically unfavorable and therefore not a problem. A study of alternate acceptor impurities produced no candidates superior to Mg. Hydrogen is found to have a beneficial effect on p-type doping: it suppresses compensation and enhances acceptor incorporation. The mechanisms for acceptor activation by post-growth annealing have been established. H diffuses readily in p-GaN, but not in n-GaN.

Some compensation of p-type material by nitrogen vacancies may occur; the vacancies are metastable, explaining observations of persistent photoconductivity. The formation energy of the vacancies decreases as x increases in $Al_xGa_{1-x}N$ alloys; vacancy compensation is the likely explanation for the decreased p-type doping efficiency in $Al_xGa_{1-x}N$. Oxygen incorporation (contamination) is likewise detrimental to obtaining good *p*-type doping.

The data contained on this page are subject to the restrictions outlined on page 1

Last, "natural" valence-band offsets between the (unstrained) nitride semiconductors have been derived. For AlN/GaN the offset is found to be 0.7 eV. For GaN/InN it is only 0.3 eV, smaller than desirable for hole confinement. Deformation potentials describing effects of strain on band structure have also obtained.

3.2 Device Development

3.2.1 LEDs

All program goals and milestones related to the development of LEDs were achieved or exceeded, at HP. An EMCORE reactor was installed in mid-1995. Since then, MOCVD epitaxial growth processes were developed to produce high quality n- and p-type GaN, AlGaN and InGaN layers. Equipment and techniques have been established to routinely characterize all wafers grown using a variety of methods including single point and wafer scanning room temperature photoluminescence, variable temperature Hall effect and x-ray crystallography. A rapid device fabrication process was developed to provide rapid feedback of device performance data to the epi growth team, often in less than one day. Both AlGaN/GaN and InGaN/GaN heterostructures have been grown, with over 30% In incorporated in the InGaN active region of double heterostructure devices. All wafer fabrication, die fabrication and packaging processes required for low cost, high volume manufacturing of nitride LEDs have been developed including reactive ion etching of n- and p-type GaN and the deposition of ohmic n- and p-type metal contacts. Several device structures have been fabricated and evaluated, culminating in the demonstration of single quantum well nitride blue LEDs with over 7 mW of output power at 50 mA and a peak external quantum efficiency of 7.3% at 25 mA, almost twice the original program goal.

Figure 6. Light emitting diode employing a single quantum well InGaN active layer.

3.2.2 Laser Diodes

Work to develop GaN-based laser diodes at SDL has met all milestones and has achieved the goal of optically pumped lasing. A laser diode has not yet been demonstrated. Development of growth processes has resulted in films equaling or exceeding those fabricated elsewhere in all respects important to a laser. Crack- and pit-free laser structures have been routinely grown on sapphire substrates. Both p- and n-type doping levels in the 10^{18}'s have been demonstrated. InGaN active layers have been grown with electroluminescent half-widths significantly narrower than reported elsewhere. Typical halfwidths are 16-20nm for 450 nm emission and 30nm for 500nm emission. These are achieved with good high-injection electroluminescent quantum efficiencies, exceeding 2% for single quantum well structures. Optically pumped stimulated emission was readily achieved in such structures, as illustrated in Fig. 7.

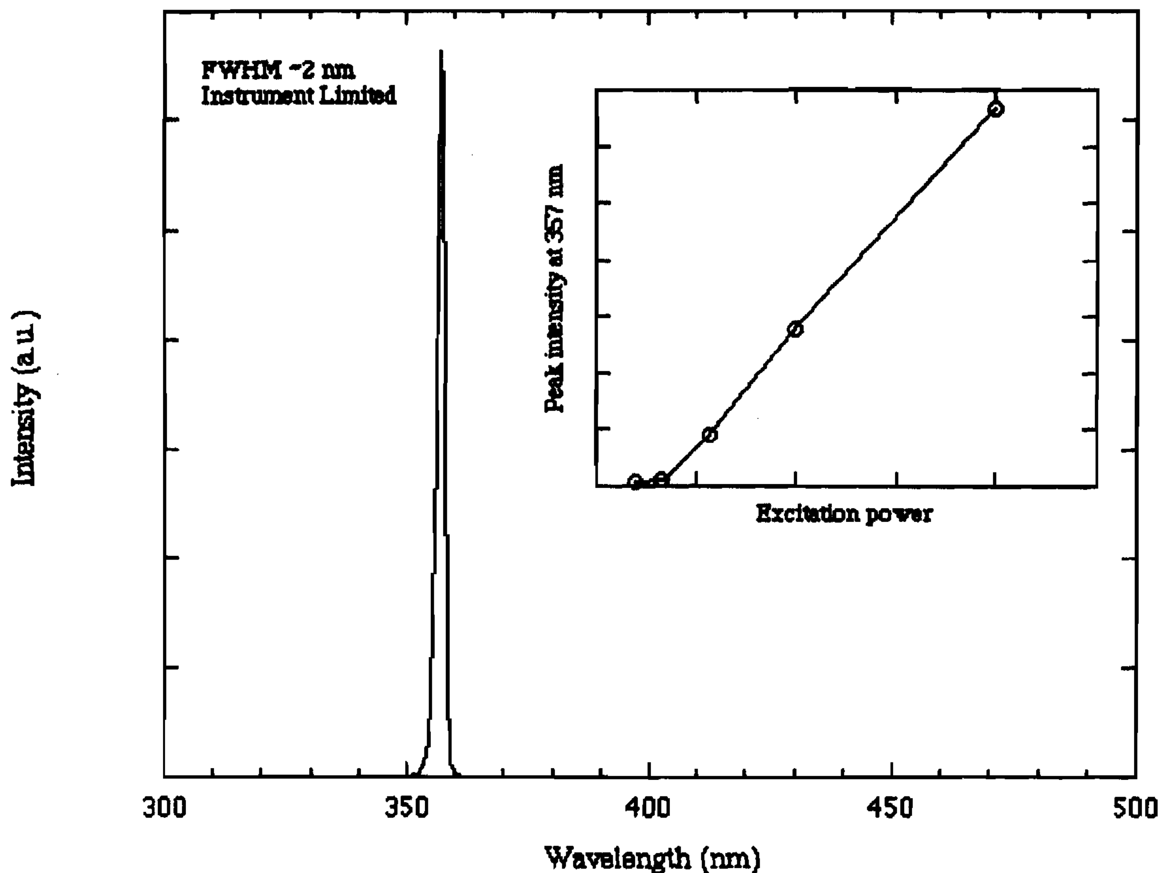

Figure 7. Optically pumped stimulated emission at 300K from a ridge waveguide structure employing a GaN active layer.

A full device fabrication process has been developed, employing chemically assisted ion beam etching to achieve exceptionally smooth facets and sidewalls and employing metallization processes yielding excellent ohmic contacts and adhesion. Differential conductivities of $<10^{-4}$ Ω-cm^{-2} have been achieved for entire devices, indicating that p-type contacts are not a problem. Turn-on is typically observed at 3-3.2V. Modeling has

((

revealed little intrinsic benefit in adopting a buried heterostructure geometry. For practical reasons, diodes currently under examination are ridge waveguides.

4 Conclusions

4.1 Devices

The development of MOCVD nitride growth on sapphire substrates in low pressure, multi-wafer reactors has been successful and will be the biggest factor in achieving a high volume, cost effective manufacturing process. The rapid feedback of characterization data and actual device performance has greatly accelerated the development of nitride epitaxial growth processes. The higher cost of nitride LEDs grown on silicon carbide substrates make them less suitable for high volume manufacturing. Lattice matched substrates are not a prerequisite for excellent LED performance, and the advanced substrates and alternative precursors studied have not yet evolved to the point of commercial feasibility for high volume manufacturing. Because of their higher quantum efficiency, narrower emission spectra and greater color saturation, quantum well device structures have been proven superior to double heterostructure devices utilizing a thick co-doped active layer.

A laser diode remains to be demonstrated, but such a demonstration appears imminent based on the status of the materials and processing, and will be attributable in great part to work performed under Blue Band. All necessary growth and fabrication processes are now in place, yielding results which equal or outstrip competitors in respects critical to realization of a commercial laser. Contact resistances are as good as any reported, with low turn-on voltages, and adhesion is excellent. Dry etched sidewalls are exceptionally smooth and uniform. Epilayers are demonstrating record electroluminescent linewidths with good efficiencies, and readily lase under optical excitation. While SDL's dry etching capability has only just come on-line, with attendant teething pains that have precluded fabrication of a satisfactory structure, realization of a diode laser appears very close.

4.2 Materials

Viable, large-area HVPE GaN-on-sapphire substrates have been produced under this program, and have been distributed to consortium members for MOVPE growth and fabrication of device layers. The LED performance of initial devices has been very encouraging. High quality GaN has been grown by HVPE on sacrificial Si templates and fast Si etching (25 µm/min) has been demonstrated. The HVPE GaN has been Si-doped to reduce the resistance in the underlying substrate by a factor of 5. Through all of these accomplishments, the HVPE process has been proven to be a viable technique for production of large area GaN substrates for short wavelength LEDs and LDs.

MOCVD growth procedures yielding high-quality AlGaN/InGaN heterostructures have been developed. This is evidenced by superior structural properties such as mirror smooth morphologies, low dislocation densities, and crack- and pit-free growths; outstanding electrical properties including demonstrations of p-type doping in the 10^{18}'s cm^{-3}; and outstanding optical properties such as record electroluminescent linewidths and quantum efficiencies almost twice those targeted under the program. Ultimately, the excellent

performance of LEDs and ease of achieving optically pumped lasing attest to the quality of the underlying materials.

MBE growth processes have likewise been successfully developed. Growth of GaN and its alloys on 6H-SiC has been achieved without use of a low temperature buffer. Films have excellent structural and optical characteristics when grown on these and conventional sapphire substrates. By contrast, MBE growth of III-V nitrides on sputtered ZnO thin films or M-plane sapphire appears undesirable. ZnO decomposes at conventional nitride growth temperatures, and MBE growth on M-plane sapphire results in undesirable epilayer orientations, resulting in high residual stresses and defect levels. M-plane sapphire may still prove useful for growth by MOCVD, as this is a higher-temperature process which could lead to growth of closely lattice matched (10-13) material.

The structural, optical, and electrical characteristics of (Al,Ga,In)N alloys and heterostructures are now substantially better understood. Energetics and microscopic mechanisms of doping, compensation, and formation of deep levels have been elucidated. Electronic properties such as band offsets have been calculated. The types and nature of structural defects have been studied in detail, as have intrinsic and extrinsic optical signatures of the materials. Each of these studies has been fed back to device growth and design parameters.

5 Recommendations for Future Work

5.1 Substrates

HVPE GaN substrates have become very promising recently, although as yet no breakthrough performance data have been reported for LEDs or laser diodes fabricated on these substrates. Many groups are currently working on the development of HVPE GaN substrates and have shown good progress towards commercialization. ATMI now sells HVPE GaN/sapphire substrates, although they are not yet available in sufficient quantity for LED manufacturing. Ultimately, the goal should be to achieve a free-standing GaN substrate so that vertically conducting devices can be fabricated, resulting in a significant cost reduction due to the smaller area required for devices. In this regard, both the growth and etch technique and the development of Si doping initiated under this program appear to be fruitful avenues for further study.

Silicon carbide substrates, which are still expensive and not required for good LED performance, have improved substantially in both surface quality and size in recent years. LEDs grown on SiC are now commercially available with about 20% the light output of those grown on sapphire substrates. SiC substrates have several potential advantages as substrates for AlInGaN lasers, including good thermal conductivity for heat dissipation and the ability to fabricate vertically-conductive device structures.

Lattice-matched spinels, garnets and intermediate layers (similar to buffer layers) have shown little progress in the last two years, and have some fundamental problems in terms of high temperature instability and diffusion that may preclude their use as substrates for AlInGaN epitaxial growth. It is recommended that research in this area be reduced, and more research efforts focused on promising substrates such as SiC or HVPE GaN, or

((

those with more desirable properties for laser applications, *e.g.* readily cleaved or having high thermal conductivities. High pressure bulk GaN crystal growth has some long range potential, but is far enough from commercialization that it is not appropriate for large companies to invest in. It is recommended that this technology be funded and developed at the university level.

5.2 Growth

Reactor modeling has been extremely useful in understanding temperature distributions and gas flow dynamics in large, multi-wafer MOCVD reactors, and the availability of the national labs and supercomputer centers has been crucial to the development of this knowledge. The continuation of this work will be necessary for improving epitaxial layer uniformity, which is crucial to the development of laser arrays and necessary for cost reduction in nitride LEDs.

In tandem with modeling, continued experimental efforts are likely to further improve the quality and reproducibility of nitride epilayers. Improvements in extrinsic characteristics and control of compositions, doping profiles, and layer thicknesses are likely to be derived from improved understanding of surface structure and growth reactions. Methods to minimize or eliminate cracks and pits must be further explored, particularly for structures containing $Al_xGa_{1-x}N$ and/or $In_xGa_{1-x}N$ poorly lattice matched to GaN. Likewise, better understanding of intrinsic and impurity-assisted dislocation dynamics is likely to yield improved control of plastic relaxation of buffers and/or epilayers.

5.3 Properties

Improved understanding of nitride properties, both intrinsic and extrinsic, is likely to guide significant improvements in material quality and in the design and performance of device structures. Areas with particular promise are studies of the properties of InGaN active layers, work on the nature and role of defects, and examination of electrical properties.

The nature of the lasing transition in nitride devices is currently unknown, although there has been extensive speculation that it is quantum-dot-like, associated with In clusters observed on the group-III sublattice in InGaN wells. As the issue is central to the operation of laser diodes and has important ramifications for device design, the nature of the transition warrants further study. In addition, numerous basic properties of these InGaN active layers remain largely unexplored. Properties of particular importance to devices are the relation between strain and band gap in InGaN MQWs and the nature of deep level defects likely to promote non-radiative recombination.

While extended defects have clearly been demonstrated to have less impact on device properties than in other III-Vs, their role in determining device performance and degradation remains unclear. Defects along dislocation cores (kinks, etc.) merit investigation as they can govern electrical activity and dislocation motion. The optical activities of various defects such as dislocations and nanotubes warrant investigation, as do their roles in enhancing diffusion processes relevant to device degradation and their utility in localizing active point defects. Such studies can be expected to focus improvements in buffers and epilayers to reducing or passivating those defects most detrimental to devices.

Incorporation and activation of p-type dopants remains an important area of study in nitrides as it is essential to achieving modest LED and laser diode turn-on and operating voltages, affecting both operation and degradation of these devices. Promising areas for further study include investigations of the effects of H in AlGaN alloys as well as the thermodynamics of H incorporation, as this is central to compensation. The effects of ion implantation on electrical conductivity remain undercharacterized in GaN, as do the electrical properties of dislocations and associated point defects. Last, identifying alternative, shallower dopants for AlGaN could be highly beneficial.

5.4 Processing

New methods of etching GaN need to be developed in order to improve feature uniformity over larger areas, to increase throughput for high volume LED fabrication, and to fabricate small features accurately for edge emitting laser and VCSEL arrays. Recently developed techniques such as Low Energy Electron Enhanced Etching (LE4) and photo-assisted electrochemical etching have shown promise, and research should be funded at the university level (perhaps in conjunction with a semiconductor equipment manufacturer) to scale up these methods.

5.5 Devices

Good progress has been made in the development of nitride edge emitting lasers by several groups around the world, but little progress has been made with nitride VCSELs. Mirror research for VCSELs is likely to be the most crucial issue. The n-type mirrors can probably be fabricated using conventional MOCVD epitaxial growth techniques. The critical problems will be maintaining a sharp enough refractive index contrast at the interfaces and minimizing scattering and interference at the rough interfaces. A suitable p-type mirror would be extremely difficult to fabricate through epitaxial growth in the nitride system, and reliable wafer bonding techniques must be developed. Further improvements in crystal quality may be required in order to commercialize these devices, and advanced substrate technologies such as HVPE nitride and bulk GaN growth should be supported. P-type contacts may also require further development to support the higher current density required for carrier injection in laser device structures.